AD-A169 732 STATIC AND DYNAMIC TESTING OF INTERCEPTOR SUBSTRUCTURES 1/2
(U) TERRA TEK INC SALT LAKE CITY UT M L WILSON ET AL.
MAR 86 RTRE-82-18 MTL-TR-86-5 DAAG29-81-C-0023
UNCLASSIFIED F/G 11/4 NL

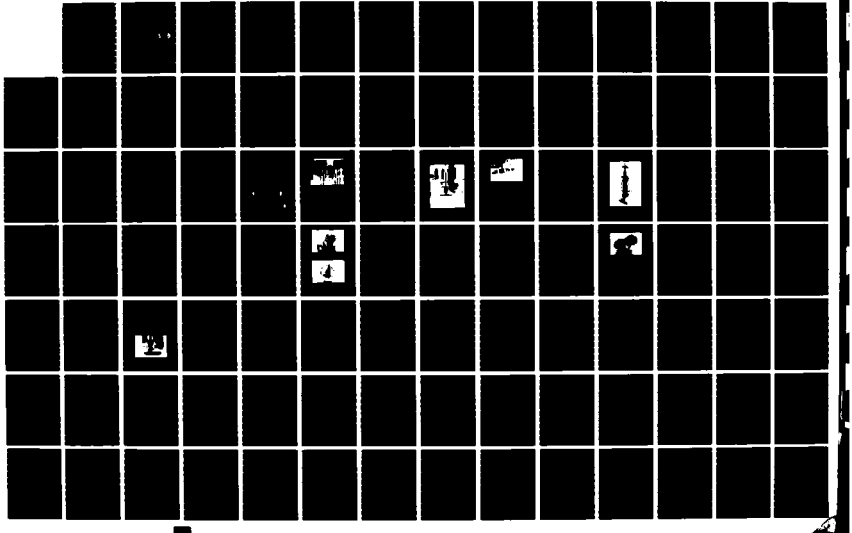

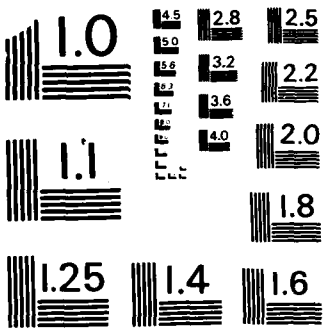

MICROCOPY RESOLUTION TEST CHART
NATIONAL BUREAU OF STANDARDS - 1963 - A

(2)

AD

US ARMY
LABORATORY COMMAND
MATERIALS TECHNOLOGY
LABORATORY

AD-A169 732

MTL TR 86-5

STATIC AND DYNAMIC TESTING OF INTERCEPTOR SUBSTRUCTURES

March 1986

M. L. WILSON and R. H. TODD
TerraTek
University Research Park
420 Wakara Way
Salt Lake City, Utah 84108

DTIC
ELECTE
JUL 0 8 1986
S D
D

FINAL REPORT Contract No. DAAG46-81-C-0023

Approved for public release; distribution unlimited.

DTIC FILE COPY

Prepared for

U.S. ARMY MATERIALS TECHNOLOGY LABORATORY
Watertown, Massachusetts 02172-0001

86 7 7 103

The findings in this report are not to be construed as an official Department of the Army position, unless so designated by other authorized documents.

Mention of any trade names or manufacturers in this report shall not be construed as advertising nor as an official indorsement or approval of such products or companies by the United States Government

DISPOSITION INSTRUCTIONS

Destroy this report when it is no longer needed
Do not return it to the originator

SECURITY CLASSIFICATION OF THIS PAGE (When Data Entered)

REPORT DOCUMENTATION PAGE		READ INSTRUCTIONS BEFORE COMPLETING FORM
1 REPORT NUMBER MTL TR 86-5	2 GOVT ACCESSION NO	3 RECIPIENT'S CATALOG NUMBER
4 TITLE (and Subtitle) STATIC AND DYNAMIC TESTING OF INTERCEPTOR SUBSTRUCTURES		5 TYPE OF REPORT & PERIOD COVERED Final Dec 80 to Apr 81
		6 PERFORMING ORG. REPORT NUMBER RTRE 82-18
7 AUTHOR(s) M. L. Wilson and R. H. Todd		8 CONTRACT OR GRANT NUMBER(s) DAAG46-81-C-0023
9 PERFORMING ORGANIZATION NAME AND ADDRESS Terra Tek, Inc. 420 Wakara Way Salt Lake City, Utah 84108		10 PROGRAM ELEMENT PROJECT, TASK AREA & WORK UNIT NUMBERS AMCMS Code: 693000.21500
11 CONTROLLING OFFICE NAME AND ADDRESS U. S. Army Materials Technology Laboratory Watertown, MA 02172-0001 ATTN: SLCMT-ISC		12 REPORT DATE March 1986 13 NUMBER OF PAGES 175
14 MONITORING AGENCY NAME & ADDRESS(if different from Controlling Office)		15 SECURITY CLASS (of this report) Unclassified 15a DECLASSIFICATION DOWNGRADING SCHEDULE

16 DISTRIBUTION STATEMENT (of this Report)

Approved for public release; distribution unlimited.

17 DISTRIBUTION STATEMENT (of the abstract entered in Block 20, if different from Report)

18 SUPPLEMENTARY NOTES

19 KEY WORDS (Continue on reverse side if necessary and identify by block number)

Structural Testing
Frustums
Dynamic Loads
Aluminum Alloys
Boron/Aluminum Composites
Metal Matrix Composites
Fracture

20 ABSTRACT (Continue on reverse side if necessary and identify by block number)

SEE REVERSE

DD FORM 1 JAN 73 1473 EDITION OF 1 NOV 65 IS OBSOLETE

SECURITY CLASSIFICATION OF THIS PAGE (When Data Entered)

Block No. 20

ABSTRACT

Truncated, conical, half-scale, interceptor substructures were tested under axial and shear/bend loads. The substructures, designed and fabricated by General Dynamics, were manufactured with 20 ply boron/aluminum composite tape, each ply was 0.0069 to 0.0080 inch thick. Boron filaments made up 47.0 + 3.0 percent of the composite tape. Average substructure dimensions were 5.80 inches (outside) forward diameter, 7.79 inches (outside) base diameter, and 9.112 inches high (total apex angle 12.46°). The wall thickness was 0.144 inches. Axial loading (both static and dynamic) as well as shear/bend loading (static only) tests were performed; one sample was tested at each test condition. An upper bound to the failure load under static axial loading was estimated at between 600,000 pounds and 700,000 pounds. Under dynamic axial loading failure was initiated at a defect in the substructure and occurred at 519,000 pounds. Failure load in shear/bend was 44,000 pounds for the load applied laterally 1 inch forward of the truncated nose (bending moment of 383,300 in-lbs at the built-in section, 1.4 inches above the base of the cone). General Dynamics reported 10 to 20 percent higher bending moments at failure (43,300 pounds to 48,000 pounds shear applied 2 inches forward of the substructure corresponding to between 420,000 in-lbs and 465,600 in-lbs bending moment at the built-in section, 1.4 inches above the base of the cone). No axial failure load data was previously reported. Under axial load the frusta exhibited sudden brittle failure. In the shear/bend loading tests, failure was at the frustum bondline with vertical splits into the frustum.

PREFACE

This report was prepared by Terra Tek, Inc. under Army Materials Technology Laboratory Contract No. DAAG46-81-C-0023. It covers work conducted from December 1, 1980 through April 30, 1981. The contract was administered under the direction of the Ballistic Missile Defense Materials Program Office, Army Materials Technology Laboratory, with Mr. John F. Dignam as Program Manager and Dr. S. C. Chou as Technical Monitor.

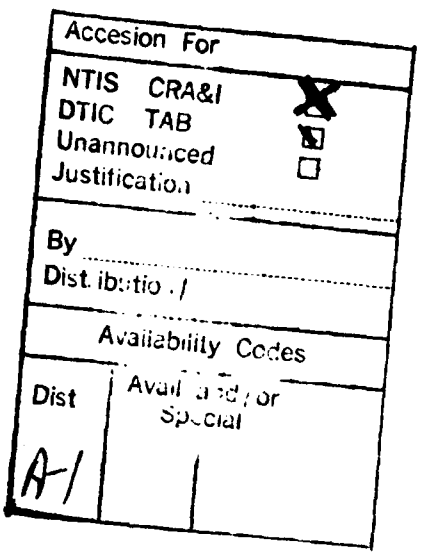

TABLE OF CONTENTS

LIST OF ILLUSTRATIONS

LIST OF TABLES

1. INTRODUCTION AND SUMMARY

The need for lightweight, stiff, structural materials, has been identified for interceptors designed to undergo high performance maneuvers. To meet these demands, the Army Materials Technology Laboratory (AMTL) has conducted the research and development of advanced materials including beryllium, graphite epoxy, boron/aluminum, etc. (References 1, 2 and 3). Characterization of these materials have generally been performed on small test coupons. The need remains to establish confidence that the missile frusta manufactured from these materials meets design, i.e. reveals no weaknesses or defects due to material handling and normal variability in manufacturing operations.

Static simulation of flight loading require intricate fixturing to provide structural data under combined loads for evaluating the strength and stiffness properties of the missile frustum. This loading is often a complex relationship of surface pressures, shears, bending moments and axial loads. To evaluate the factor of safety in designs, the selected loads are increased to failure, failure being defined as a structural component failure or excessive deformation which could prevent the successful accomplishment of the mission.

1.1 Summary of Test Program

The primary objective of the program reported here was the evaluation of the strength and stiffness properties of half-scale, ultra-high modulus, boron/aluminum cone frusta. Both axial and combined shear/bend loading tests were performed. Loads and strains were measured directly in all tests to monitor the onset of failure, i.e.:

1. Fracture from combined tensile and shear stresses.

2. Instability or buckling collapse.

A 1.7 million pound test machine at Terra Tek was modified to perform the work. The modified machine is capable of testing frusta up to 36 inches diameter and 48 inches long. Test frame characteristics are:

Loading Mode	Capacity	Maximum Loading Rate
Axial	1.70×10^6 lb	1.0×10^6 lb/sec
Shear	0.30×10^6 lb	1.0×10^6 lb/sec
Bending	15.0×10^6 in-lb	2.0×10^6 in-lb/sec

Machine control was effected by four servocontrollers which provided for completely independent control of the four separate hydraulic actuators (axial, shear and two bending moment actuators). The loading rates were precisely regulated via Exact Function Generators which supplied the command input to the servocontrollers. Loads and strains data were collected by a DEC PDP 11-34 Computer via a Soundstream 14 Bit A/D Convertor.

1.2 Summary of Test Results

Six frusta were tested according to the schedule in Table 1.1. Three were fabricated from aluminum 6061-T6 and three from the boron/aluminum composites. All six frusta were of approximately the same dimensions--right-circular, truncated, cylindrical cones, 5.80 inches outer diameter at the forward end increasing to 7.79 inches outer diameter at the base. Frusta height were 9.112 inches, i.e., 6.23^0 taper. Wall thickness was nominally 0.144 inches.

The aluminum 6061-T6 cone frusta were tested first to check out the system performance and to optimize machine setting for the boron/aluminum frusta

tests. This was an economic expediency to minimize the chance of invalid tests with the high cost boron/aluminum frusta.

Test results are summarized in Table 1.1. In static axial loading the aluminum frustum failed at 122,000 lbs. Under dynamic axial loading conditions the frustum was subjected to eccentric loads. Accordingly, failure was at a lower axial load, 109,500 lbs. Under dynamic loading the observed failure tended to exhibit a five node plastic buckling as compared to the three node plastic buckling under static loading.

In contrast the boron/aluminum frusta failed in a brittle manner. Failure under static axial load was by elastic buckling near the forward end. Since the load cell failed during the test, the load at failure was calculated based on the assumption that the frustum behaved totally elastically. The estimated failure load was 600,000 to 700,000 lbs. Under dynamic load, failure occurred at 519,000 lbs. A small amount of nonlinear response is observed in one set of gages which is totally absent in the diametrically opposite set. It is not at all clear how this condition could prevail unless local inhomogeniety existed at the gore overlap. Failure was sudden and violent.

In shear/bend loading of the aluminum frusta, plastic deformation was initiated at approximately 15,000 lbs shear load with ultimate failure at 23,250 lbs shear (i.e. 202,300 in-lbs bending moment at the base). Failure was caused by plastic buckling. The boron/aluminum frustum tested in shear/bend loading failed at the attachment to the base steel ring. Vertical splits subsequently developed in the frustum as the failure propagated. The failure load was 44,000 lbs shear (i.e. 383,300 in-lbs bending moment at the base). Result for this shear/bend loading test is 10 to 20 percent lower than for similar tests reported in Reference 4.

Table 1.1. Summary of Test Results

Material	Loading	Loading Rate	Failure Load	Comments
Al 6061-T6	Axial	Static	122,000 lbs	Buckling Failure (three-node plastic deformation)
Al 6061-T6	Axial	0.85×10^6 lb/sec	109,500 lbs	Frusta subjected to eccentric loading. Buckling Failure (five-node plastic deformation)
Al 6061-T6	Shear/Bend	Static	23,250 lbs (202,300 in-lbs bending moment)	Plastic Buckling
Boron/Aluminum	Axial	Static	600,000 lbs to 700,000 lbs	Frusta subjected to eccentric loading. Brittle Failure.
Boron/Aluminum	Axial	0.94×10^6 lb/sec	519,000 lbs	Brittle Failure initiated at inhomogeniety
Boron/Aluminum	Shear/Bend	Static	44,000 lbs (383,300 in-lbs bending moment)	Failed at frustum bondline; vertical splits in frustum

2. MATERIALS DESCRIPTION AND SUBSTRUCTURES FABRICATION

As indicated in the previous section, two sets of tests were performed. The first series of tests were with aluminum 6061-T6 truncated cones fabricated to approximately the same dimensions as the boron/aluminum frusta. These tests were to verify the test procedures prior to initiating tests on the boron/aluminum frusta.

2.1 Aluminum 6061-T6 Material Properties

The aluminum cones were machined from 8 inches diameter bar stock to approximately the same dimensions as the boron/aluminum frusta. Typical dimensions for the right-circular cones and typical material properties for the aluminum 6061-T6 are listed in Tables 2.1 and 2.2, respectively.

Table 2.1. Typical Aluminum Cone Dimensions

Outside Diameters (ins)		Height (ins)	Wall Thickness (ins)
Forward	Base		
5.781	7.752	9.100	0.144

Table 2.2. Typical Tensile Material Properties for Aluminum 6061-T6 Bar Stock

Young's Modulus (psi)	Poisson's Ratio	Yield Strength (psi)	Ultimate Strength (psi)
10.0×10^6	0.3	41,800	46,800

2.2 Description of Boron/Aluminum Sheet Material

The boron/aluminum sheet material was purchased by General Dynamics, Convair Division, and used to manufacture the frusta tested in this program. Complete details of the material, manufacturing process and inspection data are provided in Reference 4. For completness, details essential to evaluating the structural test data are duplicated here from Reference 4.

The boron/aluminum sheet material was obtained by General Dynamics from Amercom, Inc., Chatsworth, CA. Receiving inspection analysis of the boron/-aluminum tape after it was diffusion bonded by the supplier into a single layer tape is shown in Table 2.3. Results were in compliance with General Dynamics specifications.

Table 2.3. Receiving Inspection Tests Results on Incoming Boron/Aluminum Material (from Reference 4)

Material Property	Test Results
Filament Count and Alignment	137 to 138 per inch
Tape Thickness	0.0069 to 0.0080 inch
Boron Volume Percent	45.2 to 47.2 v/o
Boron Filament Diameter	0.00569 to 0.00572 inch
Aluminum Foil Base	0.002094 to 0.002113 inch
Aluminum Foil Cover	0.002088 to 0.002131 inch
Filament Bend Test	4.1 percent maximum
Surface Condition	Acceptable
Internal Defects	Acceptable
Carbon Content	0.005 percent maximum

2.3 Fabrication and Testing of Heat Treated Boron/Aluminum Material Test Specimens

Tests were conducted by General Dynamics to provide more complete boron/-aluminum properties data base for the heat treated materials. Boron/aluminum

laminates (0°_{6} and 0°_{8}) required for these test specimens were made from a single layer tape material which was laminated, encapsulated, and diffusion bonded in the General Dynamics autoclave. Test specimen configurations are shown in Figures 2.1, 2.2 and 2.3. Test results are summarized in Tables 2.4,

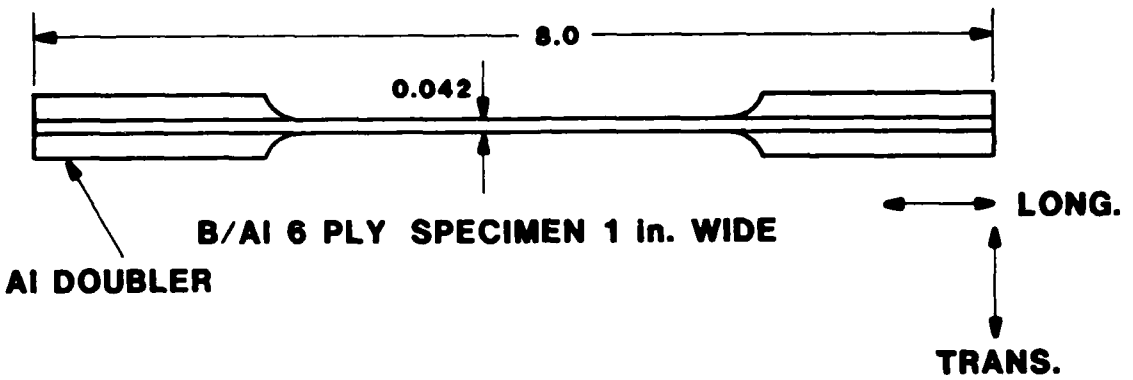

Figure 2.1. Longitudinal and Transverse Tensile Specimen. All dimensions are in inches (from Reference 4).

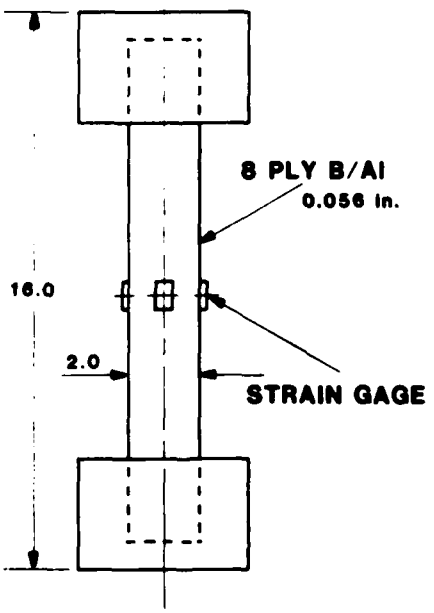

Figure 2.2. Tubular Column Compression Specimen. All dimensions are in inches (from Reference 4).

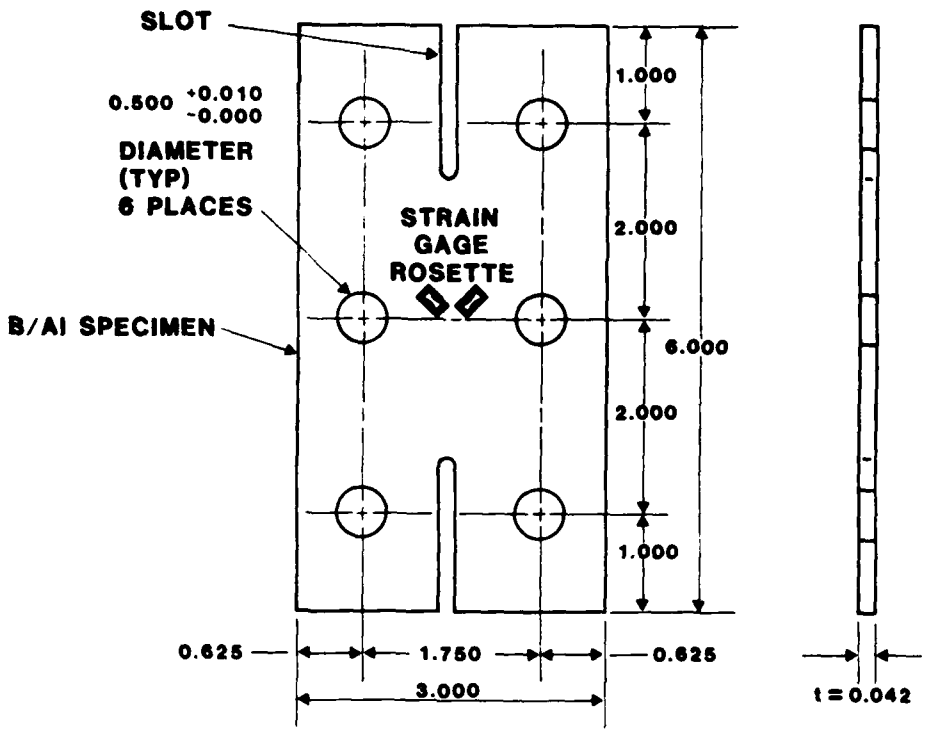

Figure 2.3. Rail Shear Specimen. Dimensions are in inches (from Reference 4).

2.5 and 2.6. The longitudinal tensile strength and modulus were slightly lower than expected; nevertheless, the values are very good and indicate a wide margin of safety for the frusta. The transverse tensile strength was slightly higher than expected. This was interpreted to mean that the heat treatment was close to optimum for the aluminum but caused a slight degradation of the filaments and the longitudinal properties. The compression strengths are exceptionally high. Shear strengths, as measured by the rail shear test, were adequate for this application. The shear strength of "as-fabricated" boron/aluminum is 12,000 psi to 16,000 psi. The heat treated values are substantially higher (25,000 psi).

Table 2.4. Longitudinal and Transverse Test Results for Heat Treated Boron/Aluminum (from Reference 4)

Test	Specimen Number		Strength, ksi	Modulus of Elasticity, 10^6 psi
Longitudinal Tensile	2-2		155	32.1
	2-5		133	29.8
	4-1		129	29.3
	4-3		158	29.7
	6-5		144	31.2
	6-4		183	31.3
		Average	150	30.6
Transverse Tensile	2TT-1		24.9	20.5
	2TT-2		28.5	21.7
	4TT-1		36.3	21.6
	4TT-3		36.1	21.4
	6TT-2		39.4	22.0
	6TT-3		41.1	22.2
		Average	34.4	21.6

Table 2.5. Compression Test Results for Heat Treated Boron/Aluminum (from Reference 4)

Test	Specimen Number		Strength, ksi	Modulus of Elasticity, 10^6 psi
Compression	1		297	33.0
	2		305	33.9
	3		324	33.9
	4		332	33.2
	5		330	33.1
	6		296	34.0
		Average	314	33.5

Table 2.6. Rail Shear Test Results for Heat Treated Boron/Aluminum (from Reference 4)

Test	Specimen Number		Shear Strength, ksi	Shear Modulus, 10^6 psi
Rail Shear	S1-1		24.2	9.8
	S1-3		25.8	9.5
	S1-5		27.0	9.7
	S2-1		24.5	9.1
	S2-3		23.1	9.0
	S2-5		27.0	9.5
		Average	25.2	9.4

2.4 Fabrication of Boron/Aluminum Frusta

The frusta wall thickness was 20 ply or approximately 0.140 inch. The filaments were oriented in an uniaxial direction to maximize strength and stiffness. Each layer was arbitrarily divided into four segments so the maximum filament deviation from true axial direction would not vary by more than 2.44^{o}, assuming the center filament of each gore is in the axial direction. Strength and modulus are practically unchanged at any angle less than 5^{o} (Reference 5).

Each layer of gore segments was assembled from the outside wall inward in the female tool. Each of the 20 layers of four connected segments was rotated $4\text{-}1/2^{o}$ (1/20 of 90^{o}) so that none of the seams lined up. In addition, the edges of each layer were allowed to overlap approximately 1/4 inch to allow for expansion of the layers during consolidation. As layers were stacked into the tool, the circumference changes required a periodic change in the gore size. Four gore segment sizes were used, i.e. gore sizes were changed every fifth layer.

The thin inner mandrel was pushed down upon the stacked gores and weld rings were installed on both ends of the hollow encapsulation. The pack was evacuated through the vent tube, previously installed on the thick outer mandrel, which was pinched off after evacuation and welded shut prior to placing of the tool assembly in the autoclave.

The high pressure autoclave cycle used in fabricating the boron/aluminum conical frusta is listed below:

a) Pressure autoclave at room temperature to 9750 $\pm$ 250 psi.

b) Heat to 800^{o} to 900^{o}F.

c) Stabilize pressure and temperature before reaching 900^{o}F.

d) Raise temperature to 970 $\pm$ 15^{o}F at a rate not less than 1.5^{o}F/minute.

e) Reduce temperature to below 900^{o}F at a rate not less than 1.5^{o}F/minute.

f) Release pressure any time between 800^{o}F and room temperature.

g) Remove tool at any temperature below 600^{o}F.

The isostatic pressure in the autoclave acts primarily on the thin inner mandrel, which yields most easily. Pressure pushes the inner diaphragm and the boron/aluminum layers to the outside. The outward movement of the boron/-aluminum in the thick female mandrel ensures a replicate of the machined tool surface as well as a duplication of the machined tolerances. Diffusion of the layers results in a homogeneous bond.

The transverse and shear properties of the cone are greatly increased by subsequently heat treating the 6061 aluminum matrix as follows:

a) Heat to 970^{o}F and hold for one-half hour.

b) Quench. (The quench tank contained Ucon A--primarily polyalkylene glycol--diluted to 18 to 22 percent

and kept vigorously agitated in a large tank so that the temperature never exceeded 90°F.)

c) Cryogenic soak in liquid nitrogen for five minutes.

d) Age at 350°F for eight hours.

After each cone was heat treated, approximately three quarters of an inch was trimmed from each end.

Dimensional analysis, including measurement of the frusta wall thickness is necessary because of wall thickness variation. Expansion of the thin inner mandrel during pressurization plus the overlapping edges of the gore sections give the inside of the cone an uneven surface. The outside, however, is forced against a heavy-wall smooth tool and is therefore smooth. Relative to roundness, the cones before heat treatment assume the shape of the mandrel. After heat treatment, the cones usually distort. The amount of distortion is generally small. Table 2.7 shows the dimensions and weight after heat treatment of frusta 6 through 10 (three of which were tested in this program). The

Table 2.7. Dimensions and Weight after Heat Treatment, Boron/Aluminum Frusta 6 through 10 (from Reference 4)

Cone Number	Height (inches)	Roundness Tolerance 4 Places (mils)	Average Thickness 12 Places 3 Levels (inches)	Standard Deviation Sample Thickness (mils)	Weight (grams)
6	9.109	14.5	0.145	4.8	1198
7	9.110	18.0	0.147	3.0	1203
8	9.118	21.0	0.141	8.2	1195
9	9.113	26.0	0.142	11.5	1191
10	9.108	28.0	0.143	8.3	1178
Average	9.112	21.5	0.144	7.2	1193 or (2.63 lb)

measured thickness can be compared with the 0.140 inches predicted thickness for 20 layers. The predicted weight was 2.63 pounds at a density of 0.094 lb/in^3. The predicted thickness and weight closely coincide with the data, shown in Table 2.7.

3. TEST FACILITIES AND PROCEDURES

3.1 Test System Load Capacity Requirements for Testing Boron/Aluminum Frusta

The maximum substructure loads and deformations under axial loading and shear/bend loading can be estimated using the material properties data listed in Section 2. Axial membrane forces (N_x) at a section with radius r to the middle surface, as shown in Figure 3.1, is given by

$$N_x = \frac{P}{2\pi r \cos \alpha}$$

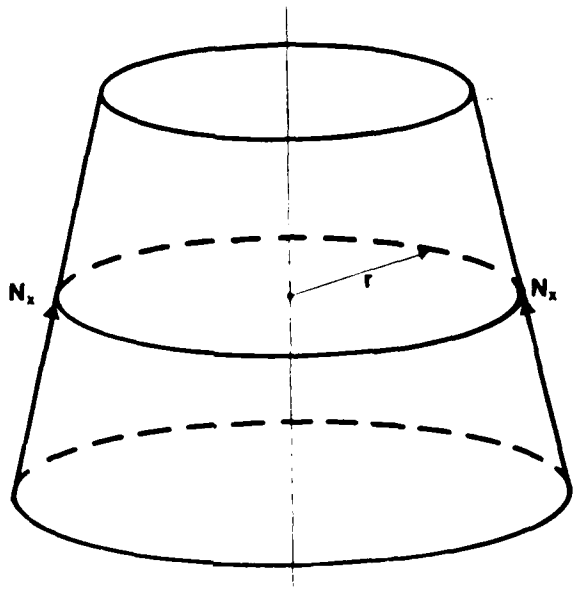

Figure 3.1. Membrane Forces Resulting from Axial Load.

where α is one-half the apex angle, and P the axial load. N_θ, the circumferential membrane force, is zero. The maximum axial membrane force occurs at the forward end of the frusta where r = 2.84 ins. With a wall thickness h = 0.144 ins, the compressive failure load is

$$P = 2\pi r \sigma_c h \qquad 3.2$$

$$= 799{,}000 \text{ lbs}$$

Under shear/bend loading (M) the maximum membrane load (N_x) in the axial direction is

$$N_x = \frac{M}{\pi r^2} \qquad 3.3$$

where r is the radius of the cone to the middle surface. For a lateral load P at a distance δ above the truncated end of the frusta, the bending moment at a section distance x below the truncated face is P (δ + x) and Equation 3.3, becomes:

$$N_x = \frac{P(\delta + x)}{\pi (a + x \tan \quad)^2} \qquad 3.4$$

where a is the radius at the forward end of the frustum. For $\delta/a \leq 1$ the maximum value of N_x (tensile strength = 21,600 lbs/in) occurs at the base of the frusta. Taking δ = 1 inch, the maximum expected shear load of 98,100 lbs would result in tensile failure. The shear load to failure would increase should the forward end be constrained from rotating. Under pure bending, tensile failure is expected to also initiate at the smaller end where the maximum bending moment at failure calculates to 547,500 in-lbs.

3.2 Support Ring For Frusta Testing

Structural testing of frusta, without the advantage of built-in fixture attachment, presents the problem of design for shear transmission of test loads into the shell ends. This problem was addressed in Reference 6 where a

form of bonded mounting rings which could withstand the high test loads was designed. The same system was subsequently successfully adapted by General Dynamics (Reference 4) in testing the boron/aluminum frusta. A schematic of the General Dynamics system, which was used also in the present program, is shown in Figure 3.2 The frustum is bonded at each end, both on the inside and outside surfaces to 1.4 inches thick steel rings. Bonding was with Hysol EA9309 Structural Adhesive. Vendor strength data for EA 9309 shows the following:

Shear Strength (psi)	Peel Strength (psi)
4750	39

Koo and Seinberg (Reference 6) evaluated bond strength of the Hysol EA9309 for the testing of graphite/epoxy frusta. They performed shear tests with 8.60 inches long, 7 inches diameter, by 0.25 inch thick, aluminum cylinders bonded to an aluminum plate with a 0.125 inch thick, 0.75 inch overlay bondline. Two tests were performed in which the cones were point loaded, normal to their axes at the end removed from the bond. Effective average bond strength resisting pull out of the cylinder calculated to 3,980 psi and 4,900 psi.

Using these pull-out strengths, the calculated bondline failure for the test configuration shown in Figure 3.2 would occur at

Axial Load	257,000 to 316,000 lbs
Shear Load	54,000 to 67,000 lbs

These are significantly lower than the estimated test design loads for failure (799,000 lbs axial load and 98,000 lbs shear load). Nevertheless, General

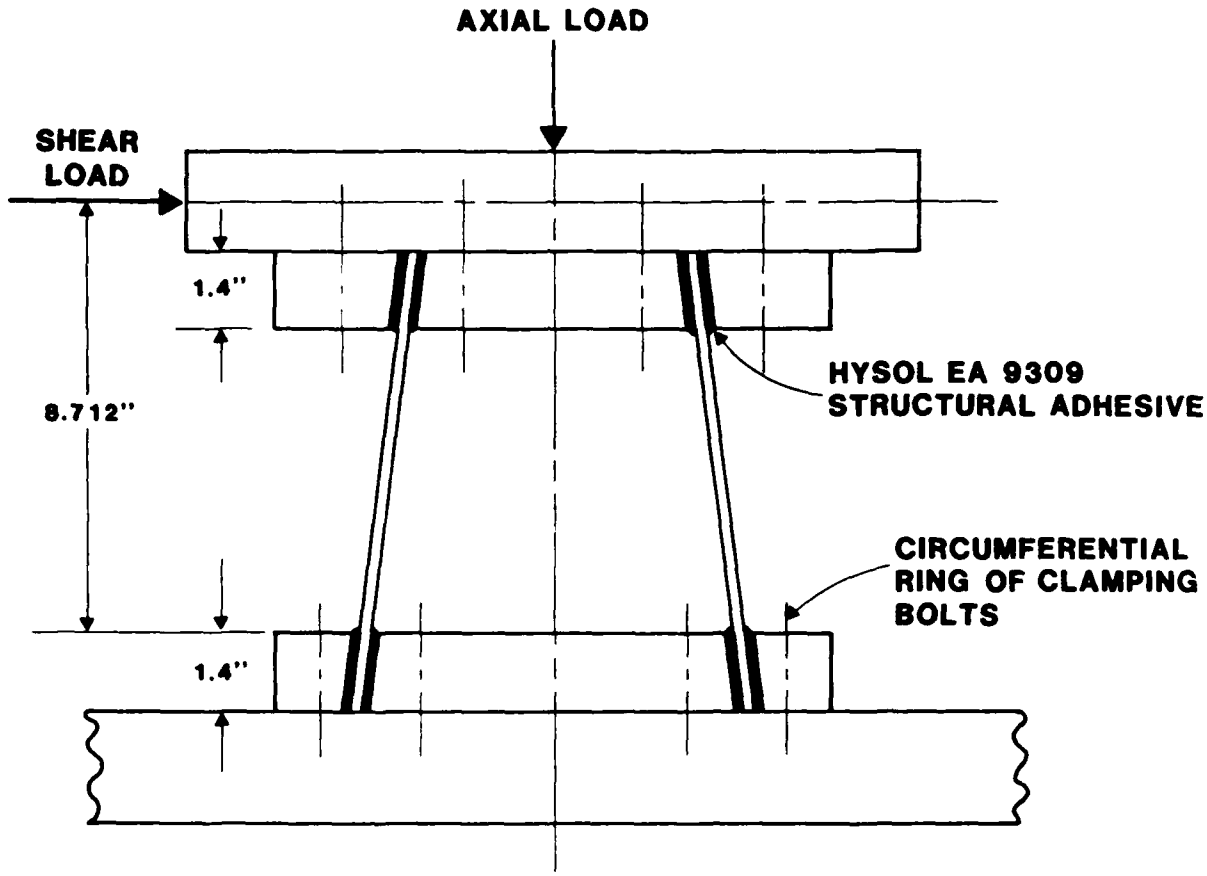

Figure 3.2 Schematic Drawing Showing the Axial and Shear/Bend Load System for Testing the Boron/Aluminum Frusta.

Dynamics (Reference 4) noted that in axial loads to 600,000 lbs the only damage that could be observed was that the boron fibers have indented the loading heads. Based on General Dynamics experience, it was decided to use the same mounting rings design for the axial load tests. Great care was taken in sample preparation to assure intimate contact between the frusta and bearing plates in axial loading. Under shear loading General Dynamics (Reference 4) observed frusta failure at 43,000 lbs to 48,000 lbs, much lower than the calculated failure load. The mounting rings design, therefore, is adequate for the expected shear loads based on data from Reference 4.

3.3 Test Facilities

Table 3.1 summarizes the load capabilities required to test the half-scale frusta to failure. The existing 1.7 million pound test machine was

Table 3.1. Summary of Test System Requirements for Testing Half-Scale Substructure

Loading Mode	Capacity
Axial Load	799,000 lbs
Shear Load	98,000 lbs
Bending Moment	542,500 in-lbs

modified to meet these requirements. In actuality the accumulators chosen have sufficient capacity to test full-scale frusta. Three Miller Fluid Power Rams were installed to provide the shear and bending moment. Figure 3.3 schematically illustrates the modifications made. The hydraulic systems are depicted in Figure 3.4. High-performance, high-flow, servocontrol valves used in conjunction with each actuator allowed for the large flow rates in the dynamic tests.

Each loading system is discussed in detail below and a photograph of the completed facility is shown in Figure 3.5.

Axial System: The axial piston has an area of 322 in^2 and a total thrust of 966,000 lbs at 3,000 psi pressure. The servovalve, controlling pressurized fluid flow to the actuator was rated at 1,000 psi total pressure drop at 55 gallons per minute. Total valve pressure drop was proportional to the square of the flow rate.

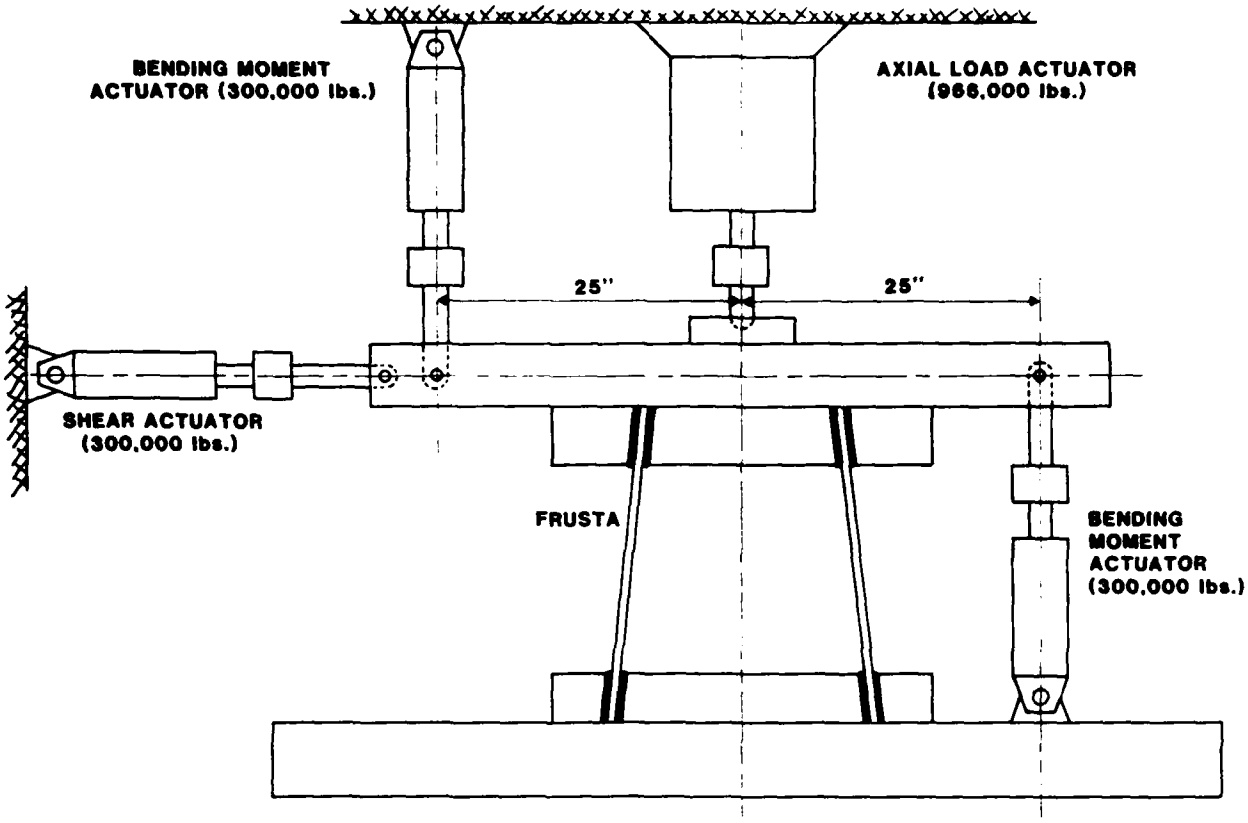

Figure 3.3. Schematic Showing Combined Axial Compression, Shear and Bending Moment Actuators for Frusta Tests. Actuator loads are specified for 3,000 psi operating pressure.

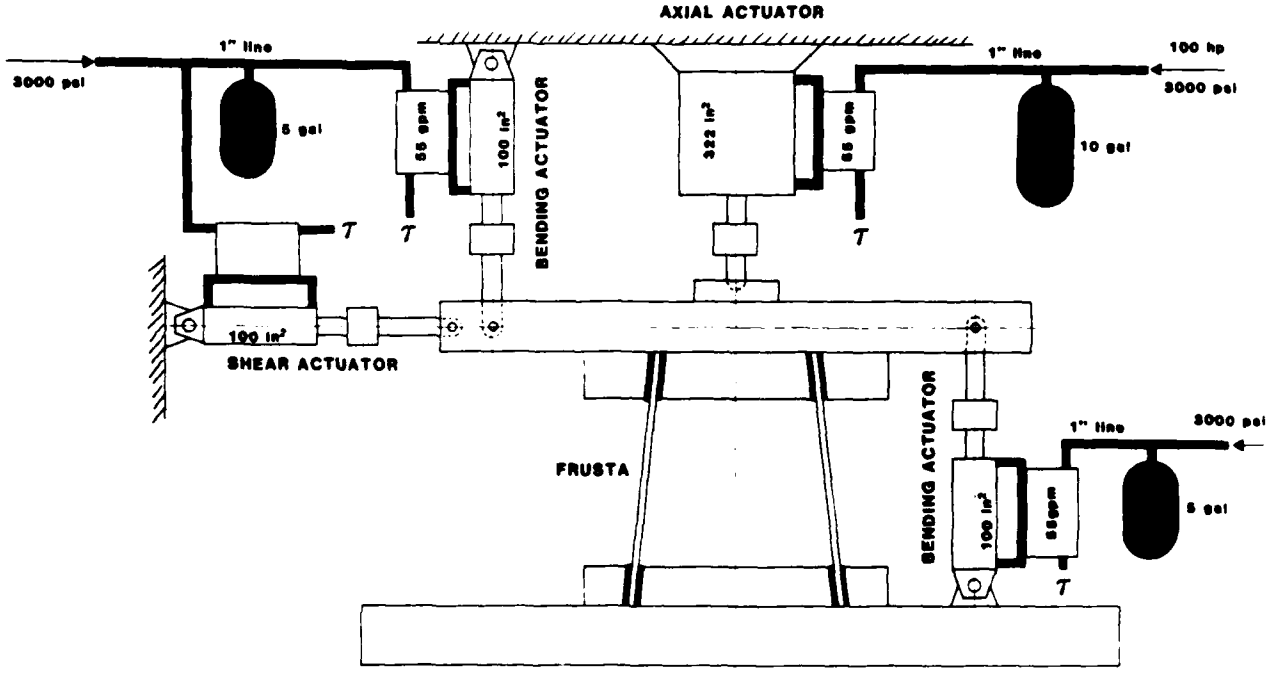

Figure 3.4. Schematic of the Hydraulics for Frusta Test System.

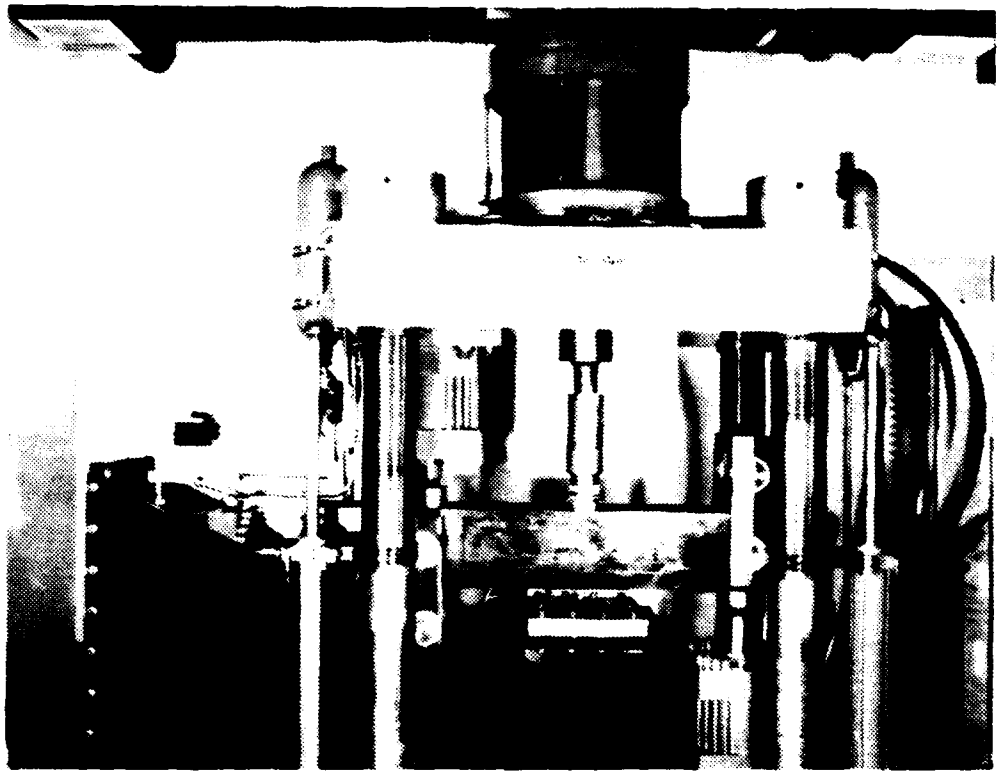

Figure 3.5. Frusta Test System. Axial, shear and bending actuators and hydraulic accumulators are shown.

To achieve the high rate loading a 10 gallon accumulator precharged with gas to 1,500 psi was added to the system. With the test frame stiffness of 6,000,000 lbs/inch, the accumulator reservoir alone has sufficient hydraulic fluid reserve to achieve axial loads in excess of 800,000 lbs in testing the boron/aluminum structure. Achievable loading rates are controlled by the servovalve and are calculated to be on the order of 1,000,000 lb/second.

Shear System: The shear system utilized a single, 100 in^2, horizontal actuator having a thrust of 300,000 lbs at a hydraulic fluid pressure of 3,000 psi. The servovalve was identical to the one used for the Axial System described above.

A 5 gallon accumulator, precharged with gas to 1,500 psi facilitated the dynamic tests. Maximum loading rates to 1,000,000 lbs/sec are possible for the boron/aluminum frusta tests.

Bending System: Bending was introduced by two 100 in^2 actuators operating to 3,000 psi. Each actuator was equipped with a 55 gallon per minute servovalve and attached to a 5 gallon accumulator precharged with gas to 1,500 psi. Figure 3.4 shows the accumulator for one bending actuator to be common with the shear actuator. Maximum bending moment rates to 2,000,000 in-lbs/sec are possible with the boron/aluminum frusta.

The test system capabilities for testing the boron/aluminum frusta are summarized in Table 3.2.

Table 3.2. System Characteristics for Testing Boron/Aluminum Frusta

Loading Mode	Capacity	Maximum Rate
Axial	1.70×10^6 lbs	1×10^6 lbs/sec
Shear	0.30×10^6 lbs	1×10^6 lbs/sec
Bending	15.0×10^6 in. lbs	2×10^6 in. lbs/sec

The system was designed and constructed to provide easy adjustment for frusta up to 36 inches in length and 30 inches diameter. Photographs of the test system, the control and instrument panel, are shown in Figures 3.5, 3.6 and 3.7.

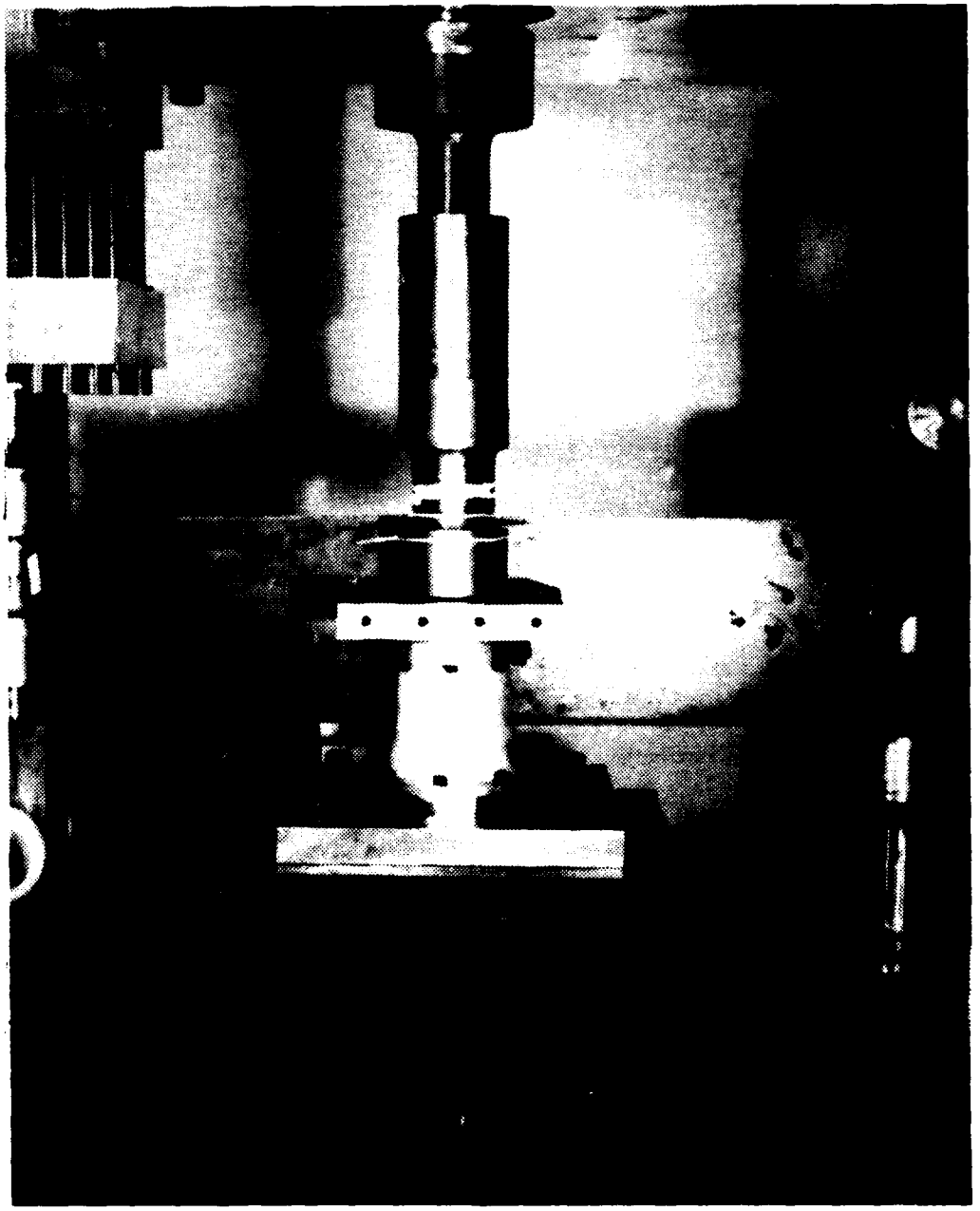

Figure 3.6. Loading System with Front Shear/Bend Beam Removed.

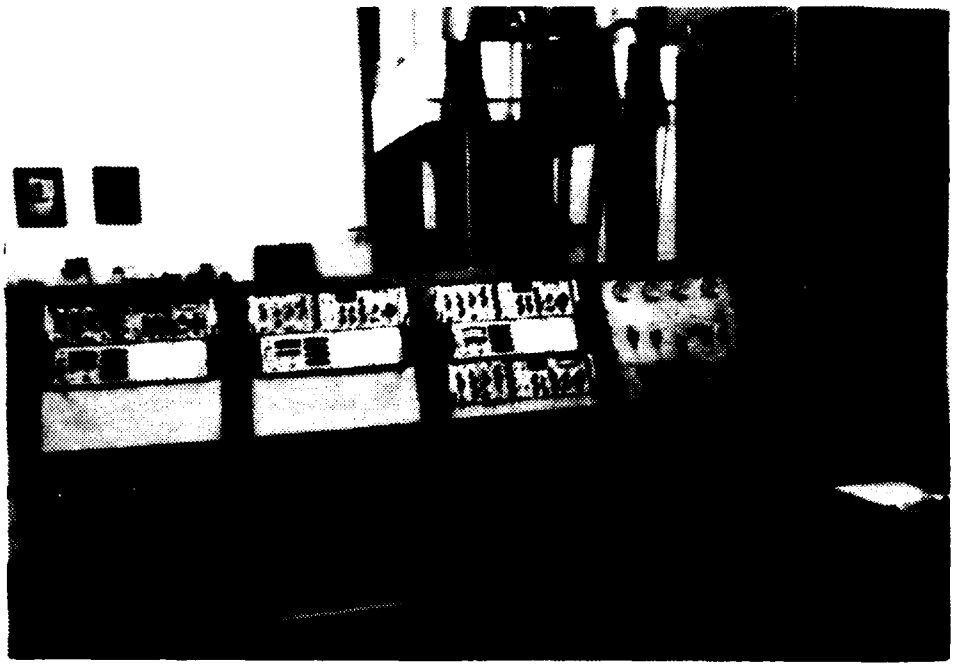

Figure 3.7. Test System Control Panels. Signal conditioning equipment is on the extreme right hand side.

3.4 Test Procedures

The three 6061-T6 aluminum frusta and the three boron/aluminum frusta were prepared identically for testing. The frusta were lightly grit blasted and then degreased in order to provide a suitable surface for strain gaging and for attaching the upper and lower clamping rings. The frusta were then scribed to provide precise locations for the thirty-three strain gage stations as shown in Figure 3.8. Each frustum was gaged using Micro Measurements 120 ohm gages adhered with M-Bond 200 cement. As described previously, the instrumented frusta were epoxied to the upper and lower clamping rings with Hysol EA9309 structural adhesive and bolted to loading plates. Figure 3.9 shows the aluminum frustum prepared for axial loading.

Prior to the actual test each frustum was gradually loaded to 1,000 lbs to check if all systems were operational and to assure load alignment. Shims

were added as necessary until all corresponding gages on a cross-section responded equally to load. Each gage was calibrated by placing a short resistance (0.01 percent tolerance) across the gage. The loading rate was selected and a trigger pulse was used to simultaneously initiate loading and data acquisition. Load and strain data was amplified and then sampled. The sampling rate was approximately 10 microseconds per point for fifty channels

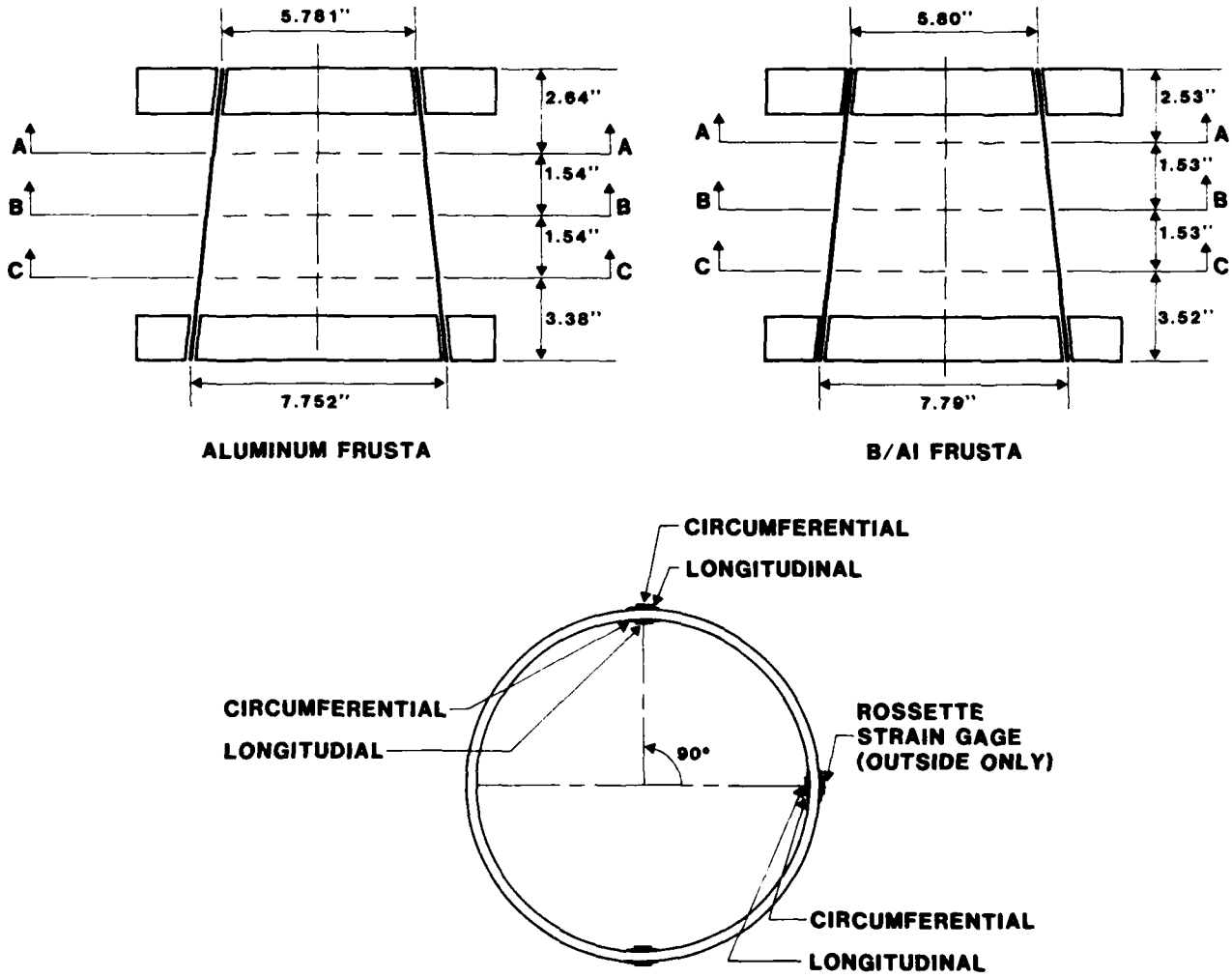

Figure 3.8. Strain Gages Locations on Both the Aluminum 6061-T6 and Boron/Aluminum Frusta.

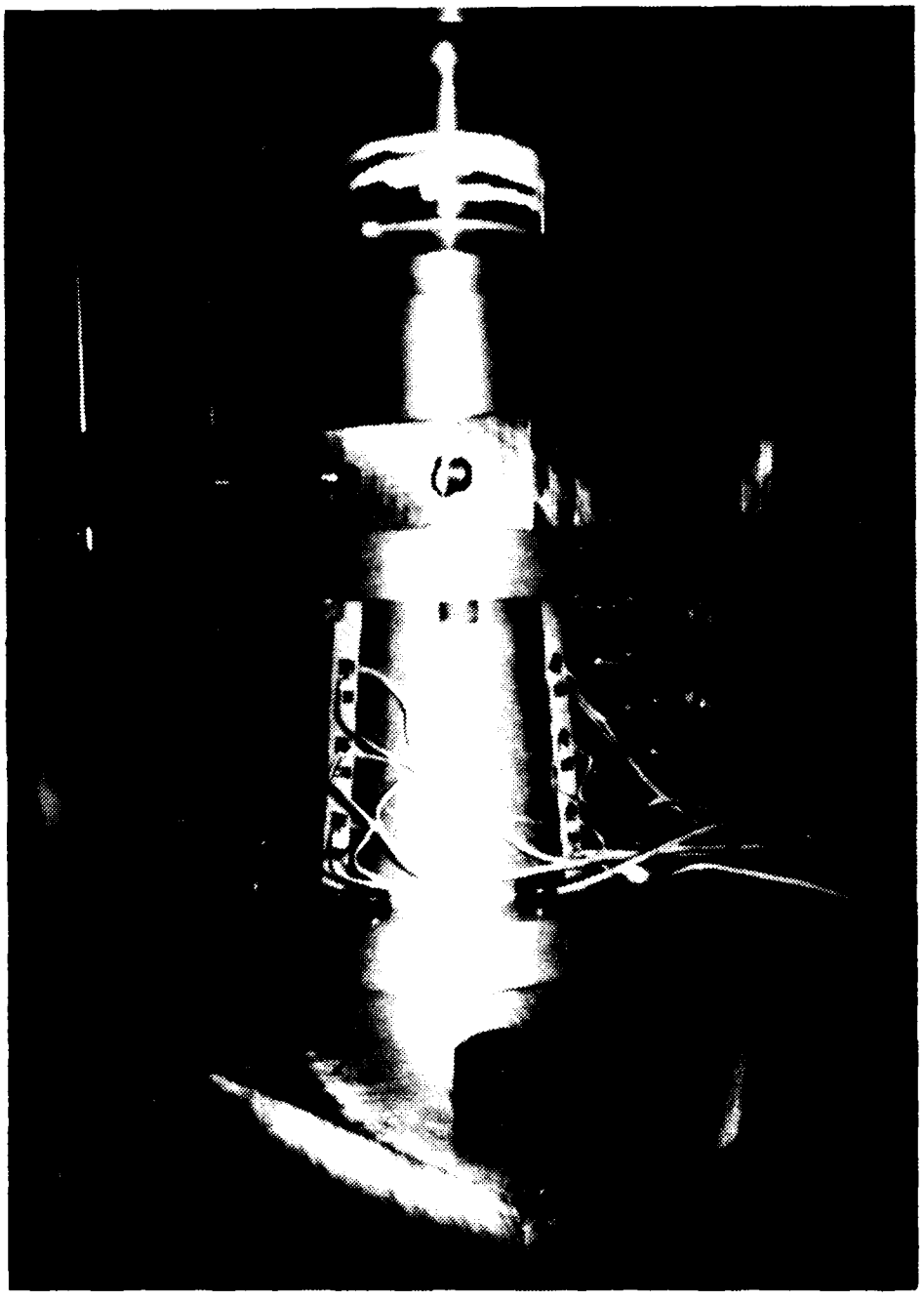

Figure 3.9. Aluminum Frusta Prepared for Static Axial Loading. Strain gages are protected with a clear plastic adhesive.

of data: thirty-three strain gages, four loads (axial, shear and two bending loads), four displacements and nine spare channels. A 0.5 millisecond slew time results between the first channel sampled and the last channel for each fifty channel sweep. This was discounted as being insignificant for the quasi-static tests but was included during reduction of the dynamic test data.

Test control was effected by Exact Function Generators which provided the input command to the servocontrollers. Data was collected in real-time by a DEC PDP 11-34 computer via a Soundstream 14 Bit A/D convertor. Not all the A/D convertor data channels functioned as designed and resulted in a stepped response. These channels were used for monitoring the transverse gages. Data analysis was performed with the same data acquisition computer after the tests.

4. TEST RESULTS

Data for selected gages from each test are appended. Each set of data is designated according to test and gage position (corresponding to locations shown in Figure 3.8); for example:

STATIC AXIAL: ALUMINUM FRUSTUM

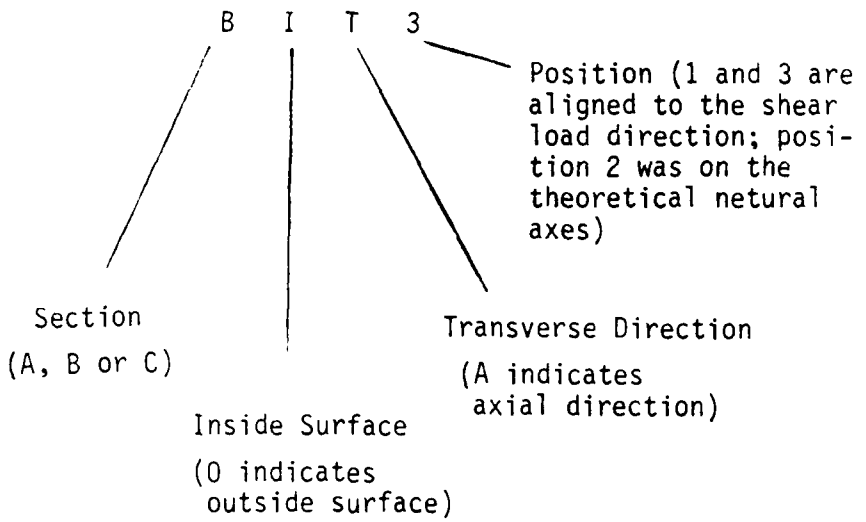

Compressive strains are shown positive.

Tests were performed for three loading conditions:

Static Axial Load

Dynamic Axial Load

Static Shear/Bend Load

A preliminary series of tests were undertaken with aluminum 6061-T6 frusta to evaluate the system performances prior to testing the boron/aluminum frusta.

4.1 Static Axial Loading: Aluminum Frustum

Load-time and selected load-strain curves for the static axial loading tests on aluminum frustum are shown in Appendix A. Response of gages AOA1, BOA1, and COA1, shown in Figure 4.1, conform with the elastic membrane theory predictions for loads to 100,000 lbs. Plasticity effects become pronounced at Section A for loads greater than 100,000 lbs. At 100,000 lbs load the calculated axial stress in the frustum at Section A is 36,000 psi as compared to the expected yield stress of 41,800 psi. From Figure 4.2 the ratio of the absolute values of the lateral strain to the axial strains in this load range is approximately 0.36, slightly higher than the expected Poisson's ratio for 6061-T6 aluminum. Section B shows a lesser degree of plastic flow prior to frusta failure. No plastic strain is obvious at Section C.

Bending effects become more pronounced at each gage location with increased load above 100,000 lbs as exhibited by the differences in strain through the wall thickness illustrated in Figures 4.3 and 4.4 for gages AOA1/AIA1 and AOA3/AIA3 respectively. The reversal in strain increments at AIA1 and AIA3 to those at AOA1 and AOA3 suggests the failure mode to be plastic buckling. Load at failure was 122,000 lbs. Figure 4.5 shows photographs of the failed frusta; a through-going fracture is seen to have formed at the buckled-plastic hinge. The three-lobed form in the failed region is clearly seen in the two photographs.

4.2 Dynamic Axial Loading: Aluminum Frustum

A maximum loading rate of 500,000 lb/sec was achieved during the dynamic, axial loading test on an aluminum frustum with failure occurring at 109,500 lbs. The lower failure load during the dynamic test results from the introduction of a bending component due to eccentricity. Load-time and strain-load

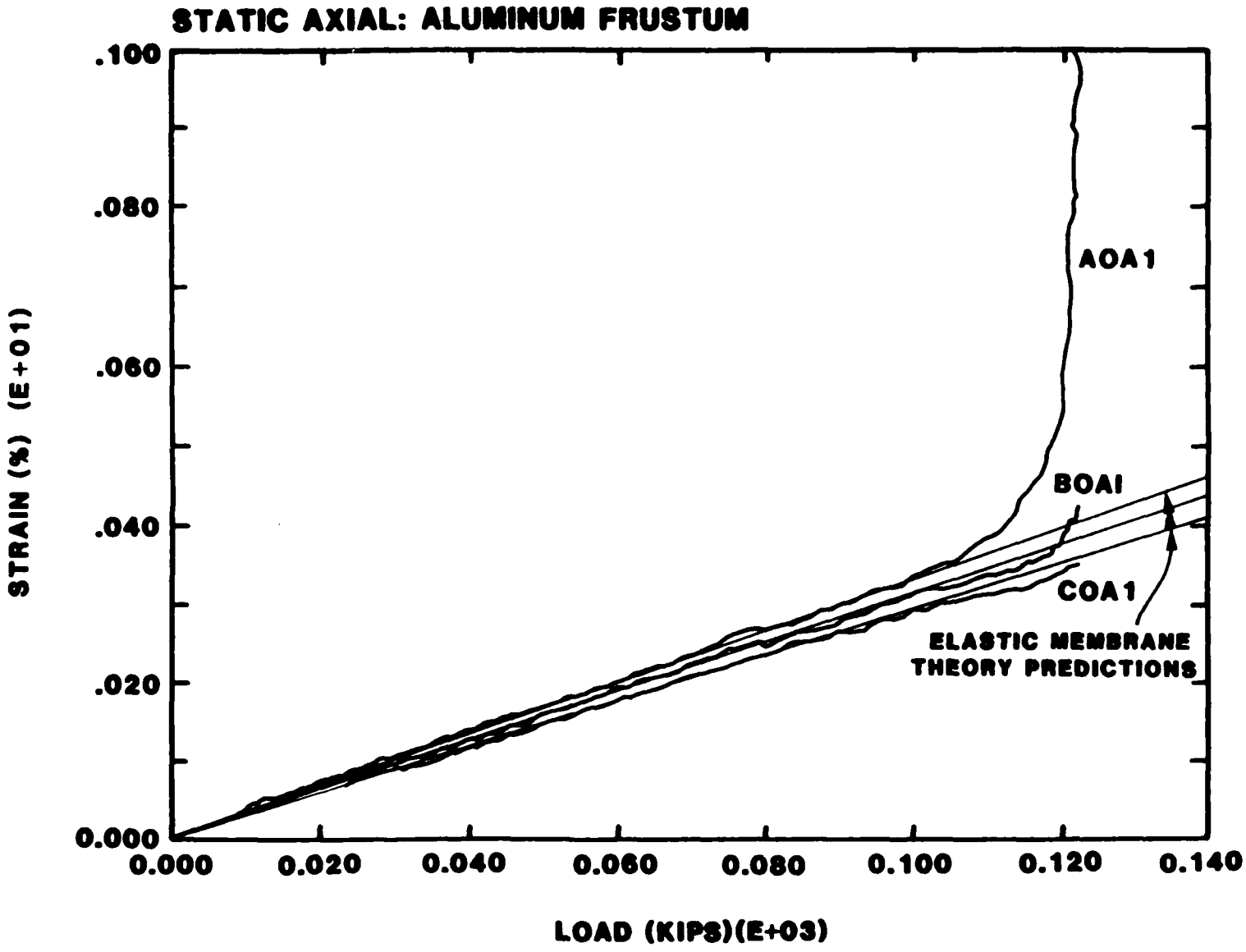

Figure 4.1. Response of Gages AOA1, BOA1, and COA1 on the Aluminum Frustum during Static Axial Loading. The straight lines are predictions based on Elastic Membrane Theory.

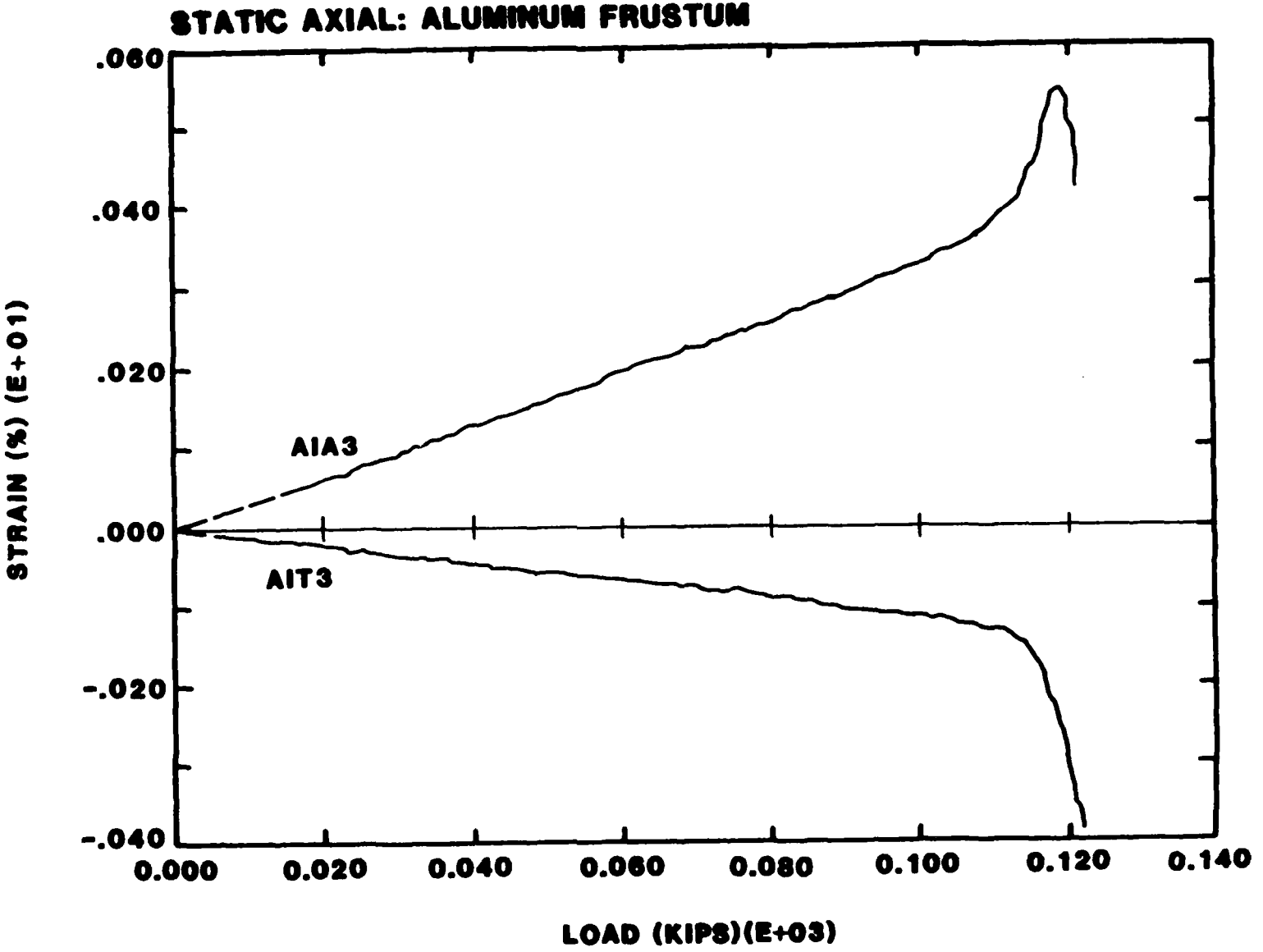

Figure 4.2. Axial and Lateral Strains at the Same Location (AIA3 and AIT3) on the Aluminum Frustum during Static Axial Loading.

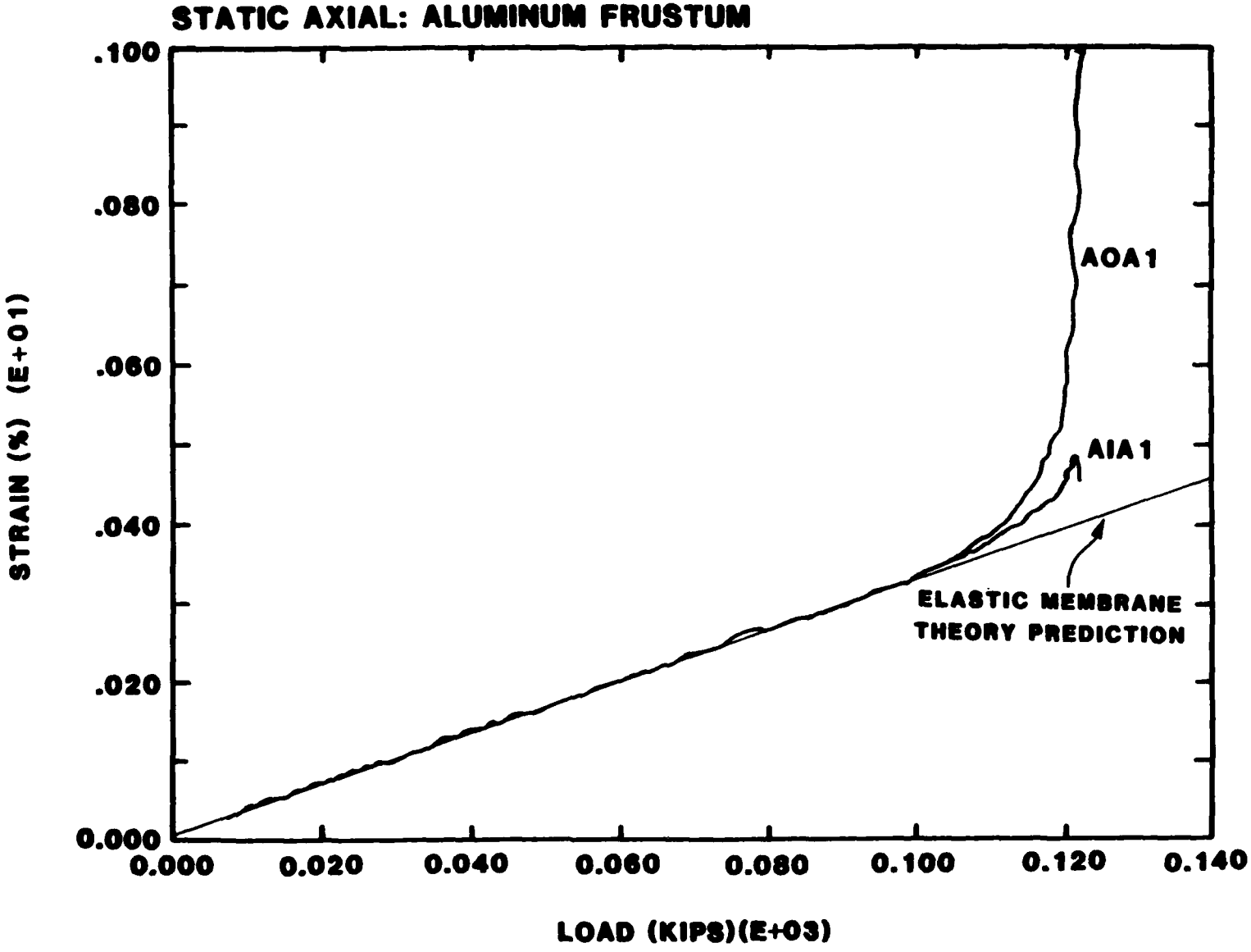

Figure 4.3. Comparison of the Response of Gages AOA1 and AIA1 on the Outside and Inside Surfaces of the Aluminum Frustum during Static and Axial Loading.

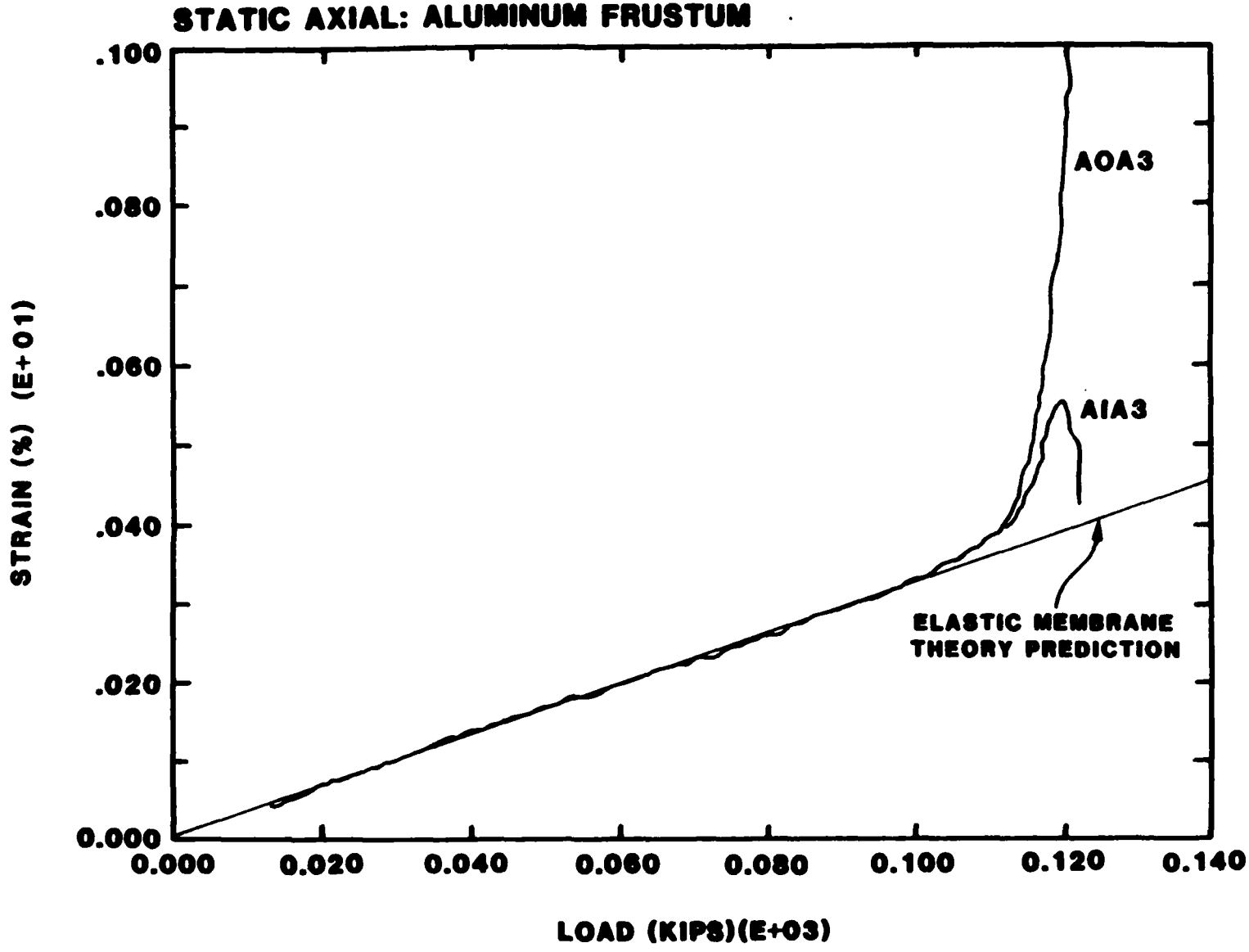

Figure 4.4. Comparison of the Response of Gages AOA3 and AIA3 on the Outside and Inside Surfaces of the Aluminum Frustum during Static Axial Loading.

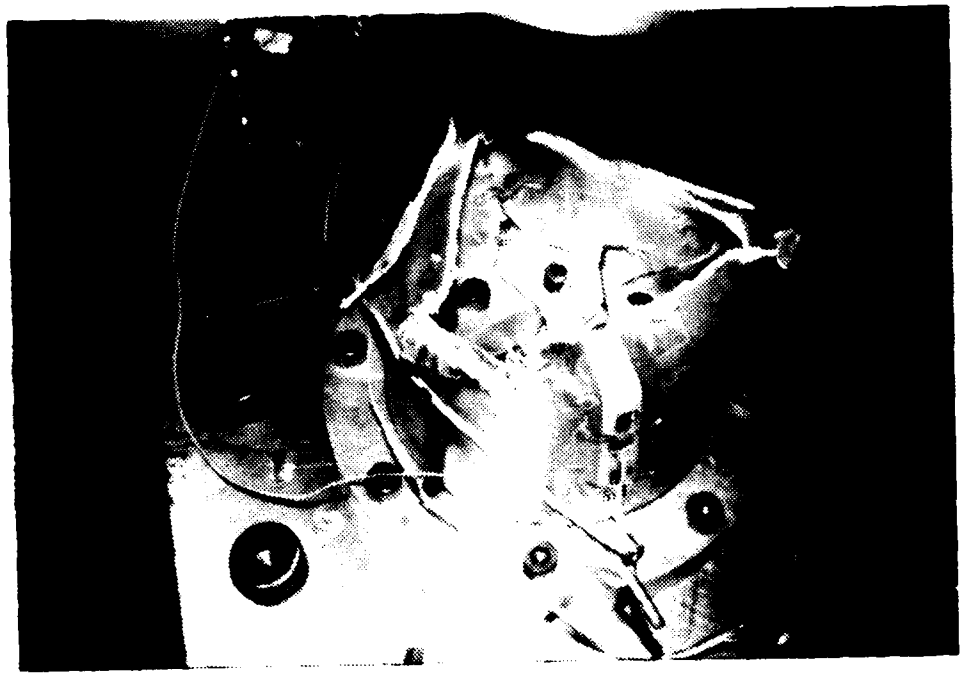

Figure 4.5a. Aluminum 6061-T6 Frustum after Failure under Static Axial Load. The upper clamp rings have been removed.

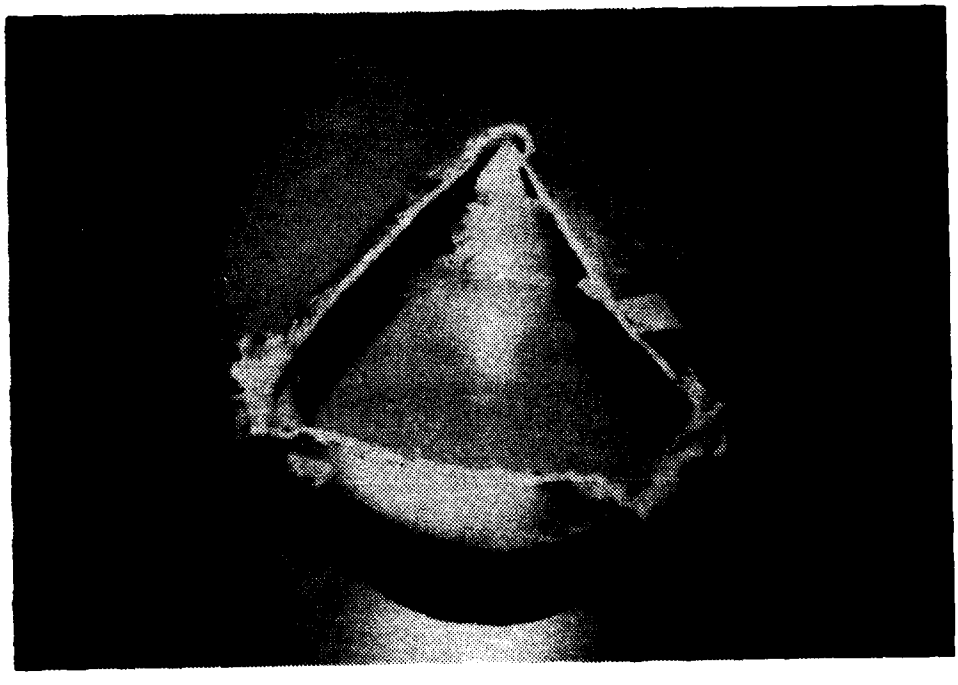

Figure 4.5b. Top View of the Aluminum 6061-T6 Frustum after Failure under Static Axial Load.

curves for the test are provided in Appendix B. Comparison of the load-strain response for gages AOA1 and AIA1 in Figure 4.6 shows the eccentric loading results in higher strains in the AOA1 and AIA1 gages. Between 40,000 lbs and 80,000 lbs axial load, the strain paths parallel the response predicted by elastic membrane theory. The effects of eccentric loading can be much better appreciated in the response of gages AIA1, AIA2, and AIA3 shown in Figure 4.7 and CIA1, CIA2 and CIA3 shown in Figure 4.8.

Figure 4.6 show negligible frustum wall bending at the AOA1/AIA1 location prior to the onset of yielding. Based on the divergence in the strains measured at AOA1 and AIA1, plastic buckling was the cause of failure. Figure 4.9 shows the failed frustum on removal from the test machine. A through-going fracture again developed at the plastic hinge. A second circumferential fracture, which was incompletely formed, can be seen below the A gages locations. The buckled shape shows a deviation from the three-lobed failure observed under static loading; the appearance is more of a five-lobed failure surface.

4.3 Shear/Bend Loading: Aluminum Frustum

Shear load was applied to the aluminum frustum as depicted in Figure 3.3. Gages #1 were on the theoretical bend axis nearest to the point of load application and in the region subjected to tensile bending stresses. Gages #3 were diametrically opposite to the Gages #1 and subjected to compressive stresses. Gages #2 were located at the theoretical neutral axis of the section. The load-time and selected strain-load curves for this test can be found in Appendix C.

Both the load-time and strain-load records were noisy. This is illustrated in Figure 4.10 for gage AOA1 which is in good agreement with elastic theory predictions to a load of 15,000 lbs. At higher loads the strain versus load becomes nonlinear. Figure 4.11 shows the strain recorded at the AIA2 gage

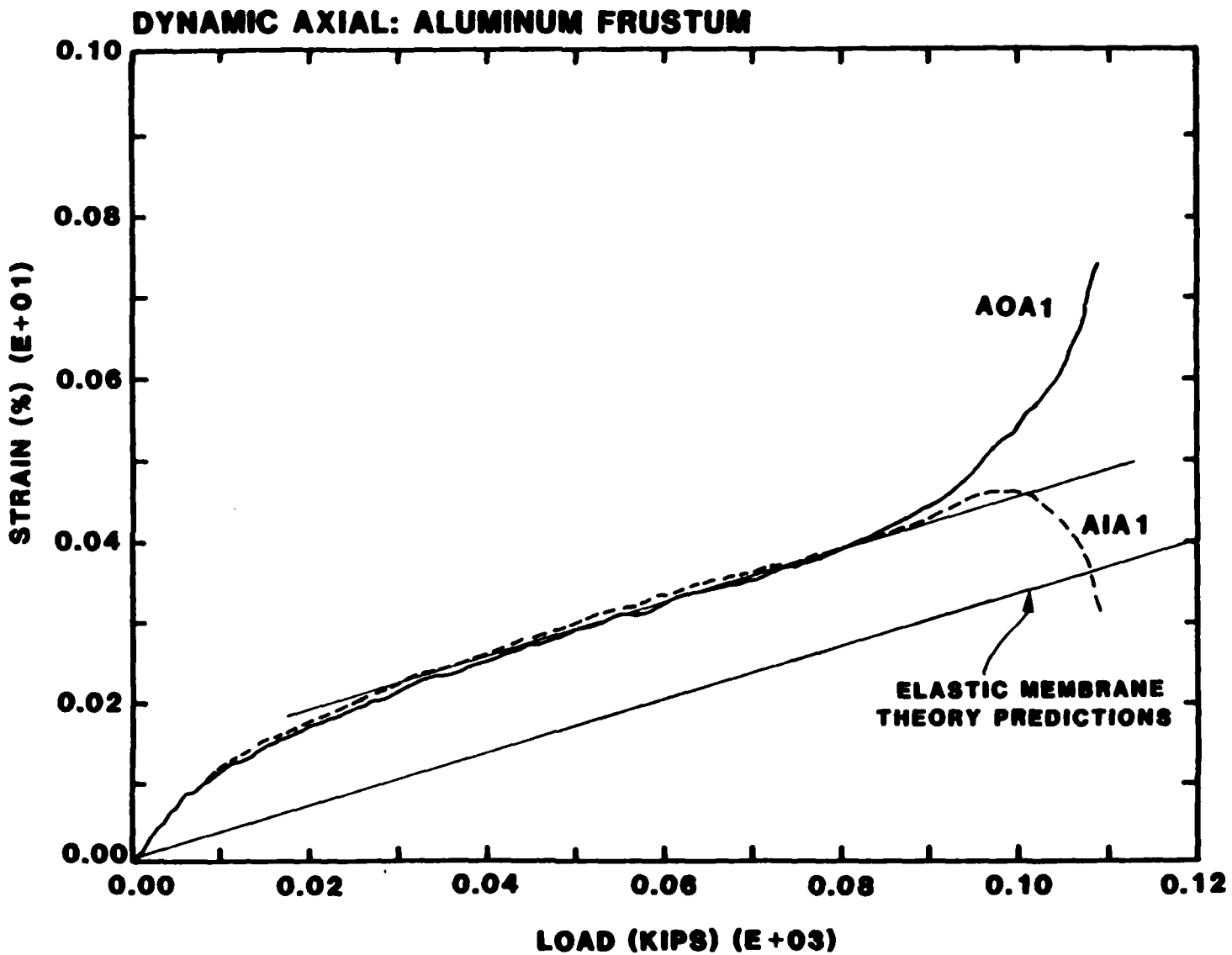

Figure 4.6. Response of Gages AOA1 and AIA1 on the Aluminum 6061-T6 Frustum during Dynamic Axial Loading. The straight line is the prediction based on Elastic Membrane Theory.

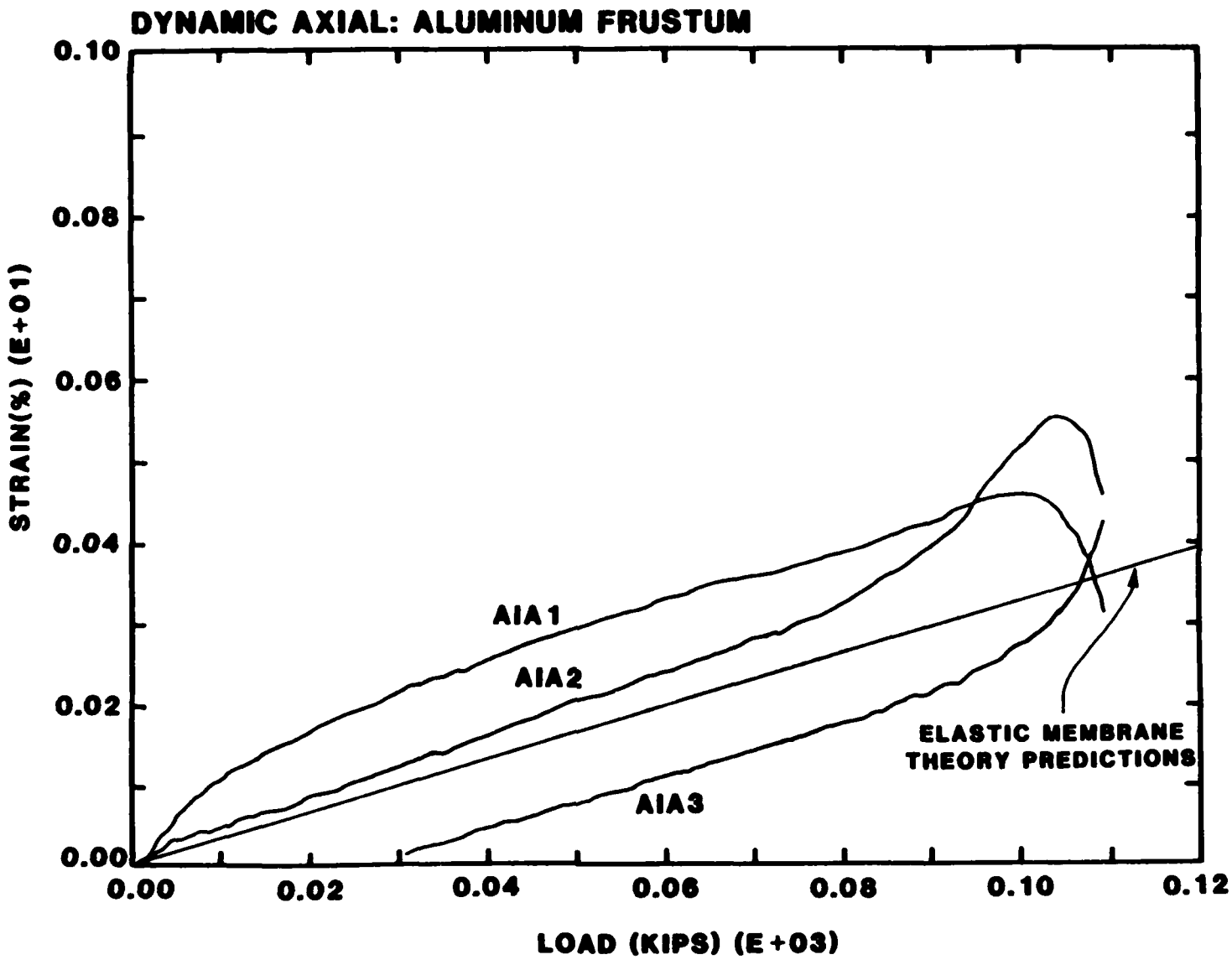

Figure 4.7. Response of Gages AIA1, AIA2, and AIA3 on the Aluminum Frustum during Dynamic Axial Loading. The straight line is the prediction based on Elastic Membrane Theory.

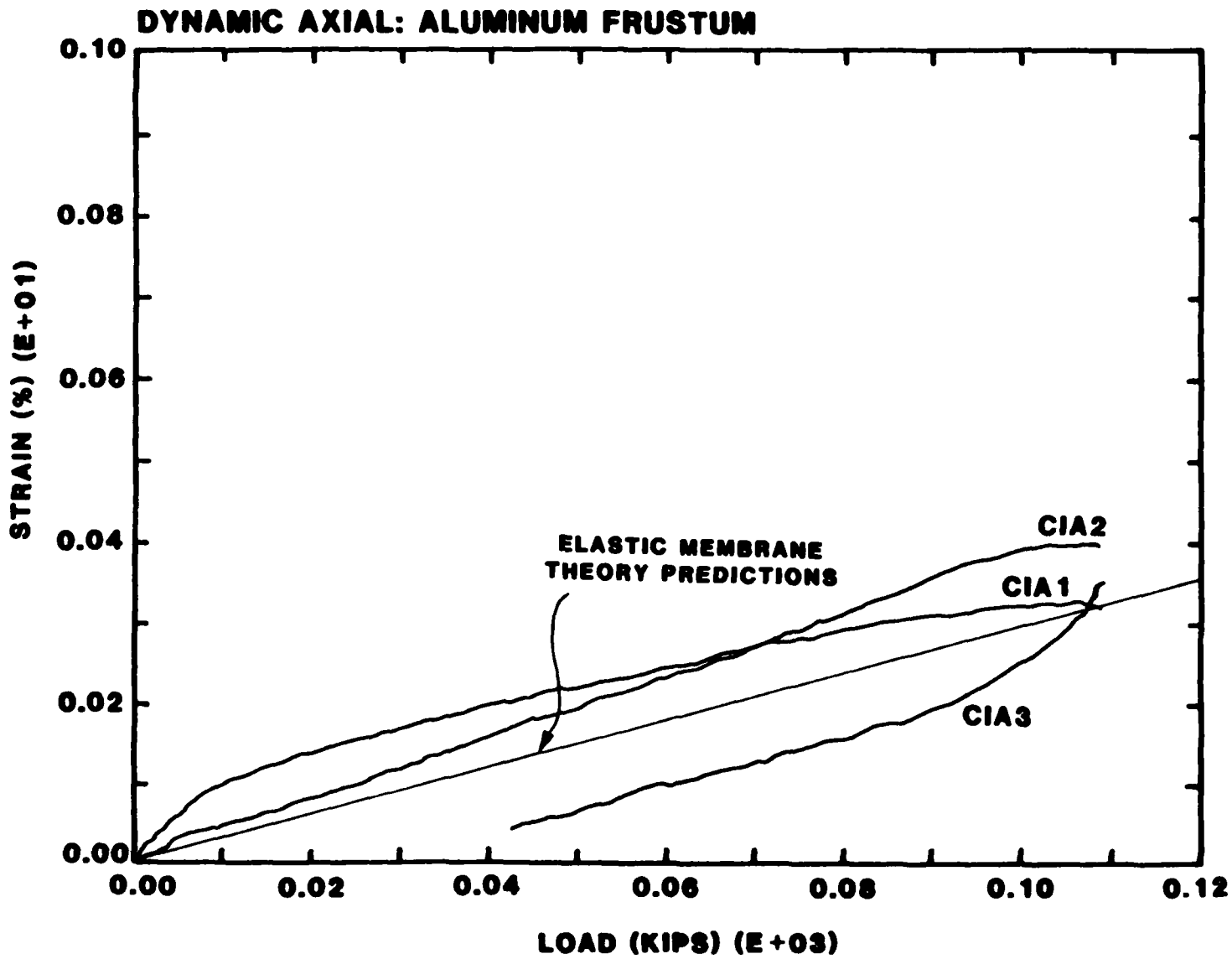

Figure 4.8. Response of Gages CIA1, CIA2, and CIA3 on the Aluminum 6061-T6 Frustum during Dynamic Axial Loading. The straight line is the predicted response based on Elastic Membrane Theory.

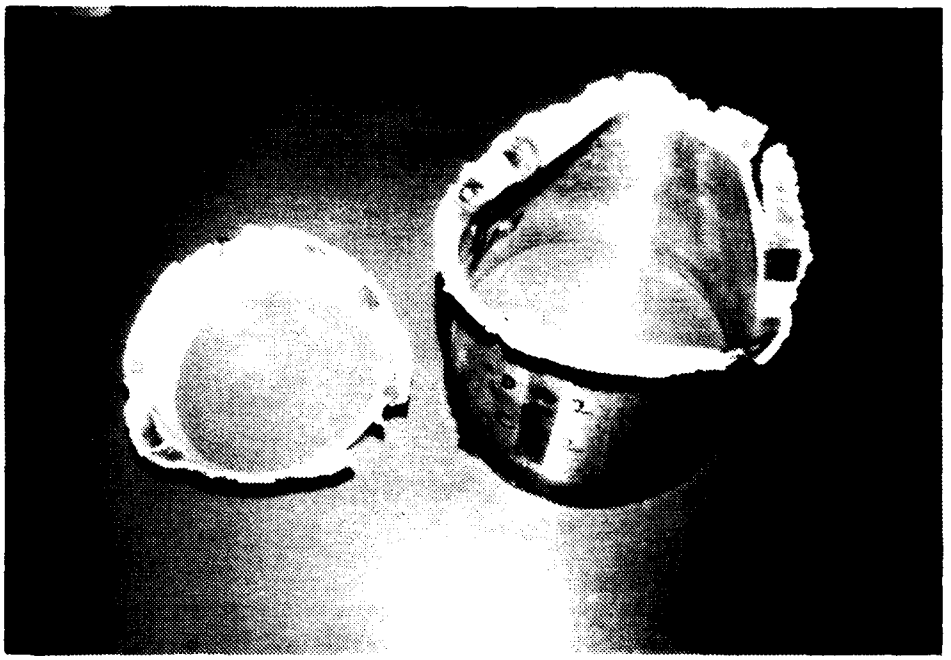

Figure 4.9. Top View of the Aluminum 6061-T6 Frustum after Failure under Dynamic Axial Load.

on the theoretical neutral axis of Section A. The strain is zero for shear loads to 20,000 lbs; however, it increases rapidly with increasing shear loads.

The higher stresses occur at Section C under shear/bending. The calculated maximum stress at Section C for 20,000 lbs shear load is 25,500 psi which is much lower than the yield stress for 6061-T6 aluminum ($\sim$ 41,800 psi). Failure, therefore, resulted from elastic buckling at 23,250 lbs shear load. The corresponding bending moment at the base/bond interface was 202,600 in lbs.

4.4 Static Axial Loading: Boron/Aluminum Frustum

The load-time and selected load-strain data for the static axial load response of the boron/aluminum frustum are shown in Appendix D. There are three distinct regions to each curve. These regions can be selected from close evaluation of Figure 4.12, 4.13 and 4.14. For the initial 100,000 lb load the strains are in good agreement with predictions based on linear

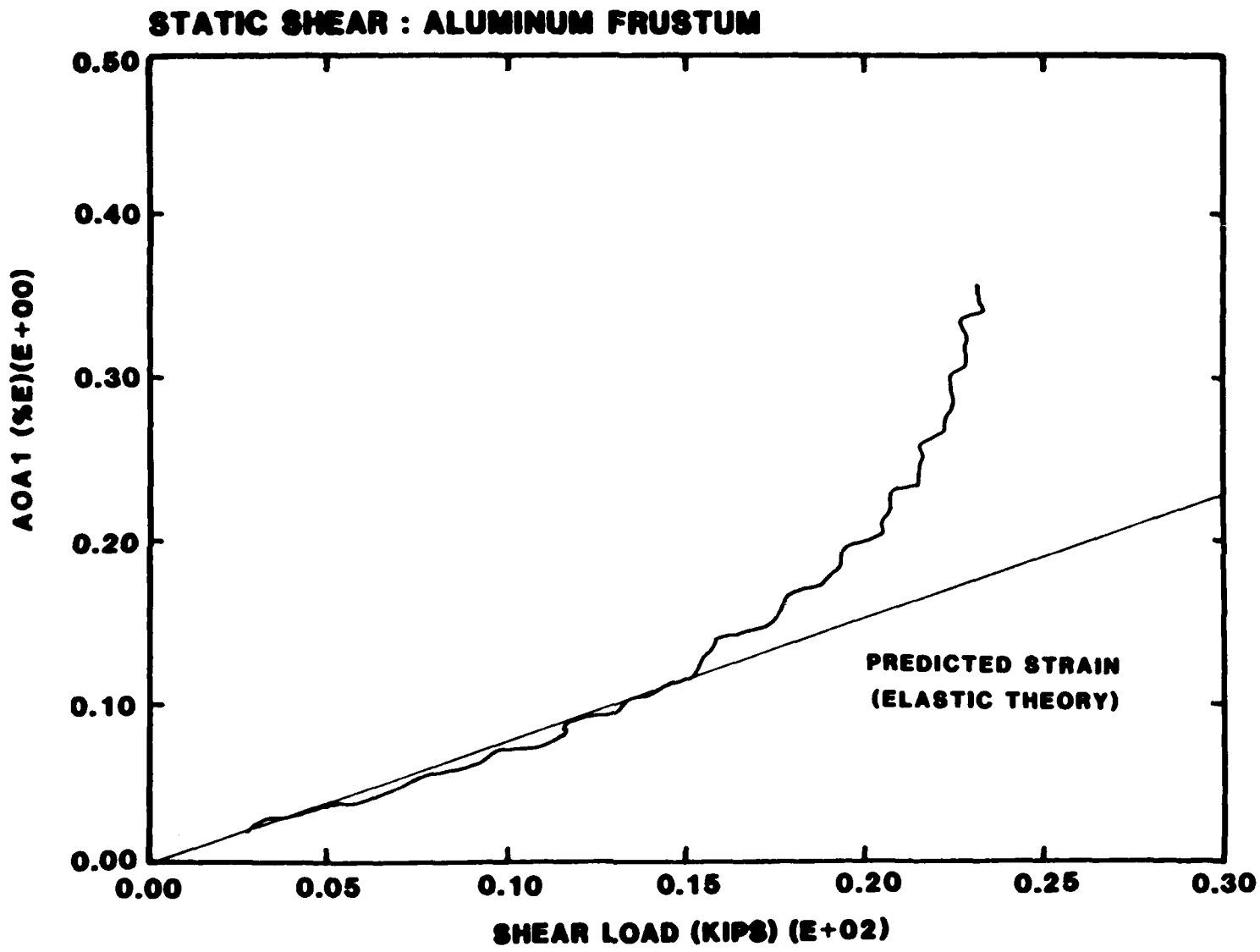

Figure 4.10. Strains Recorded at Gage AOA1 on the Aluminum Frustum during Shear/Bend Loading.

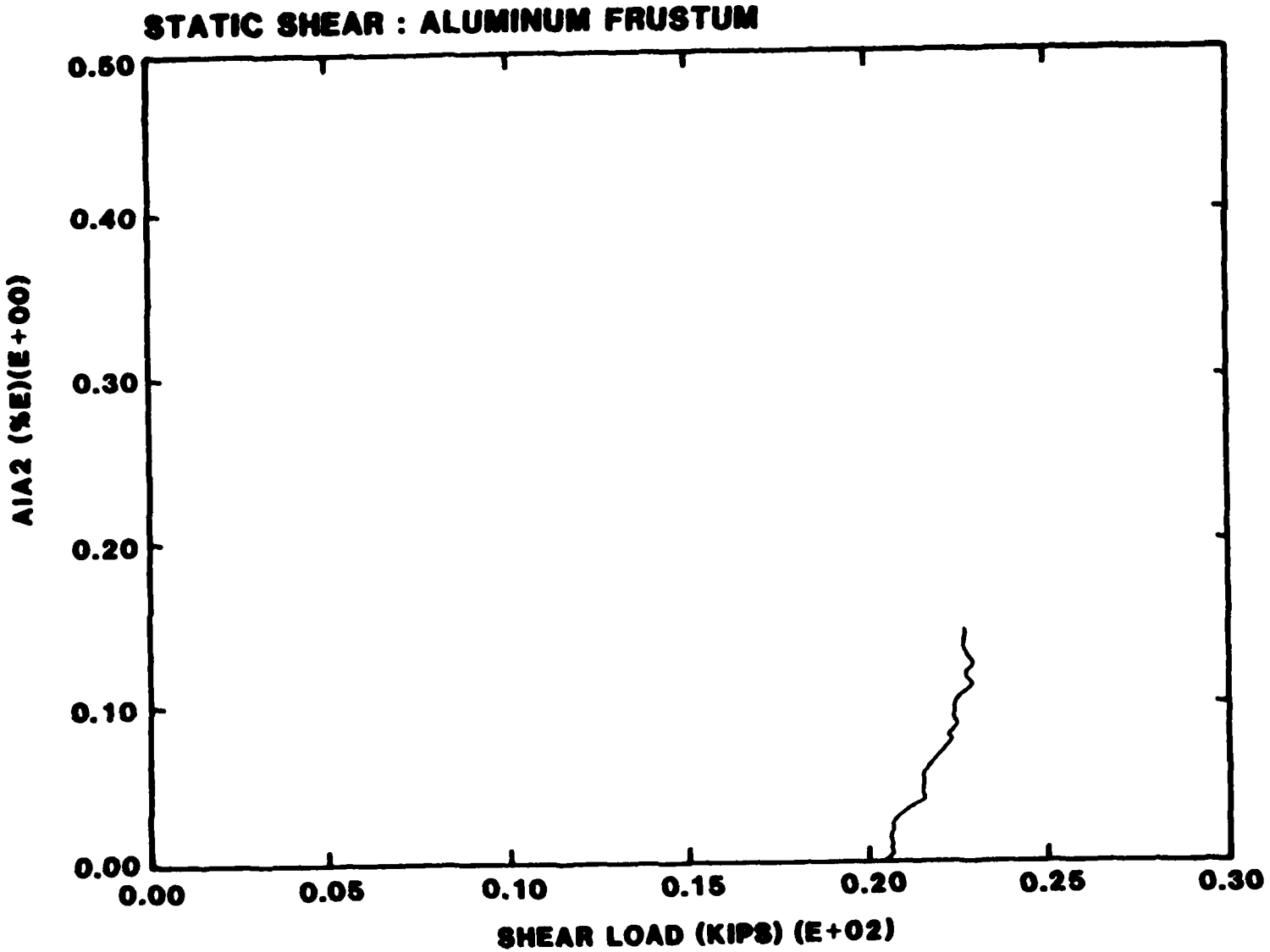

Figure 4.11. Strains Recorded by Gage AIA2 on the Theoretical Neutral Axis on the Aluminum Frustum during Shear/Bend Loading.

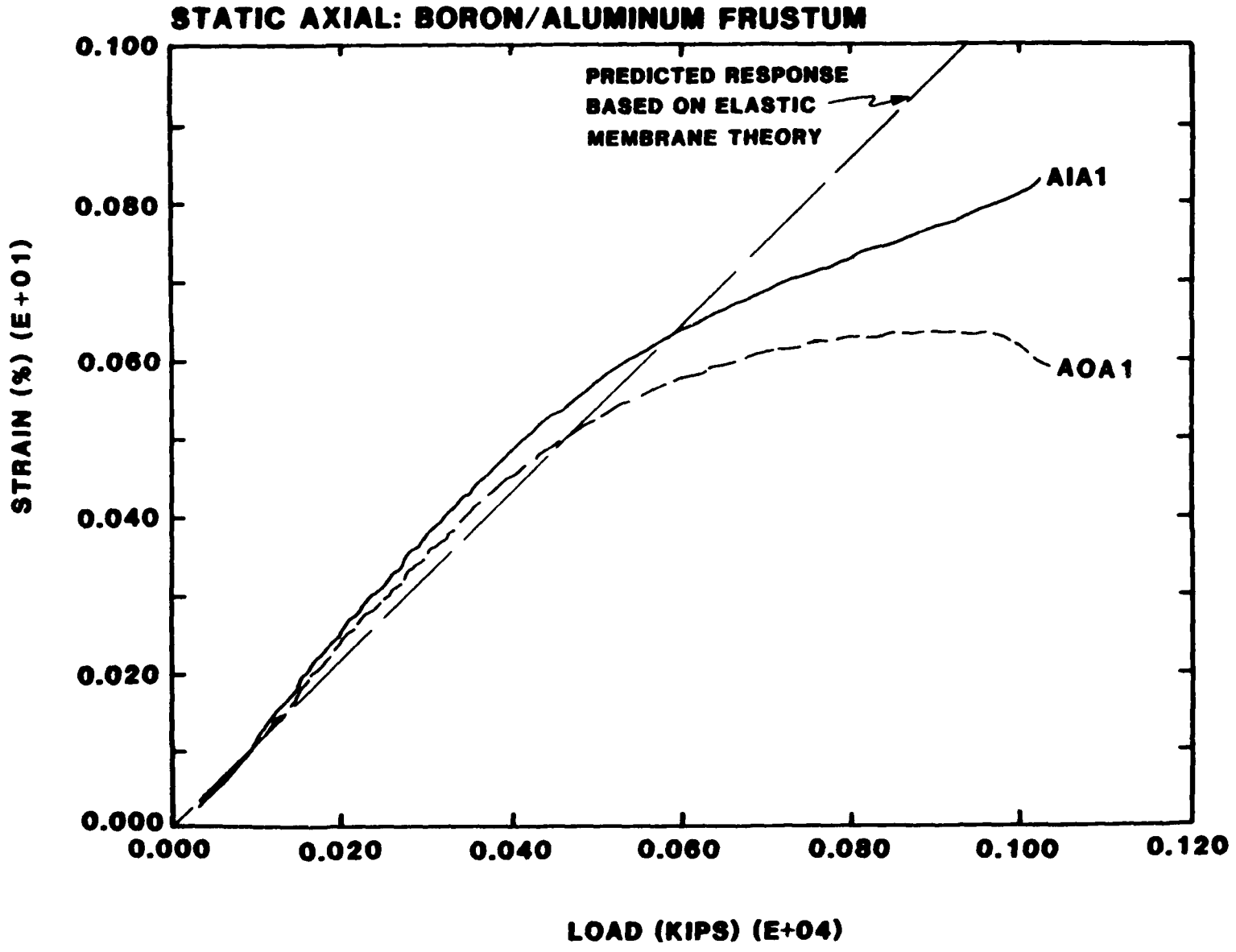

Figure 4.12. Response of Gages AOA1 and AIA1 on the Boron/Aluminum Frustum during Static Axial Loading. Gages' response is compared to the Elastic Membrane Theory Predictions. Note the measured load is in error above 400,000 lbs. Actual load at failure is estimated to be 600,000 lbs to 700,000 lbs.

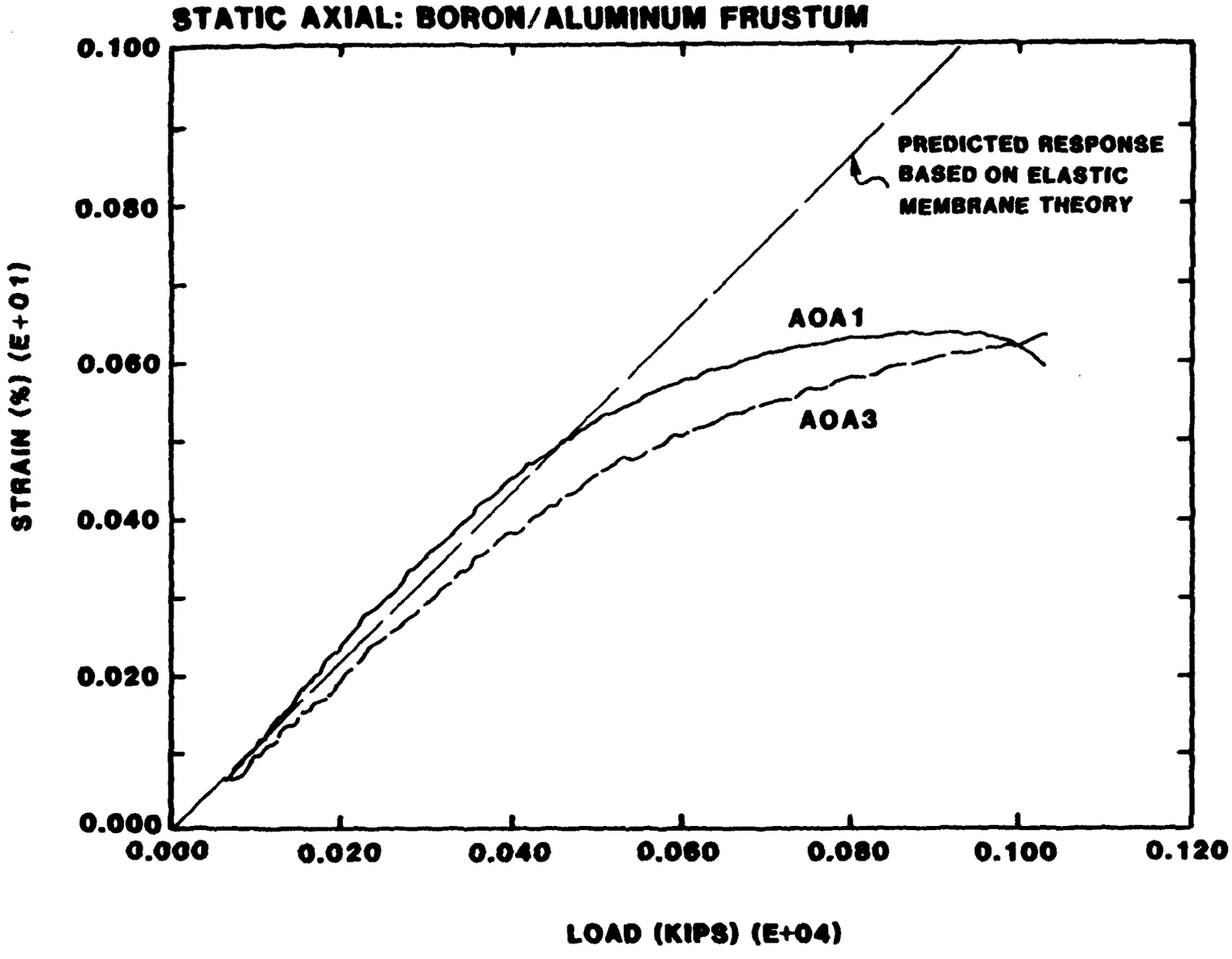

Figure 4.13. Response of Gages AOA1 and AOA3 on the Boron/Aluminum Frustum during Static Axial Loading. Gages' response is compared to the Elastic Membrane Theory Predictions. Note the measured load is in error above 400,000 lbs. Actual load at failure is estimated to be 600,000 lbs to 700,000 lbs.

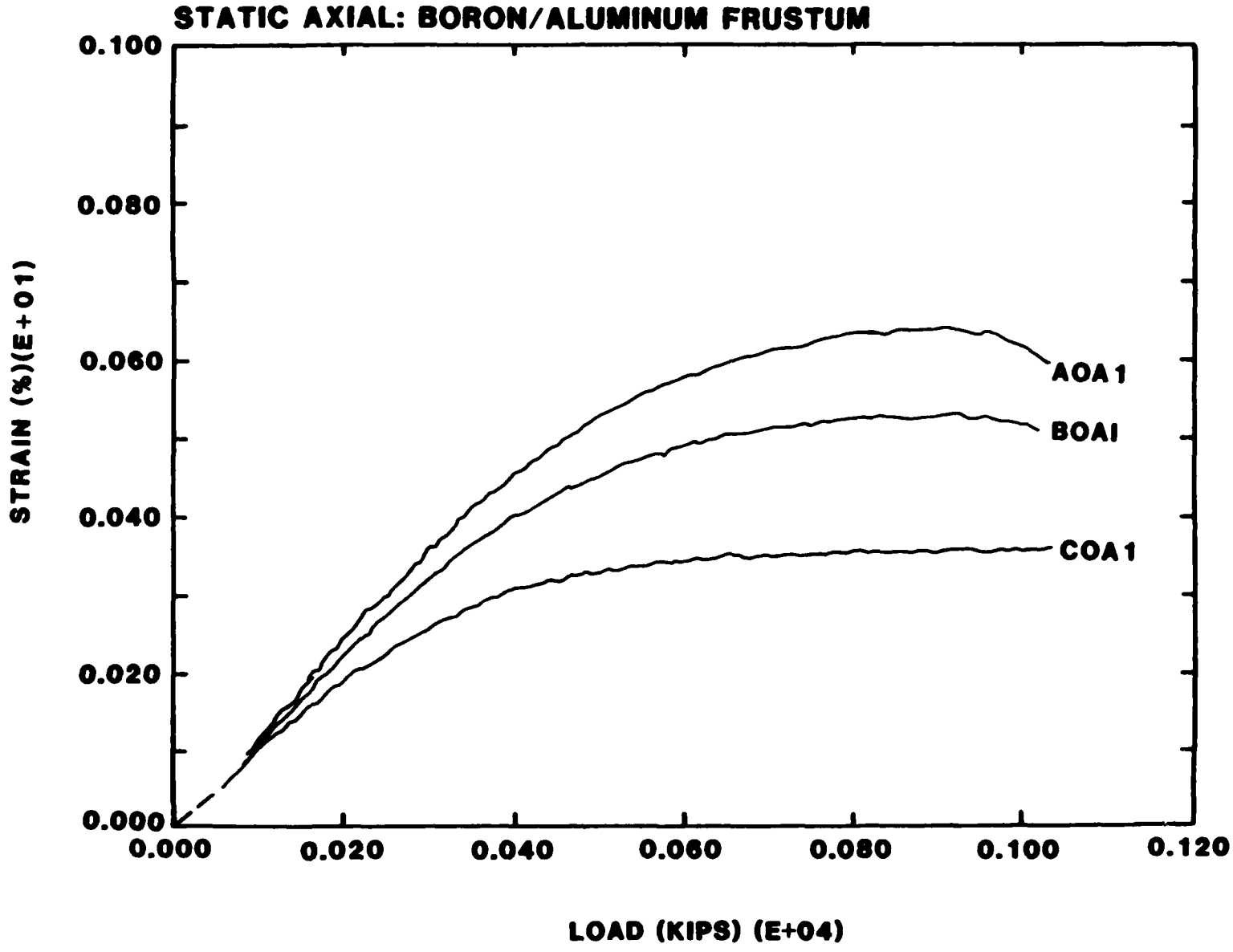

Figure 4.14. Response of Gages AOA1, BOA1, and COA1 on the Boron/Aluminum Frustum during Static Axial Loading. Note the measured load is in error above 400,000 lbs. Actual load at failure is estimated to be 600,000 lbs to 700,000 lbs.

elastic membrane theory. A small bending load appears to have been introduced at higher loads. Figures 4.12 and 4.13 show the bending imposes larger compressive stress in Gages #1. There is a corresponding lowering of the compressive stress in Gages #3 as seen in Figure 4.13. In addition, the nonlinearity in all the load-strain curves above 400,000 lbs results from plastic failure of the load cell. Assuming a linear stress-strain curve to failure for the boron/aluminum the actual failure strength lies in the range 600,000 lbs to 700,000 lbs.

Failure mode was buckling in the vicinity of Section A as seen by the trends for gages AOA1 and AIA1 in Figure 4.12. A photograph of the failed boron/aluminum frustum is seen in Figure 4.15. The lower portion of the frustum appears to be intact.

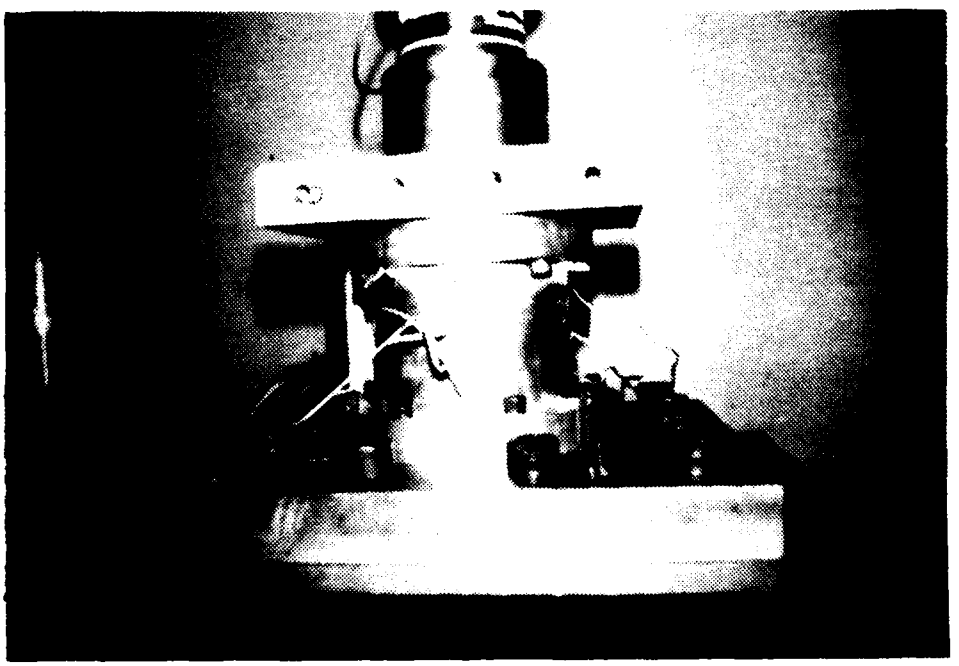

Figure 4.15. Photograph of the Failed Boron/Aluminum Frustum. Axial failure load was estimated to be between 600,000 lbs and 700,000 lbs.

During this test the boron/aluminum punched into both the upper and lower steel base plates. Prior to reuse, the grooves were filled with stellite, an extremely hard surfacing steel, and refinished.

4.5 Dynamic Axial Loading: Boron/Aluminum Frustum

A loading rate of 1,200,000 lbs/sec was achieved during the test. The test was completed in approximately 0.5 seconds with the frustum failing in a brittle manner at 519,000 lbs, significantly lower than in the static loading test.

Load-time and selected load-strain curves for the test are provided in Appendix E. Strains measured at Gages #3 on Sections A, B and C are in good agreement with elastic membrane theory predictions throughout the test to failure, as seen in Figures 4.16 and 4.17, with little bending through the frustum wall. On the other hand, Gages #1 at Sections A, B and C (Figure 4.18) show a nonlinear strain response to load. Compared to elastic membrane theory predictions the measured strains at AOA1 are higher. Lower strains are measured than predicted at COA1. Gages AOA1 and AIA1 data in Figure 4.19 show significant bending through the frustum wall. Localized inhomogenieties at Gages #1 locations (e.g. gore segment overlap) may be a possible cause for the observed data and premature frustum failure.

Punching by the frusta into the upper and lower plattens occurred as in the static test. However, the punch depth was significantly reduced for the dynamic tests.

4.6 Shear/Bend Loading: Boron/Aluminum Frustum

The shear/bend load test condition is shown schematically in Figure 3.2. Shear load was applied at the forward end resulting in maximum bending moment at the base end. Gages #1 were on the theoretical bend axis nearest to the point of load application and in the region subjected to tensile stresses

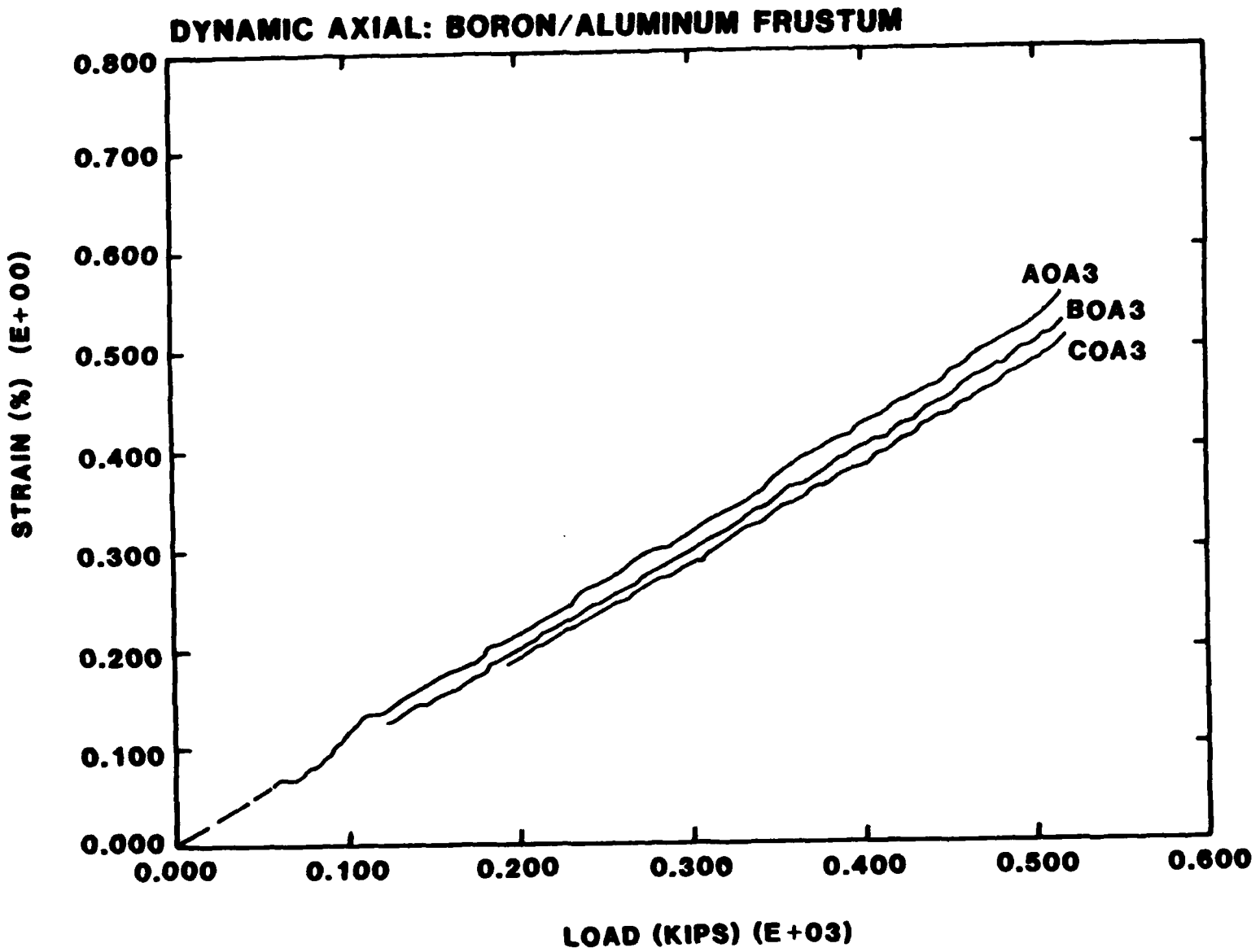

Figure 4.16. Response of Gages AOA3, BOA3, and COA3 on the Boron/Aluminum Frustum during Dynamic Axial Loading.

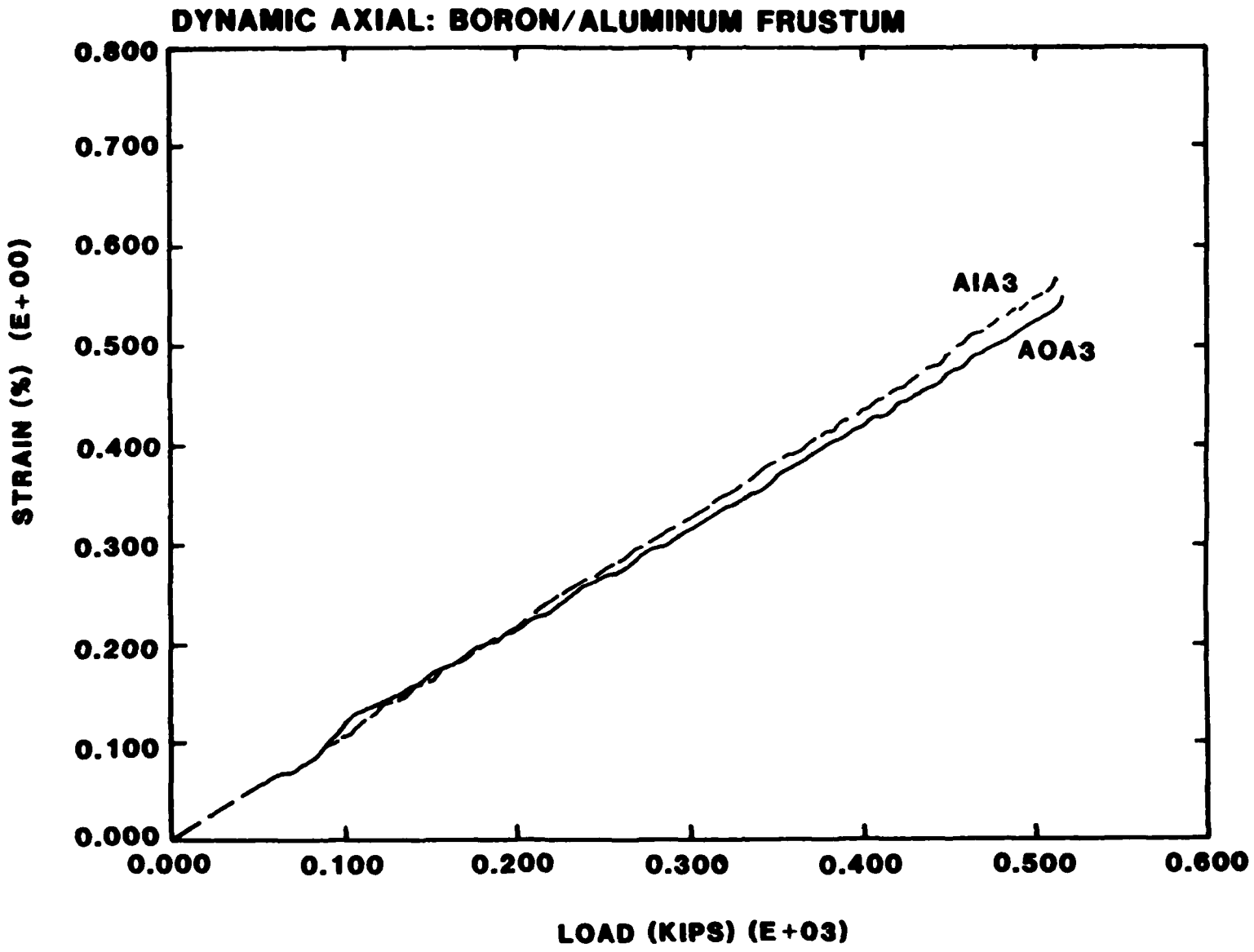

Figure 4.17. Response of Gages AOA3 and AIA3 on the Boron/Aluminum Frustum during Dynamic Axial Loading.

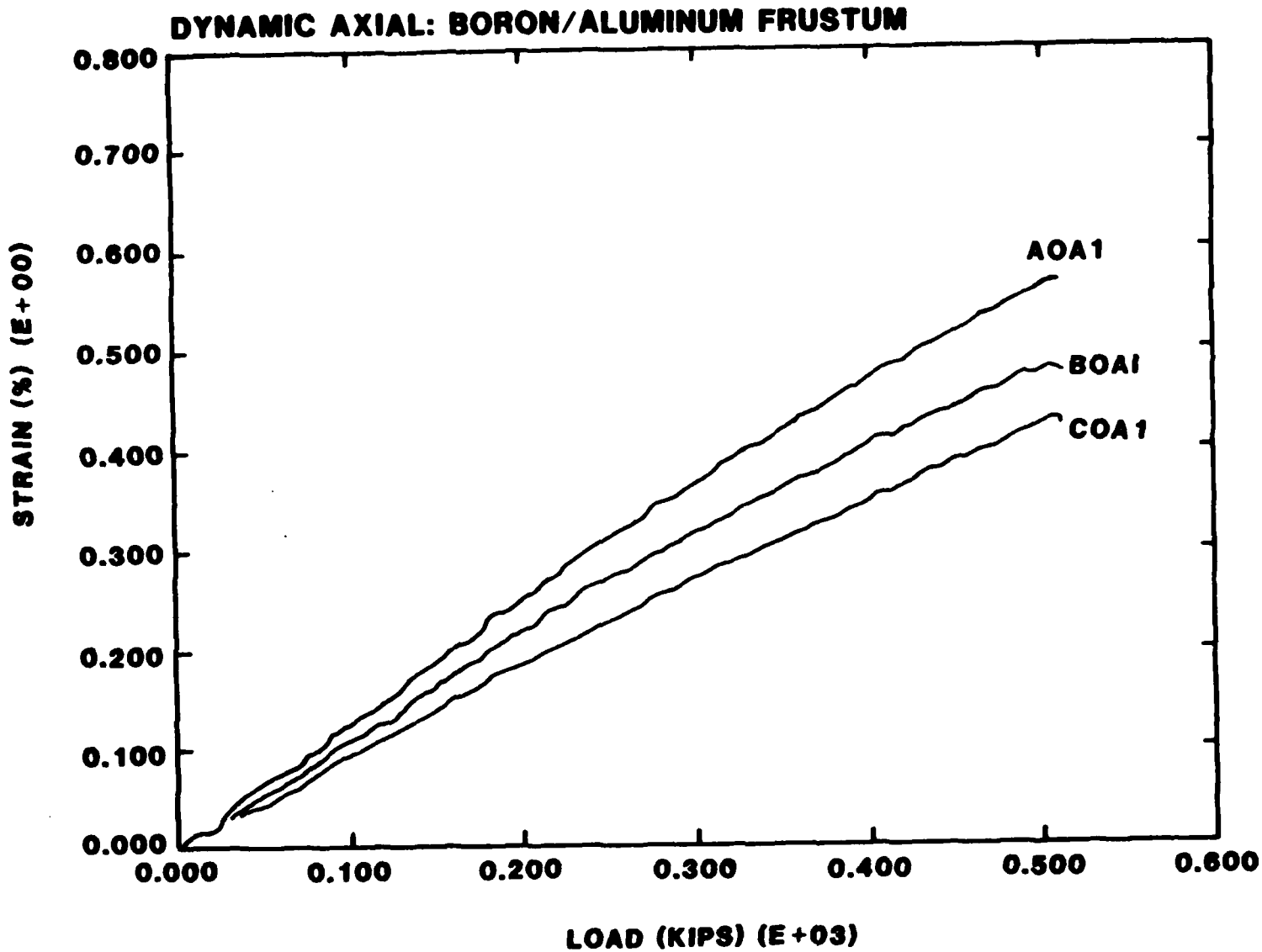

Figure 4.18. Response of Gages AOA1, BOA1, and COA1 on the Boron/Aluminum Frustum during Dynamic Axial Loading.

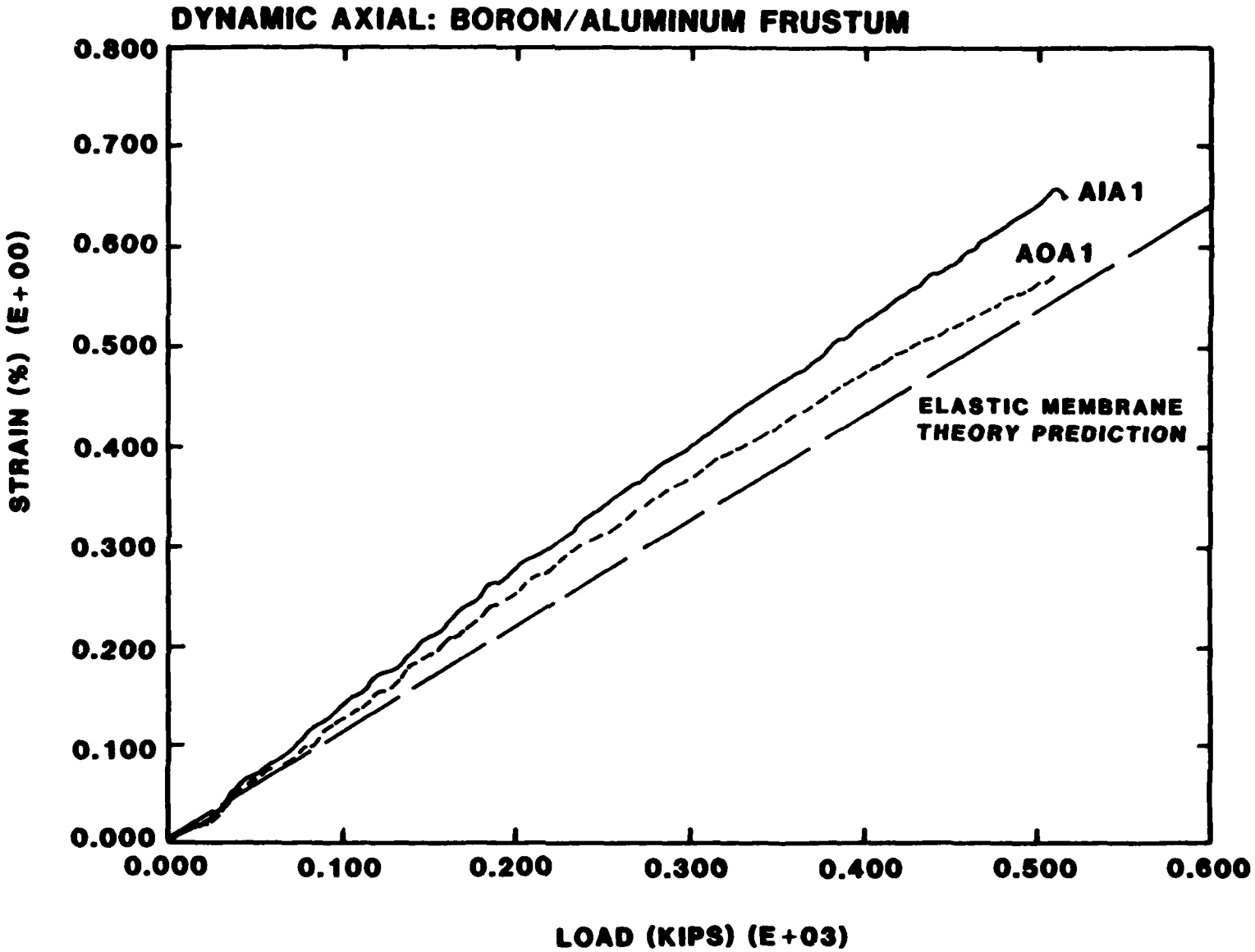

Figure 4.19. Response of Gages AOA1 and AIA1 on the Boron/Aluminum Frustum during Dynamic Axial Loading.

during bending. Gages #3 were diametrically opposite Gages #1 and are consequently subject to compressive stresses. Gages #2 were located on the theoretical neutral axis of the section.

Load-time and selected load-strain curves for the shear/bend loading test with the boron/aluminum frustum are provided in Appendix F. As in the shear/-bend loading test on the aluminum 6061-T6, the load and strain data are extremely noisy. Figure 4.20 shows the measured strains at locations AOA1 and BOA1. The measured strains compare favorably to predictions based on linear elastic theory for shear loads to approximately 28,000 lbs. A nonlinear load-strain response is observed beyond 28,000 lbs. Failure occurred at 44,000 lbs. Calculated maximum bending moment at the fixed base at failure was 383,300 in-lbs with failure occurring at the ring to frustum bondline. The result is compared to the data obtained by General Dynamics (Reference 4) in Table 4.1. Bending moment at failure determined in the present test program is

Table 4.1. Boron/Aluminum Frustum Test Results for Shear/Bend Loading

Test Results	Failure Mode	Reference
44,100 lbs 427,700 in-lbs	Shear Failure	Ref. 4
43,300 lbs 420,000 in-lbs	Bond Failure	Ref. 4
48,000 lbs 465,600 in-lbs	Bond Failure	Ref. 4
44,000 lbs 383,300 in-lbs	Bond Failure	This Work

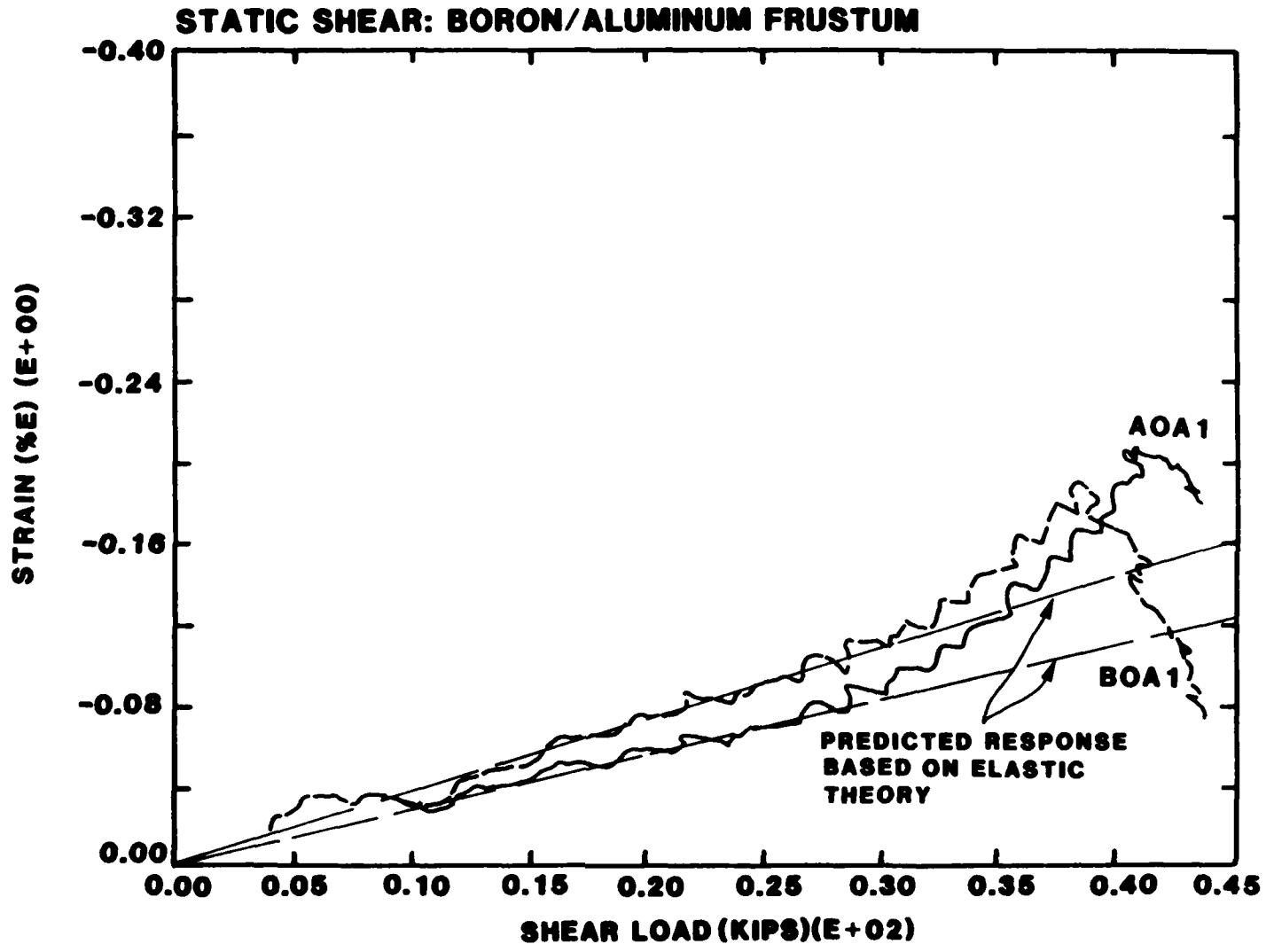

Figure 4.20. Response of Gages AOA1 and BOA1 on the Boron/Aluminum Frustum during Shear/Bend Loading. Measured responses are compared to predicted responses based on Elastic Membrane Theory.

approximately 10 to 20 percent lower than the average value of the data reported in Reference 4.

4.7 Discussion of Results

The data obtained here has been plotted, along with the data from Reference 4, in a load interaction curve of axial load versus bending moment (Figure 4.21). The plot shows that the frusta far exceeds all design strength requirements (designated DLL in Figure 4.21).

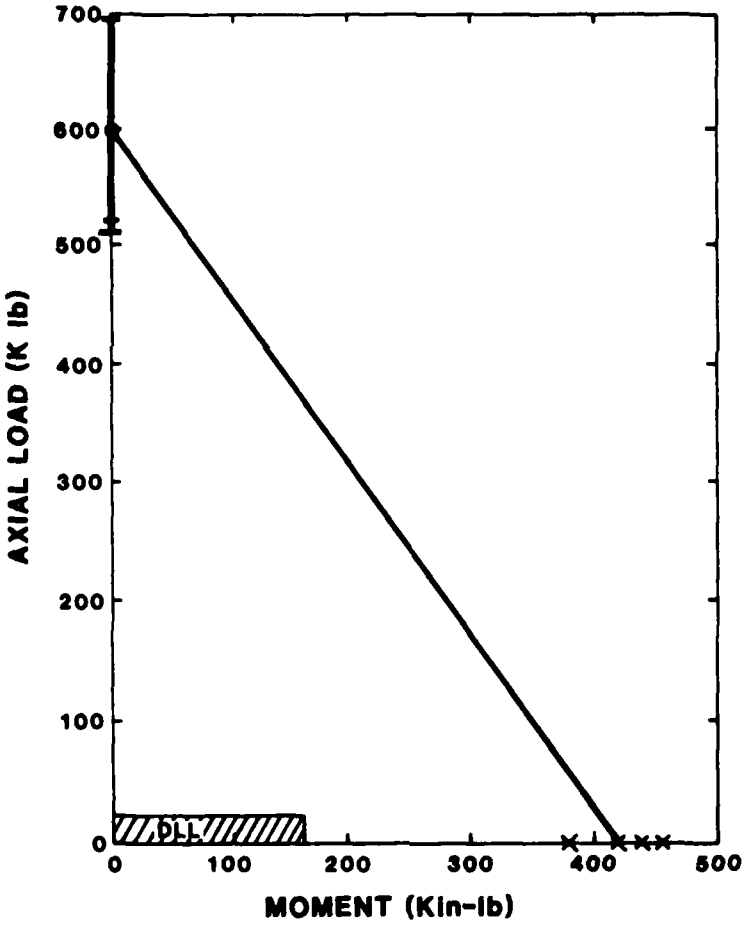

Figure 4.21. Load Interaction Curve for the Boron/Aluminum Frusta.

5. SUMMARY AND CONCLUSIONS

The following briefly summarizes the work performed under the contract and the conclusions based on results of the structural testing of the half-scale boron/aluminum frusta:

1. The 1.7 million pound load frame at Terra Tek was successfully modified to load a truncated, conical frustum in axial compression, shear/bend and pure bending. Accumulators were placed in close promixity to all actuators to provide the needed oil flow for performing dynamic tests.
2. A fifty channel data acquisition system was tied to a DEC PDP 11-34 computer via a Soundstream 14 bit A/D convertor for real-time monitoring of the tests.
3. Three aluminum 6061-T6 frusta were tested, two under static loading conditions and one at high rate of loading, to verify the systems operations.
4. Under static, axial loading, failure of boron/aluminum frustum occurred by buckling near the forward end.
5. Failure of the boron/aluminum frustum under dynamic axial load appears to have been influenced by local inhomogeniety. Seams, resulting from gore pattern layup, is a possible cause for the inhomogeniety.
6. Under shear/bend loading, failure of the boron/aluminum frustum occurred at the large end at a shear load of 44,000 lbs. The corresponding bending moment at the base calculates to 383,300 in-lbs.

7. The result of the shear/bend loading test for the boron/aluminum frustum is in good agreement with results reported earlier by General Dynamics (Reference 4).
8. The load interaction curve of axial load versus bending shows the boron/aluminum frusta strength far exceed design requirements.
9. Further investigation should be undertaken to evaluate the effects of surface flaws due to manufacturing processes on the stiffness, deformation and failure of the boron/aluminum frusta.

6. REFERENCES

1. Adsit, N. R. and Hertz, J.; "Development of Advanced Interceptor Substructural Material"; General Dynamics Convair Division, AMMRC TR 81-31, July 1981.

2. Hertz, J. and Adsit, N. R.; "Development of Advanced Interceptor Substructural Material"; General Dynamics Convair Division, AMMRC TR 80-44, August 1980.

3. Weisinger, M. D.; "Design and Fabrication of Boron/Aluminum Frusta", General Dynamics Convair Division, AMMRC TR 81-43, September 1981.

4. Adsit, N. R. and Weisinger, M. D.; "Design, Fabrication and Testing of Boron/Aluminum Frusta"; General Dynamics Convair Division, AMMRC TR 80-40, August 1980.

5. Kreider, K. G., Dardi, L. and Prewo, K.; "Metal Matrix Composite Technology"; United Aircraft Research Lab, AFML-TR-71-204, 1971.

6. Koo, F. H. and Seinberg, J. P.; "Subscale Development of Advanced ABM Graphite/Epoxy Composite Structure"; Martin Marietta Corporation (Orlando Division), AMMRC TR 78-4, January 1978.

7. APPENDICES

7.1 APPENDIX A

STATIC-AXIAL LOADING TEST DATA
FOR ALUMINUM FRUSTA

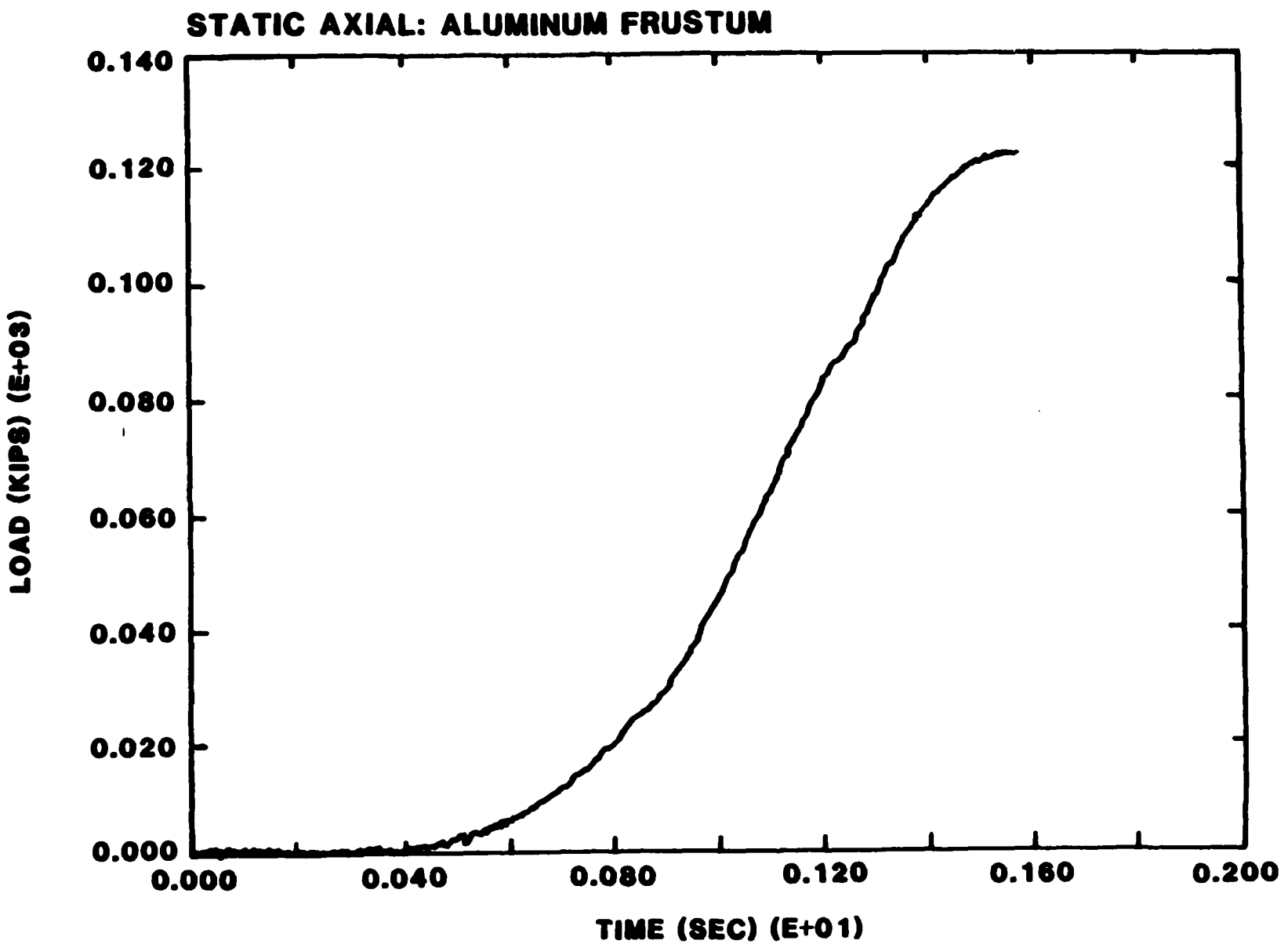
STATIC AXIAL: ALUMINUM FRUSTUM
LOAD (KIPS) (E+03)
0.140
0.120
0.100
0.080
0.060
0.040
0.020
0.000
0.000
0.040
0.080
0.120
0.160
0.200
TIME (SEC) (E+01)

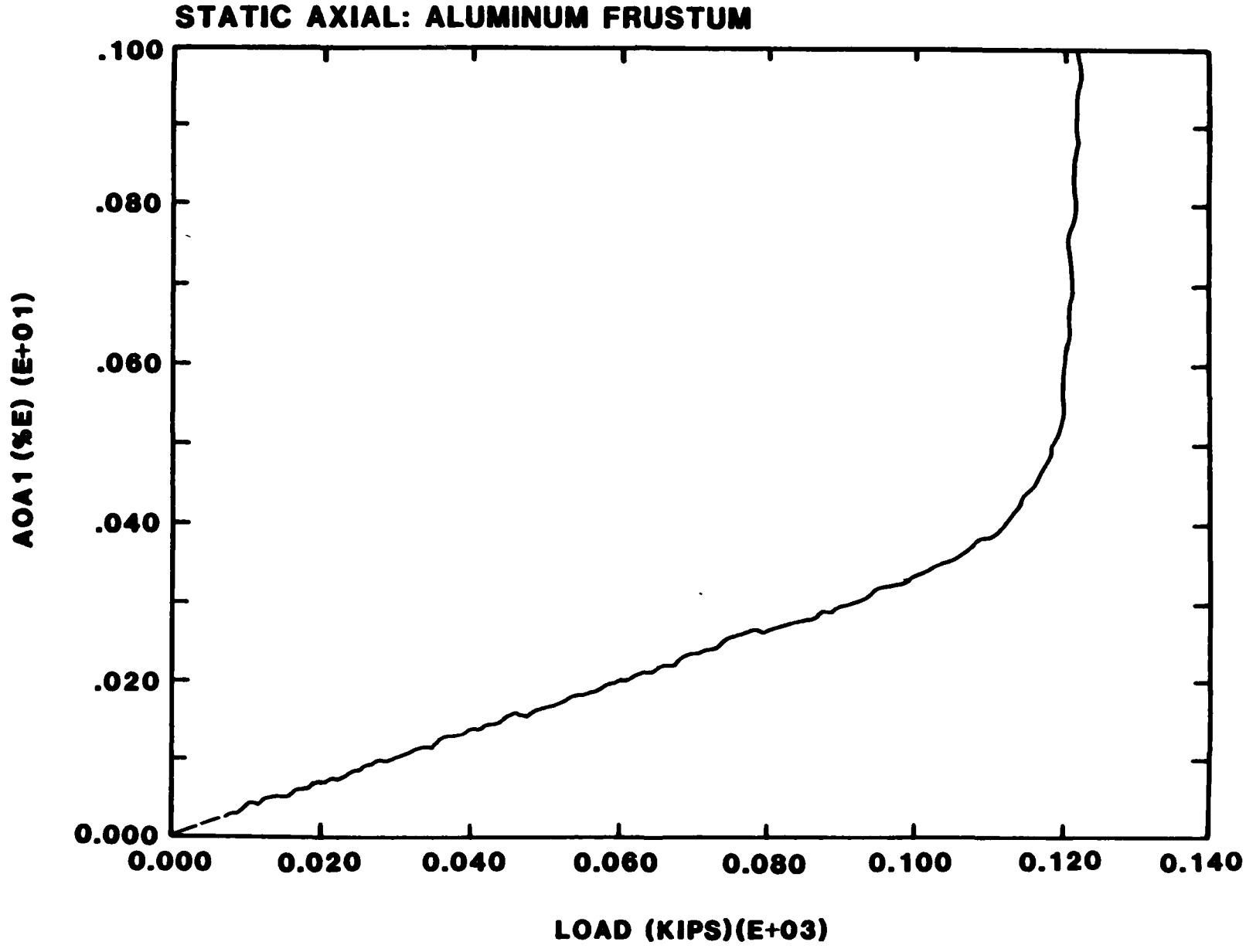
STATIC AXIAL: ALUMINUM FRUSTUM
.100
.080
.060
.040
.020
0.000
AOA1 (%E) (E+01)
0.000
0.020
0.040
0.060
0.080
0.100
0.120
0.140
LOAD (KIPS)(E+03)

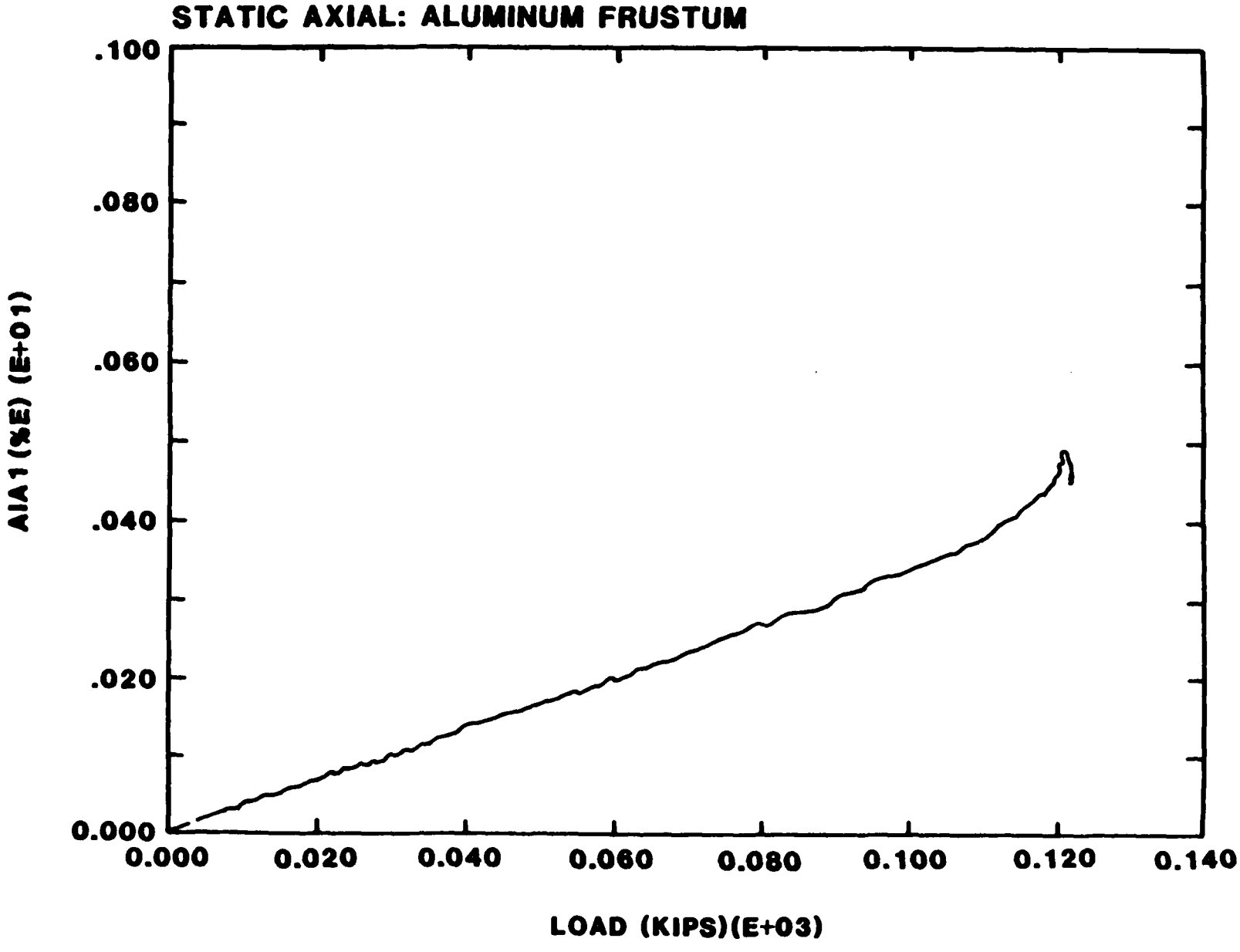
STATIC AXIAL: ALUMINUM FRUSTUM
.100
.080
.060
.040
.020
0.000
AIA1 (%E) (E+01)
0.000
0.020
0.040
0.060
0.080
0.100
0.120
0.140
LOAD (KIPS)(E+03)

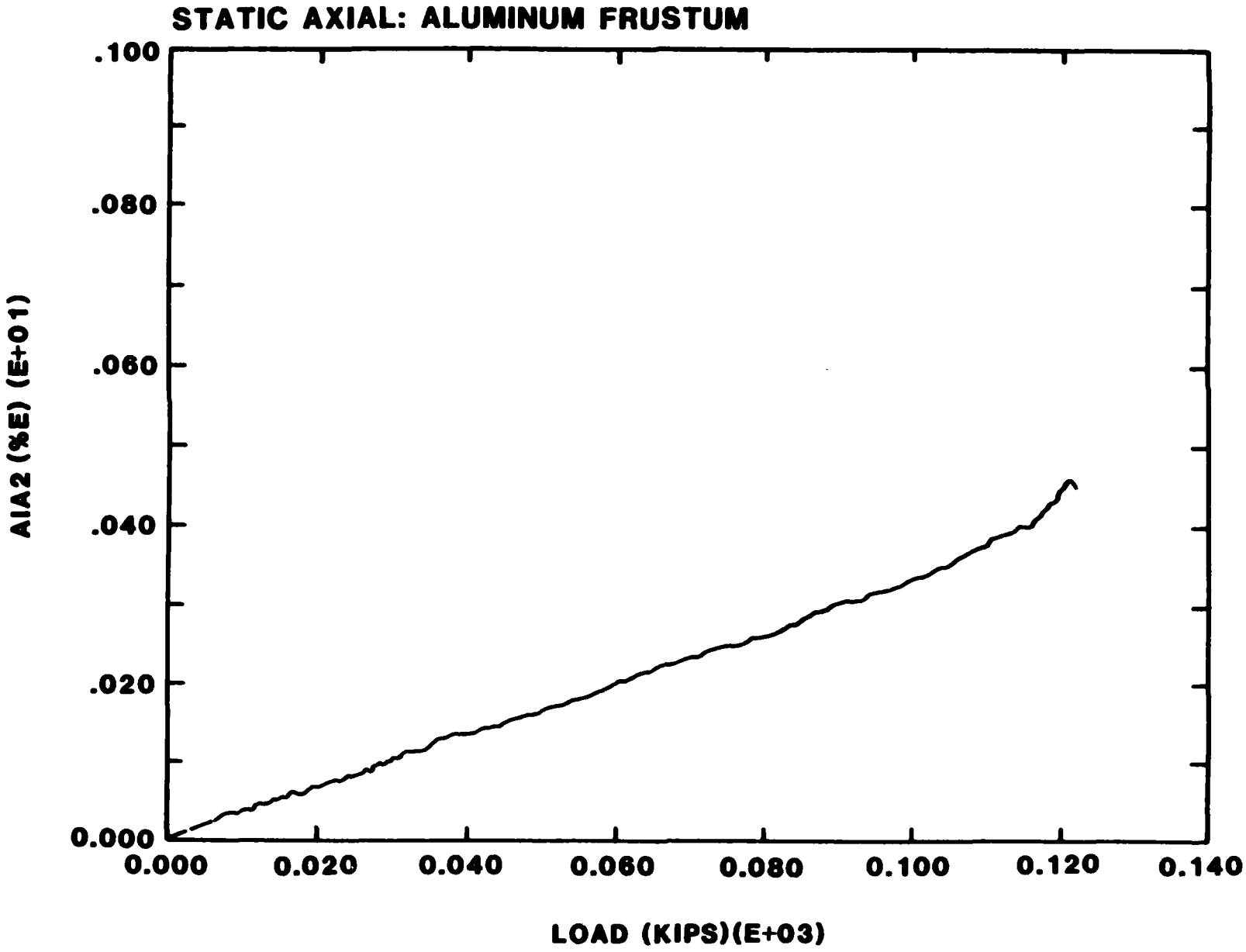
STATIC AXIAL: ALUMINUM FRUSTUM
.100
.080
.060
.040
.020
0.000
AIA2 (%E) (E+01)
0.000
0.020
0.040
0.060
0.080
0.100
0.120
0.140
LOAD (KIPS)(E+03)

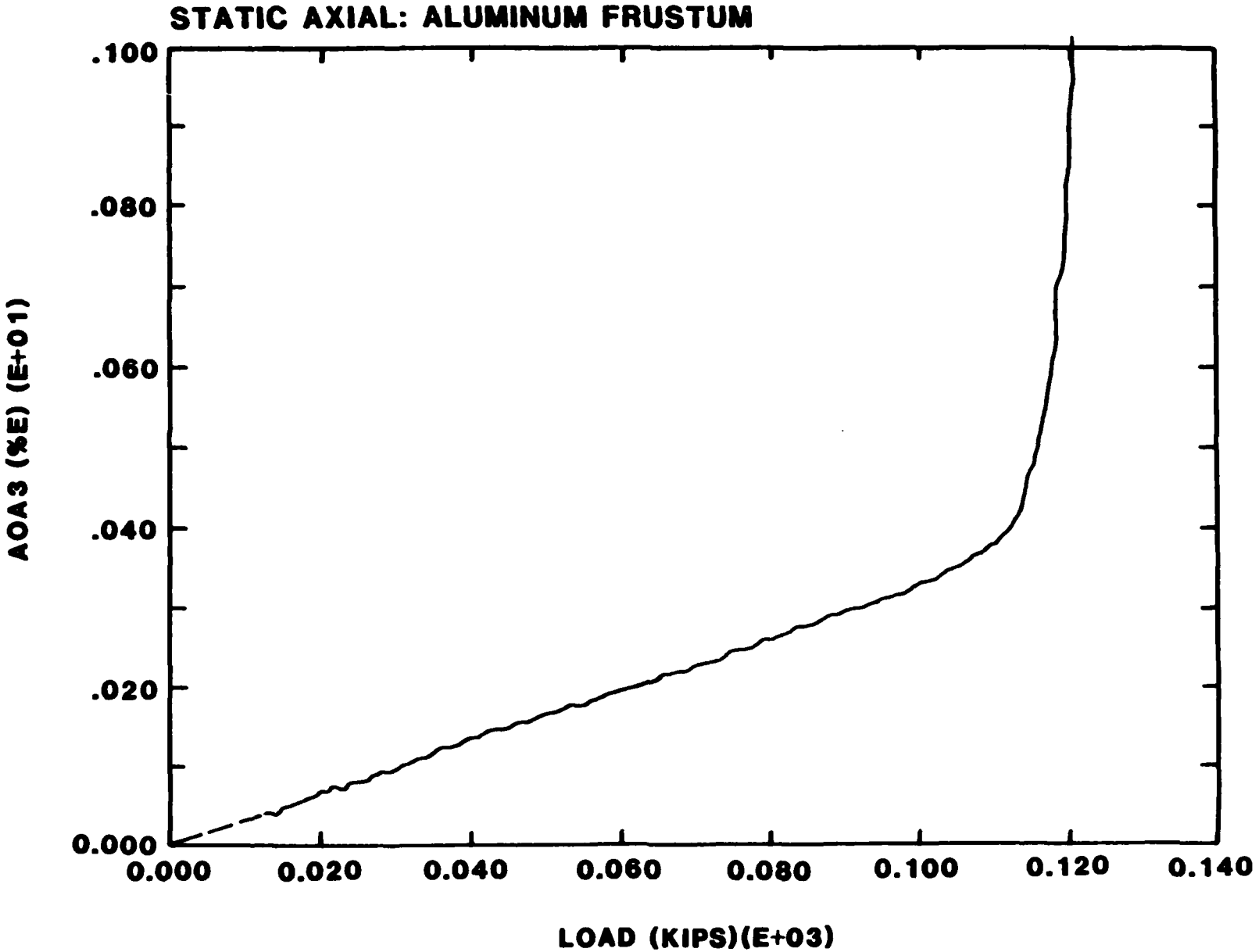
STATIC AXIAL: ALUMINUM FRUSTUM
.100
.080
.060
.040
.020
0.000
AOA3 (%E) (E+01)
0.000
0.020
0.040
0.060
0.080
0.100
0.120
0.140
LOAD (KIPS)(E+03)

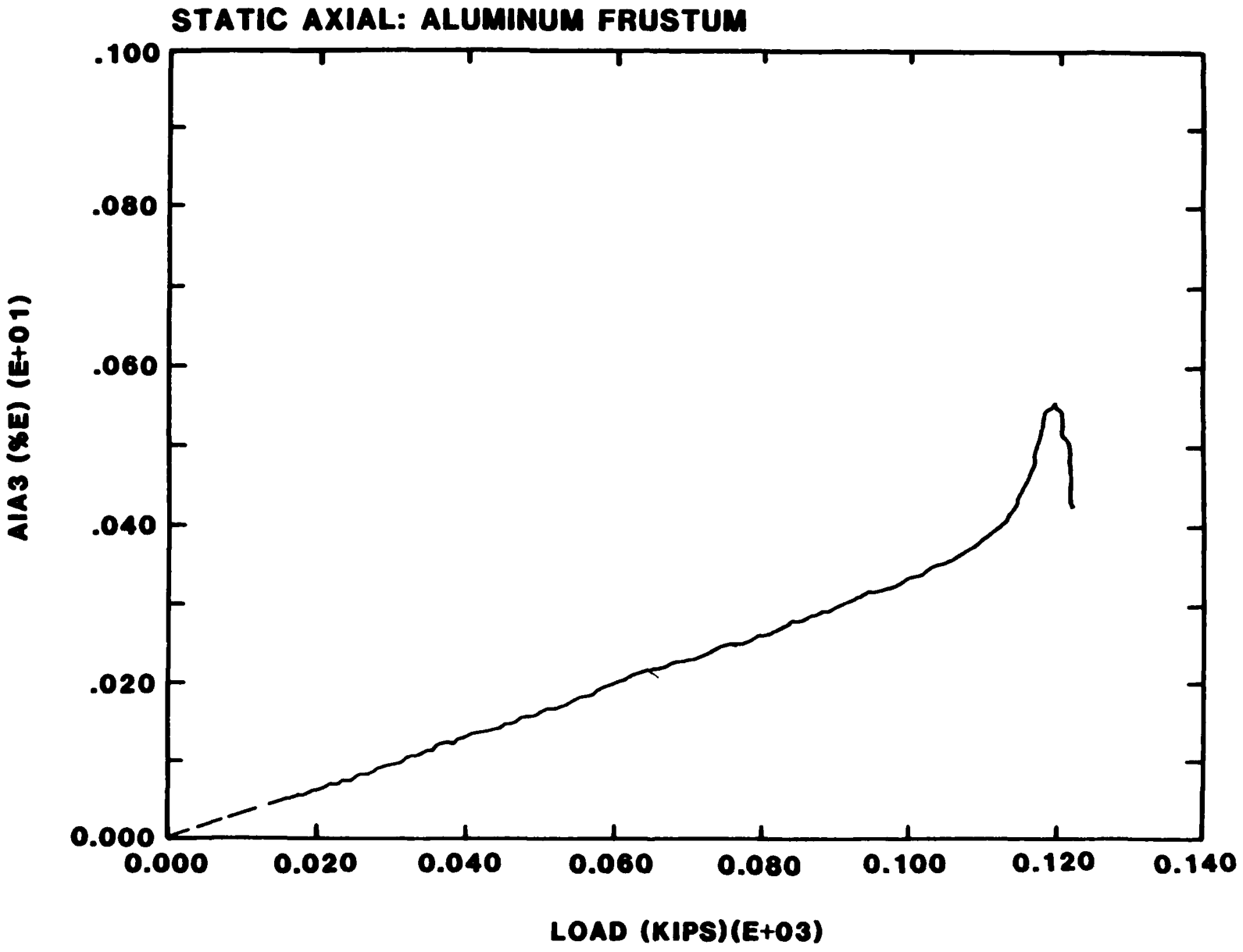
STATIC AXIAL: ALUMINUM FRUSTUM
.100
.080
.060
.040
.020
0.000
AIA3 (%E) (E+01)
0.000
0.020
0.040
0.060
0.080
0.100
0.120
0.140
LOAD (KIPS)(E+03)

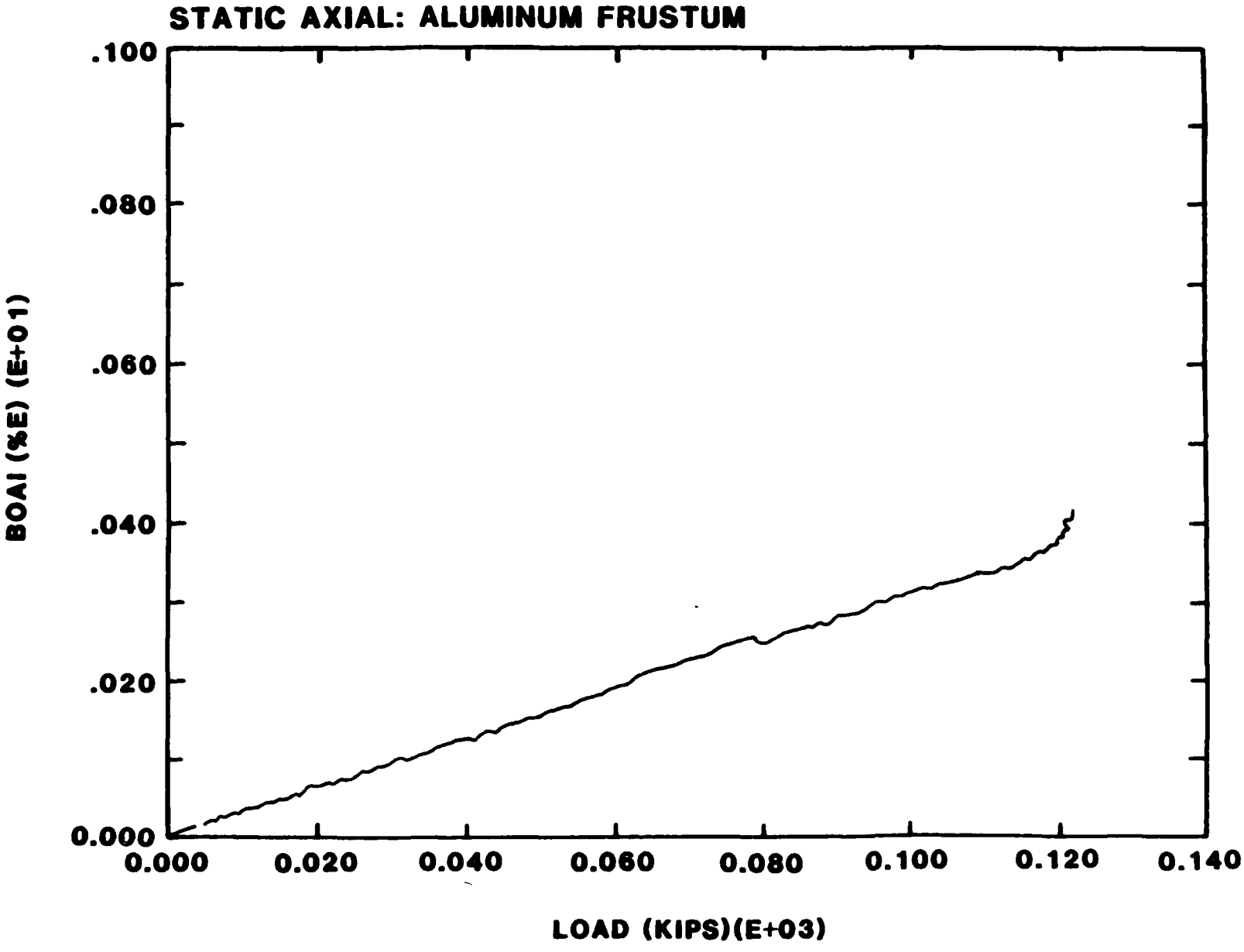
STATIC AXIAL: ALUMINUM FRUSTUM
.100
.080
.060
.040
.020
0.000
BOAI (%E) (E+01)
0.000
0.020
0.040
0.060
0.080
0.100
0.120
0.140
LOAD (KIPS)(E+03)

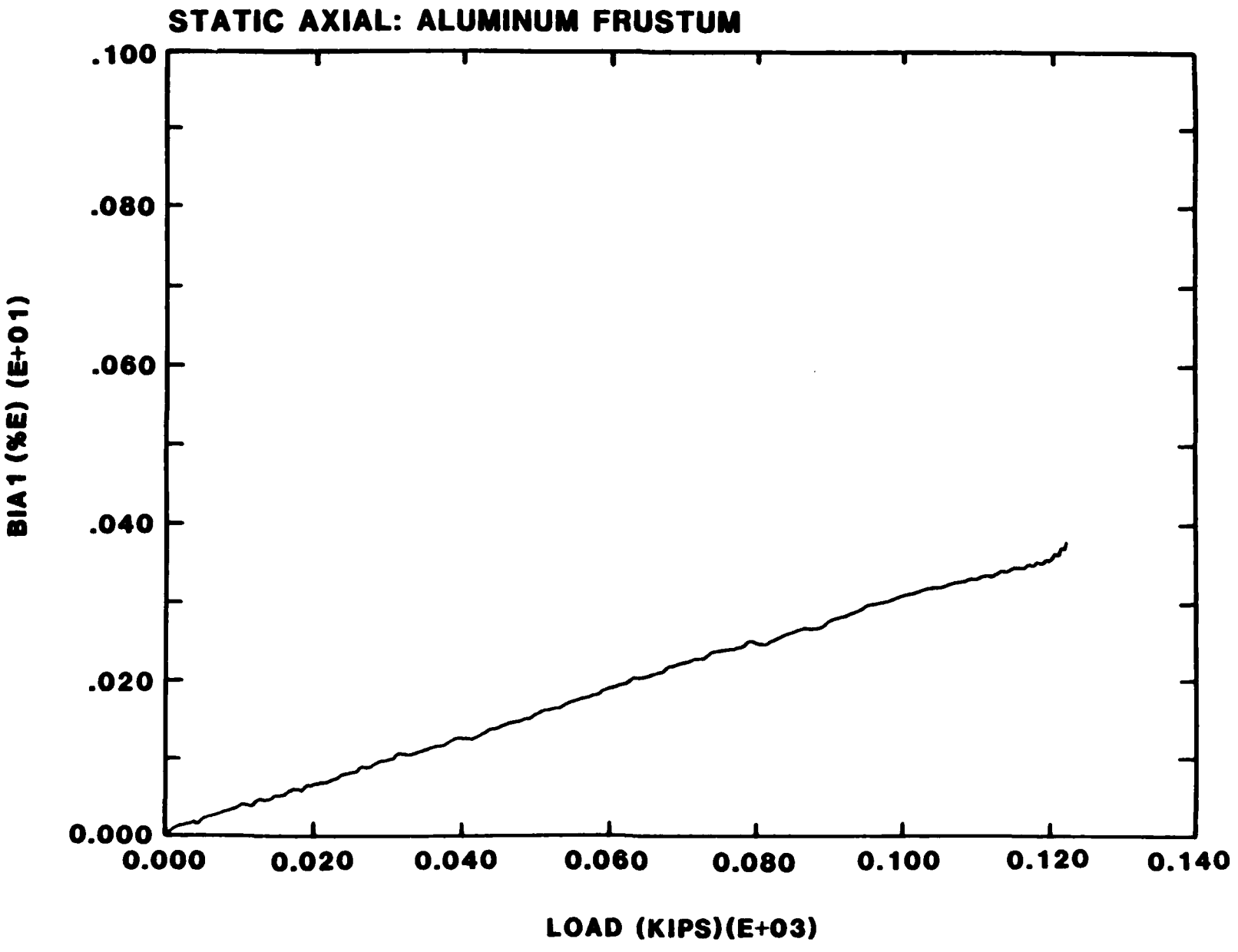
STATIC AXIAL: ALUMINUM FRUSTUM
.100
.080
.060
.040
.020
0.000
BIA1 (%E) (E+01)
0.000
0.020
0.040
0.060
0.080
0.100
0.120
0.140
LOAD (KIPS)(E+03)

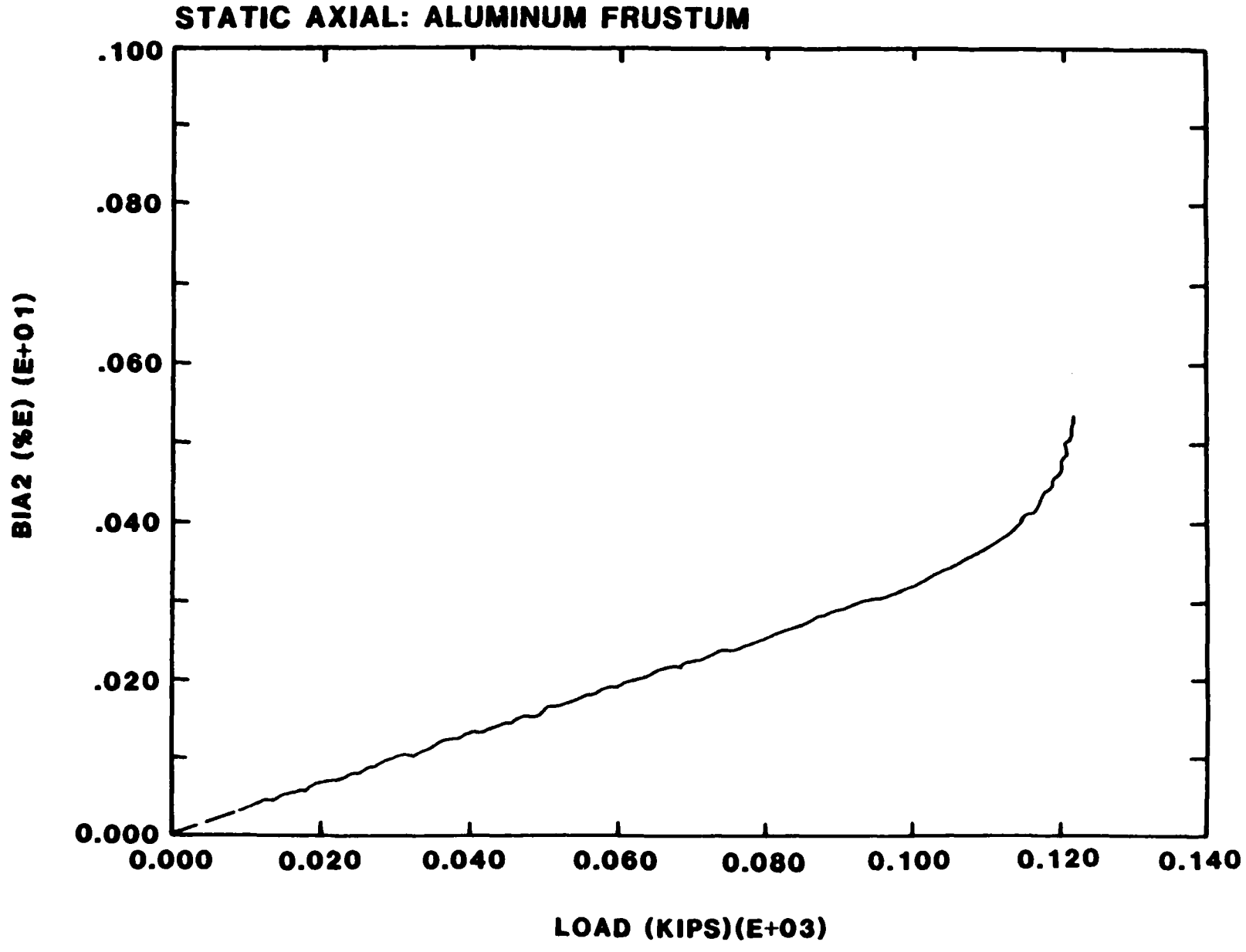
STATIC AXIAL: ALUMINUM FRUSTUM
.100
.080
.060
.040
.020
0.000
BIA2 (%E) (E+01)
0.000
0.020
0.040
0.060
0.080
0.100
0.120
0.140
LOAD (KIPS)(E+03)

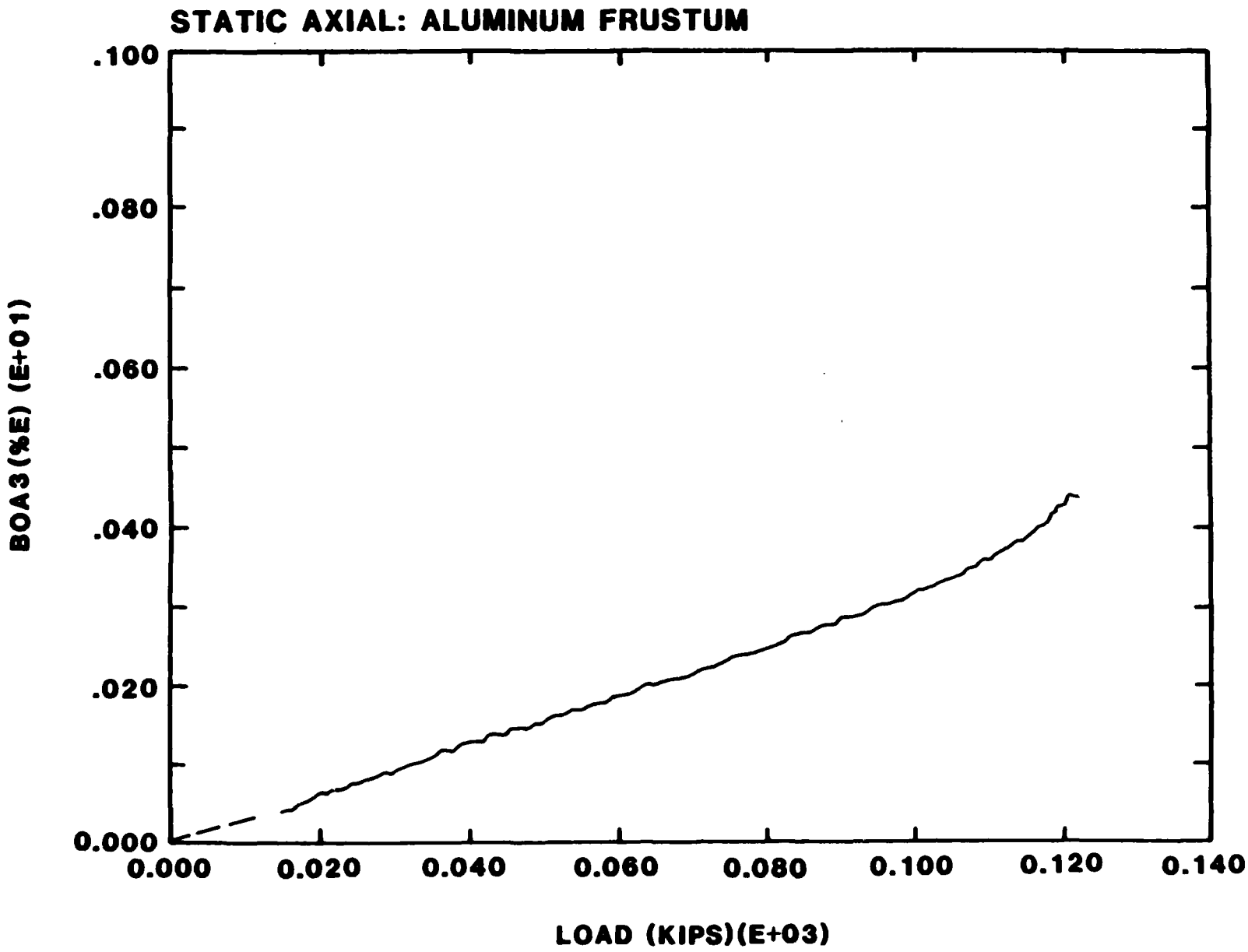
STATIC AXIAL: ALUMINUM FRUSTUM
.100
.080
.060
.040
.020
0.000
BOA3(%E) (E+01)
0.000
0.020
0.040
0.060
0.080
0.100
0.120
0.140
LOAD (KIPS)(E+03)

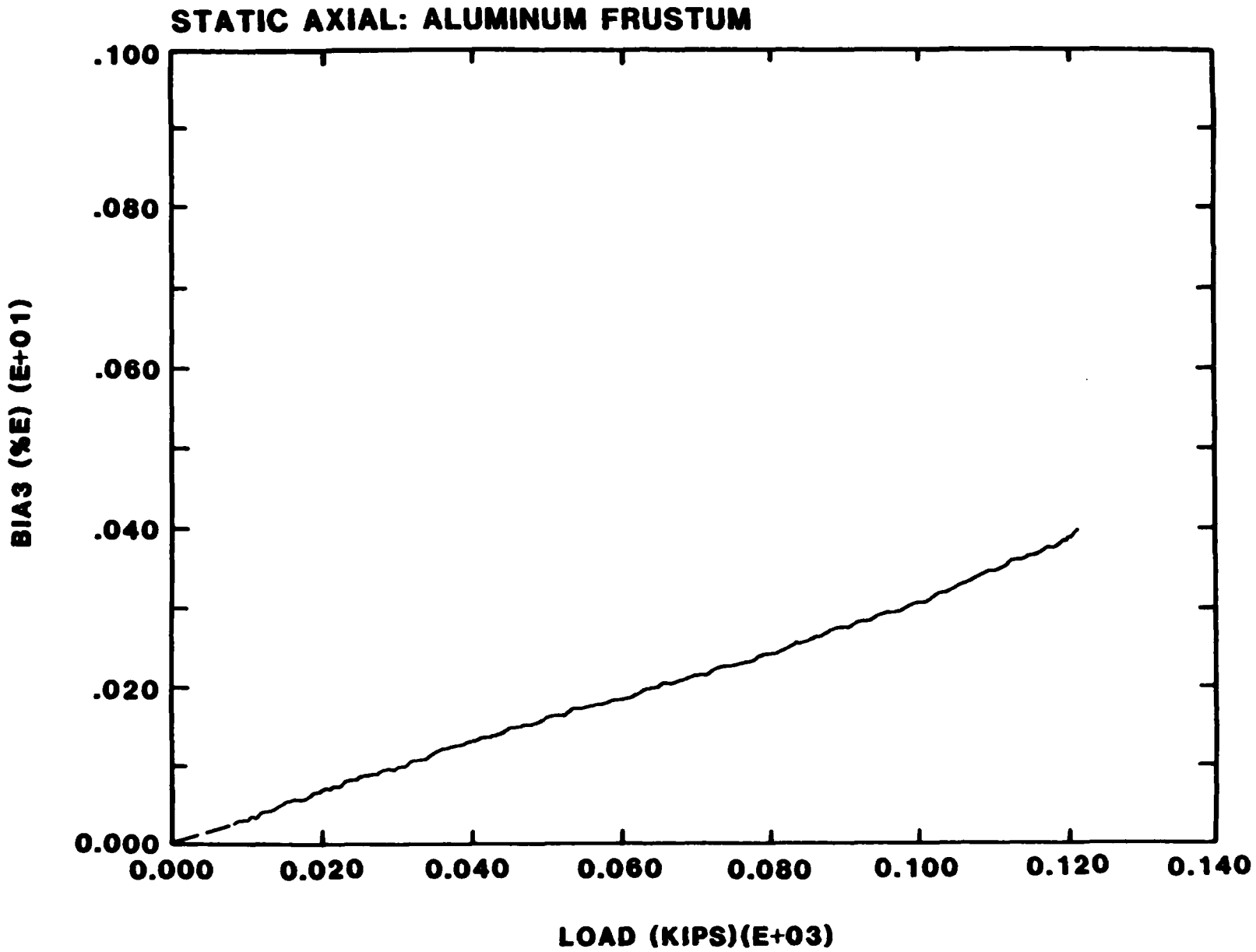
STATIC AXIAL: ALUMINUM FRUSTUM
.100
.080
.060
.040
.020
0.000
BIA3 (%E) (E+01)
0.000
0.020
0.040
0.060
0.080
0.100
0.120
0.140
LOAD (KIPS)(E+03)

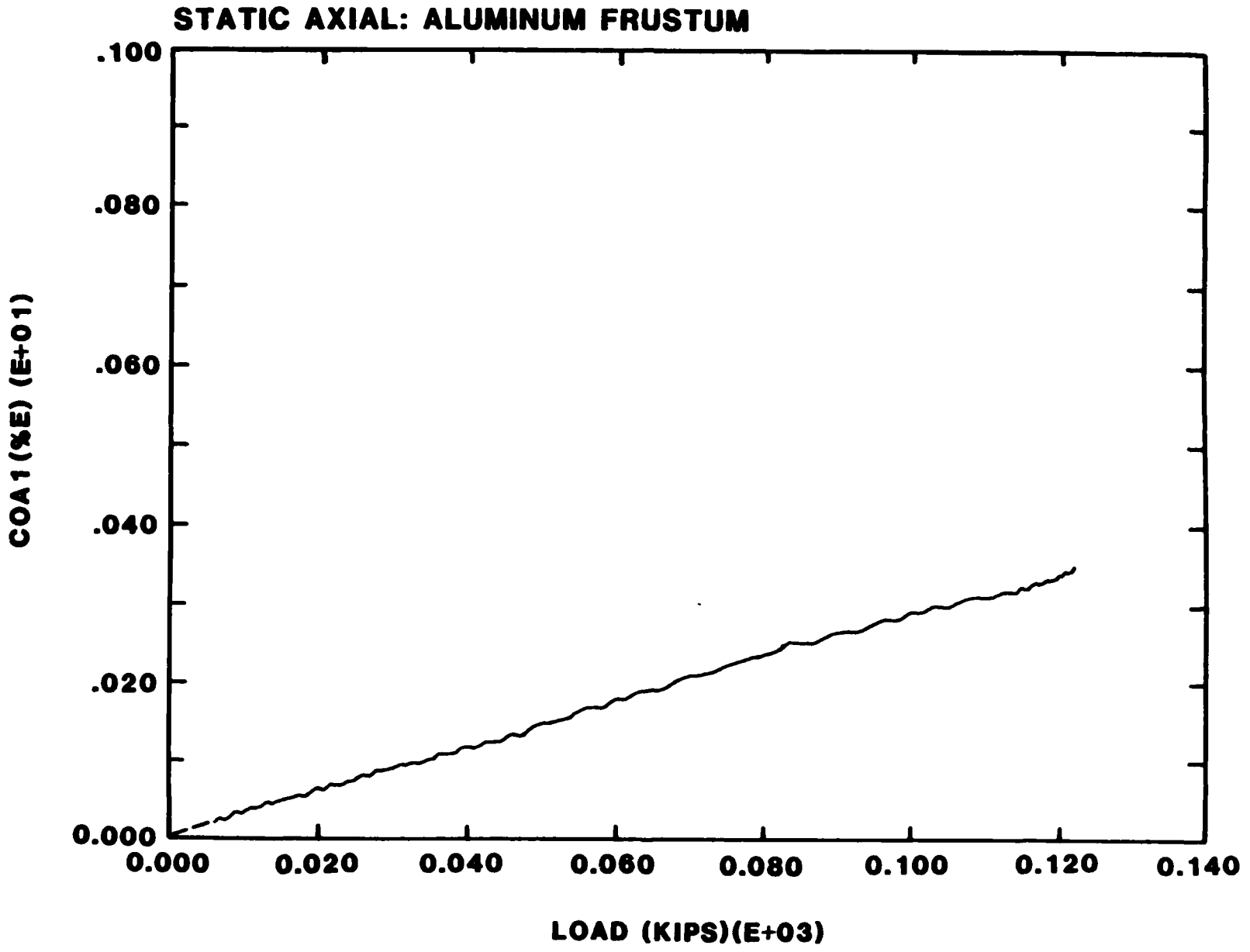
STATIC AXIAL: ALUMINUM FRUSTUM
.100
.080
.060
.040
.020
0.000
COA1(%E) (E+01)
0.000
0.020
0.040
0.060
0.080
0.100
0.120
0.140
LOAD (KIPS)(E+03)

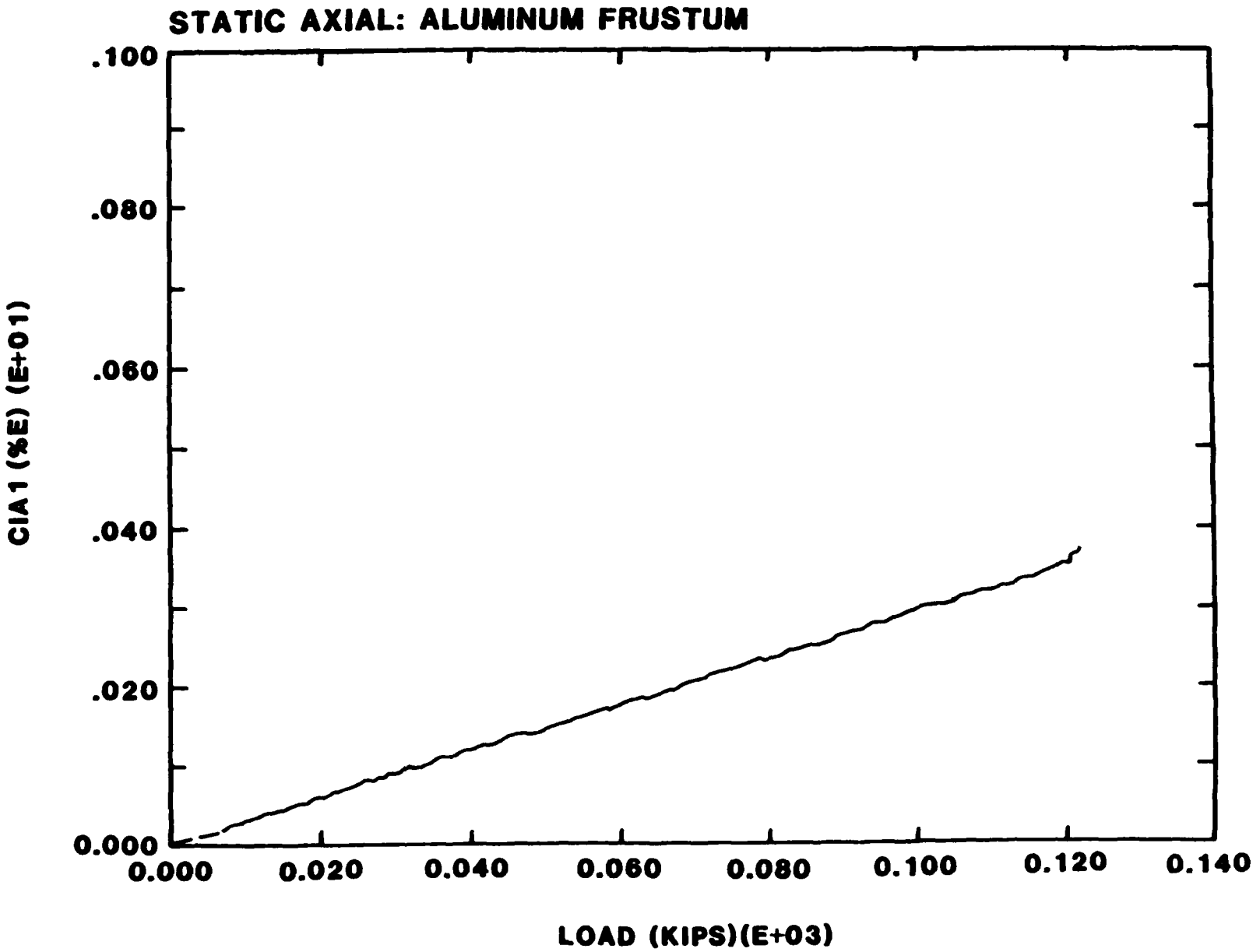
STATIC AXIAL: ALUMINUM FRUSTUM
.100
.080
.060
.040
.020
0.000
CIA1 (%E) (E+01)
0.000
0.020
0.040
0.060
0.080
0.100
0.120
0.140
LOAD (KIPS)(E+03)

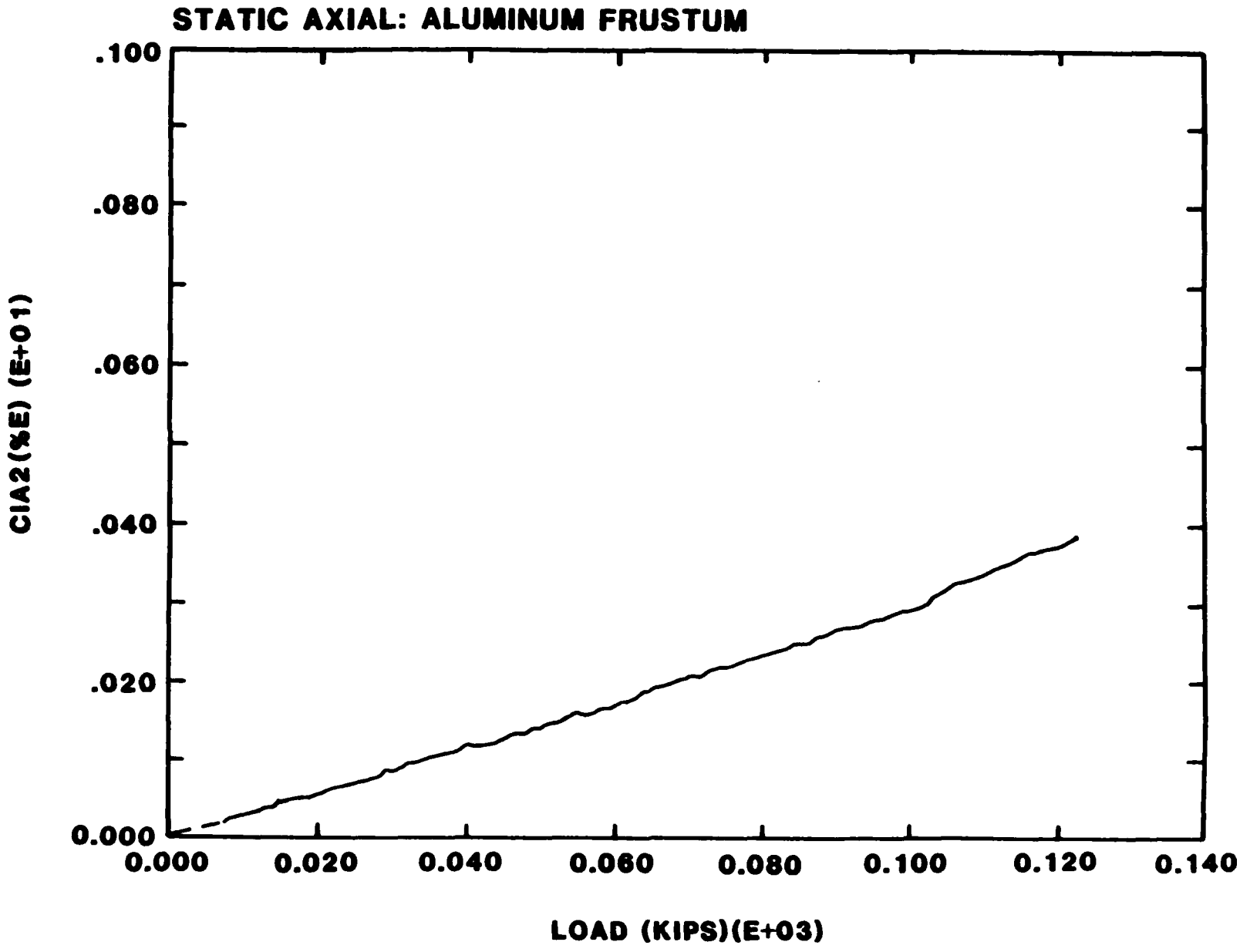
STATIC AXIAL: ALUMINUM FRUSTUM
.100
.080
.060
.040
.020
0.000
CIA2(%E) (E+01)
0.000
0.020
0.040
0.060
0.080
0.100
0.120
0.140
LOAD (KIPS)(E+03)

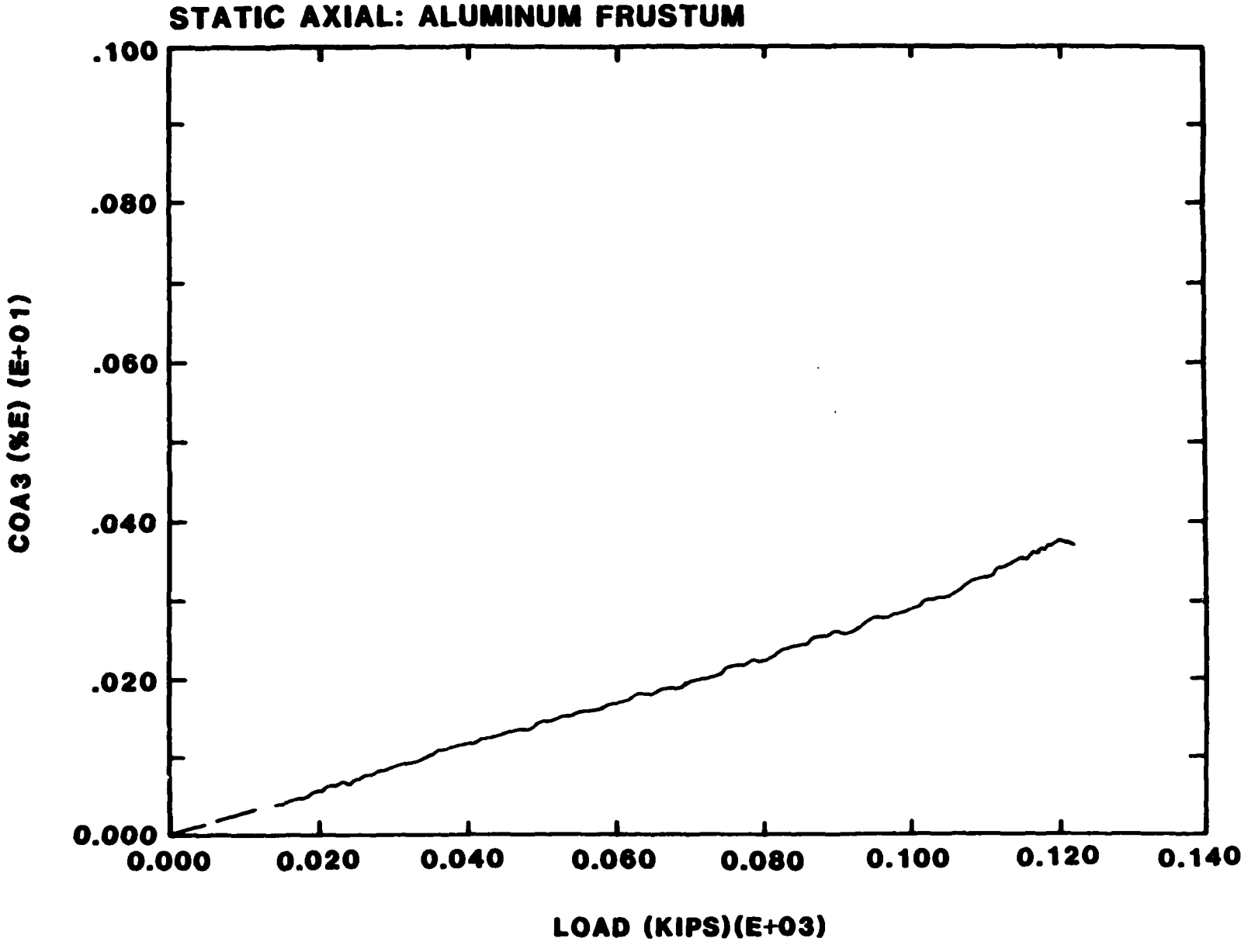
STATIC AXIAL: ALUMINUM FRUSTUM
.100
.080
.060
.040
.020
0.000
COA3 (%E) (E+01)
0.000
0.020
0.040
0.060
0.080
0.100
0.120
0.140
LOAD (KIPS)(E+03)

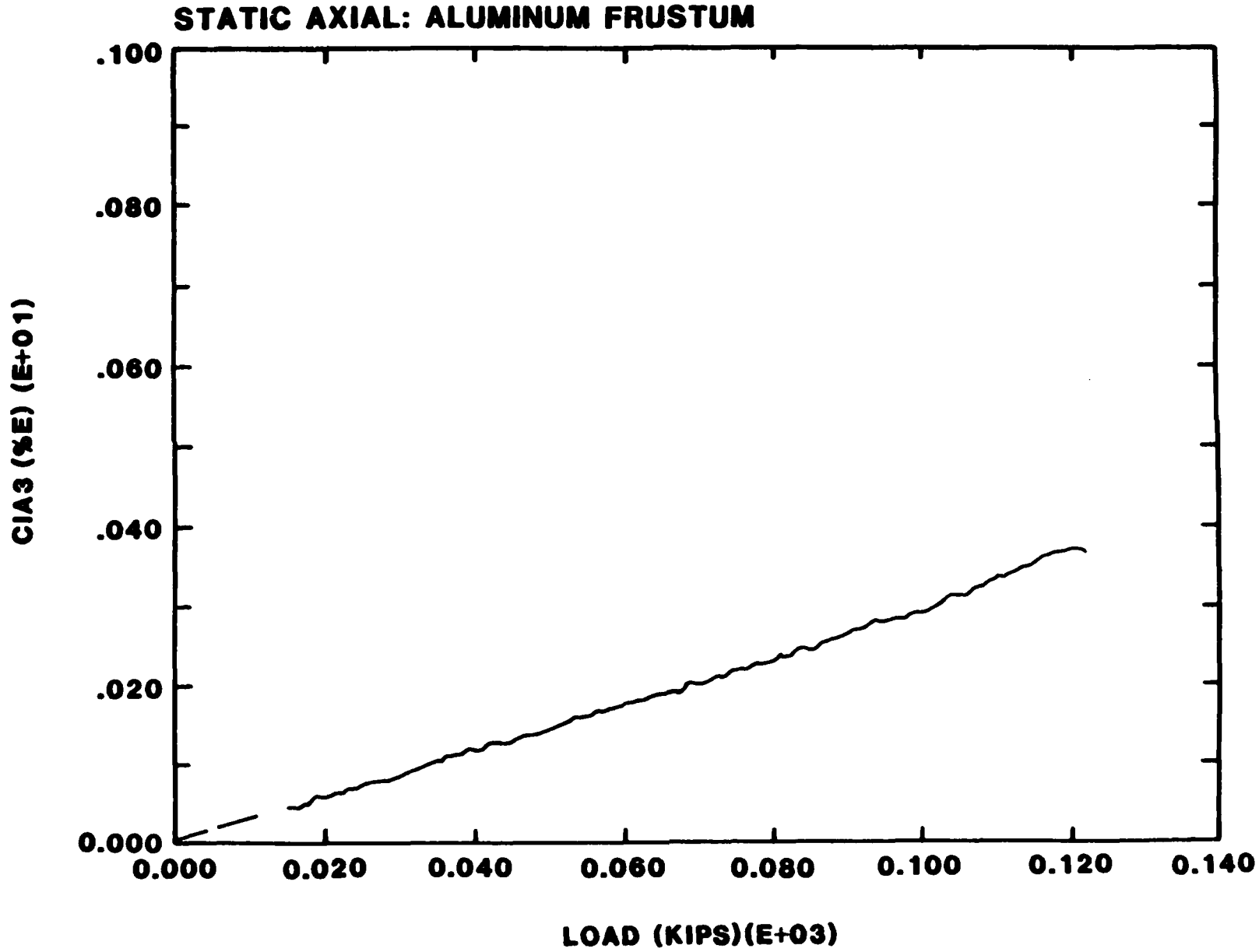
STATIC AXIAL: ALUMINUM FRUSTUM
.100
.080
.060
.040
.020
0.000
CIA3 (%E) (E+01)
0.000
0.020
0.040
0.060
0.080
0.100
0.120
0.140
LOAD (KIPS)(E+03)

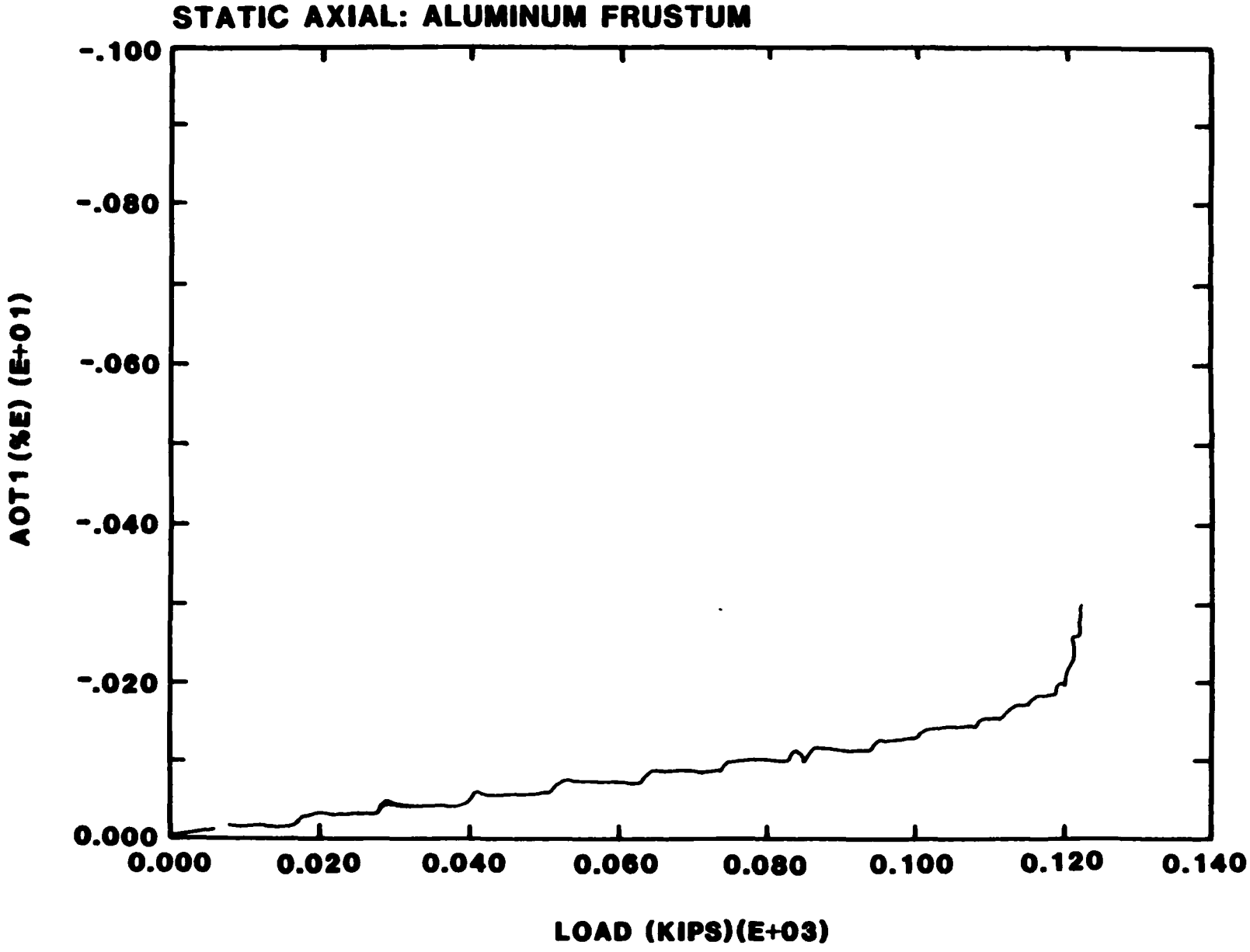
STATIC AXIAL: ALUMINUM FRUSTUM
-.100
-.080
-.060
-.040
-.020
0.000
AOT1 (%E) (E+01)
0.000
0.020
0.040
0.060
0.080
0.100
0.120
0.140
LOAD (KIPS)(E+03)

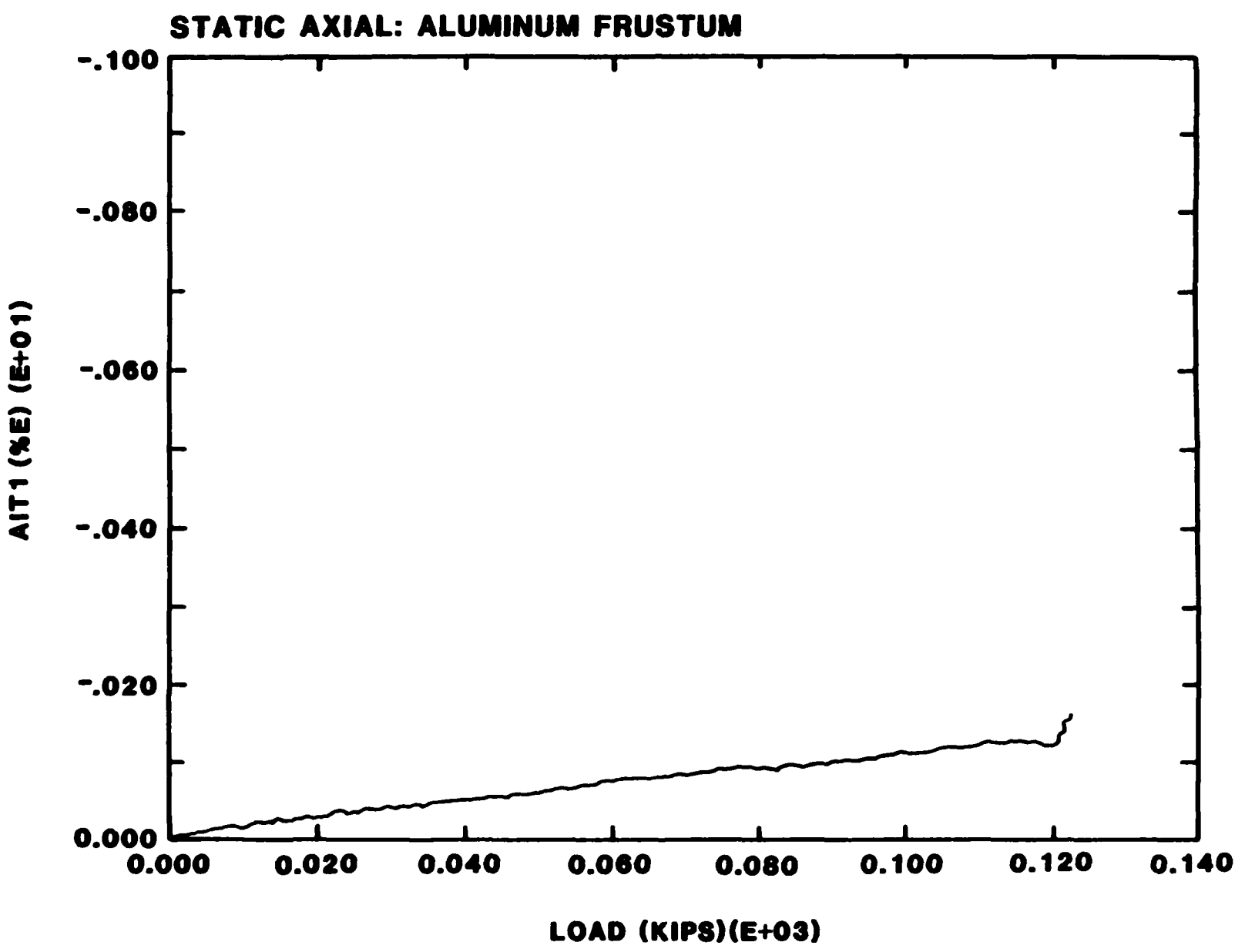
STATIC AXIAL: ALUMINUM FRUSTUM
-.100
-.080
-.060
-.040
-.020
0.000
AIT1 (%E) (E+01)
0.000
0.020
0.040
0.060
0.080
0.100
0.120
0.140
LOAD (KIPS)(E+03)

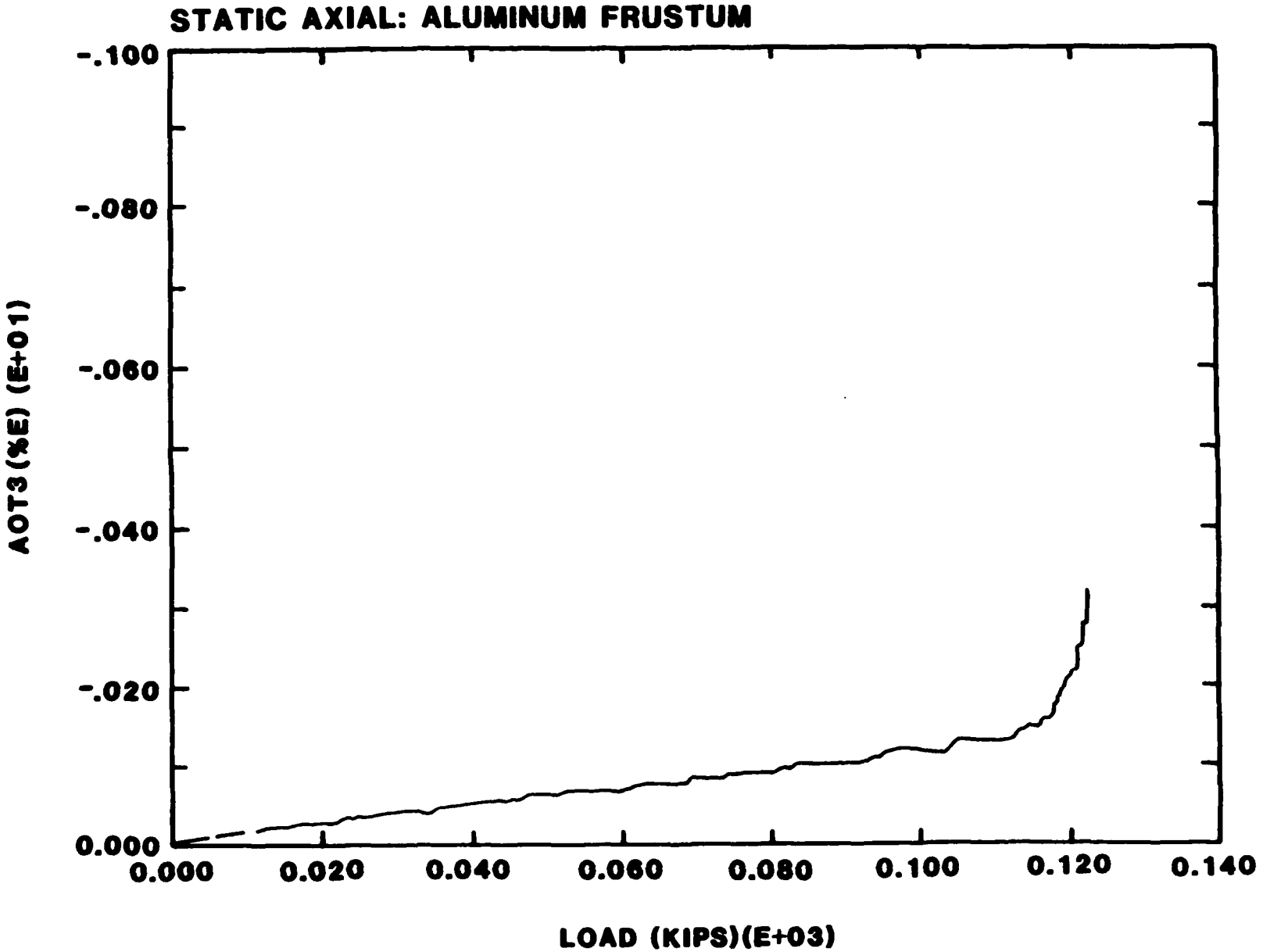
STATIC AXIAL: ALUMINUM FRUSTUM
-.100
-.080
-.060
-.040
-.020
0.000
AOT3 (%E) (E+01)
0.000
0.020
0.040
0.060
0.080
0.100
0.120
0.140
LOAD (KIPS)(E+03)

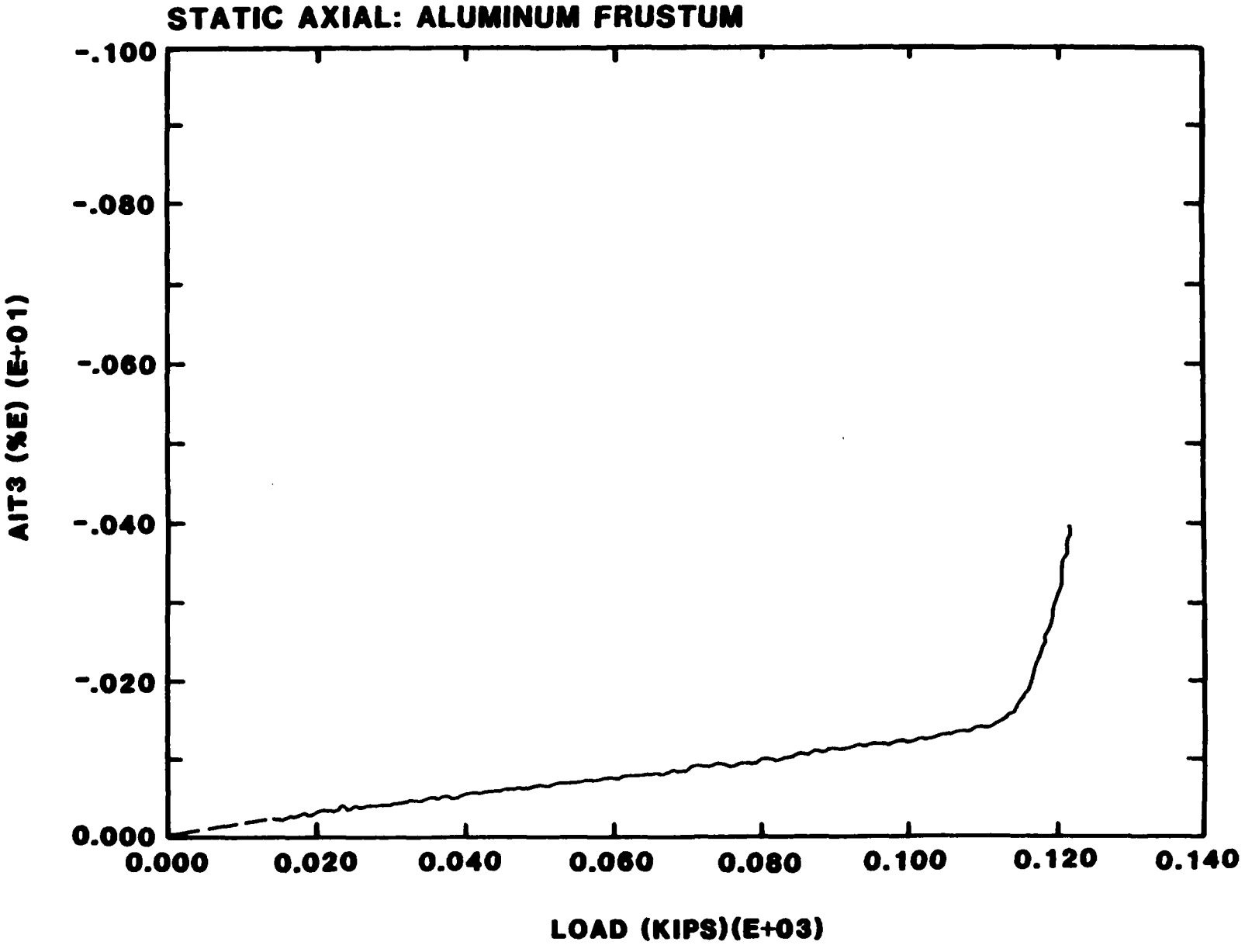
STATIC AXIAL: ALUMINUM FRUSTUM
-.100
-.080
-.060
-.040
-.020
0.000
AIT3 (%E) (E+01)
0.000
0.020
0.040
0.060
0.080
0.100
0.120
0.140
LOAD (KIPS)(E+03)

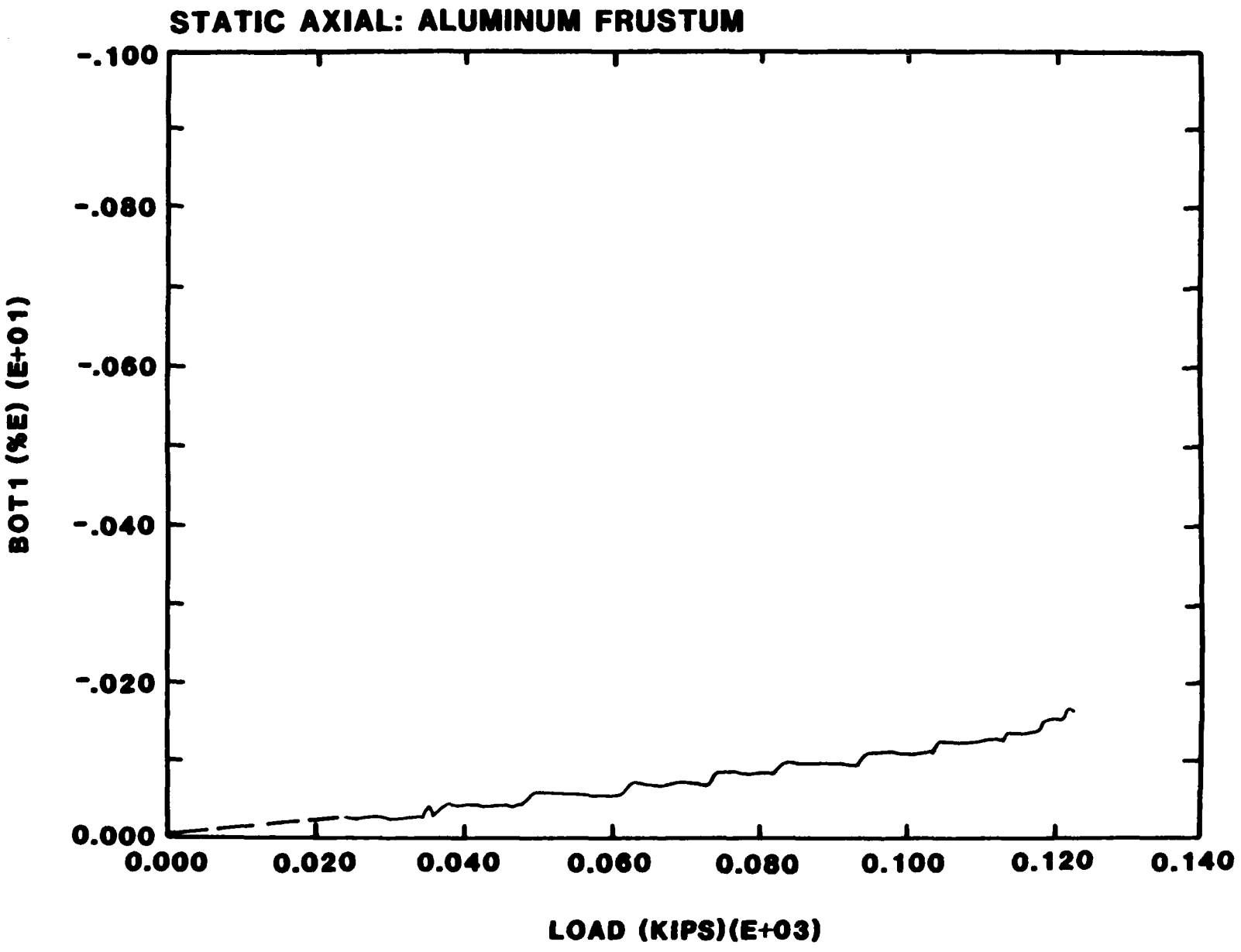
STATIC AXIAL: ALUMINUM FRUSTUM
-.100
-.080
-.060
-.040
-.020
0.000
BOT1 (%E) (E+01)
0.000
0.020
0.040
0.060
0.080
0.100
0.120
0.140
LOAD (KIPS)(E+03)

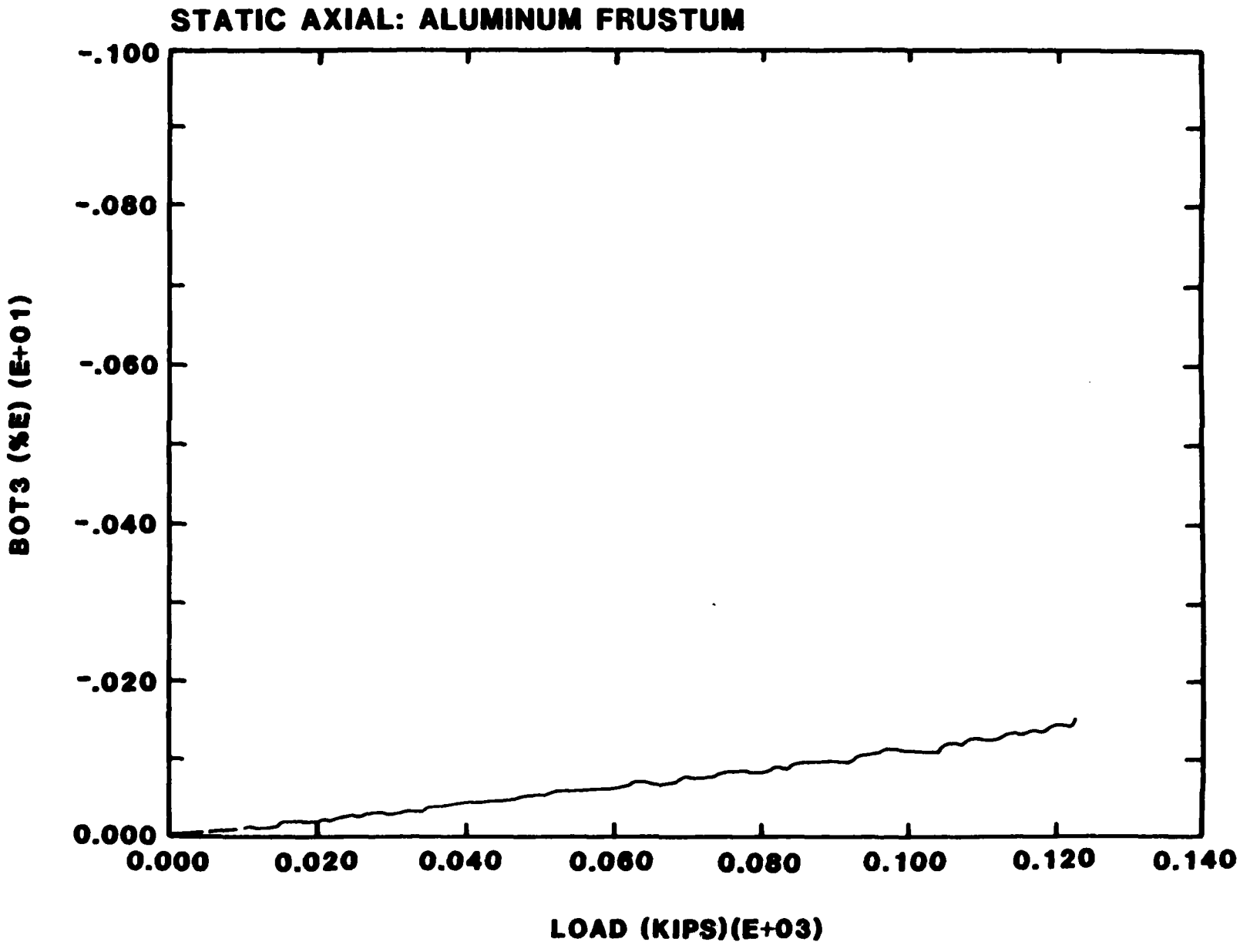
STATIC AXIAL: ALUMINUM FRUSTUM
-.100
-.080
-.060
-.040
-.020
0.000
BOT3 (%E) (E+01)
0.000
0.020
0.040
0.060
0.080
0.100
0.120
0.140
LOAD (KIPS)(E+03)

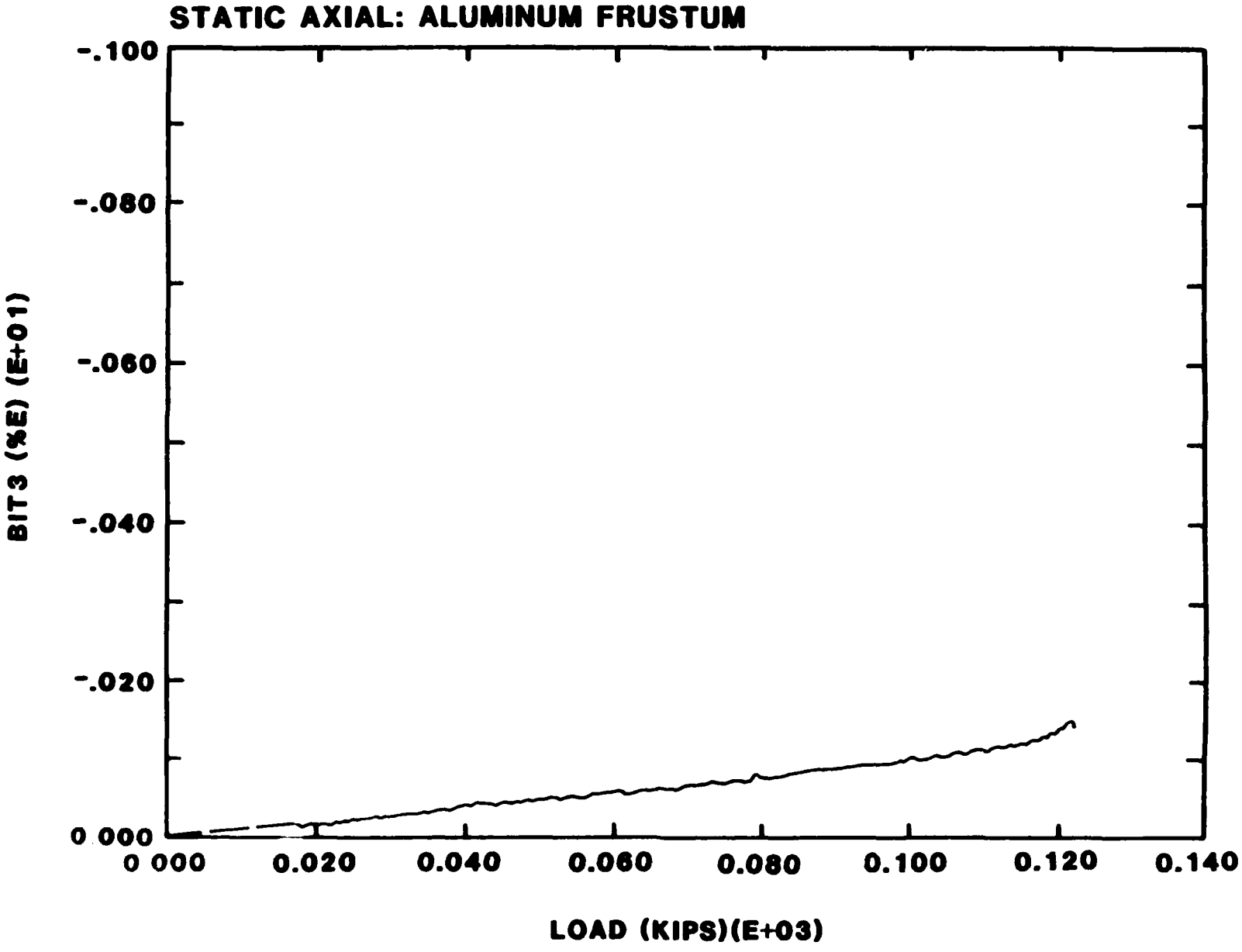
STATIC AXIAL: ALUMINUM FRUSTUM
-.100
-.080
-.060
-.040
-.020
0 000
BIT3 (%E) (E+01)
0 000
0.020
0.040
0.060
0.080
0.100
0.120
0.140
LOAD (KIPS)(E+03)

AD-A169 732 STATIC AND DYNAMIC TESTING OF INTERCEPTOR SUBSTRUCTURES 2/2
(U) TERRA TEK INC SALT LAKE CITY UT M L WILSON ET AL.
MAR 86 RTRE-82-18 MTL-TR-86-5 DAAG29-81-C-0023
UNCLASSIFIED F/G 11/4 NL

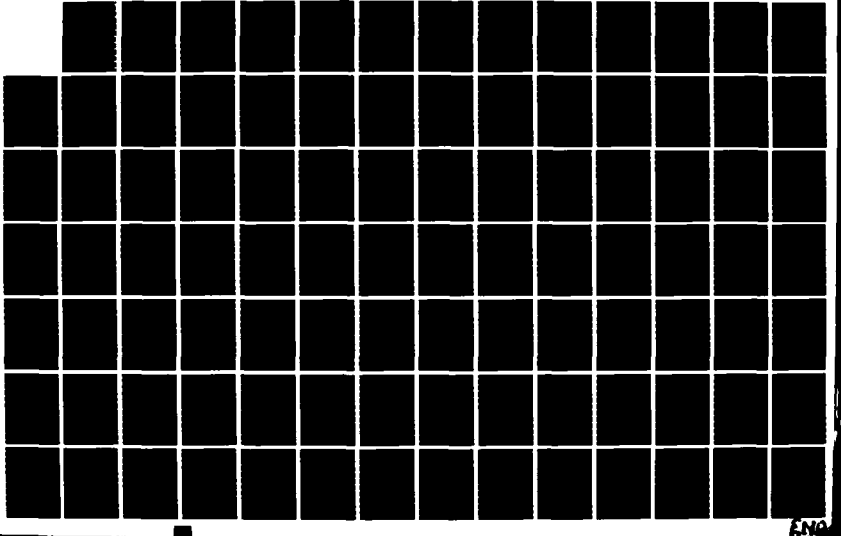

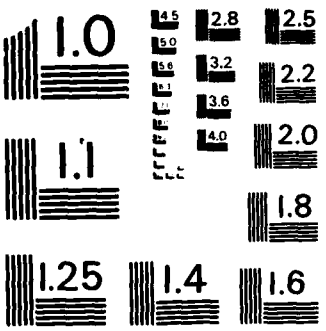

MICROCOPY RESOLUTION TEST CHART
NATIONAL BUREAU OF STANDARDS - 1963 - A

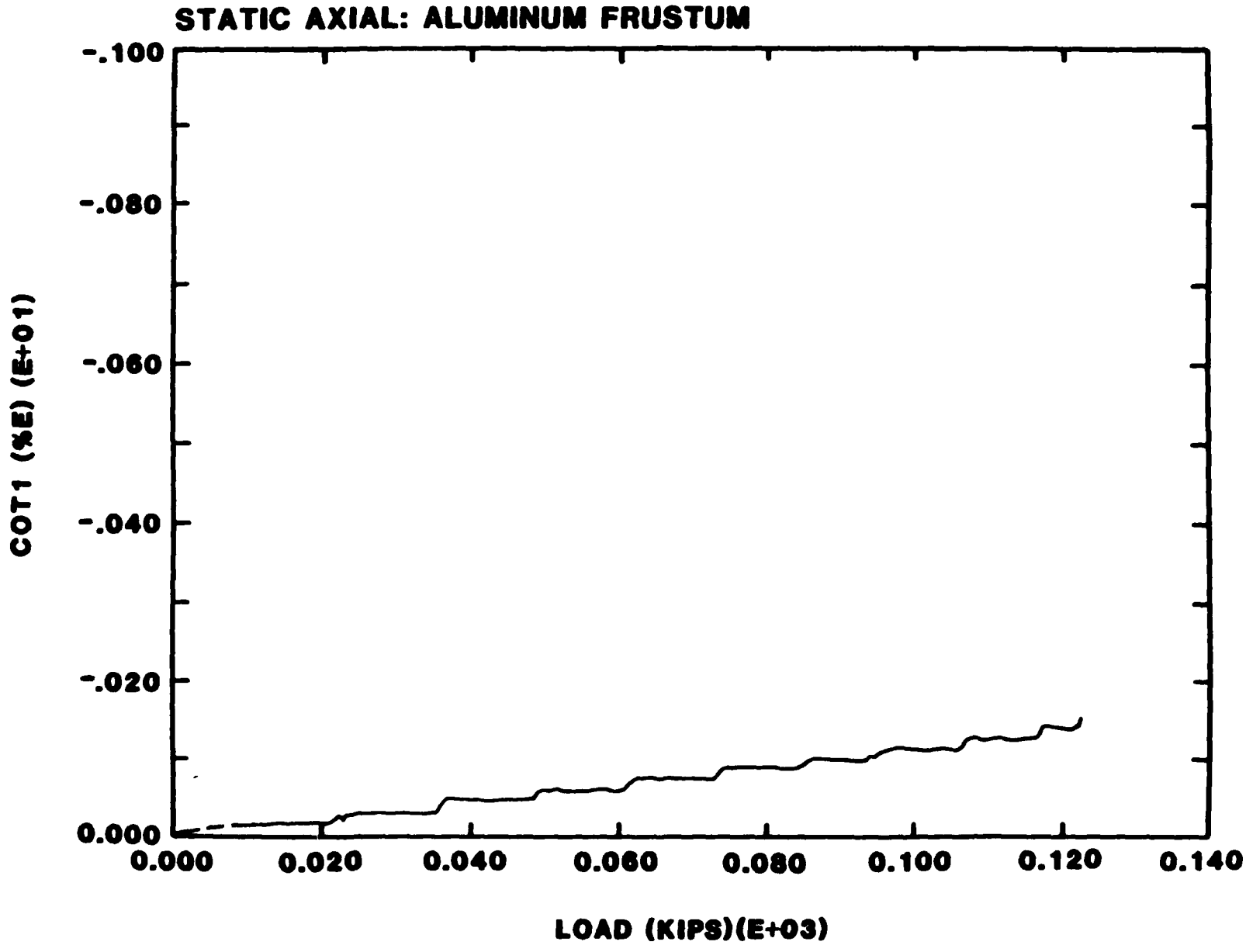
STATIC AXIAL: ALUMINUM FRUSTUM
-.100
-.080
-.060
-.040
-.020
0.000
COT1 (%E) (E+01)
0.000
0.020
0.040
0.060
0.080
0.100
0.120
0.140
LOAD (KIPS)(E+03)

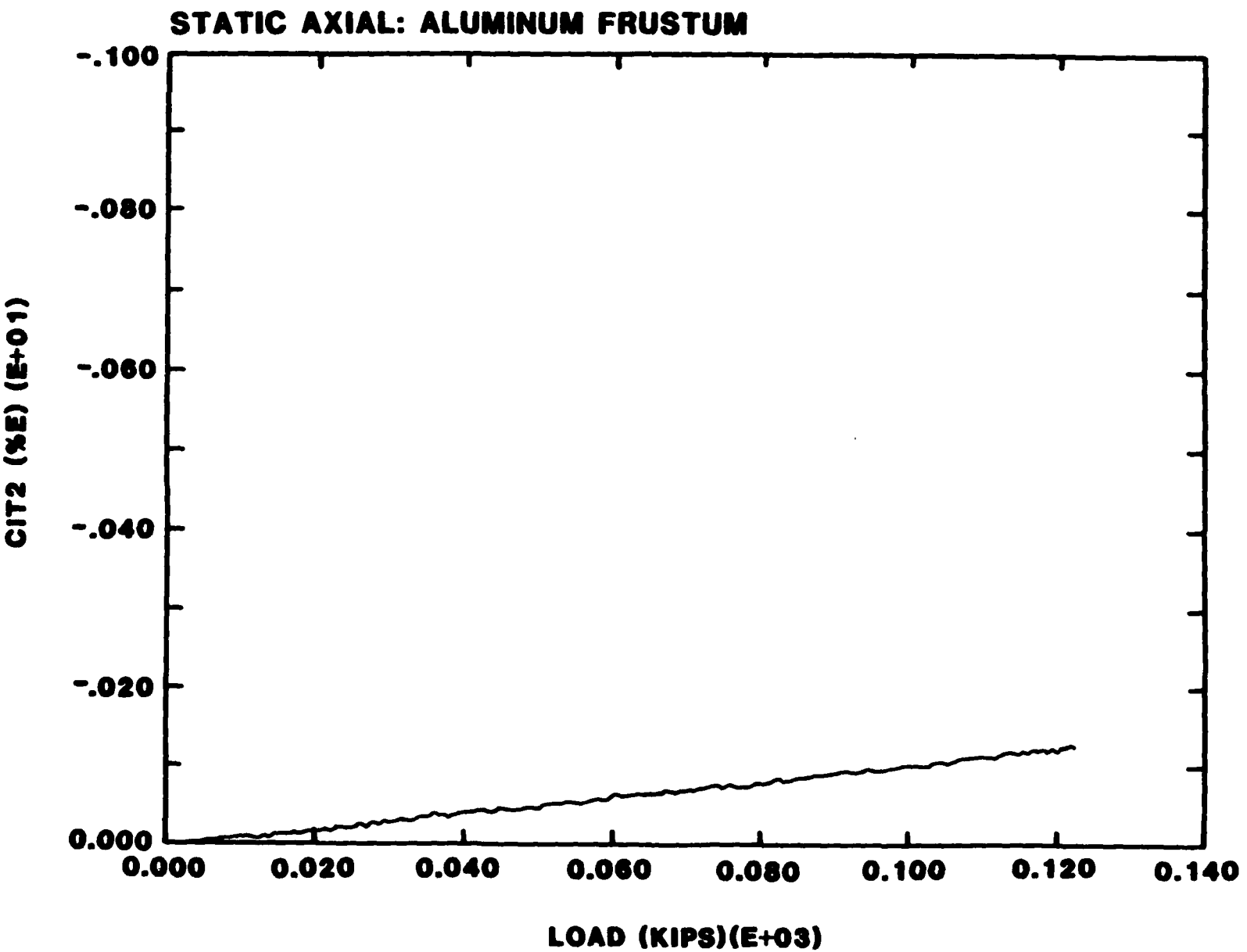
STATIC AXIAL: ALUMINUM FRUSTUM
-.100
-.080
-.060
-.040
-.020
0.000
CIT2 (%E) (E+01)
0.000
0.020
0.040
0.060
0.080
0.100
0.120
0.140
LOAD (KIPS)(E+03)

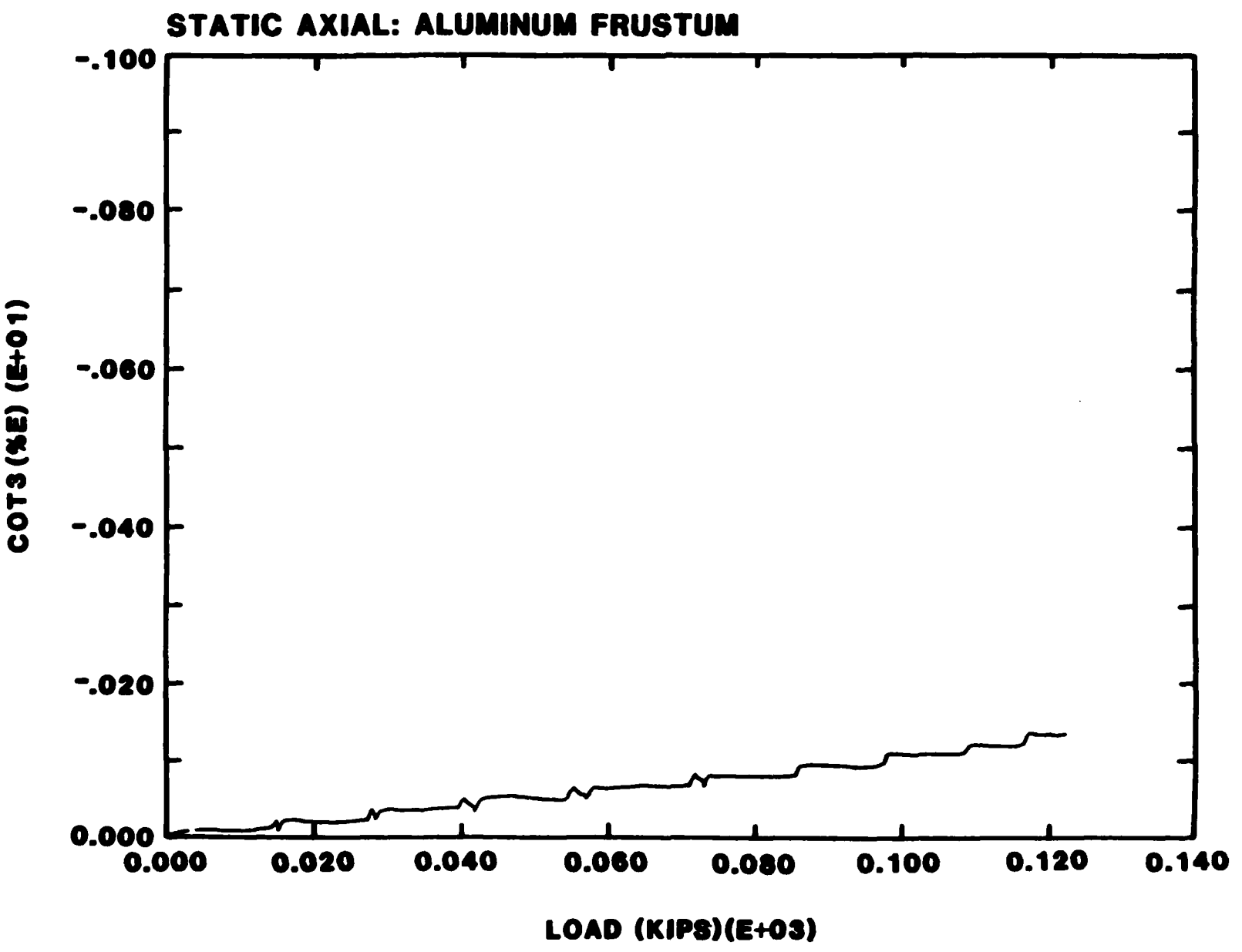
STATIC AXIAL: ALUMINUM FRUSTUM
-.100
-.080
-.060
-.040
-.020
0.000
COT3 (%E) (E+01)
0.000
0.020
0.040
0.060
0.080
0.100
0.120
0.140
LOAD (KIPS)(E+03)

7.2 APPENDIX B

DYNAMIC-AXIAL LOADING TEST DATA
FOR ALUMINUM FRUSTA

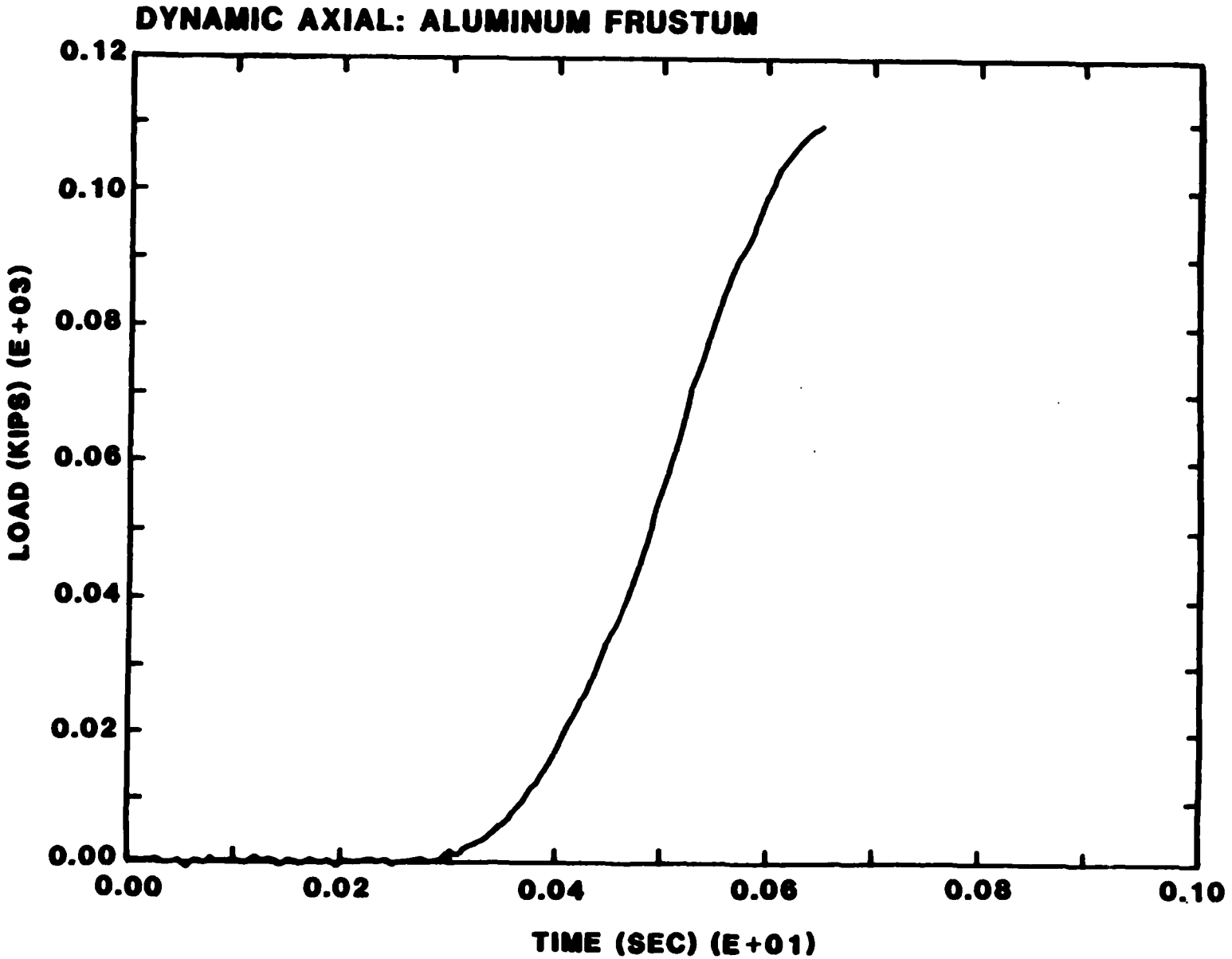
DYNAMIC AXIAL: ALUMINUM FRUSTUM
LOAD (KIPS) (E+03)
0.12
0.10
0.08
0.06
0.04
0.02
0.00
0.00
0.02
0.04
0.06
0.08
0.10
TIME (SEC) (E+01)

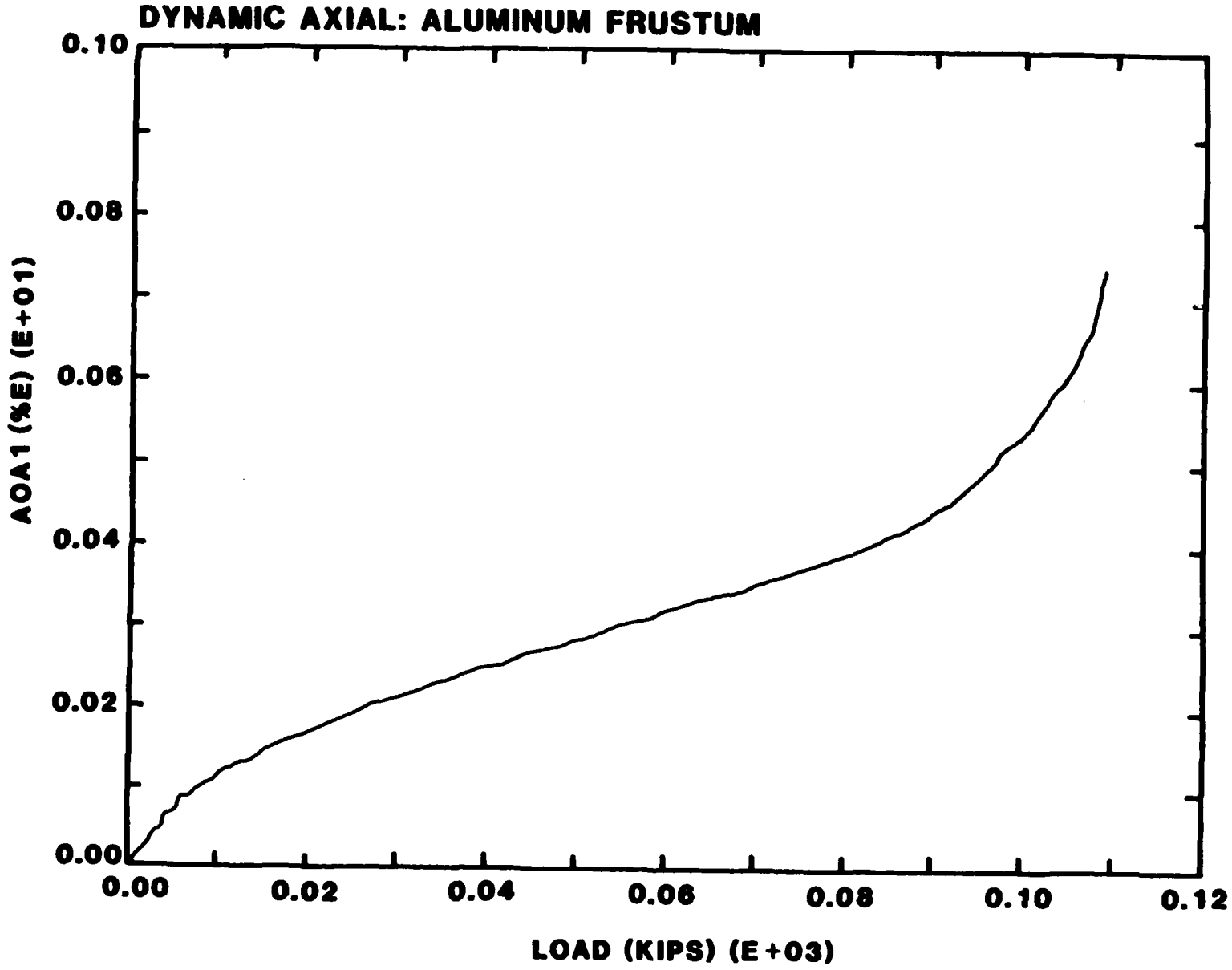
DYNAMIC AXIAL: ALUMINUM FRUSTUM
0.10
0.08
0.06
0.04
0.02
0.00
AOA1 (%E) (E+01)
0.00
0.02
0.04
0.06
0.08
0.10
0.12
LOAD (KIPS) (E+03)

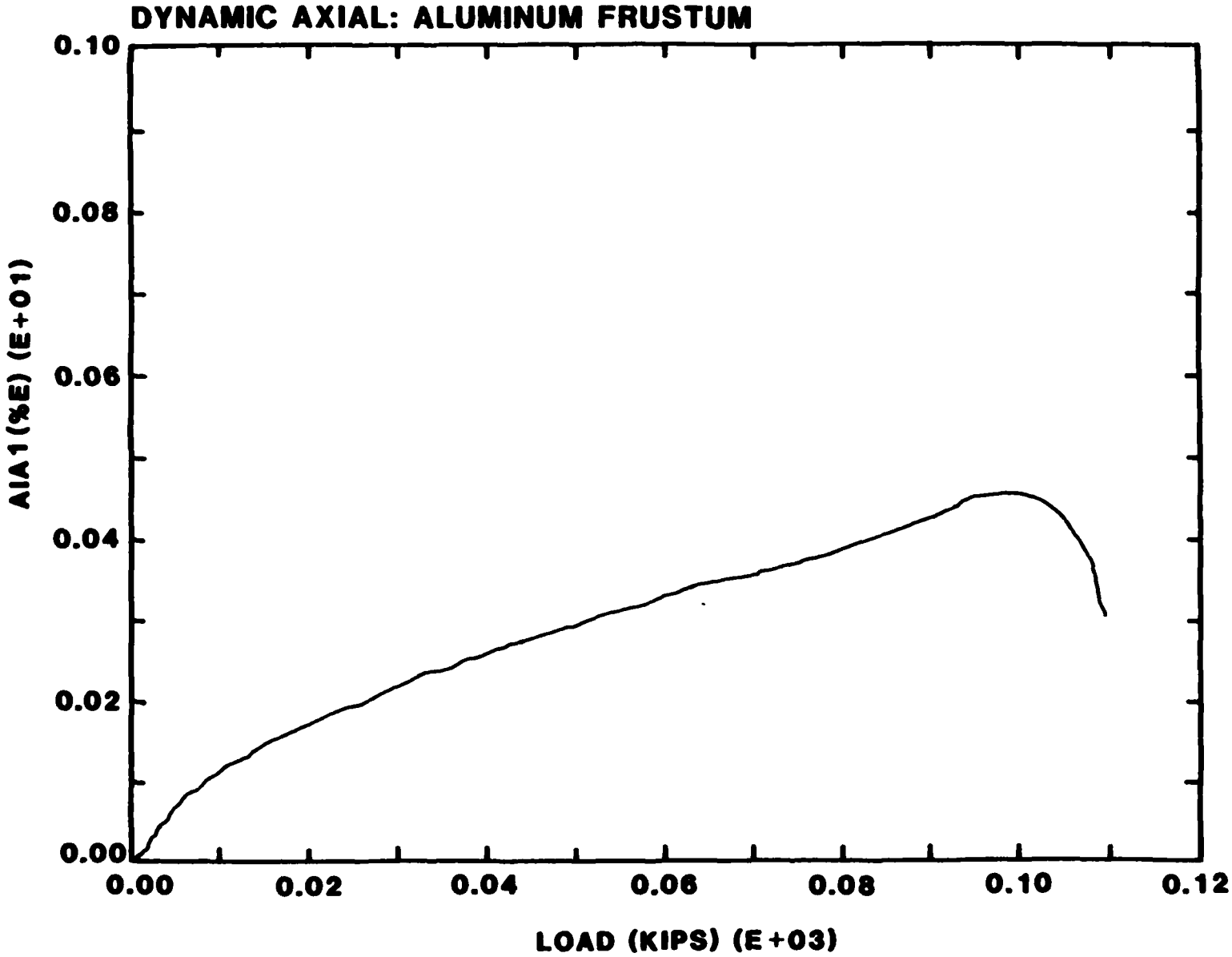
DYNAMIC AXIAL: ALUMINUM FRUSTUM
0.10
0.08
0.06
0.04
0.02
0.00
AIA1(%E) (E+01)
0.00
0.02
0.04
0.06
0.08
0.10
0.12
LOAD (KIPS) (E+03)

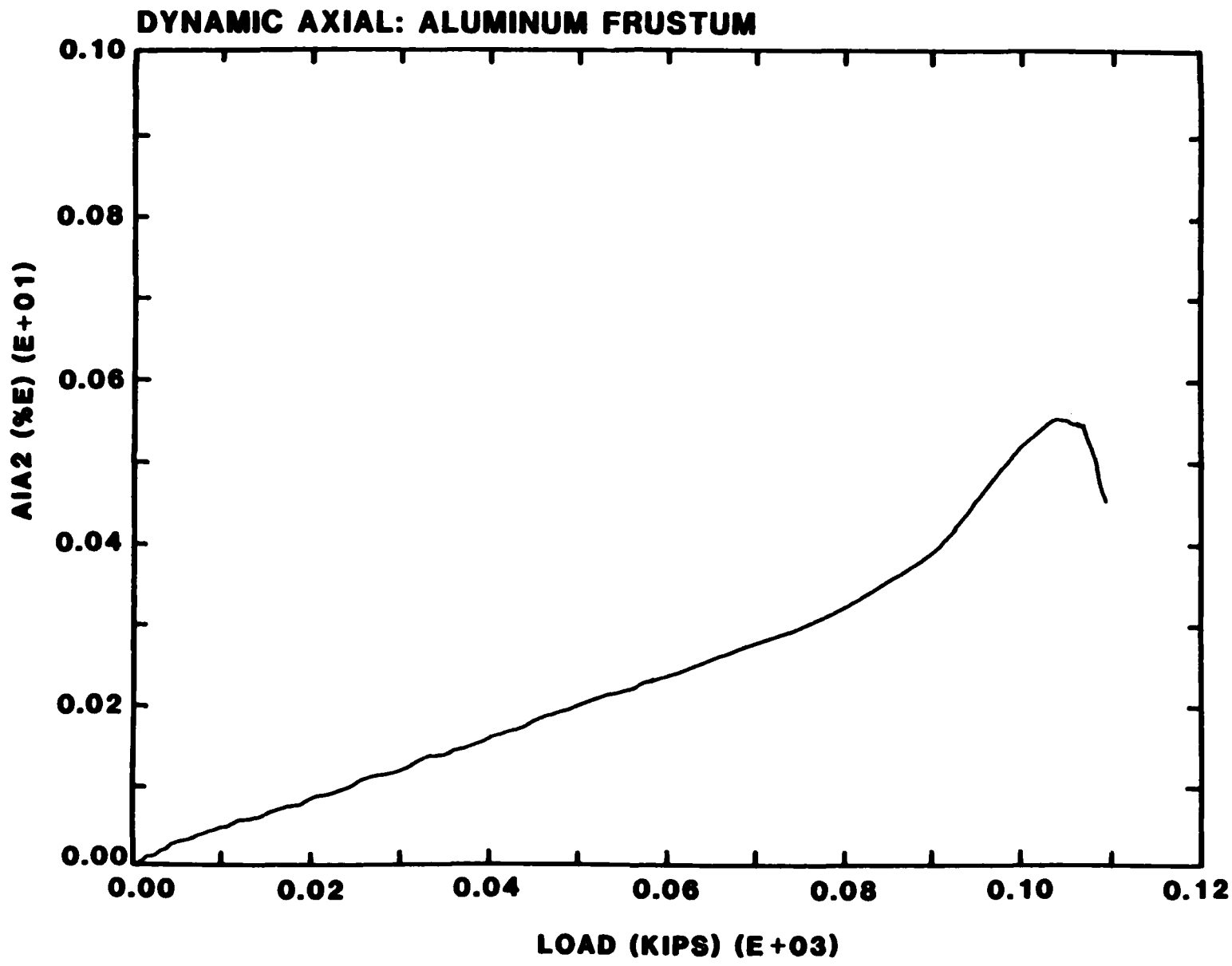
DYNAMIC AXIAL: ALUMINUM FRUSTUM
0.10
0.08
0.06
0.04
0.02
0.00
AIA2 (%E) (E+01)
0.00
0.02
0.04
0.06
0.08
0.10
0.12
LOAD (KIPS) (E+03)

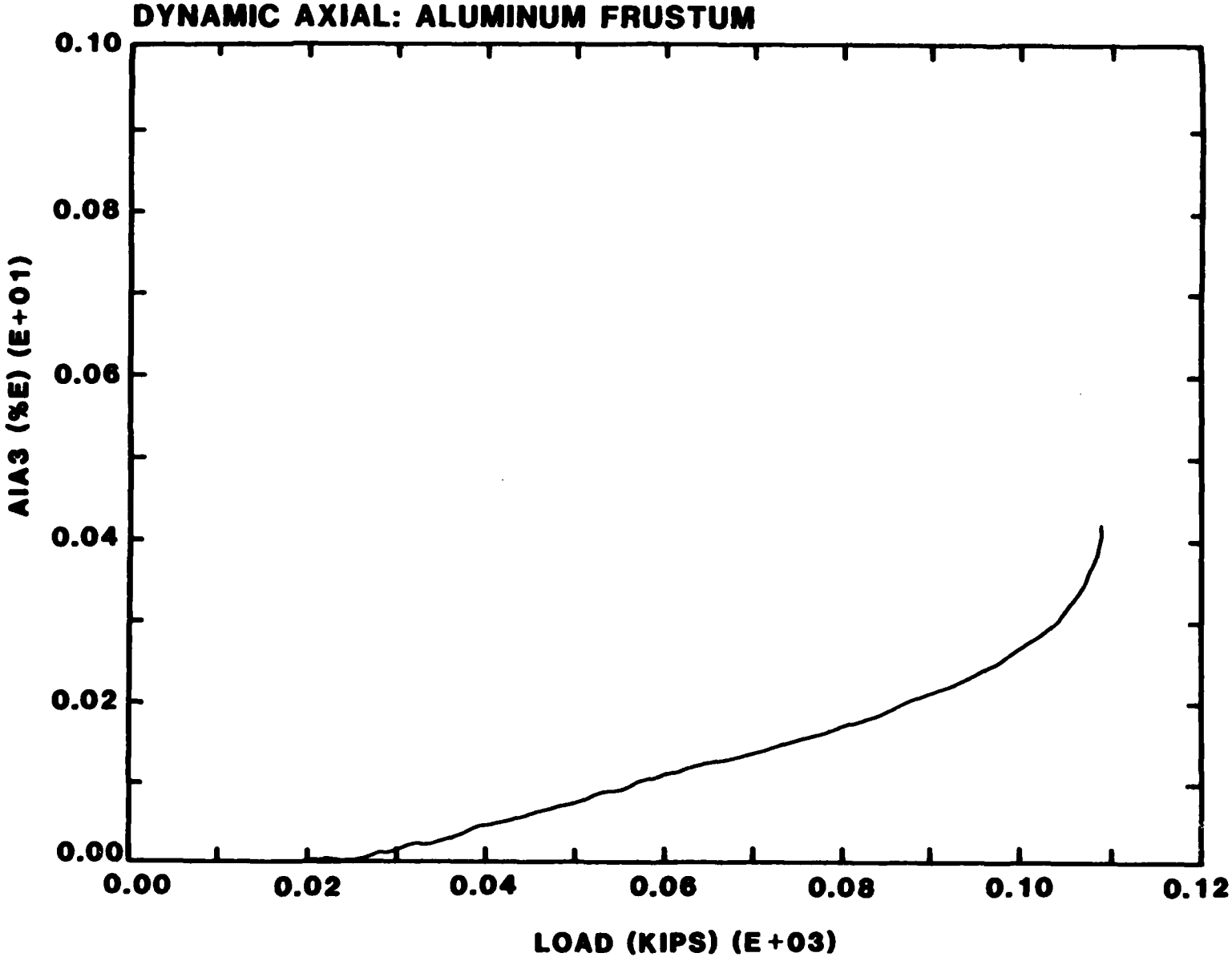
DYNAMIC AXIAL: ALUMINUM FRUSTUM
0.10
0.08
0.06
0.04
0.02
0.00
AIA3 (%E) (E+01)
0.00
0.02
0.04
0.06
0.08
0.10
0.12
LOAD (KIPS) (E+03)

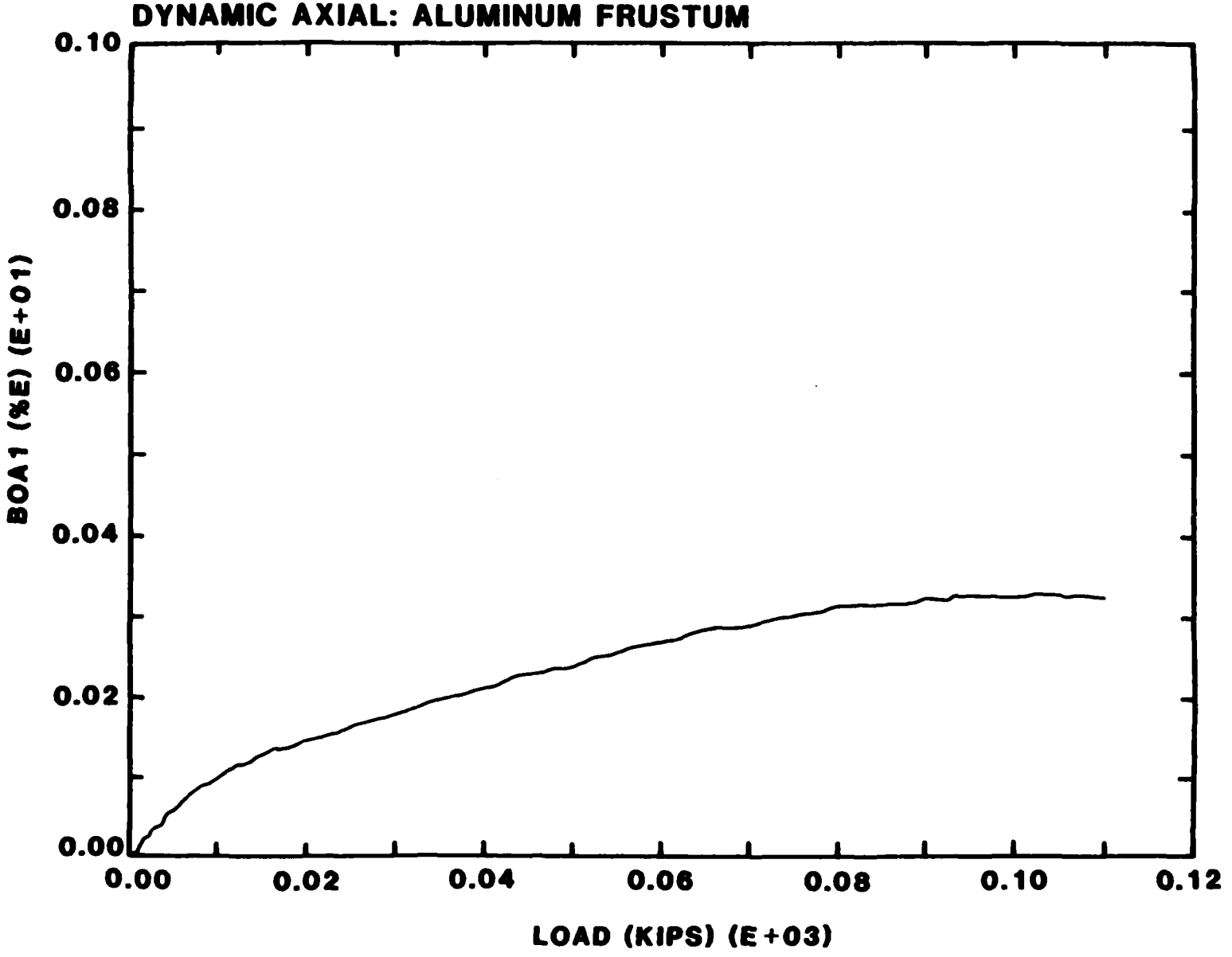
DYNAMIC AXIAL: ALUMINUM FRUSTUM
0.10
0.08
0.06
0.04
0.02
0.00
BOA1 (%E) (E+01)
0.00
0.02
0.04
0.06
0.08
0.10
0.12
LOAD (KIPS) (E+03)

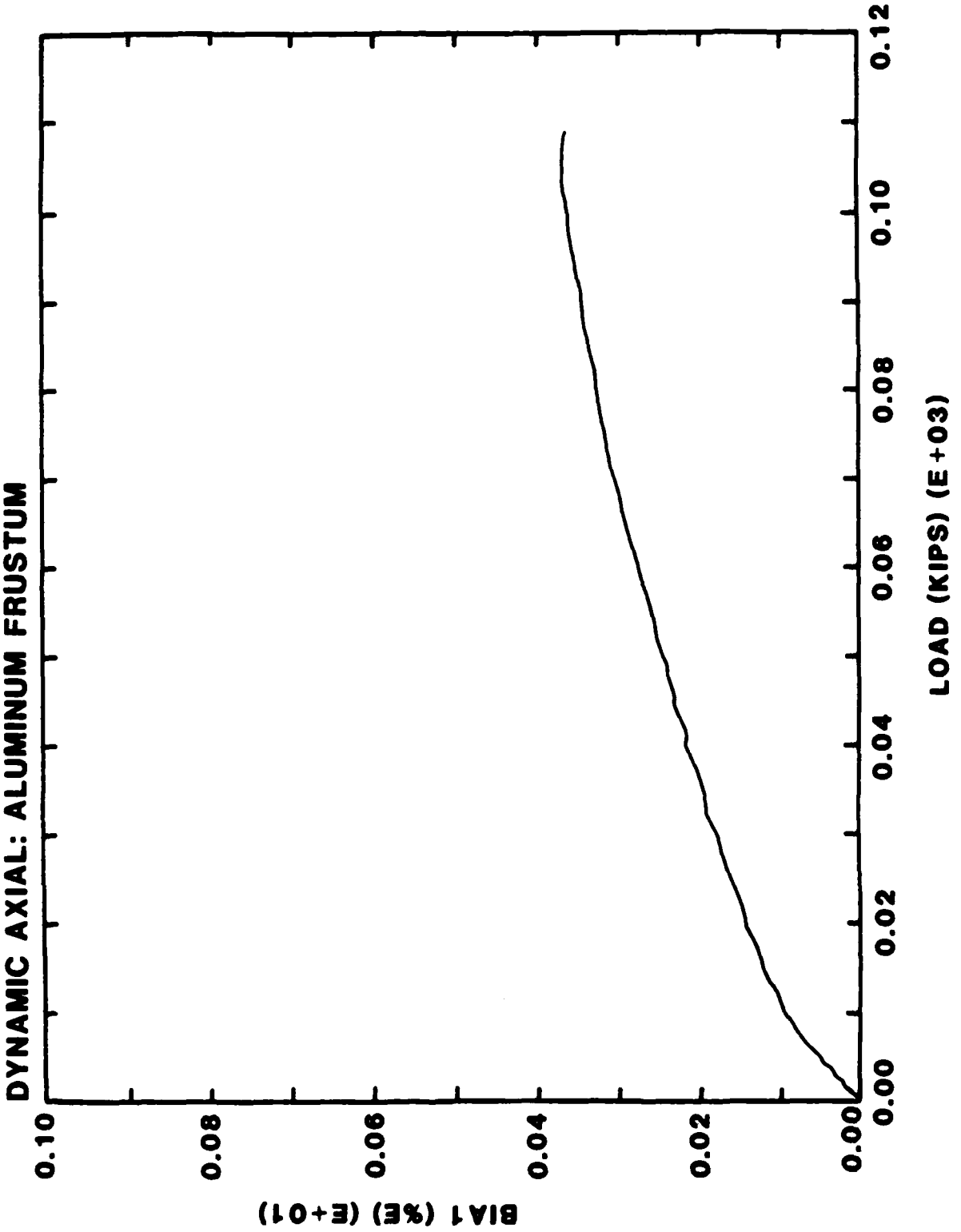
DYNAMIC AXIAL: ALUMINUM FRUSTUM
BIA1 (%E) (E+01)
0.10
0.08
0.06
0.04
0.02
0.00
0.00
0.02
0.04
0.06
0.08
0.10
0.12
LOAD (KIPS) (E+03)

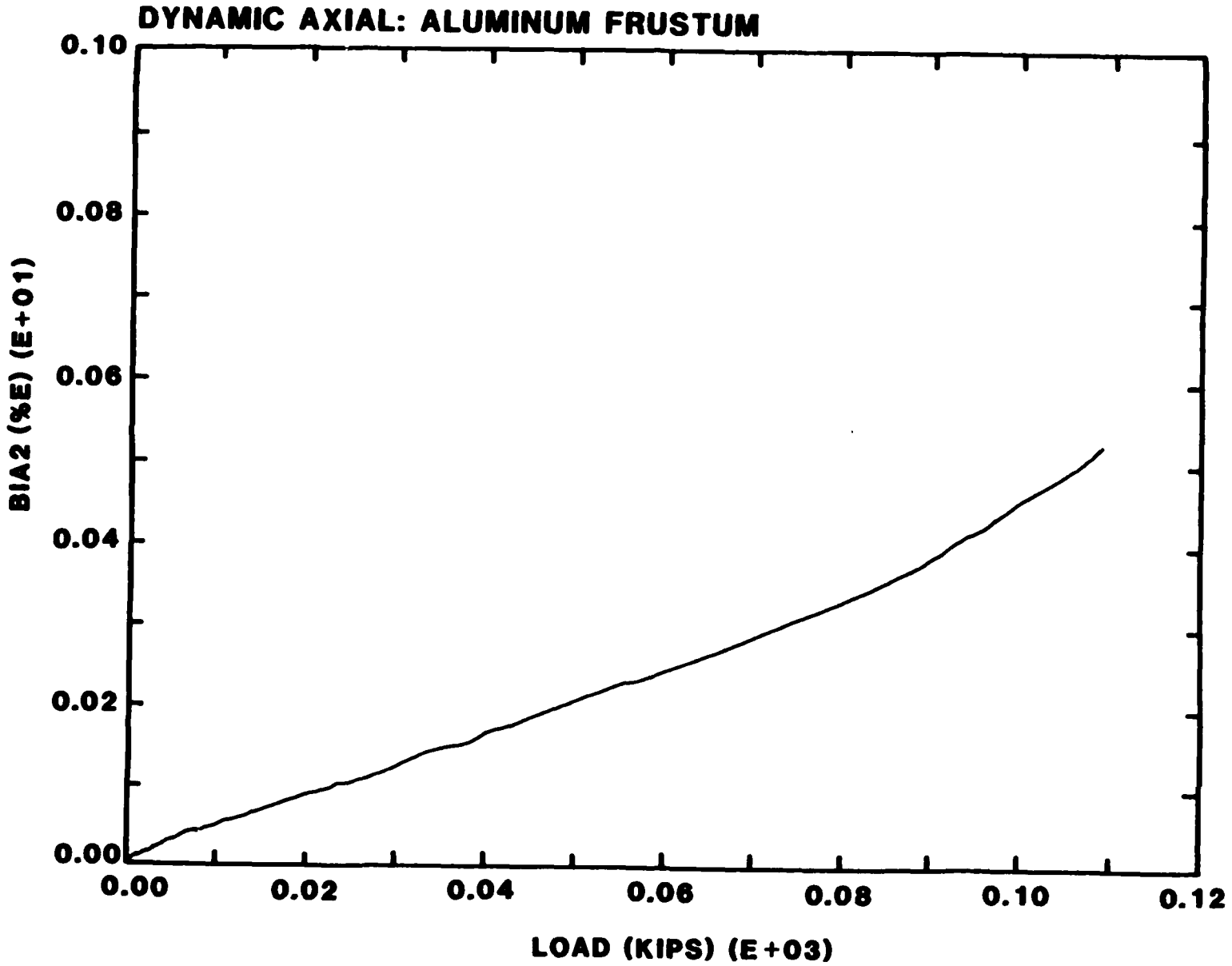
DYNAMIC AXIAL: ALUMINUM FRUSTUM
0.10
0.08
0.06
0.04
0.02
0.00
BIA2 (%E) (E+01)
0.00
0.02
0.04
0.06
0.08
0.10
0.12
LOAD (KIPS) (E+03)

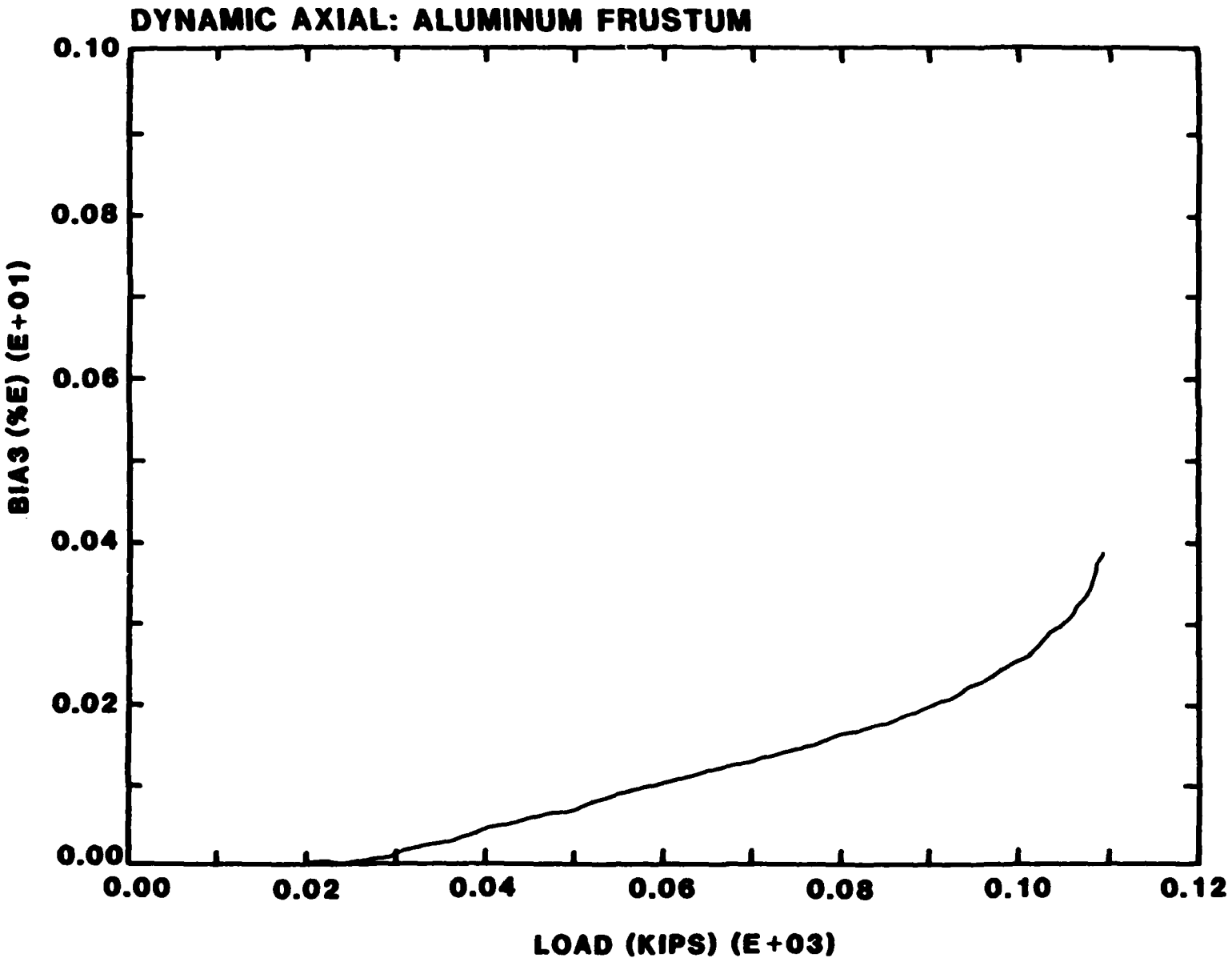
DYNAMIC AXIAL: ALUMINUM FRUSTUM
BIA3 (%E) (E+01)
0.10
0.08
0.06
0.04
0.02
0.00
0.00
0.02
0.04
0.06
0.08
0.10
0.12
LOAD (KIPS) (E+03)

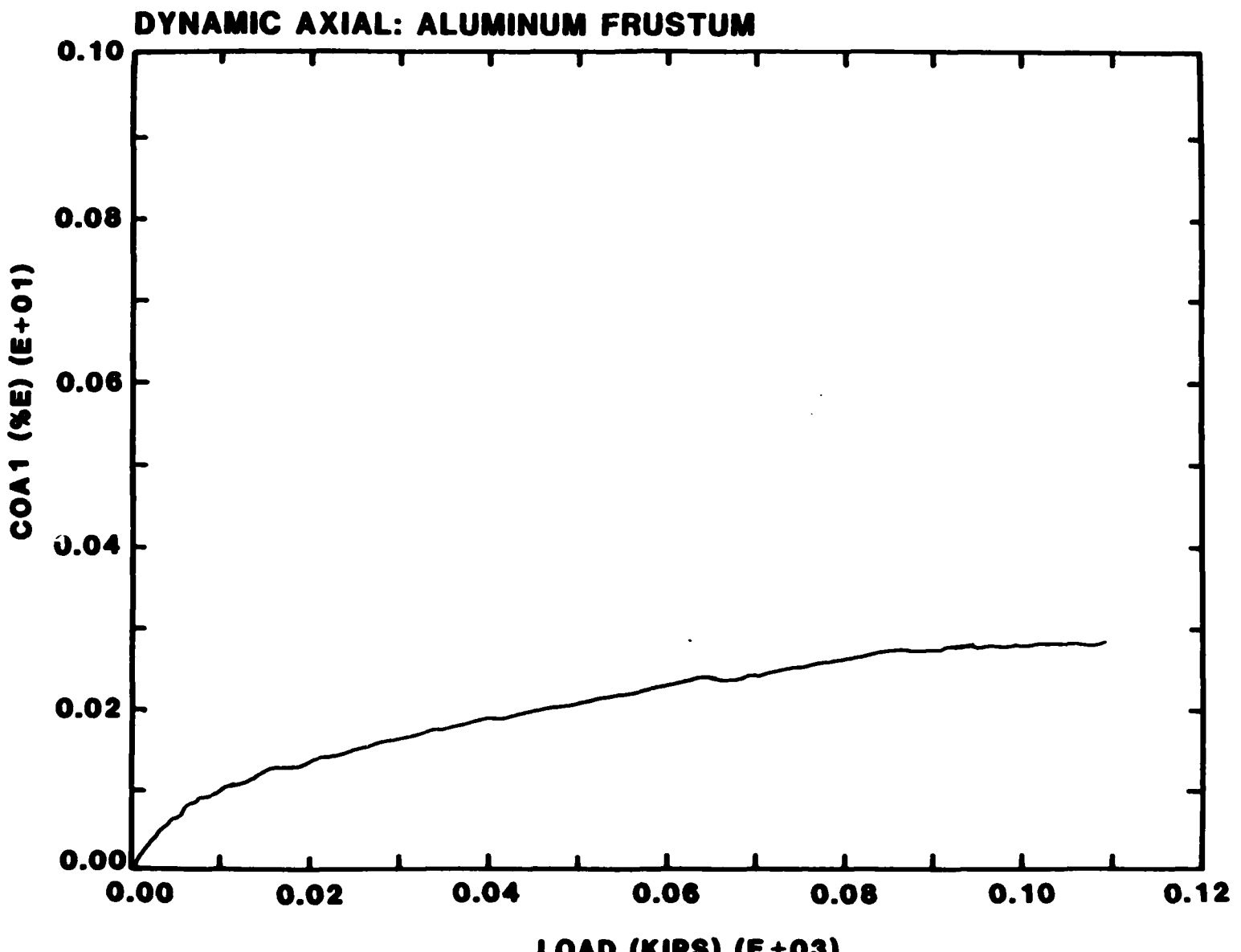
DYNAMIC AXIAL: ALUMINUM FRUSTUM
0.10
0.08
0.06
0.04
0.02
0.00
COA1 (%E) (E+01)
0.00
0.02
0.04
0.06
0.08
0.10
0.12
LOAD (KIPS) (E+03)

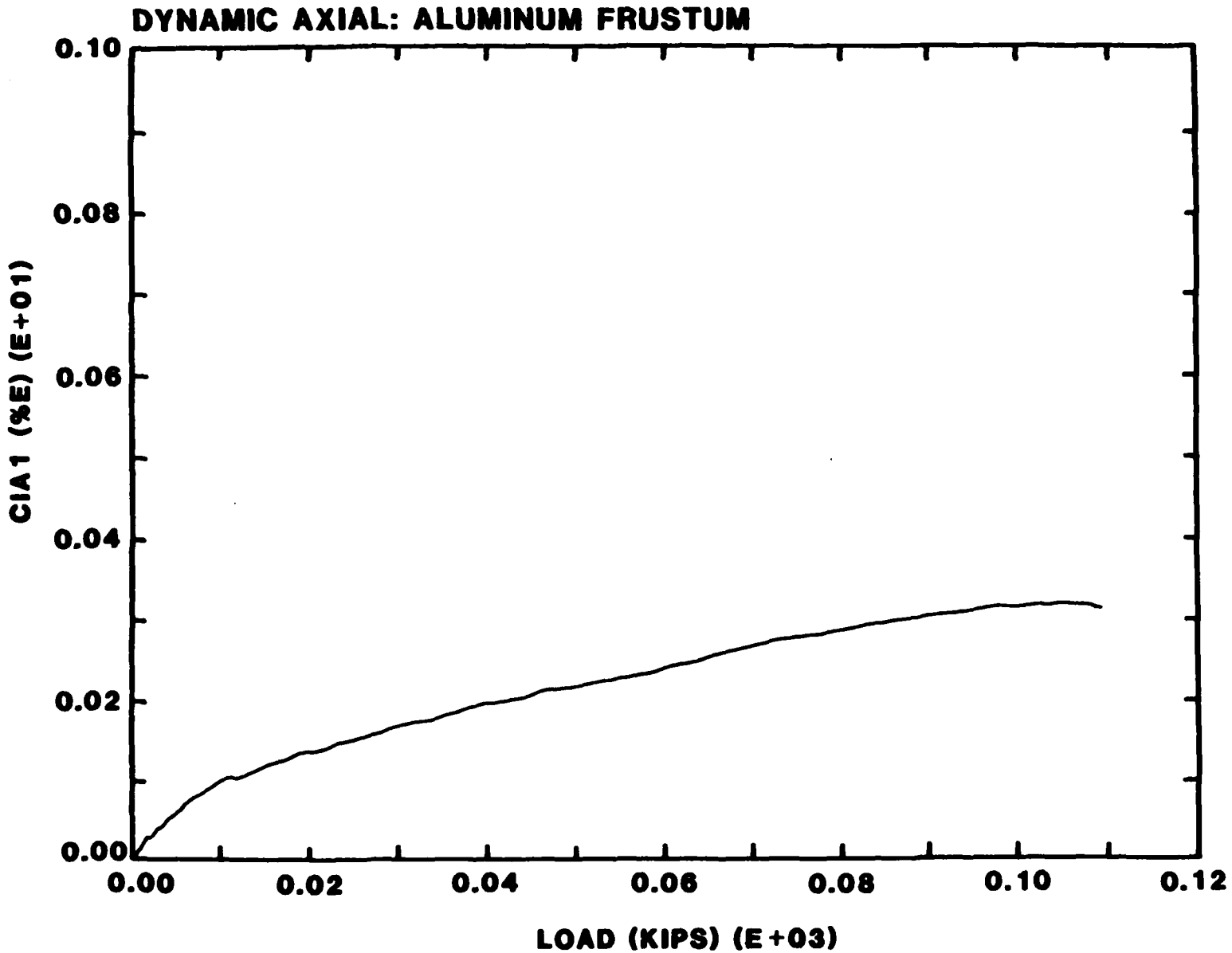
DYNAMIC AXIAL: ALUMINUM FRUSTUM
0.10
0.08
0.06
0.04
0.02
0.00
CIA1 (%E) (E+01)
0.00
0.02
0.04
0.06
0.08
0.10
0.12
LOAD (KIPS) (E+03)

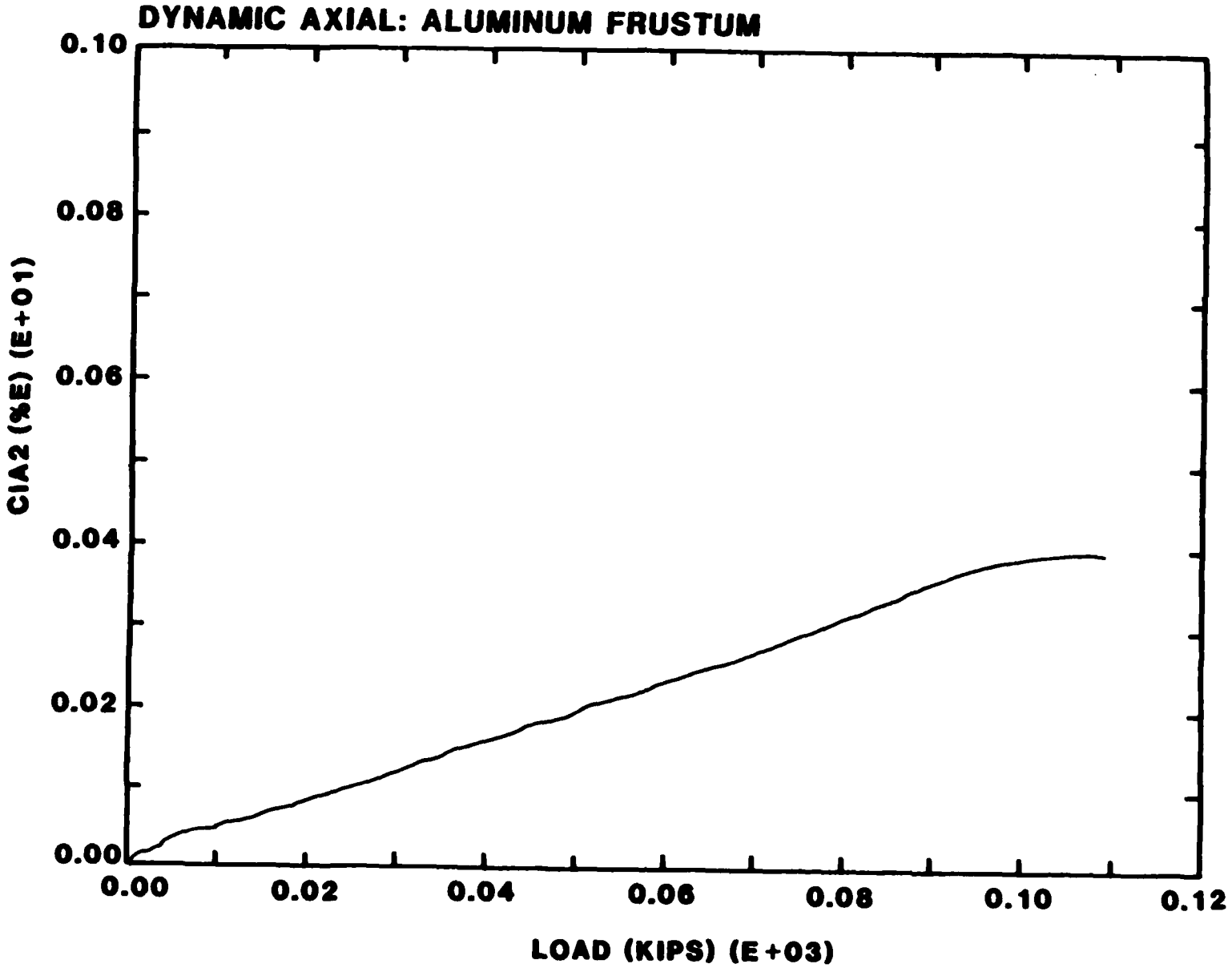
DYNAMIC AXIAL: ALUMINUM FRUSTUM
0.10
0.08
0.06
0.04
0.02
0.00
CIA2 (%E) (E+01)
0.00
0.02
0.04
0.06
0.08
0.10
0.12
LOAD (KIPS) (E+03)

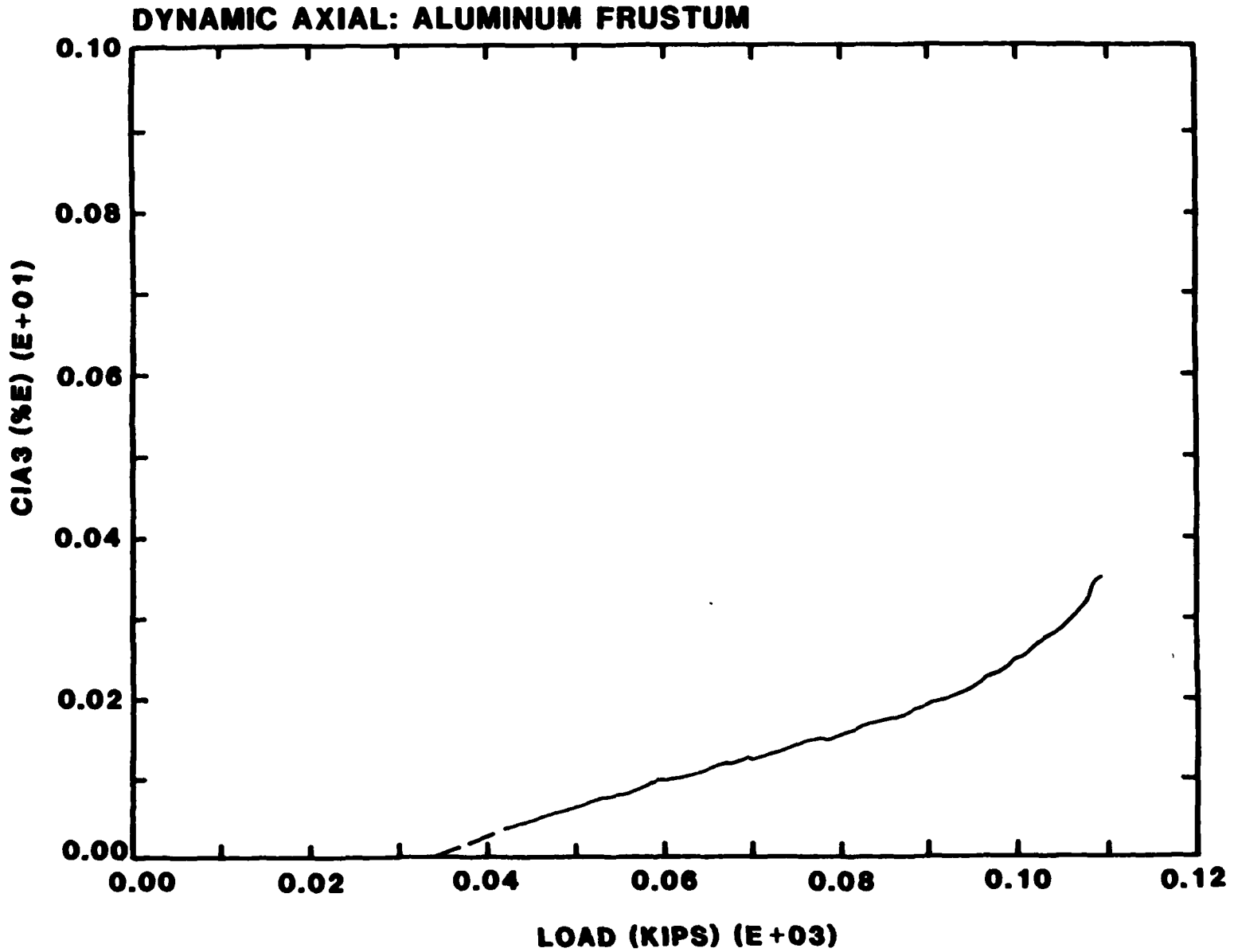
DYNAMIC AXIAL: ALUMINUM FRUSTUM
0.10
0.08
0.06
0.04
0.02
0.00
CIA3 (%E) (E+01)
0.00
0.02
0.04
0.06
0.08
0.10
0.12
LOAD (KIPS) (E+03)

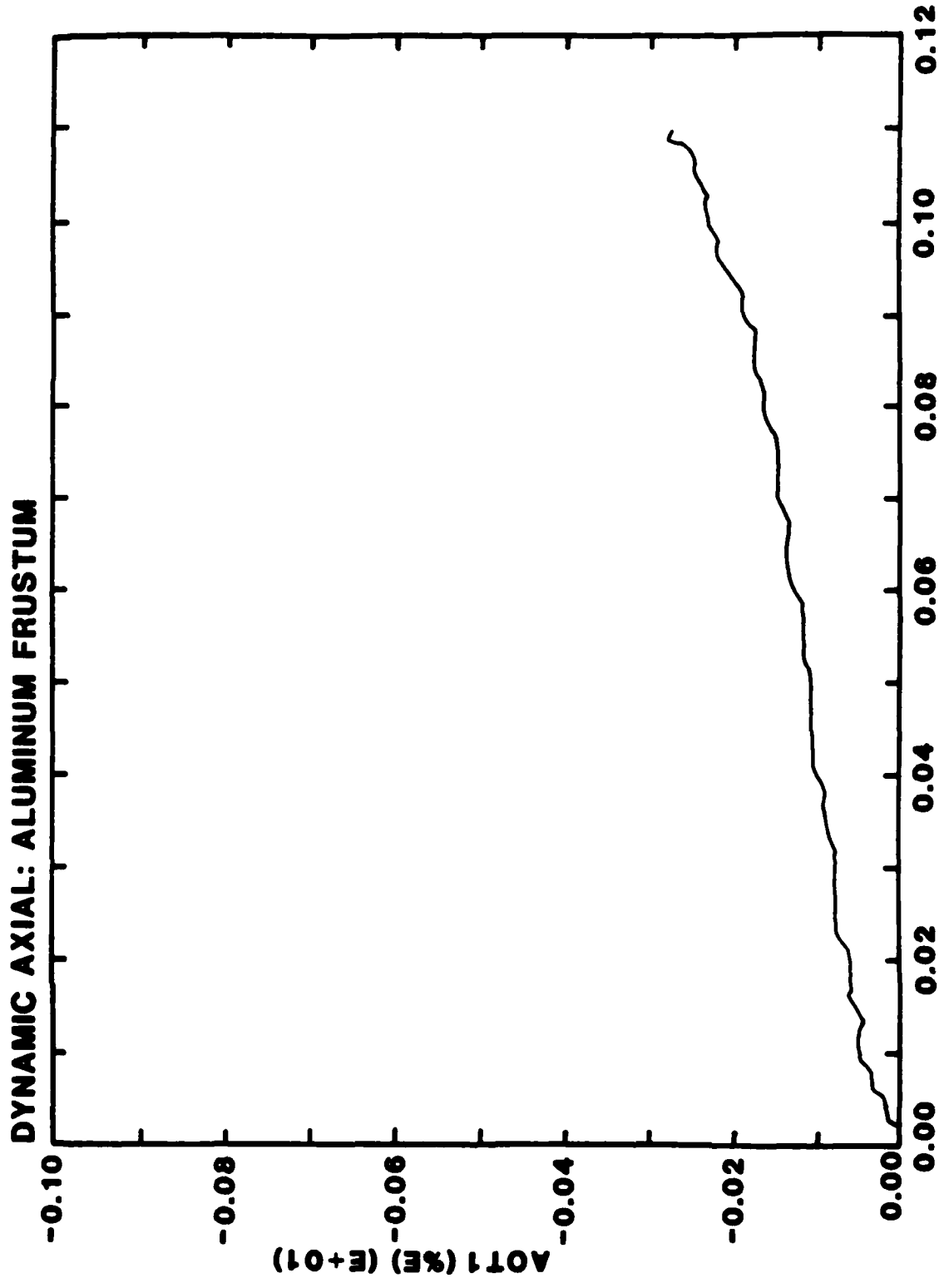
DYNAMIC AXIAL: ALUMINUM FRUSTUM
AOT1 (%E) (E+01)
-0.10
-0.08
-0.06
-0.04
-0.02
0.00
LOAD (KIPS) (E+03)
0.00
0.02
0.04
0.06
0.08
0.10
0.12

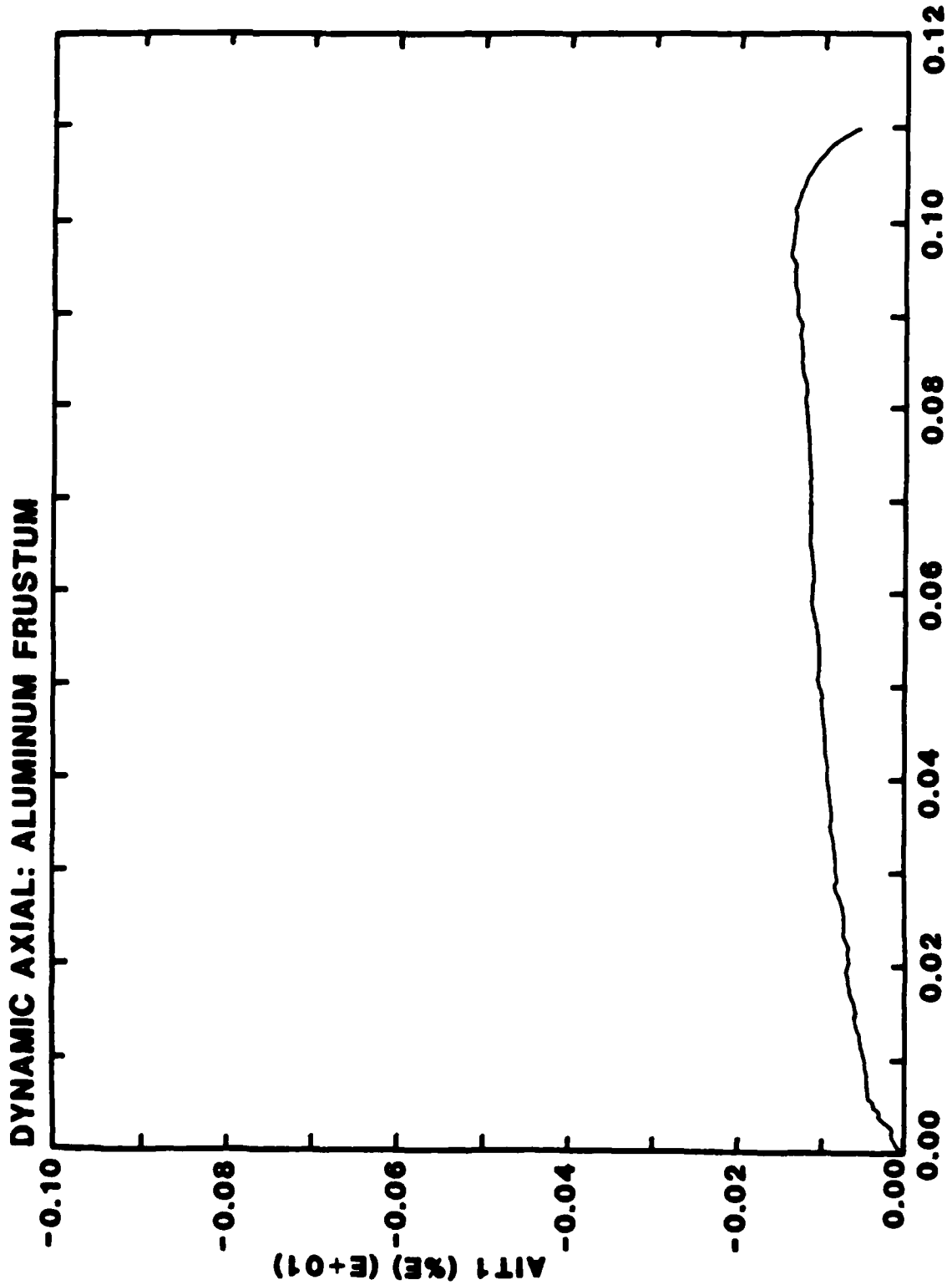
DYNAMIC AXIAL: ALUMINUM FRUSTUM
AIT1 (%E) (E+01)
-0.10
-0.08
-0.06
-0.04
-0.02
0.00
LOAD (KIPS) (E+03)
0.00
0.02
0.04
0.06
0.08
0.10
0.12

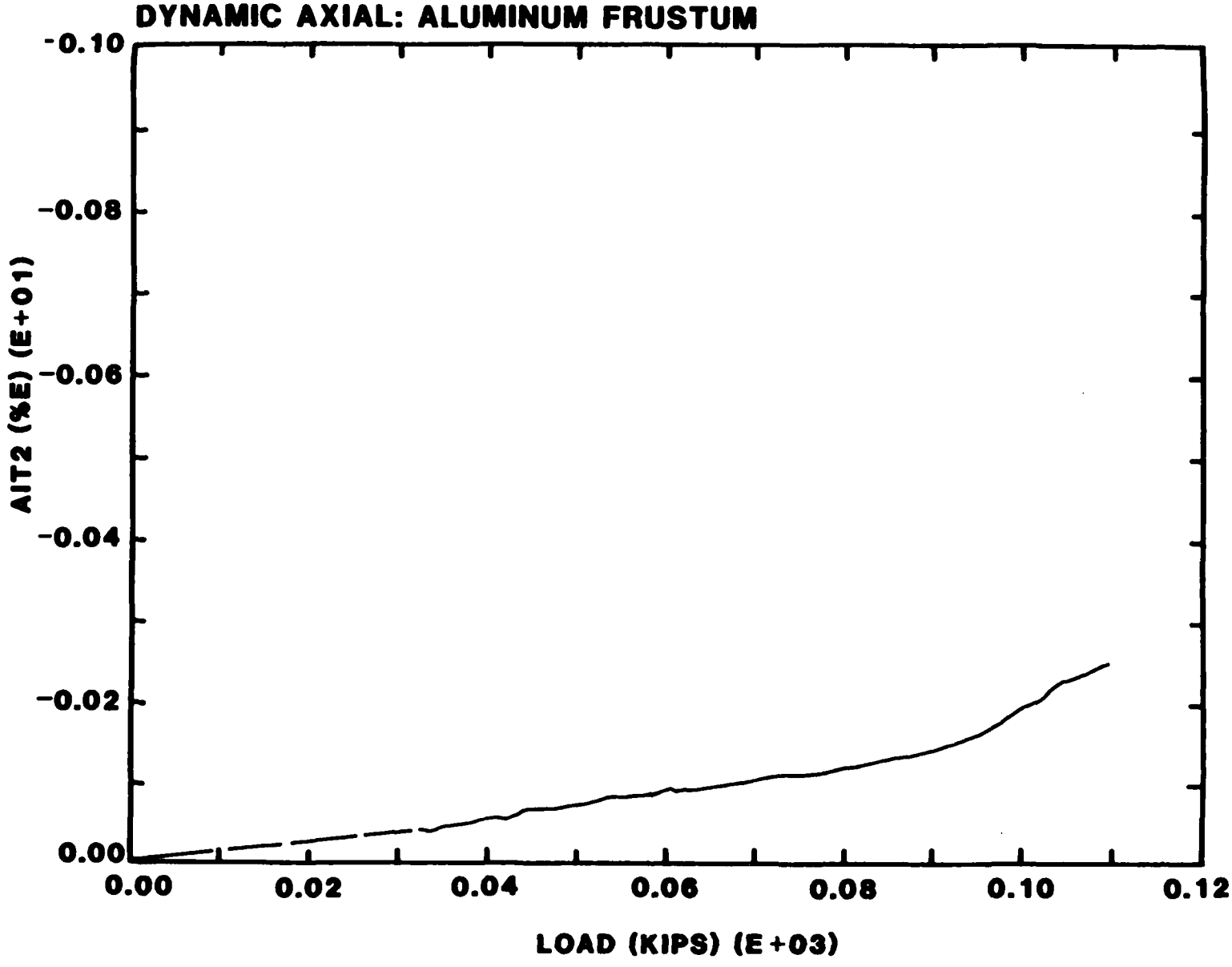
DYNAMIC AXIAL: ALUMINUM FRUSTUM
-0.10
-0.08
-0.06
-0.04
-0.02
0.00
AIT2 (%E) (E+01)
0.00
0.02
0.04
0.06
0.08
0.10
0.12
LOAD (KIPS) (E+03)

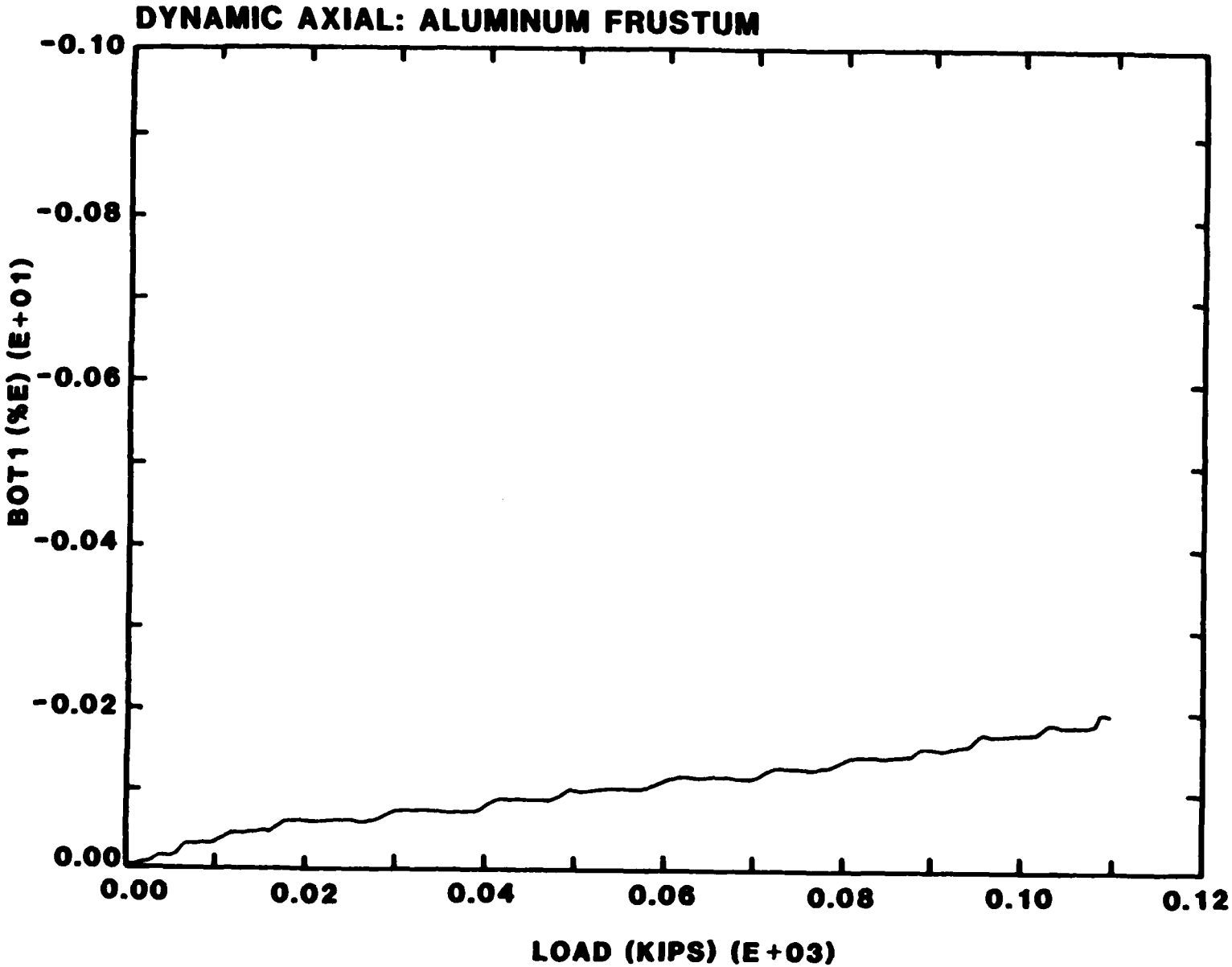
DYNAMIC AXIAL: ALUMINUM FRUSTUM
-0.10
-0.08
-0.06
-0.04
-0.02
0.00
BOT1 (%E) (E+01)
0.00
0.02
0.04
0.06
0.08
0.10
0.12
LOAD (KIPS) (E+03)

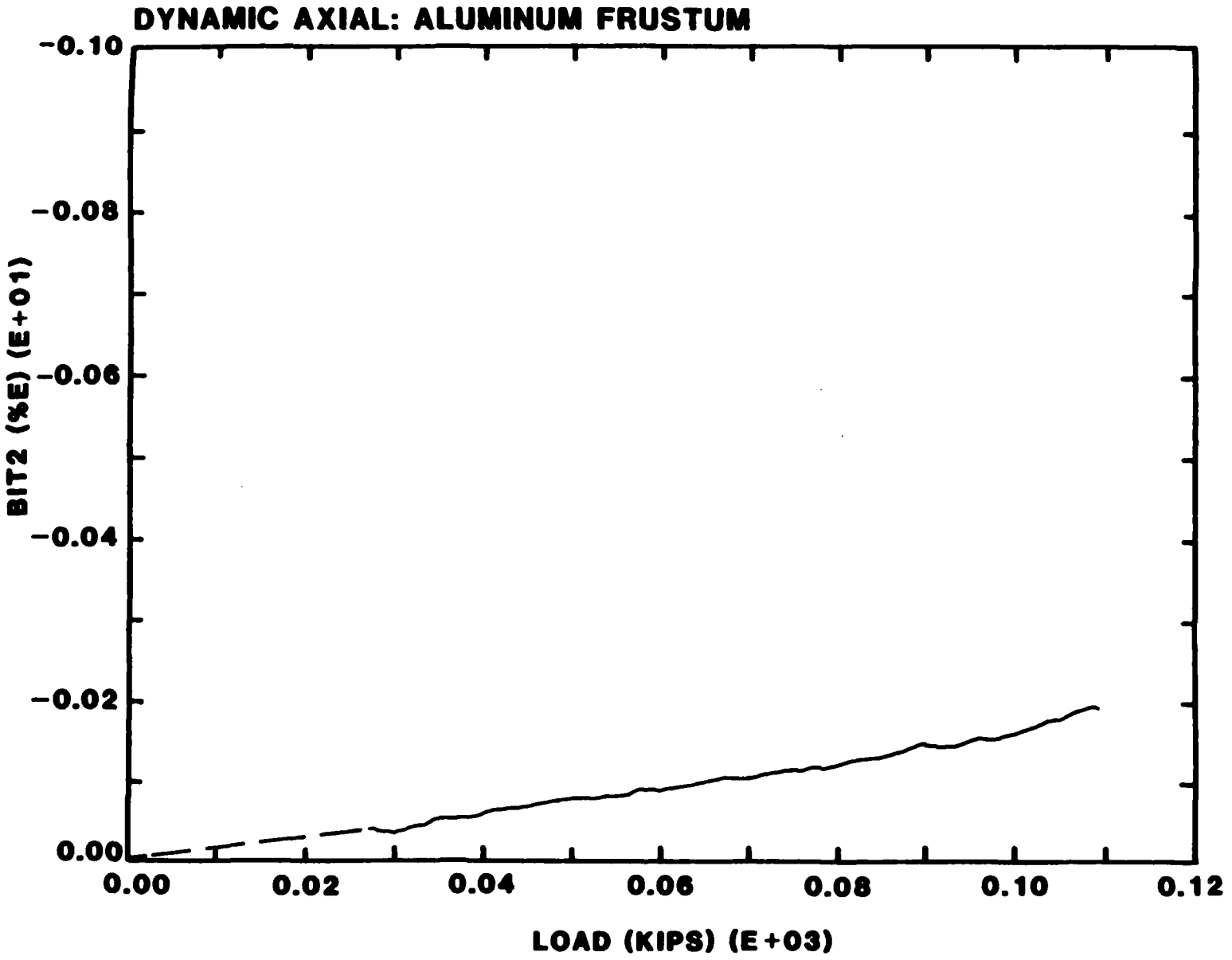
DYNAMIC AXIAL: ALUMINUM FRUSTUM
-0.10
-0.08
-0.06
-0.04
-0.02
0.00
BIT2 (%E) (E+01)
0.00
0.02
0.04
0.06
0.08
0.10
0.12
LOAD (KIPS) (E+03)

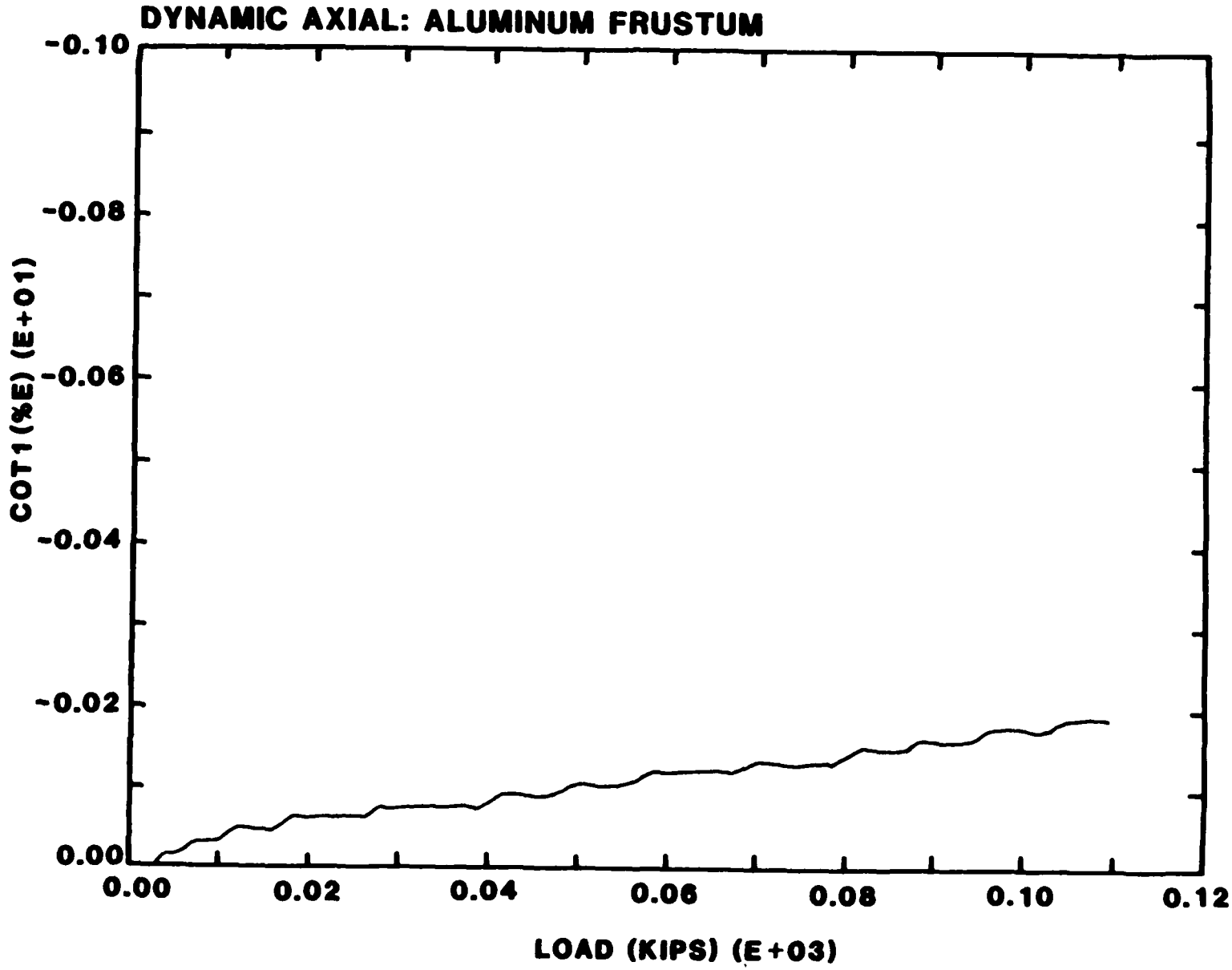
DYNAMIC AXIAL: ALUMINUM FRUSTUM
-0.10
-0.08
-0.06
-0.04
-0.02
0.00
COT1 (%E) (E+01)
0.00
0.02
0.04
0.06
0.08
0.10
0.12
LOAD (KIPS) (E+03)

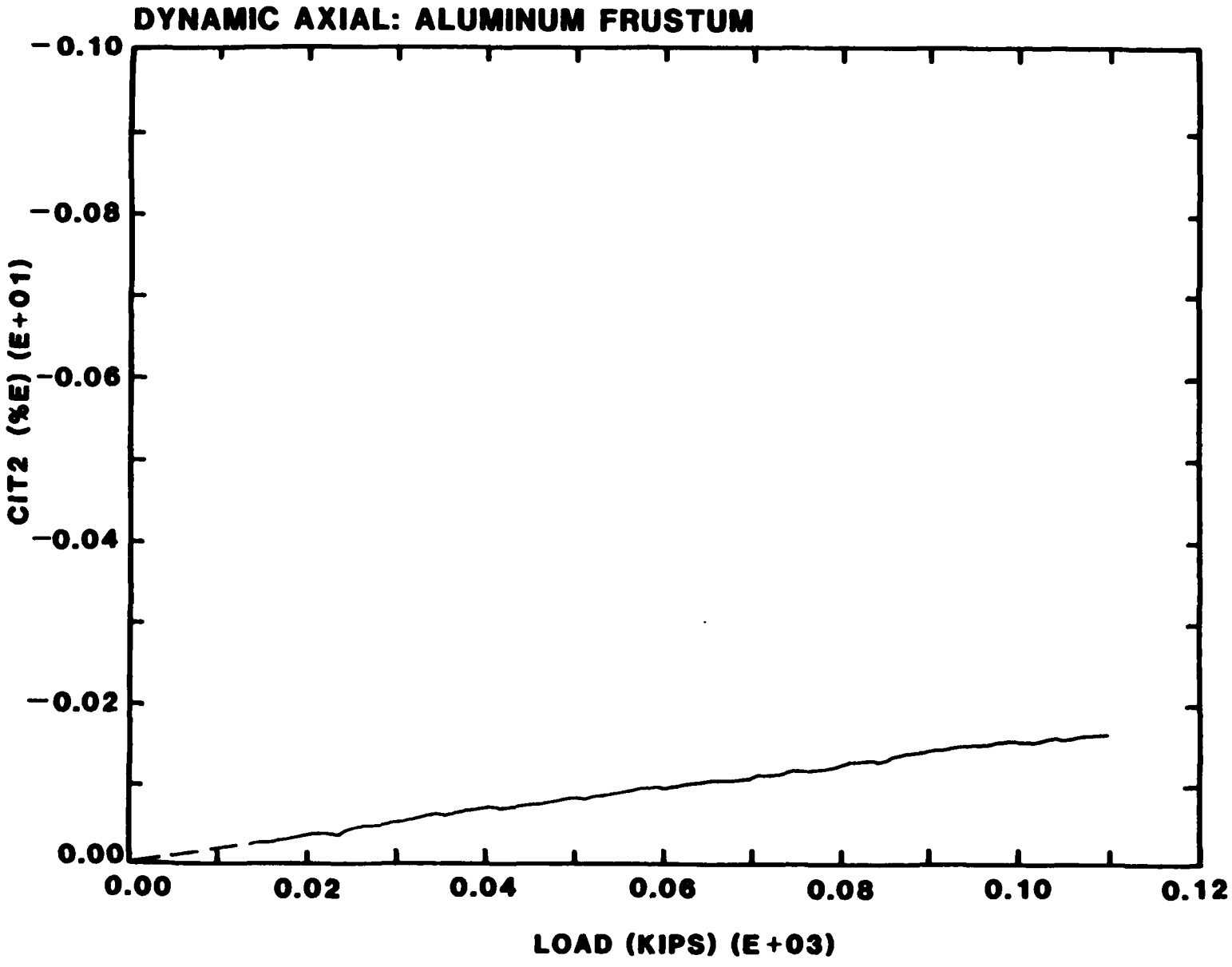
DYNAMIC AXIAL: ALUMINUM FRUSTUM
-0.10
-0.08
-0.06
-0.04
-0.02
0.00
CIT2 (%E) (E+01)
0.00
0.02
0.04
0.06
0.08
0.10
0.12
LOAD (KIPS) (E+03)

7.3 APPENDIX C

STATIC-SHEAR/BEND LOADING TEST DATA
FOR ALUMINUM FRUSTA

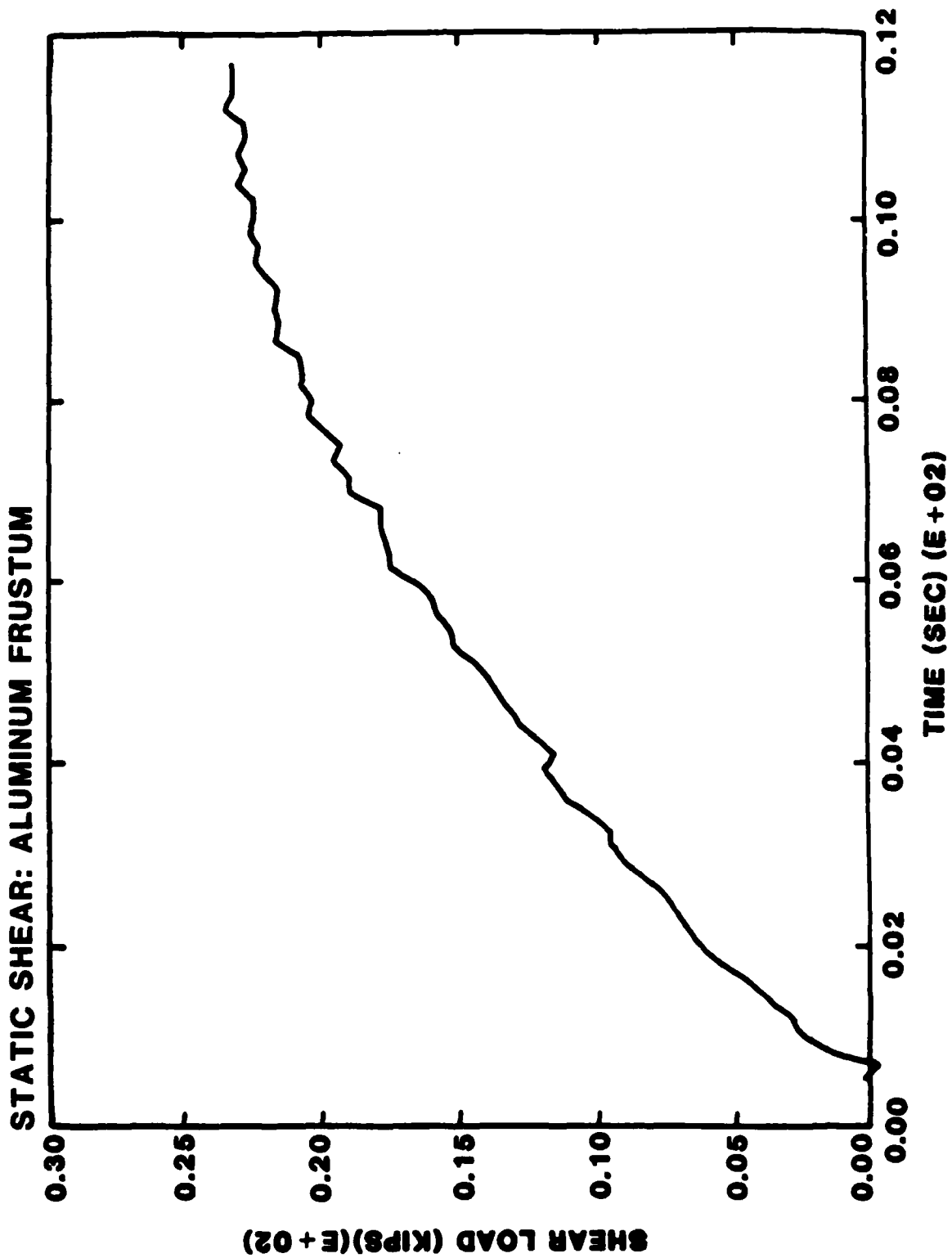
STATIC SHEAR: ALUMINUM FRUSTUM
SHEAR LOAD (KIPS)(E+02)
0.30
0.25
0.20
0.15
0.10
0.05
0.00
0.00
0.02
0.04
0.06
0.08
0.10
0.12
TIME (SEC) (E+02)

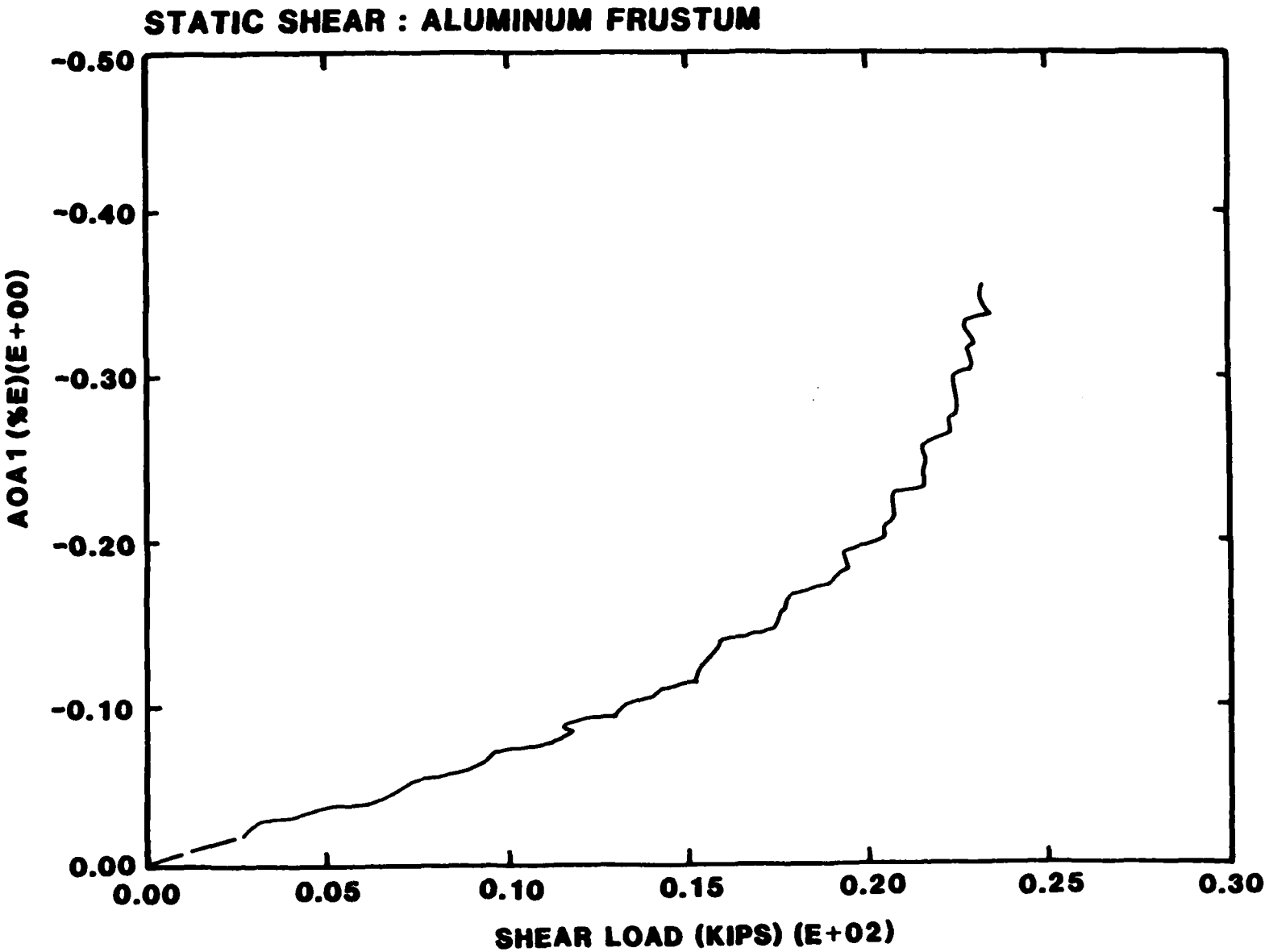
STATIC SHEAR : ALUMINUM FRUSTUM
-0.50
-0.40
-0.30
-0.20
-0.10
0.00
AOA1 (%E)(E+00)
0.00
0.05
0.10
0.15
0.20
0.25
0.30
SHEAR LOAD (KIPS) (E+02)

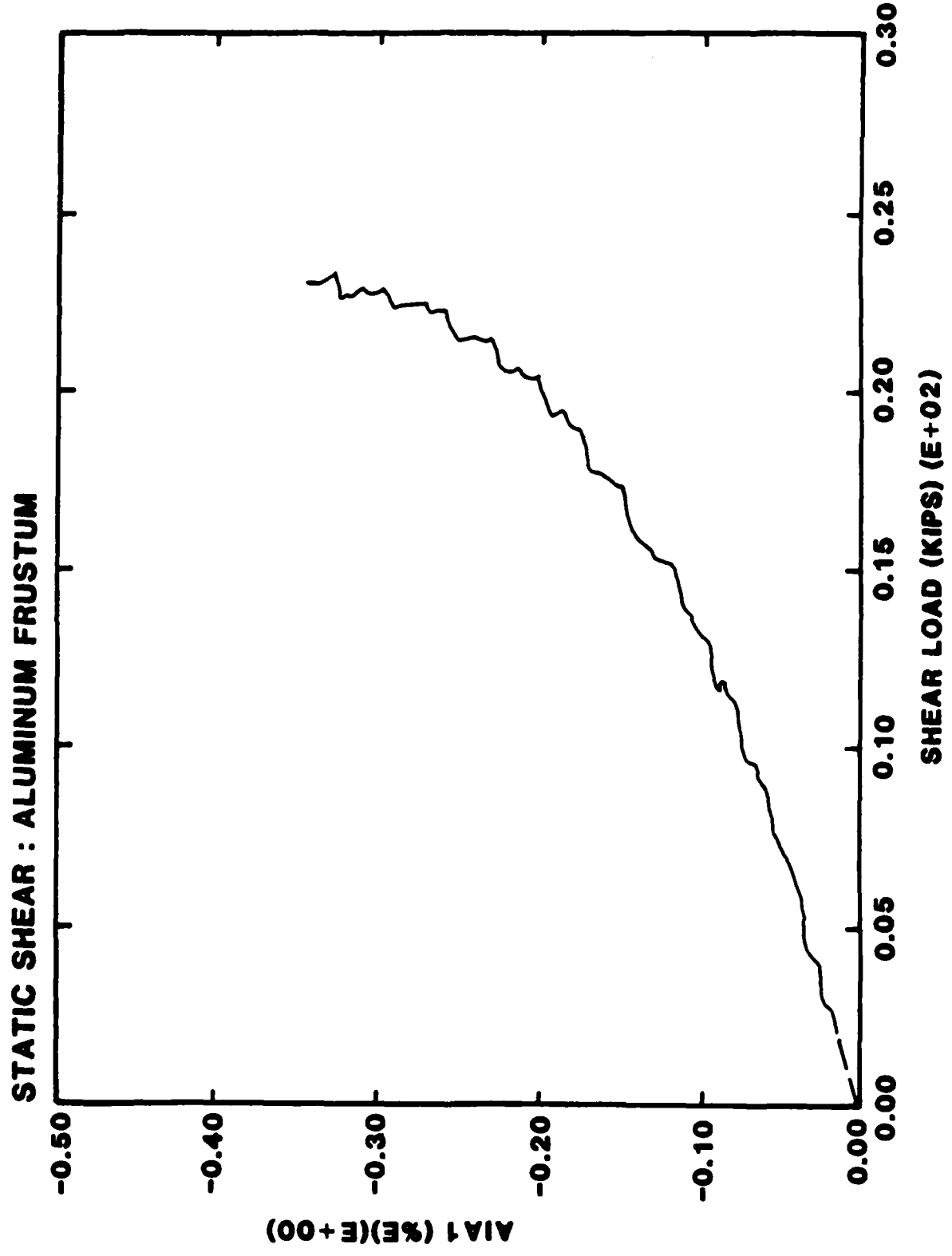
STATIC SHEAR : ALUMINUM FRUSTUM
AIA1 (%E)(E+00)
-0.50
-0.40
-0.30
-0.20
-0.10
0.00
SHEAR LOAD (KIPS) (E+02)
0.00
0.05
0.10
0.15
0.20
0.25
0.30

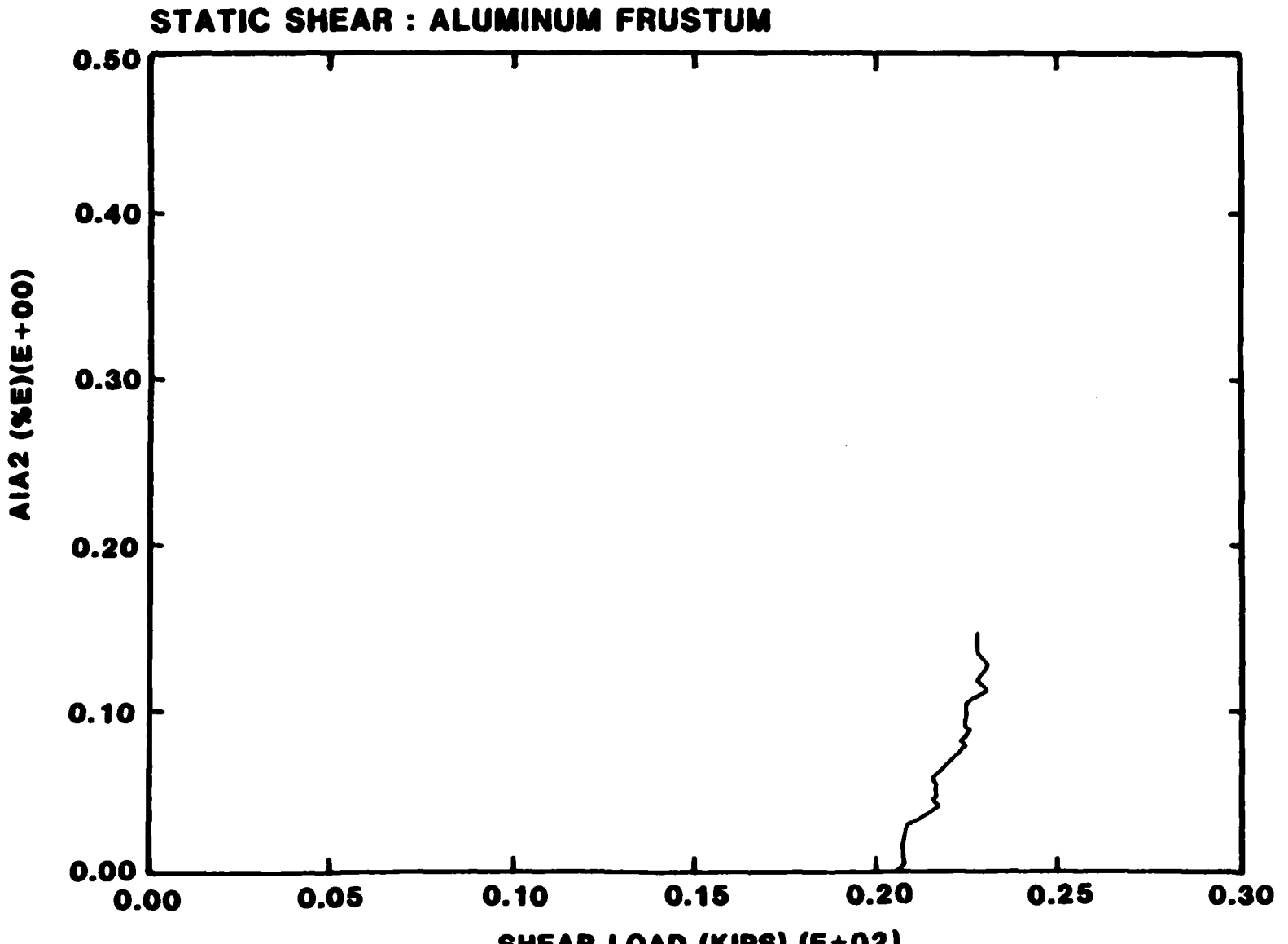
STATIC SHEAR : ALUMINUM FRUSTUM
0.50
0.40
0.30
0.20
0.10
0.00
AIA2 (%E)(E+00)
0.00
0.05
0.10
0.15
0.20
0.25
0.30
SHEAR LOAD (KIPS) (E+02)

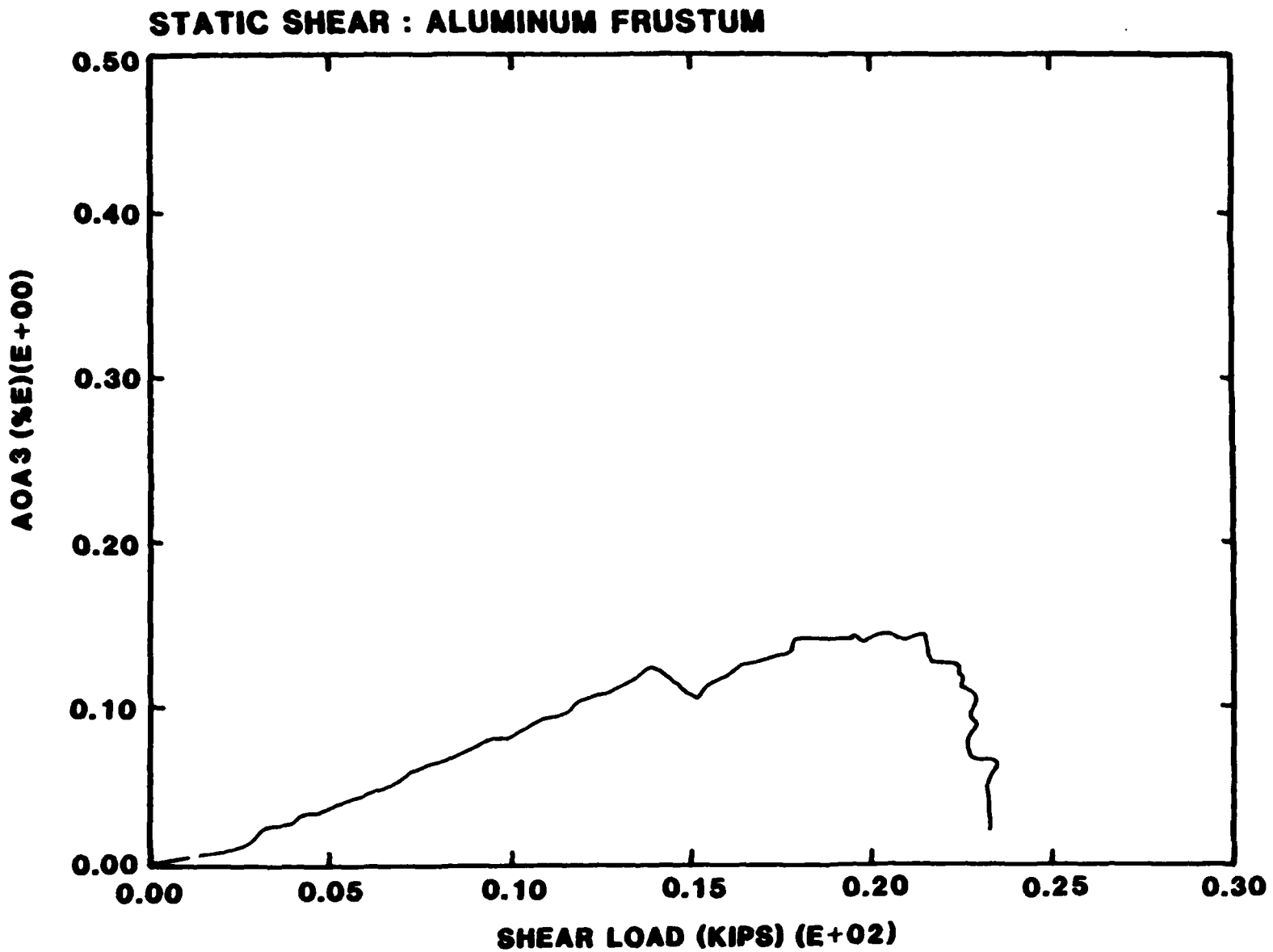
STATIC SHEAR : ALUMINUM FRUSTUM
AOA3 (%E)(E+00)
0.50
0.40
0.30
0.20
0.10
0.00
0.00
0.05
0.10
0.15
0.20
0.25
0.30
SHEAR LOAD (KIPS) (E+02)

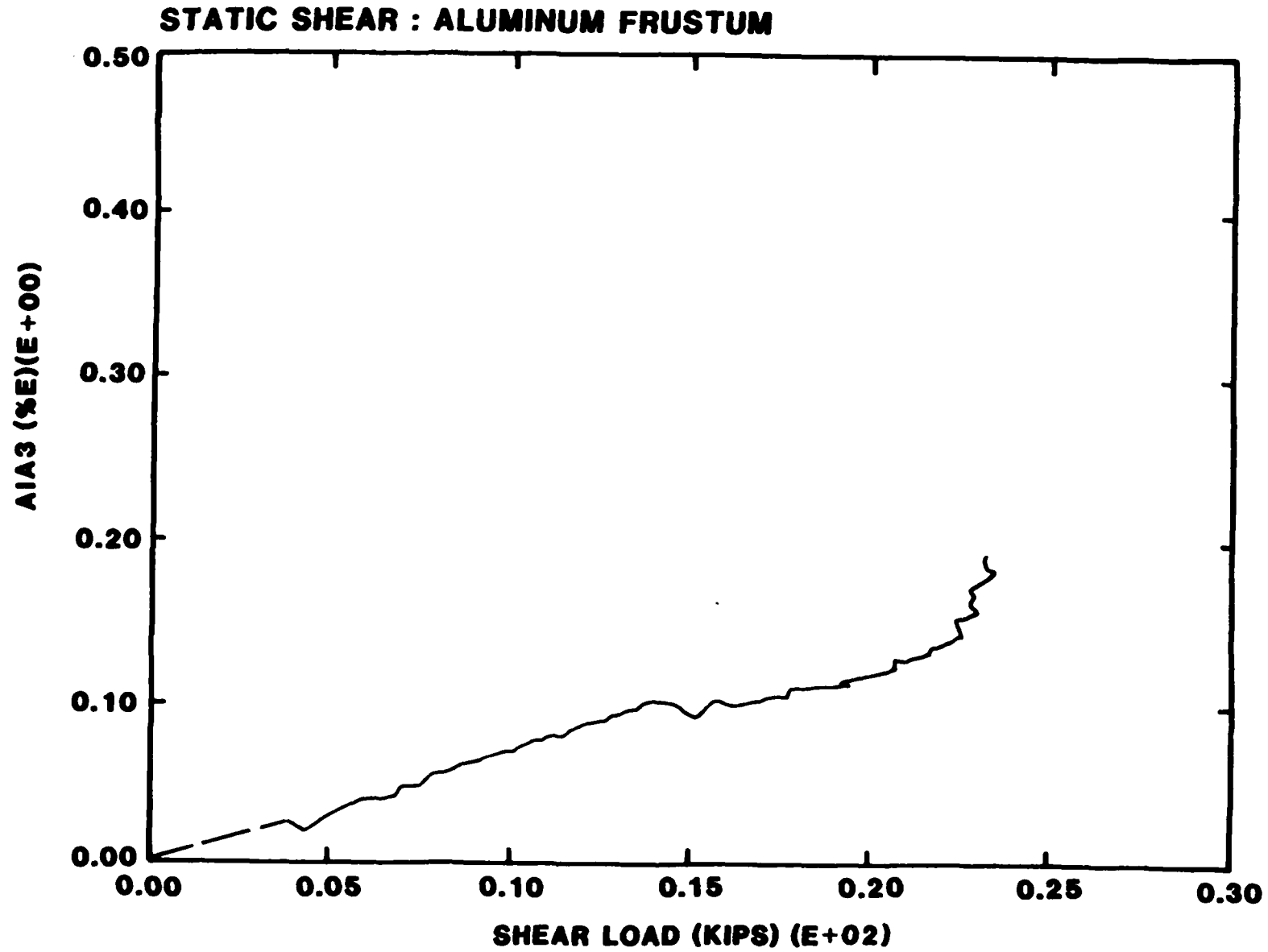
STATIC SHEAR : ALUMINUM FRUSTUM
0.50
0.40
0.30
0.20
0.10
0.00
AIA3 (%E)(E+00)
0.00
0.05
0.10
0.15
0.20
0.25
0.30
SHEAR LOAD (KIPS) (E+02)

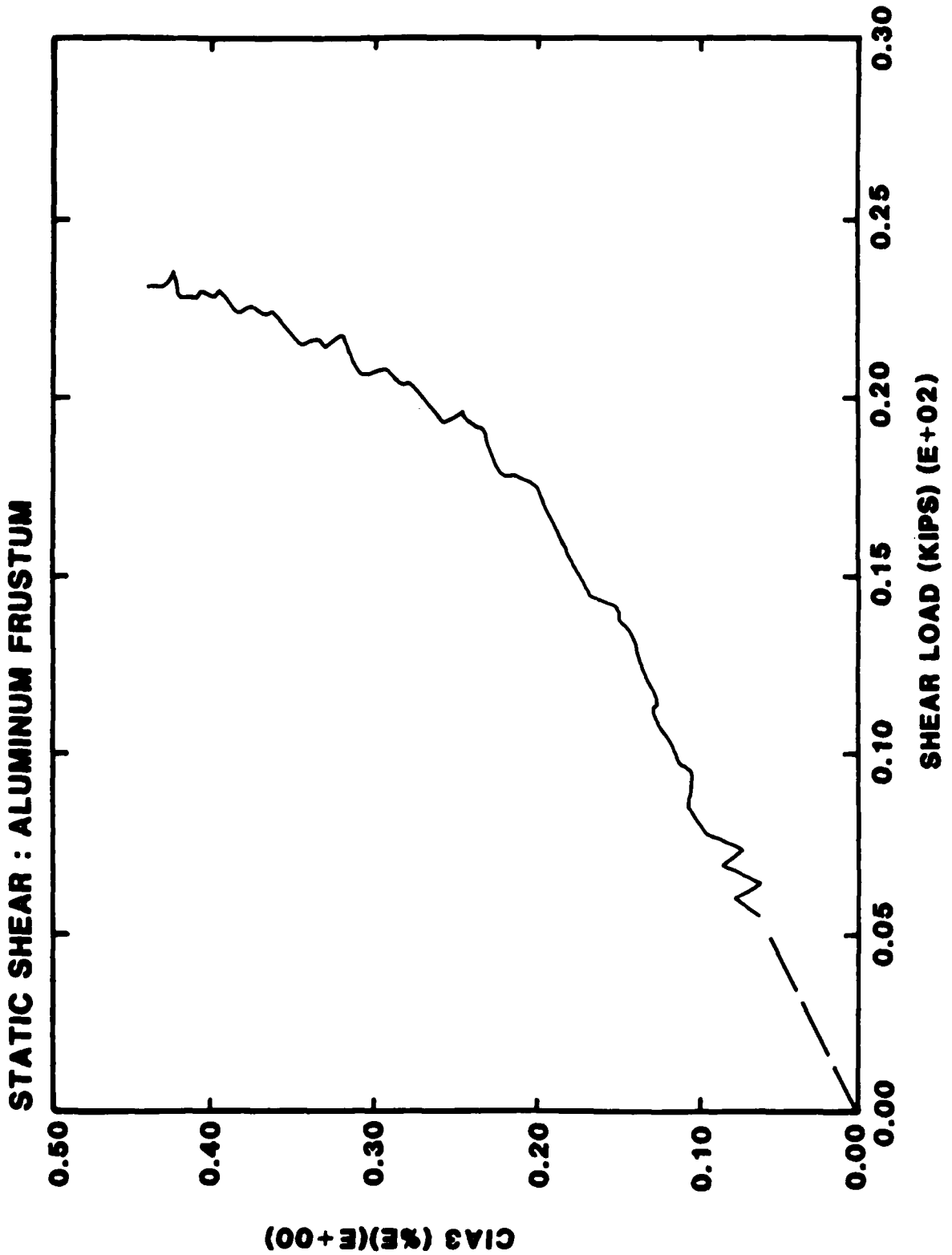
STATIC SHEAR : ALUMINUM FRUSTUM
CIA3 (%E)(E+00)
0.50
0.40
0.30
0.20
0.10
0.00
0.00
0.05
0.10
0.15
0.20
0.25
0.30
SHEAR LOAD (KIPS) (E+02)

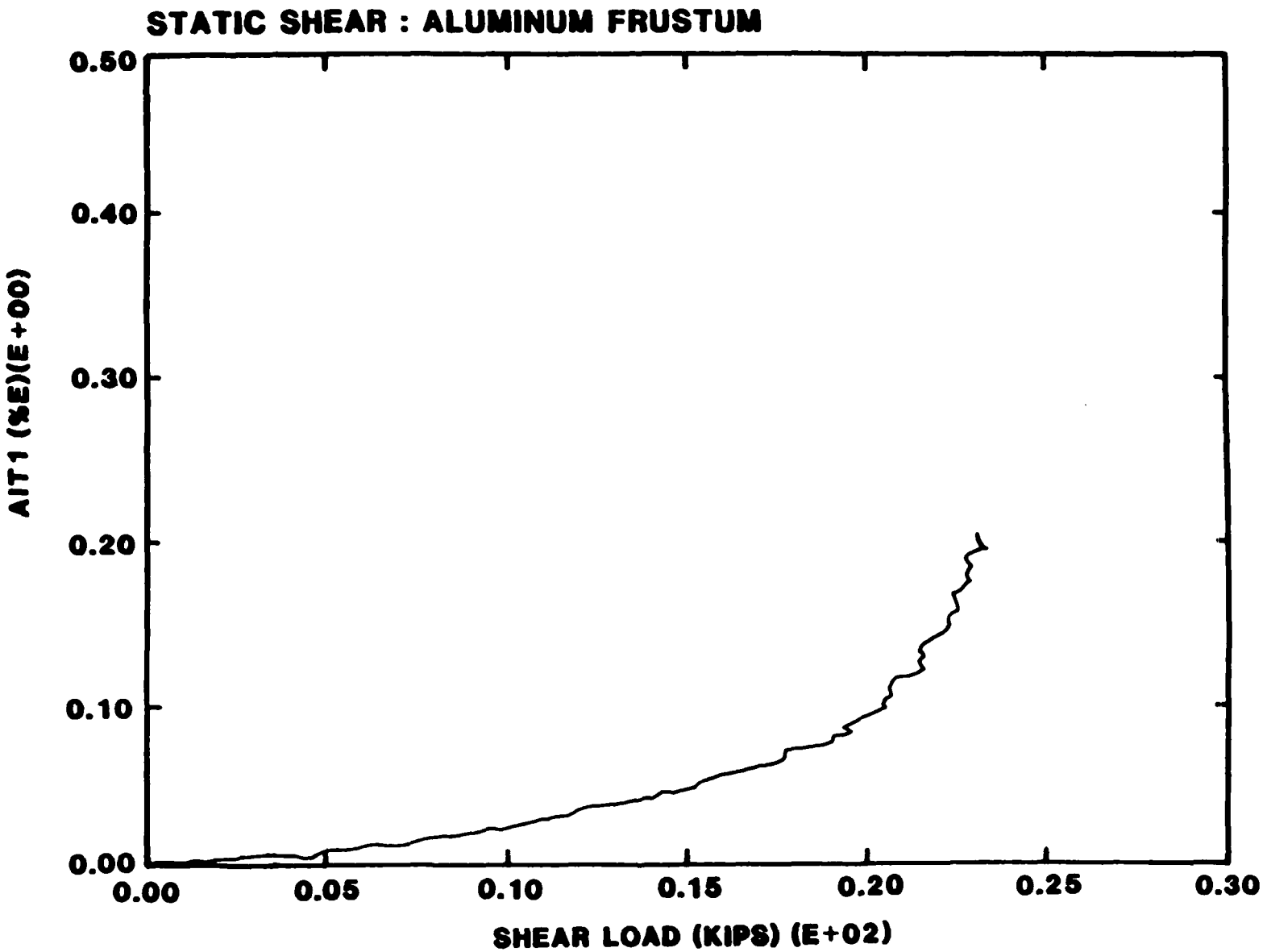
STATIC SHEAR : ALUMINUM FRUSTUM
AIT1 (%E)(E+00)
0.50
0.40
0.30
0.20
0.10
0.00
0.00
0.05
0.10
0.15
0.20
0.25
0.30
SHEAR LOAD (KIPS) (E+02)

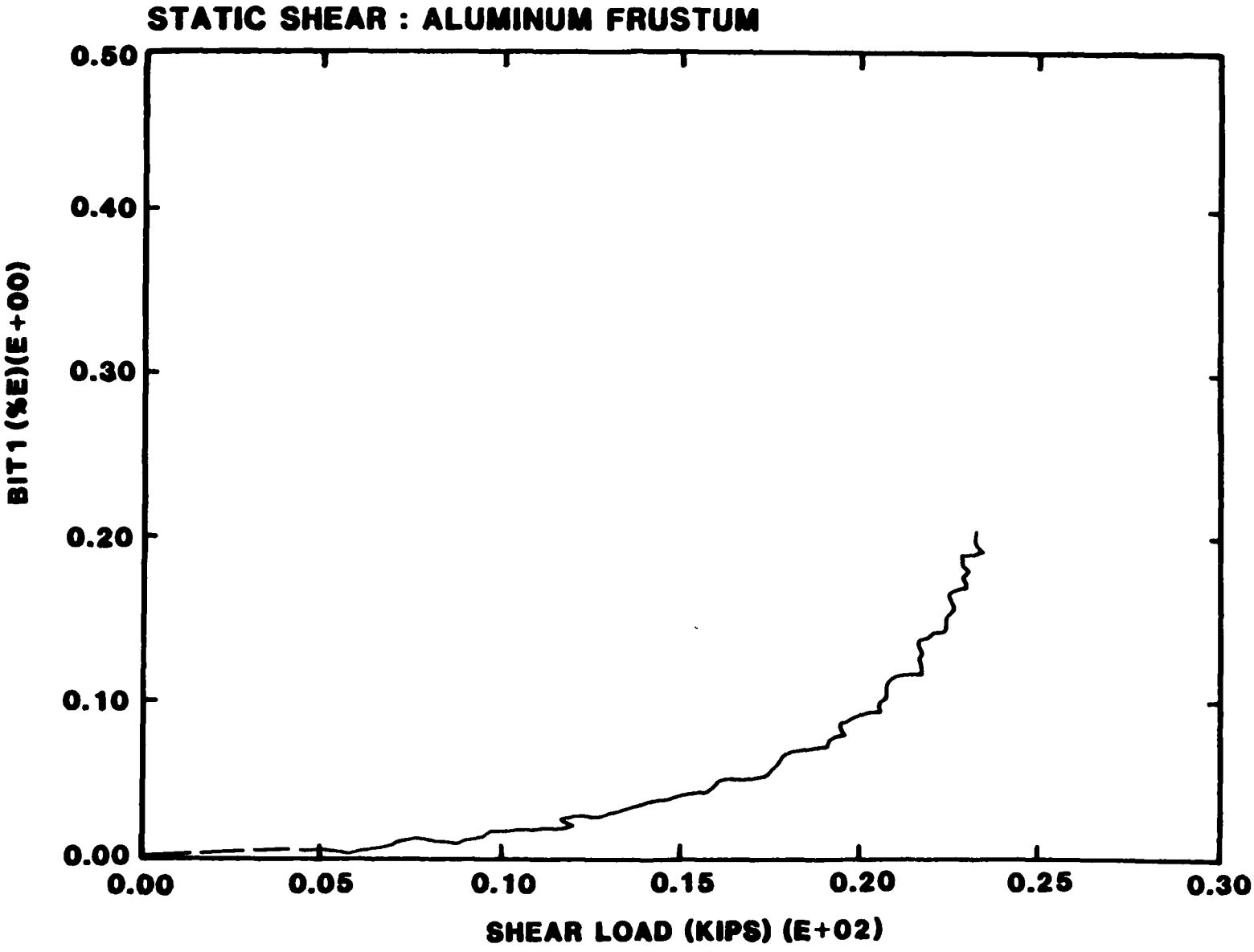
STATIC SHEAR : ALUMINUM FRUSTUM
0.50
0.40
0.30
0.20
0.10
0.00
BIT 1 (%E)(E+00)
0.00
0.05
0.10
0.15
0.20
0.25
0.30
SHEAR LOAD (KIPS) (E+02)

7.4 APPENDIX D

STATIC-AXIAL LOADING TEST DATA
FOR BORON/ALUMINUM FRUSTA

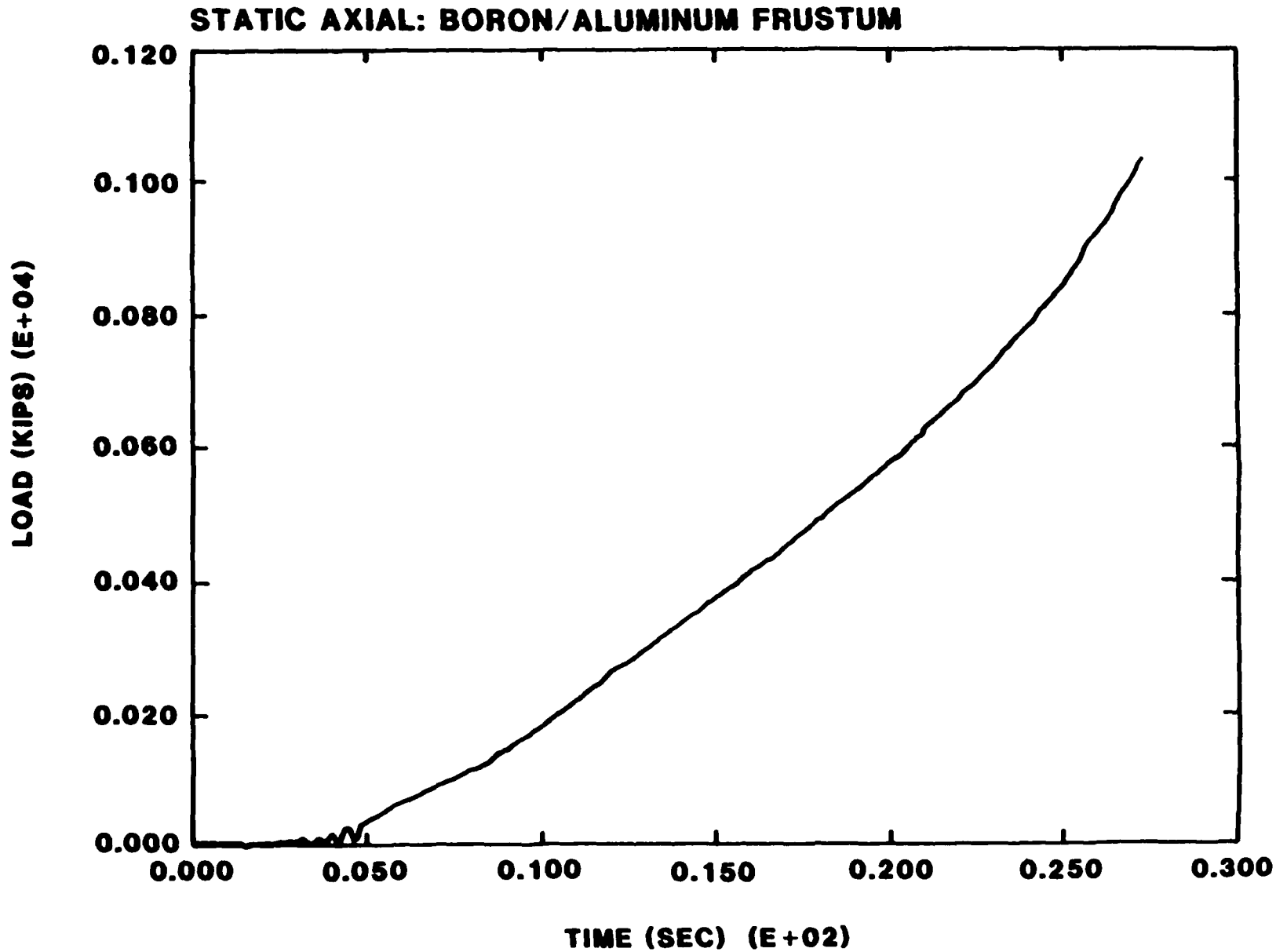
STATIC AXIAL: BORON/ALUMINUM FRUSTUM
LOAD (KIPS) (E+04)
0.120
0.100
0.080
0.060
0.040
0.020
0.000
0.000
0.050
0.100
0.150
0.200
0.250
0.300
TIME (SEC) (E+02)

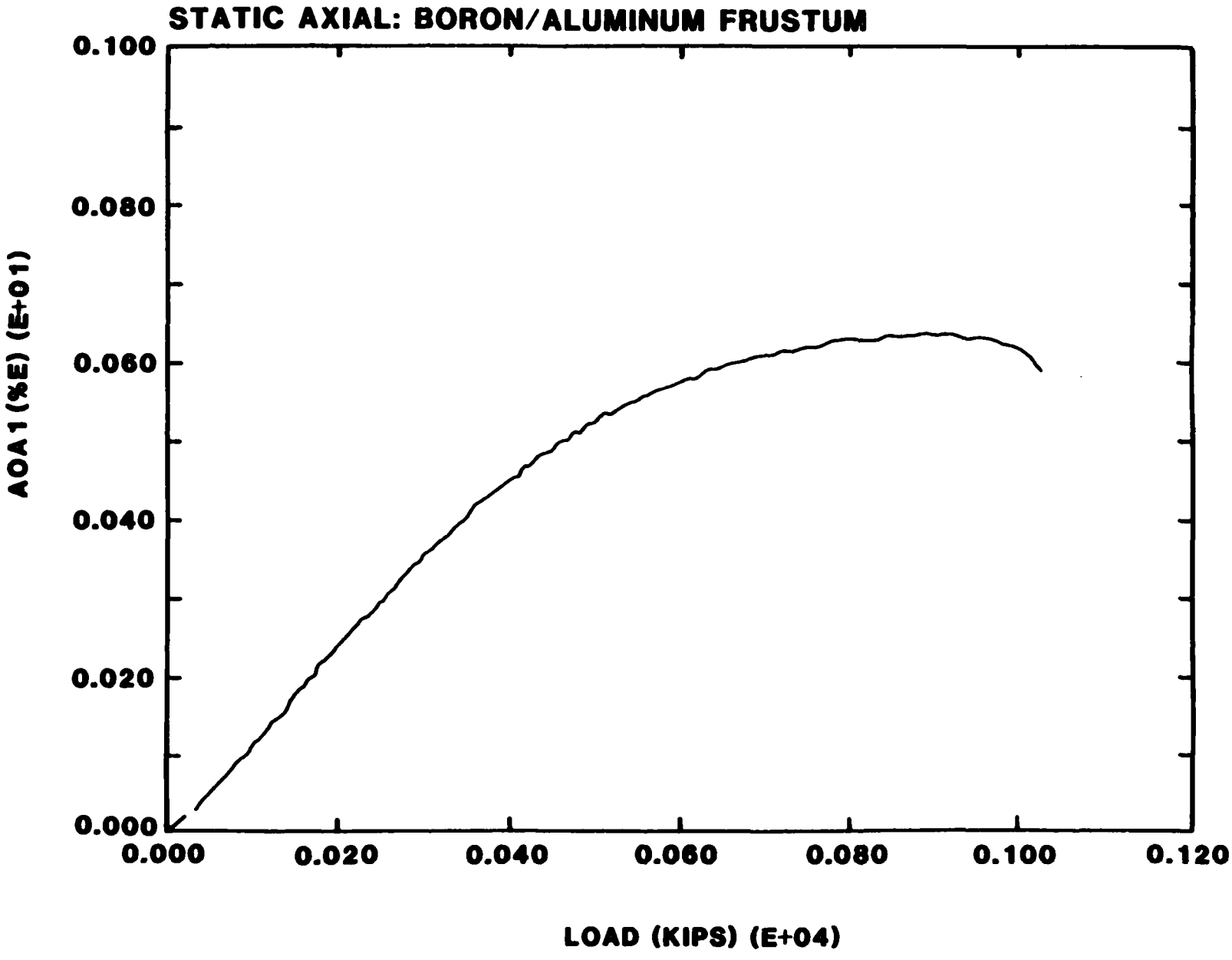
STATIC AXIAL: BORON/ALUMINUM FRUSTUM
0.100
0.080
0.060
0.040
0.020
0.000
AOA1 (%E) (E+01)
0.000
0.020
0.040
0.060
0.080
0.100
0.120
LOAD (KIPS) (E+04)

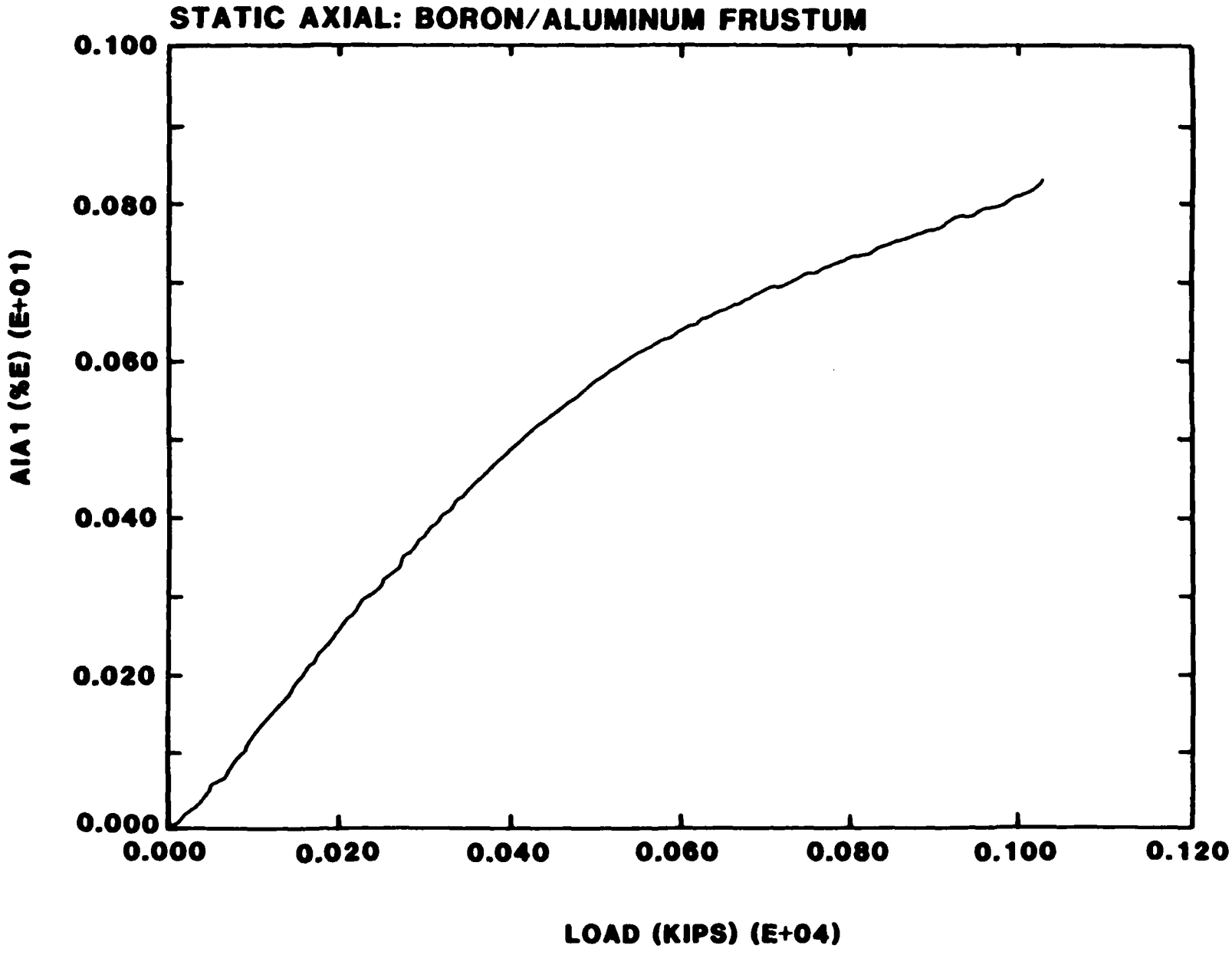
STATIC AXIAL: BORON/ALUMINUM FRUSTUM
0.100
0.080
0.060
0.040
0.020
0.000
AIA1 (%E) (E+01)
0.000
0.020
0.040
0.060
0.080
0.100
0.120
LOAD (KIPS) (E+04)

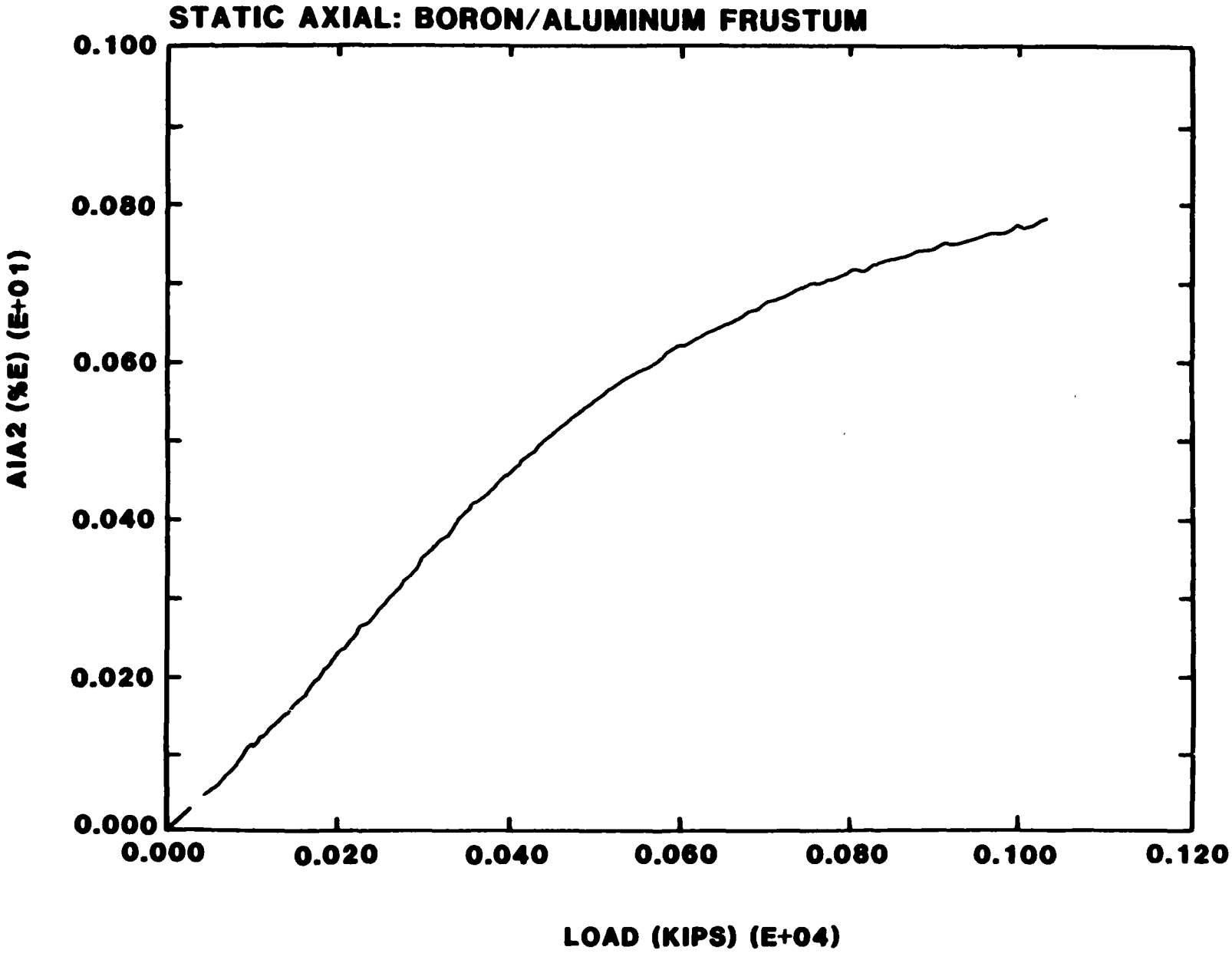
STATIC AXIAL: BORON/ALUMINUM FRUSTUM
0.100
0.080
0.060
0.040
0.020
0.000
AIA2 (%E) (E+01)
0.000
0.020
0.040
0.060
0.080
0.100
0.120
LOAD (KIPS) (E+04)

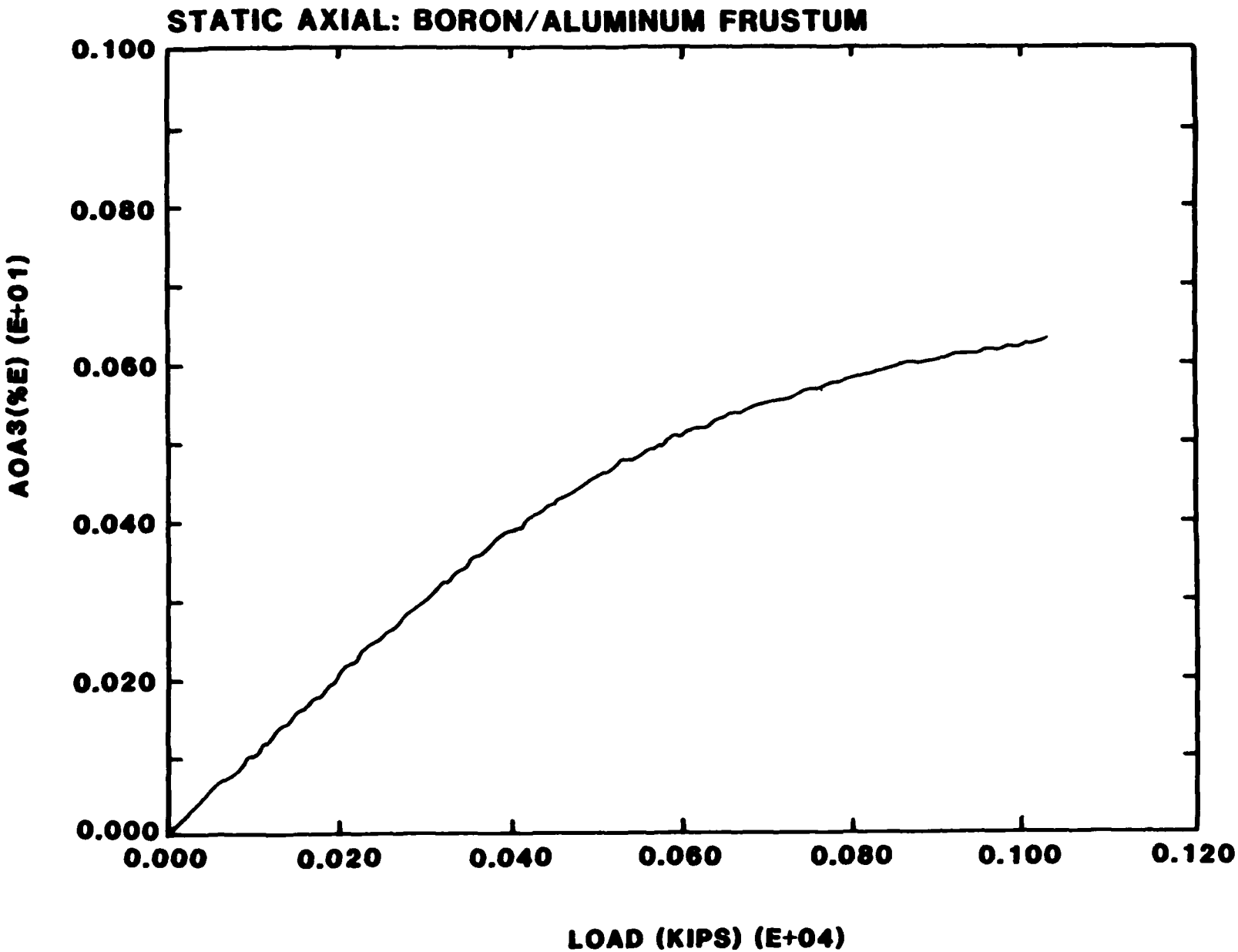
STATIC AXIAL: BORON/ALUMINUM FRUSTUM
AOA3(%E) (E+01)
0.100
0.080
0.060
0.040
0.020
0.000
0.000
0.020
0.040
0.060
0.080
0.100
0.120
LOAD (KIPS) (E+04)

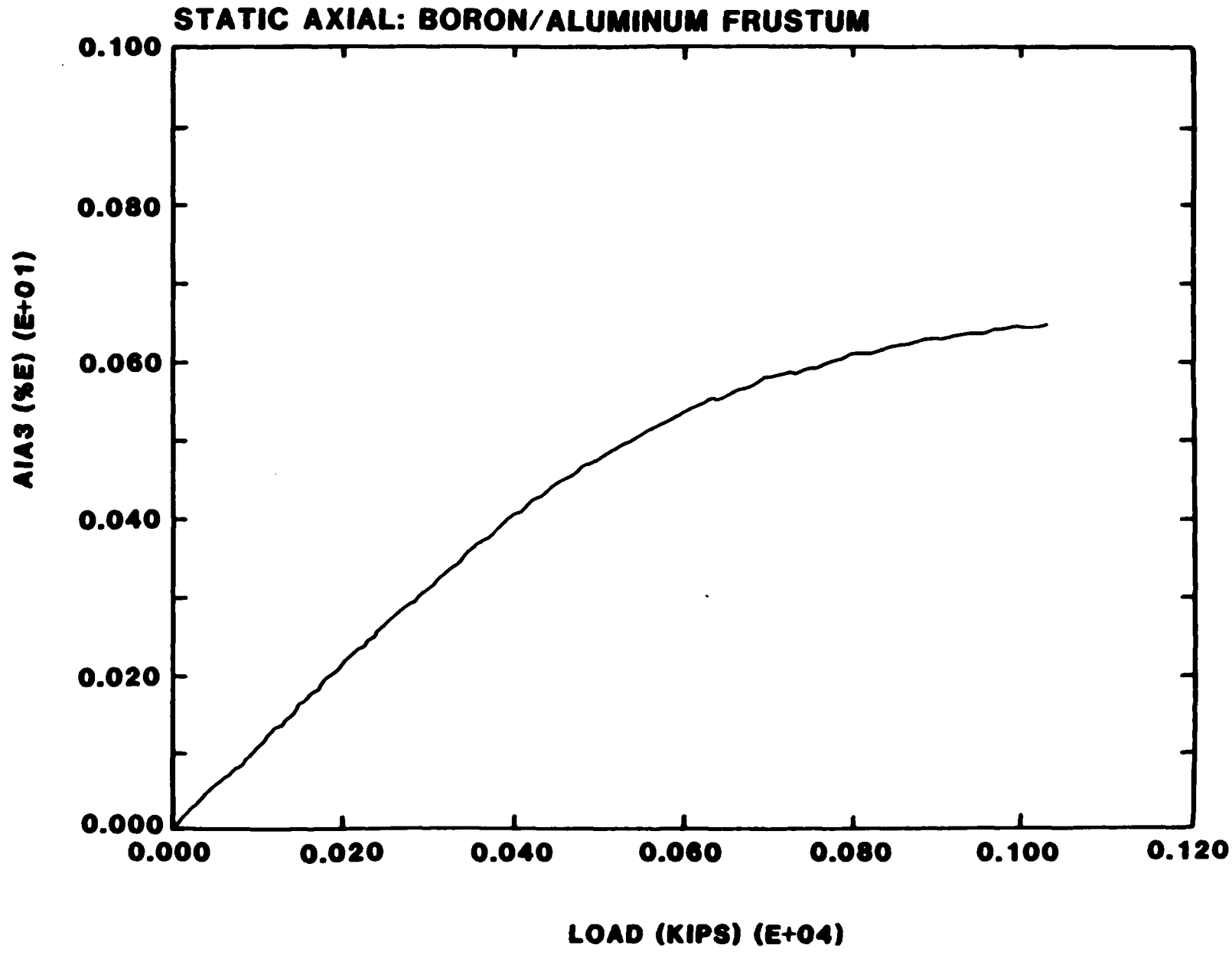
STATIC AXIAL: BORON/ALUMINUM FRUSTUM
0.100
0.080
0.060
0.040
0.020
0.000
AIA3 (%E) (E+01)
0.000
0.020
0.040
0.060
0.080
0.100
0.120
LOAD (KIPS) (E+04)

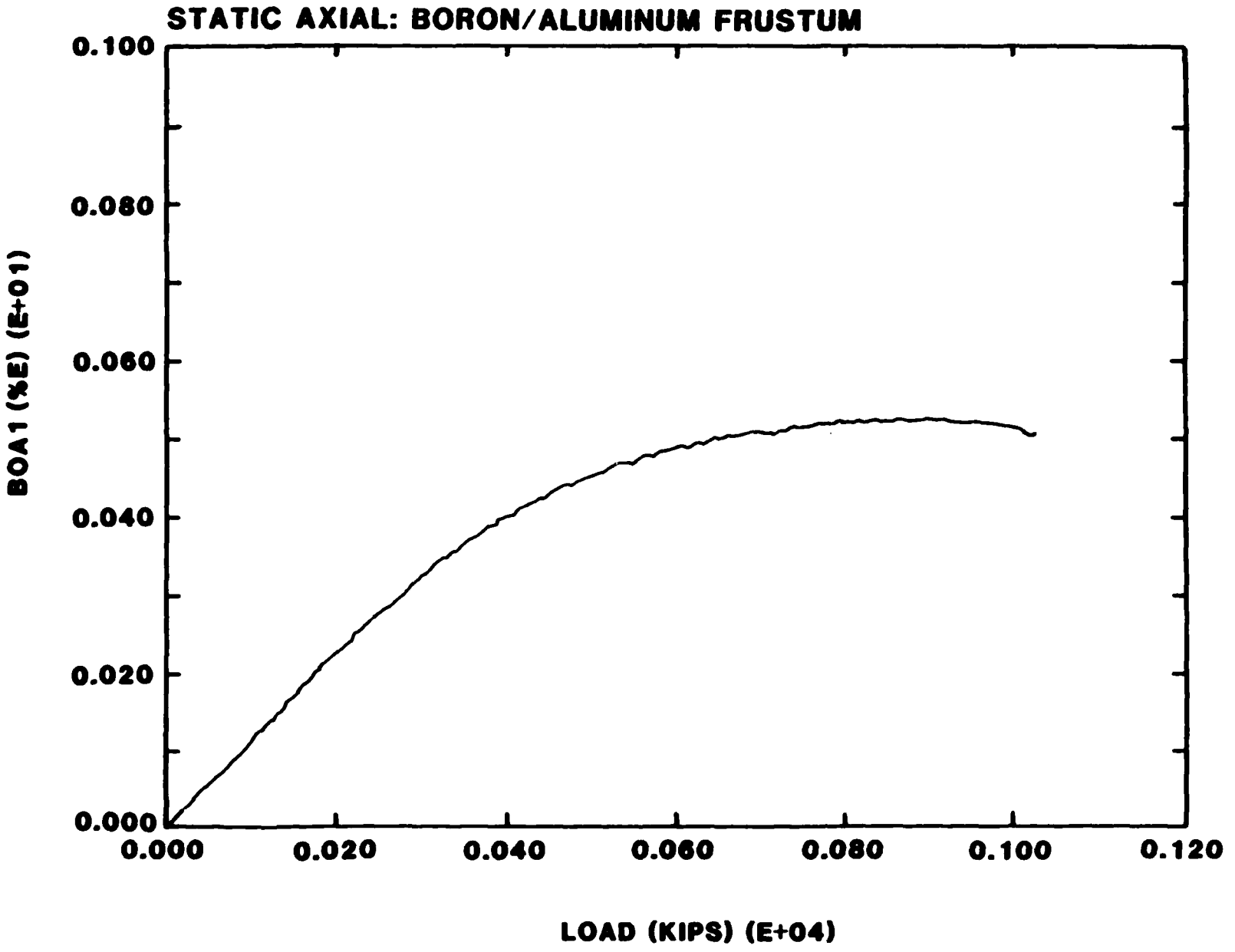
STATIC AXIAL: BORON/ALUMINUM FRUSTUM
0.100
0.080
0.060
0.040
0.020
0.000
BOA1 (%E) (E+01)
0.000
0.020
0.040
0.060
0.080
0.100
0.120
LOAD (KIPS) (E+04)

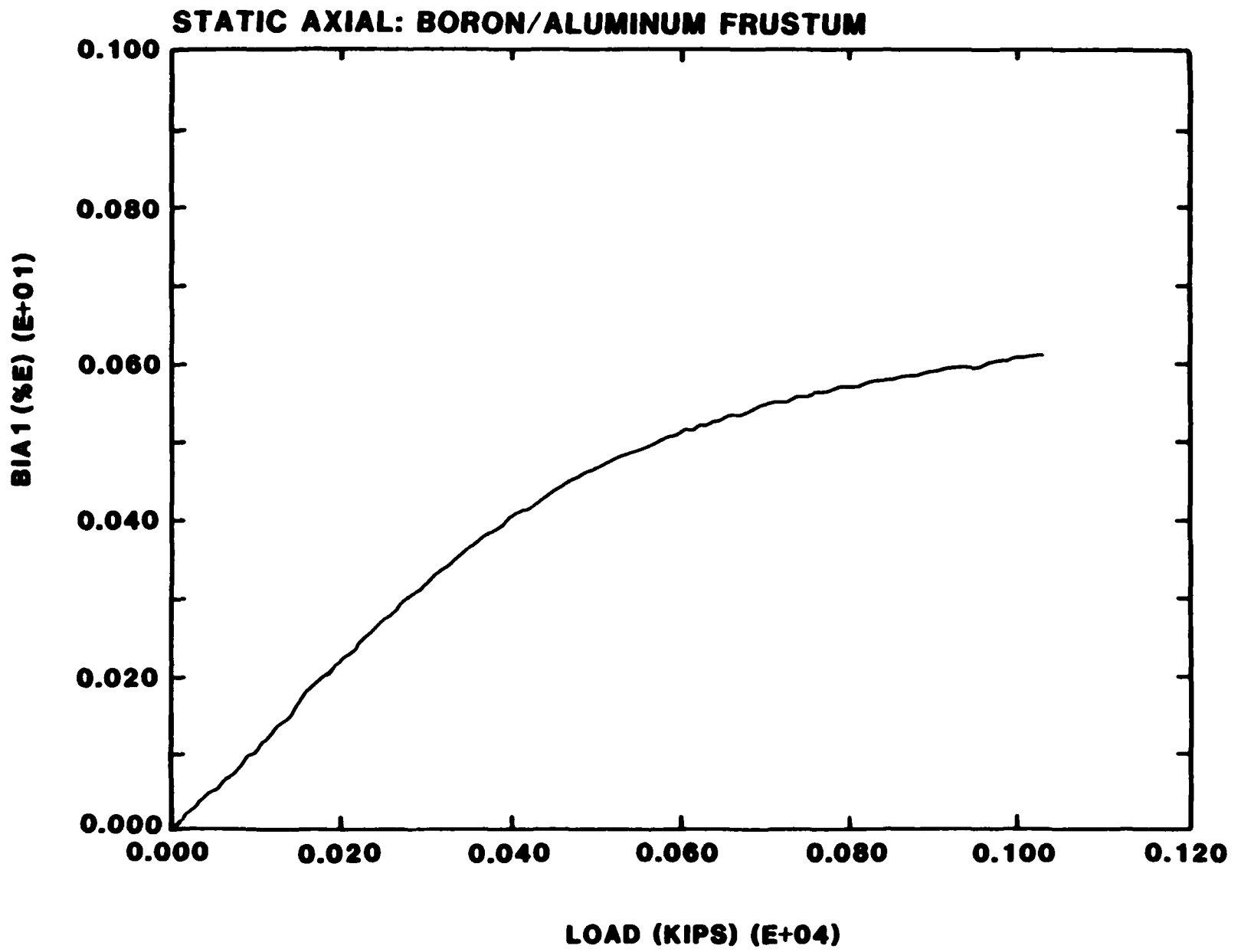
STATIC AXIAL: BORON/ALUMINUM FRUSTUM
BIA1 (%E) (E+01)
0.100
0.080
0.060
0.040
0.020
0.000
0.000
0.020
0.040
0.060
0.080
0.100
0.120
LOAD (KIPS) (E+04)

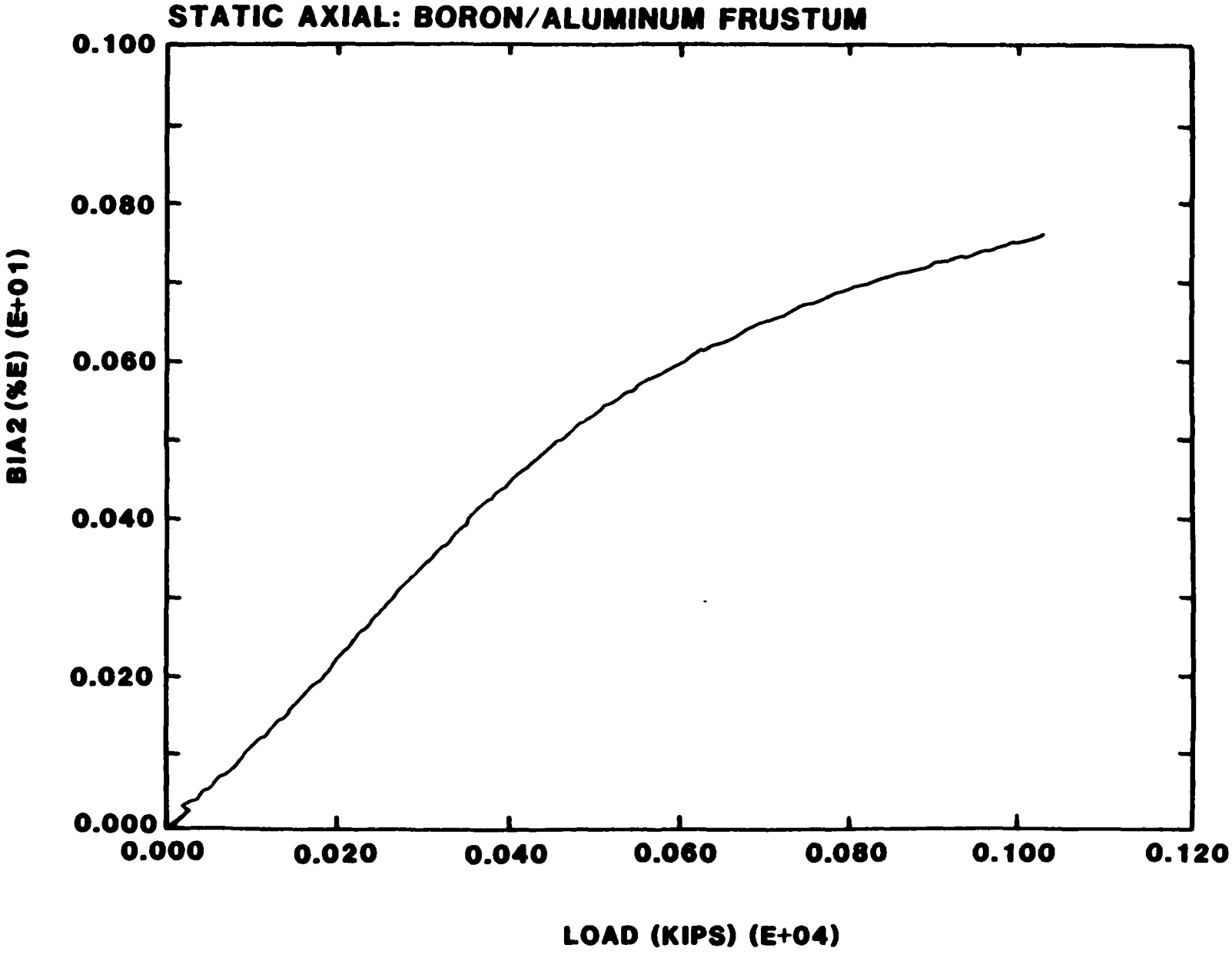
STATIC AXIAL: BORON/ALUMINUM FRUSTUM
0.100
0.080
0.060
0.040
0.020
0.000
BIA2 (%E) (E+01)
0.000
0.020
0.040
0.060
0.080
0.100
0.120
LOAD (KIPS) (E+04)

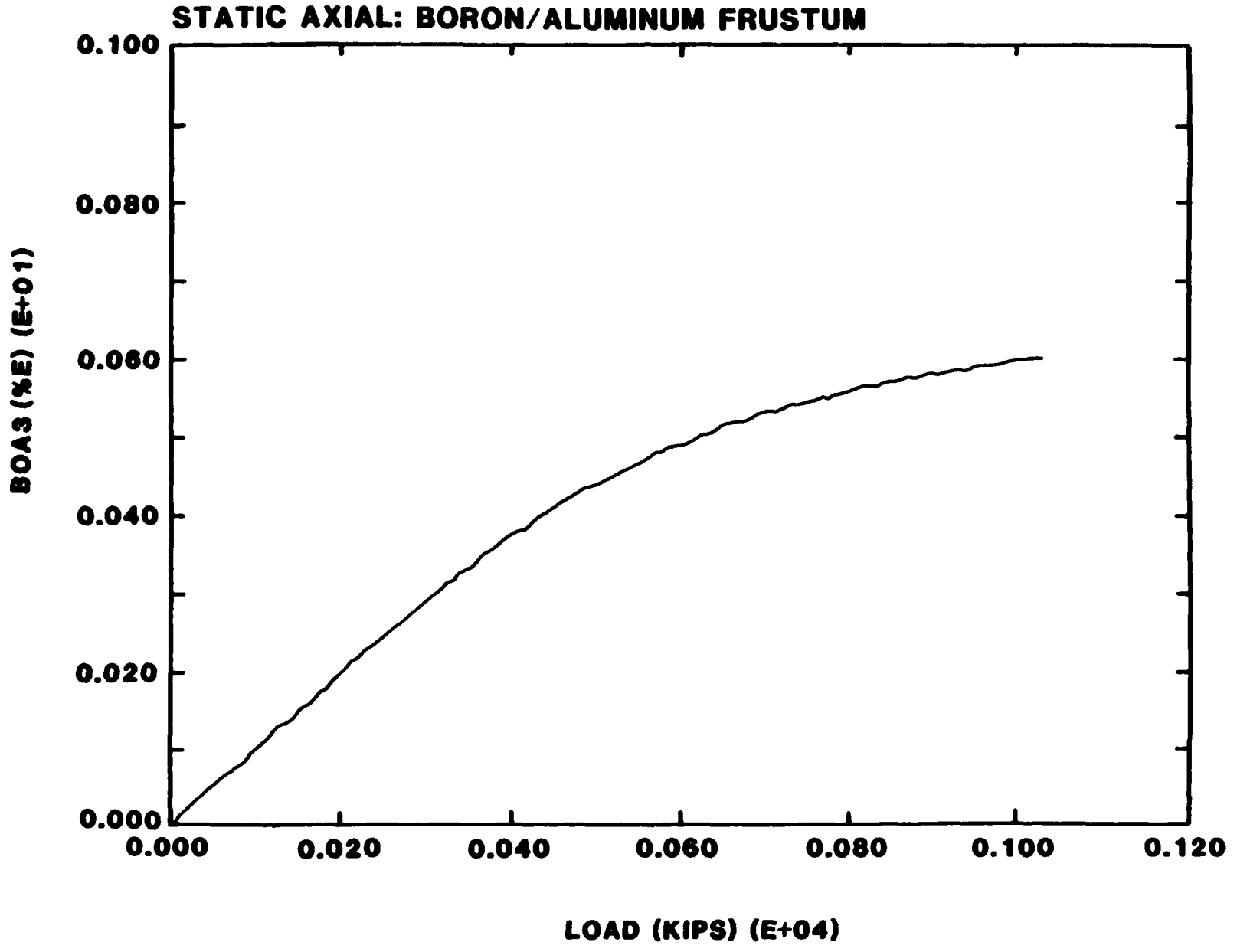
STATIC AXIAL: BORON/ALUMINUM FRUSTUM
0.100
0.080
0.060
0.040
0.020
0.000
BOA3 (%E) (E+01)
0.000
0.020
0.040
0.060
0.080
0.100
0.120
LOAD (KIPS) (E+04)

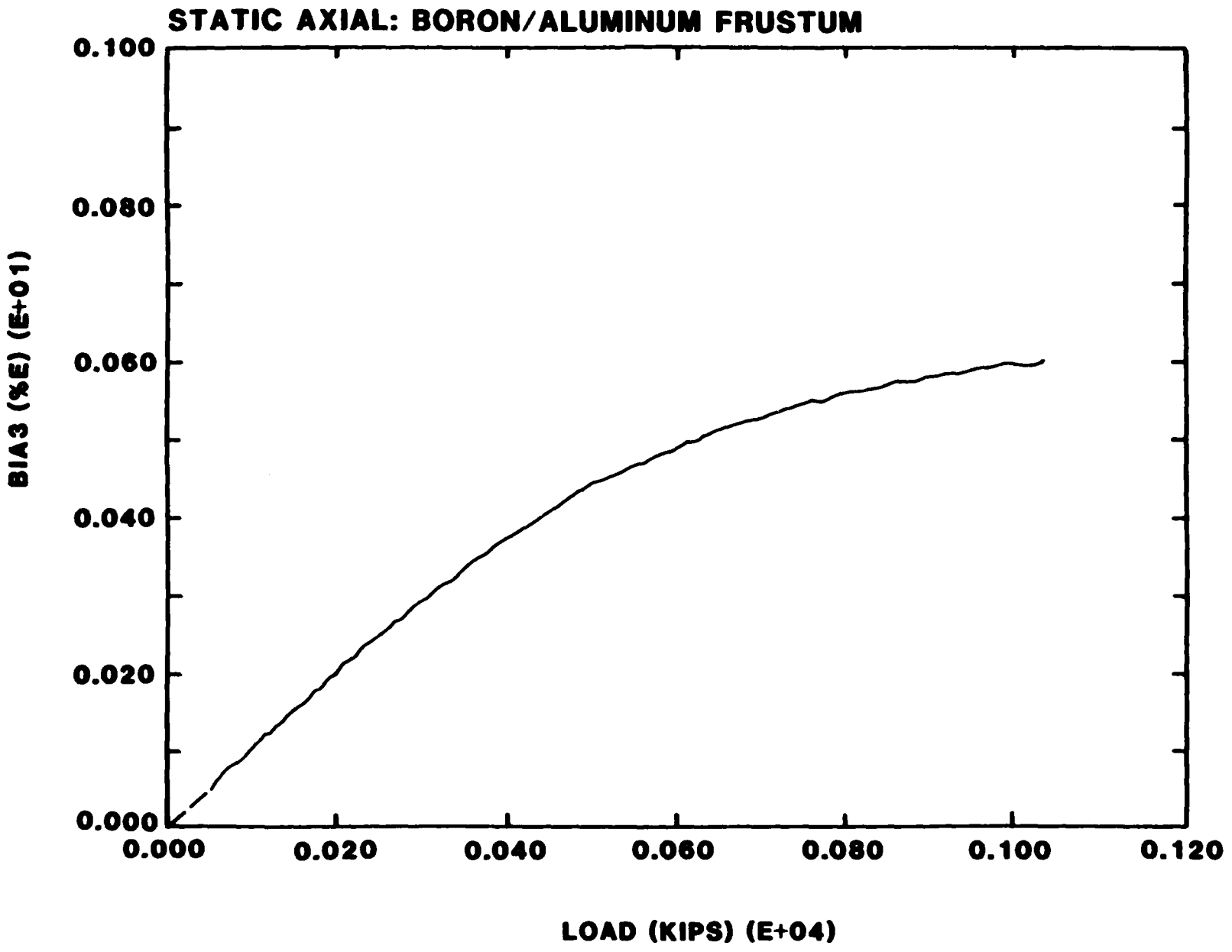
STATIC AXIAL: BORON/ALUMINUM FRUSTUM
BIA3 (%E) (E+01)
0.100
0.080
0.060
0.040
0.020
0.000
0.000
0.020
0.040
0.060
0.080
0.100
0.120
LOAD (KIPS) (E+04)

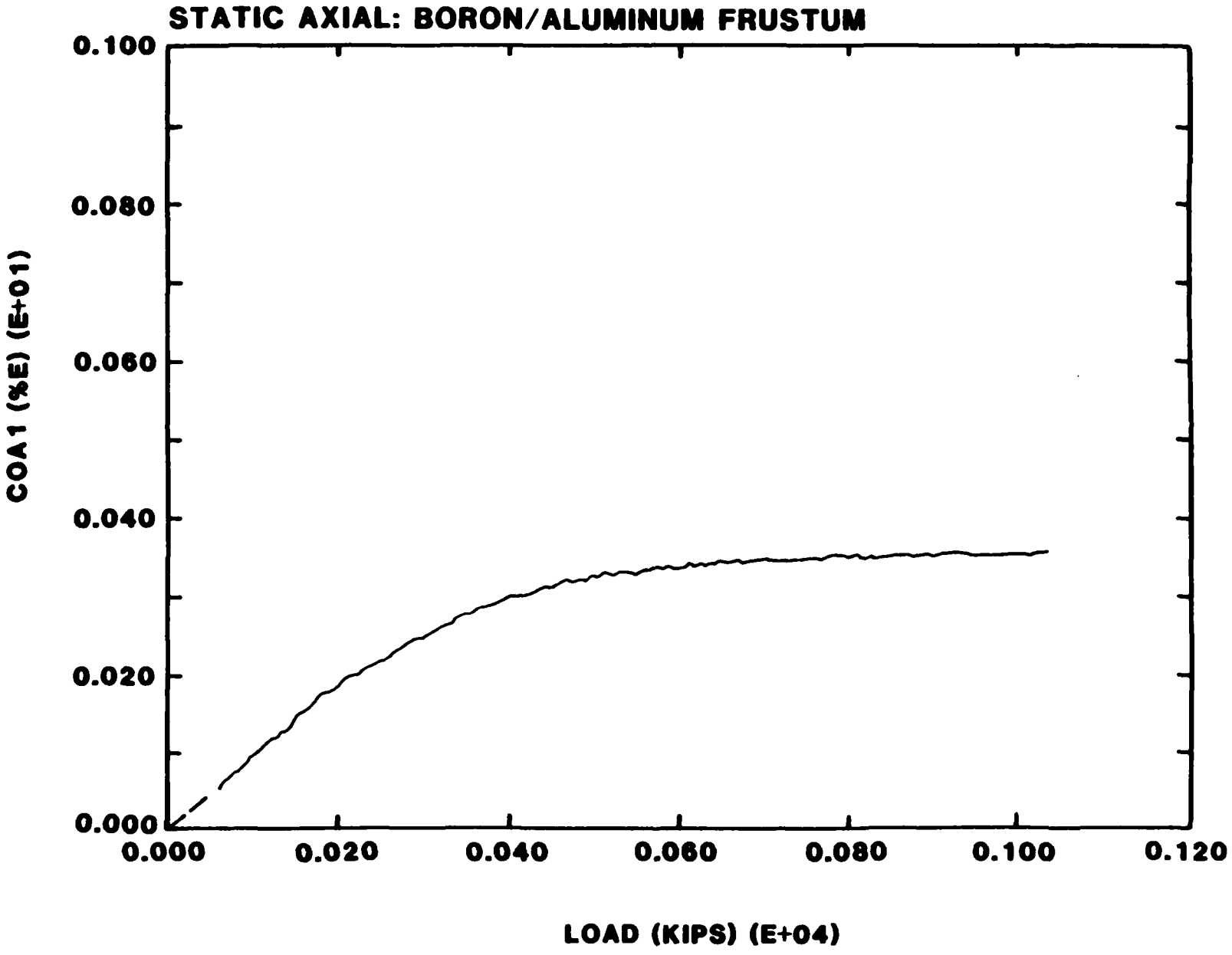
STATIC AXIAL: BORON/ALUMINUM FRUSTUM
0.100
0.080
0.060
0.040
0.020
0.000
COA1 (%E) (E+01)
0.000
0.020
0.040
0.060
0.080
0.100
0.120
LOAD (KIPS) (E+04)

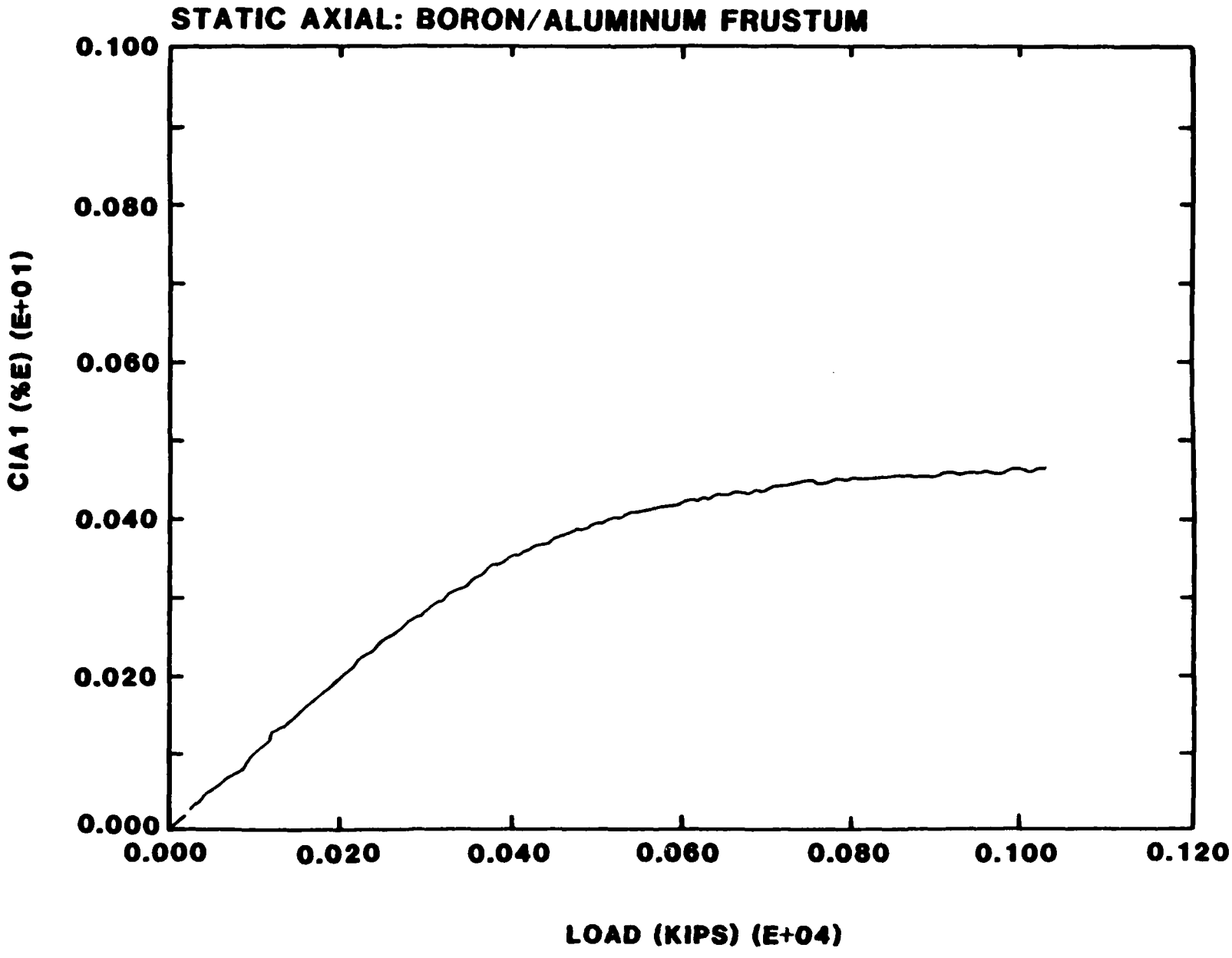
STATIC AXIAL: BORON/ALUMINUM FRUSTUM
0.100
0.080
0.060
0.040
0.020
0.000
CIA 1 (%E) (E+01)
0.000
0.020
0.040
0.060
0.080
0.100
0.120
LOAD (KIPS) (E+04)

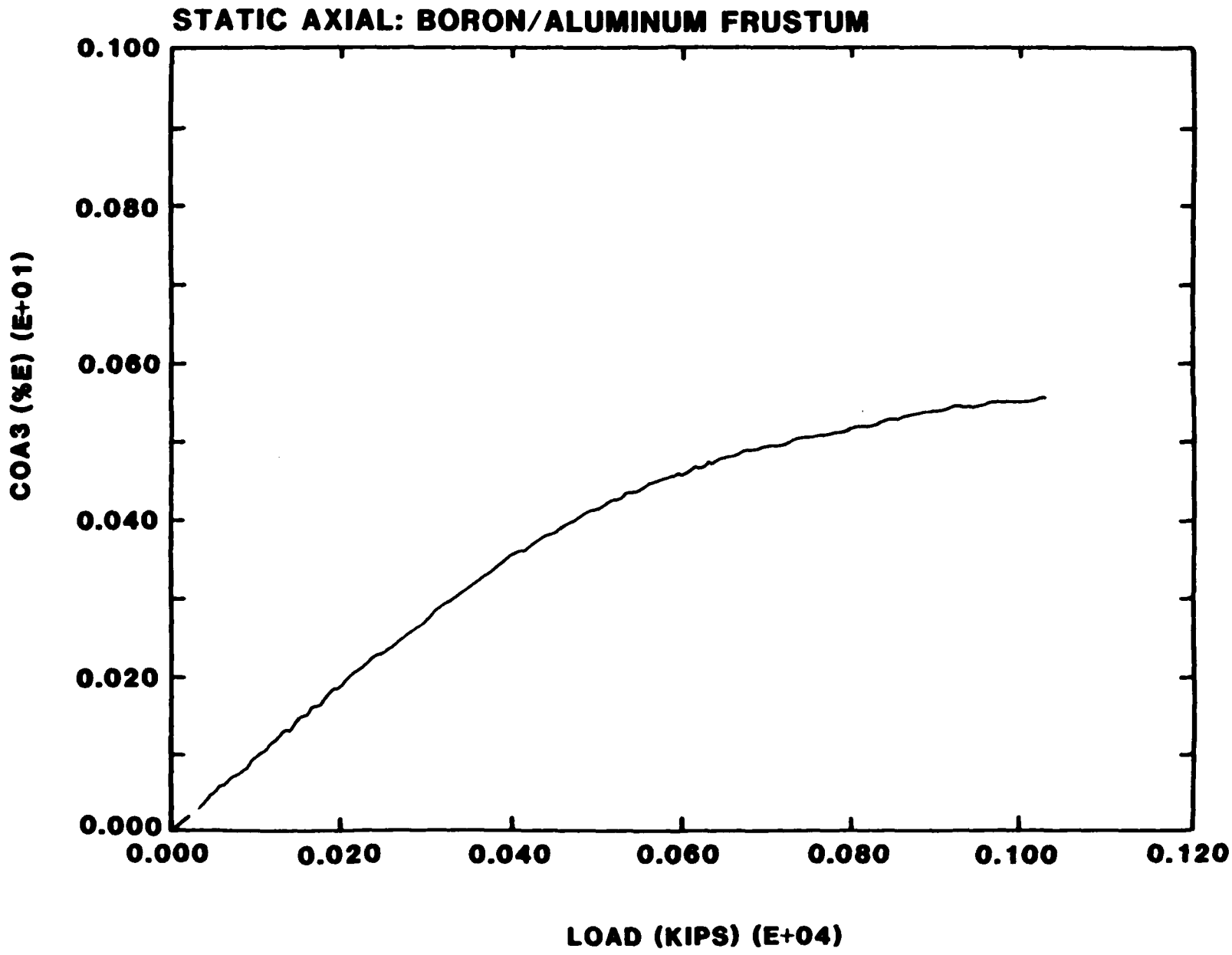
STATIC AXIAL: BORON/ALUMINUM FRUSTUM
0.100
0.080
0.060
0.040
0.020
0.000
COA3 (%E) (E+01)
0.000
0.020
0.040
0.060
0.080
0.100
0.120
LOAD (KIPS) (E+04)

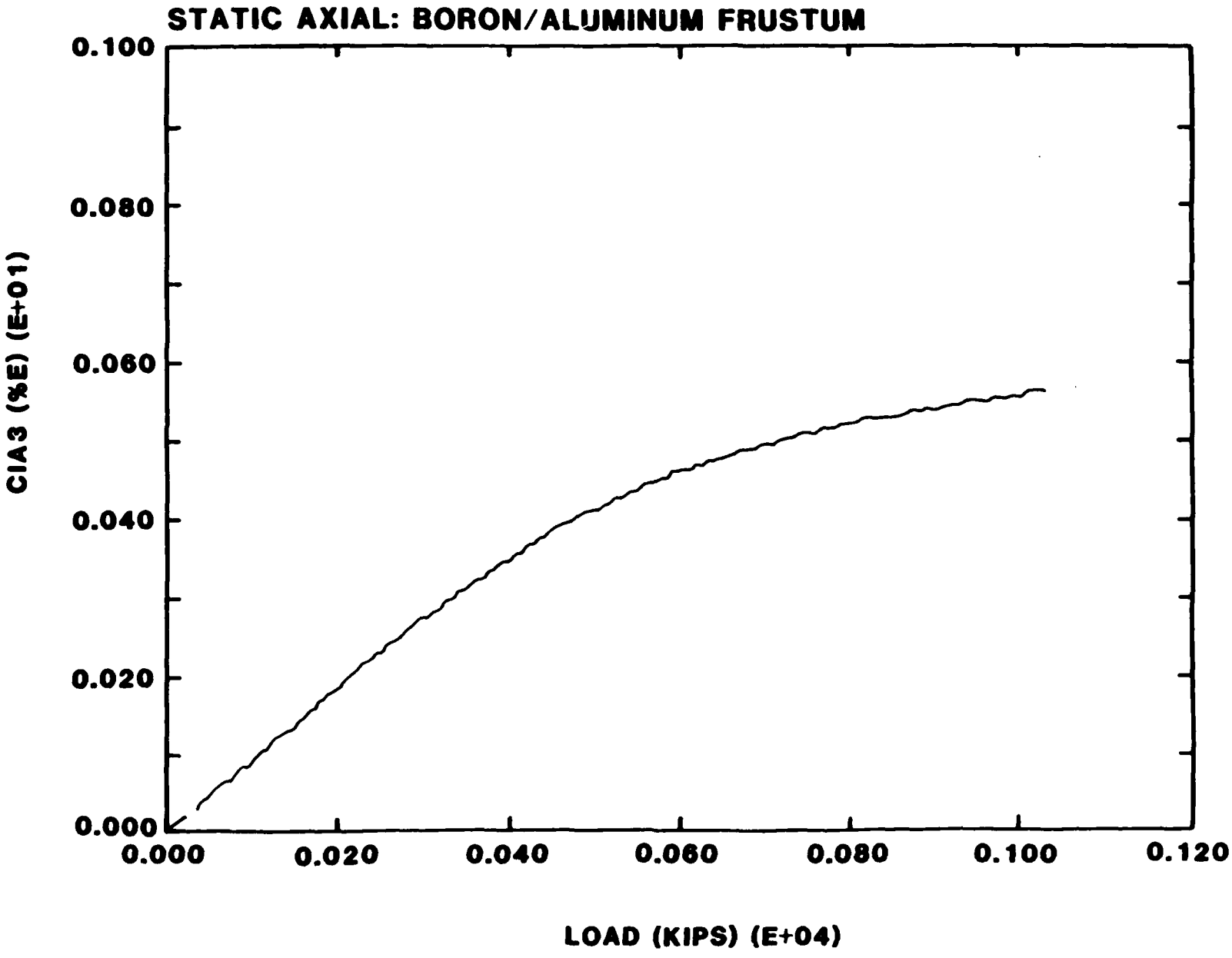
STATIC AXIAL: BORON/ALUMINUM FRUSTUM
0.100
0.080
0.060
0.040
0.020
0.000
CIA3 (%E) (E+01)
0.000
0.020
0.040
0.060
0.080
0.100
0.120
LOAD (KIPS) (E+04)

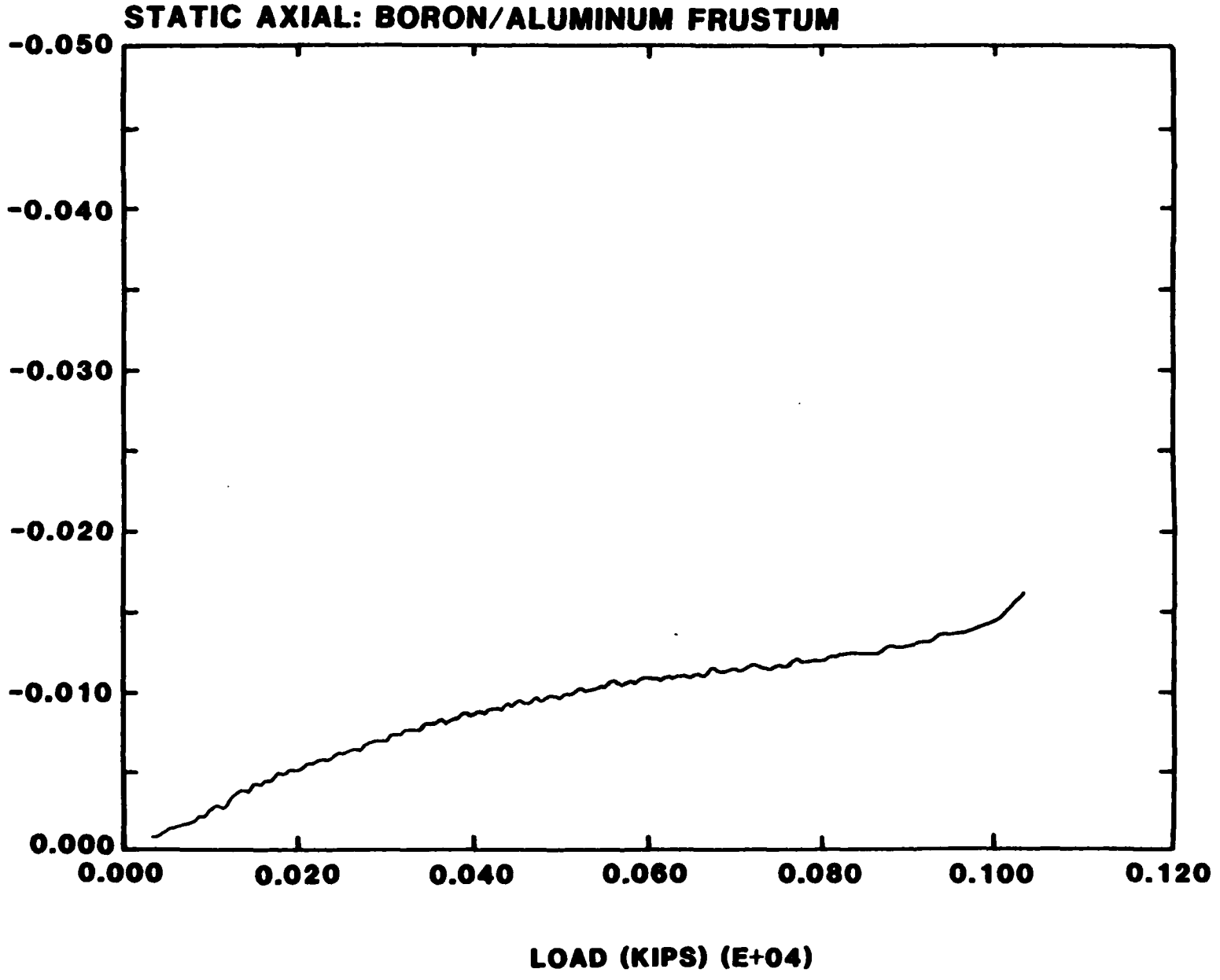
STATIC AXIAL: BORON/ALUMINUM FRUSTUM
-0.050
-0.040
-0.030
-0.020
-0.010
0.000
AIT1 (%E) (E+01)
0.000
0.020
0.040
0.060
0.080
0.100
0.120
LOAD (KIPS) (E+04)

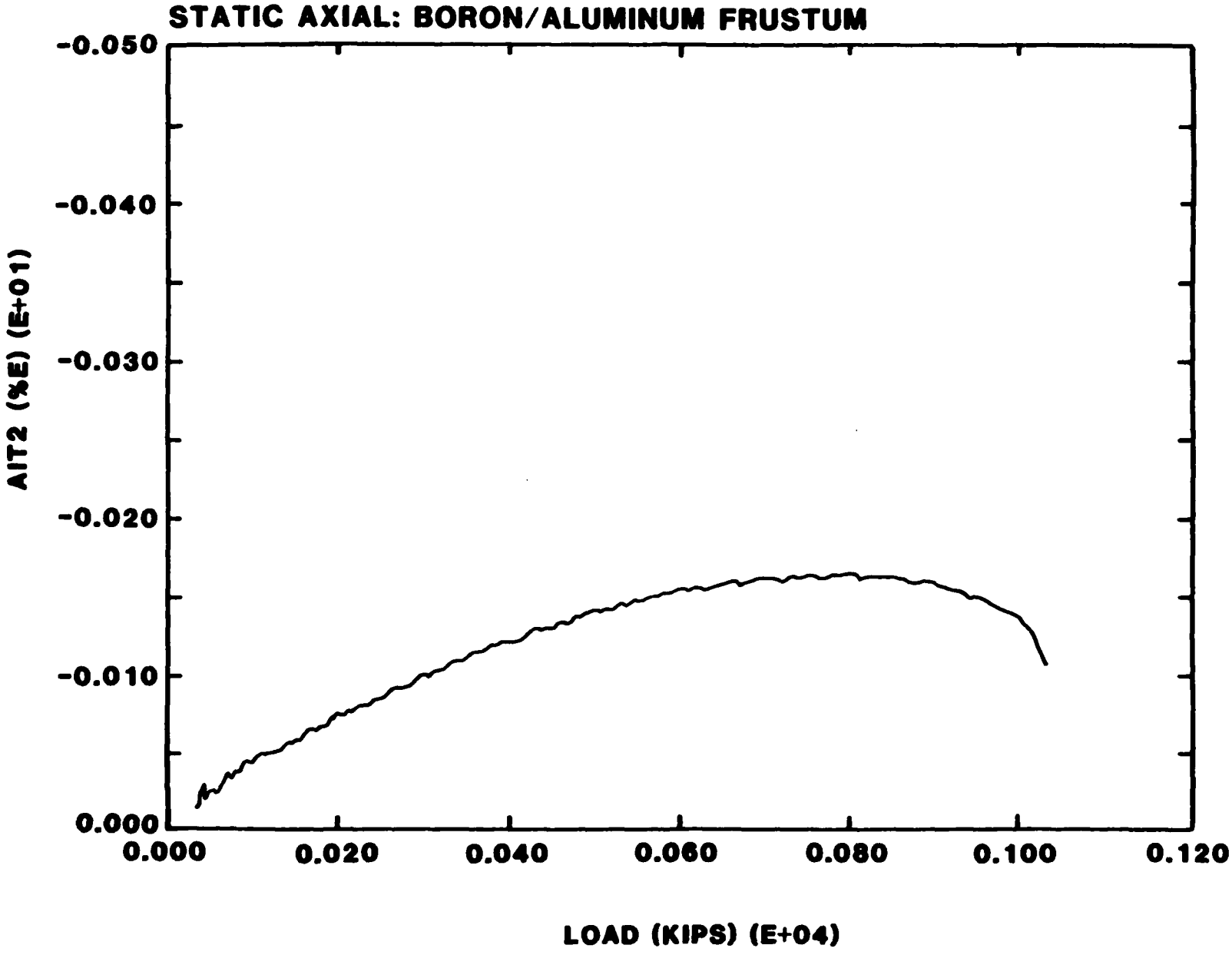
STATIC AXIAL: BORON/ALUMINUM FRUSTUM
-0.050
-0.040
-0.030
-0.020
-0.010
0.000
AIT2 (%E) (E+01)
0.000
0.020
0.040
0.060
0.080
0.100
0.120
LOAD (KIPS) (E+04)

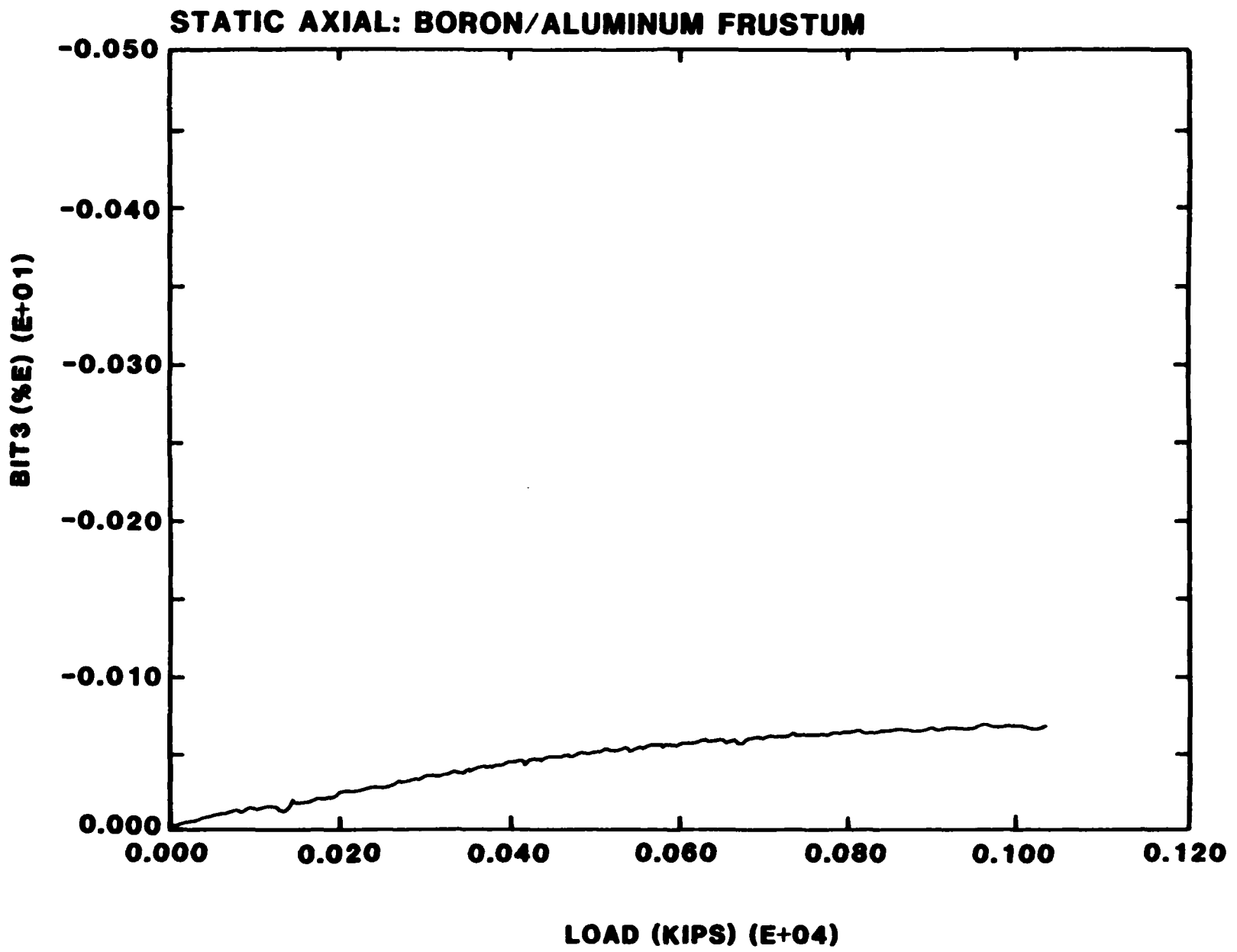
STATIC AXIAL: BORON/ALUMINUM FRUSTUM
-0.050
-0.040
-0.030
-0.020
-0.010
0.000
BIT3 (%E) (E+01)
0.000
0.020
0.040
0.060
0.080
0.100
0.120
LOAD (KIPS) (E+04)

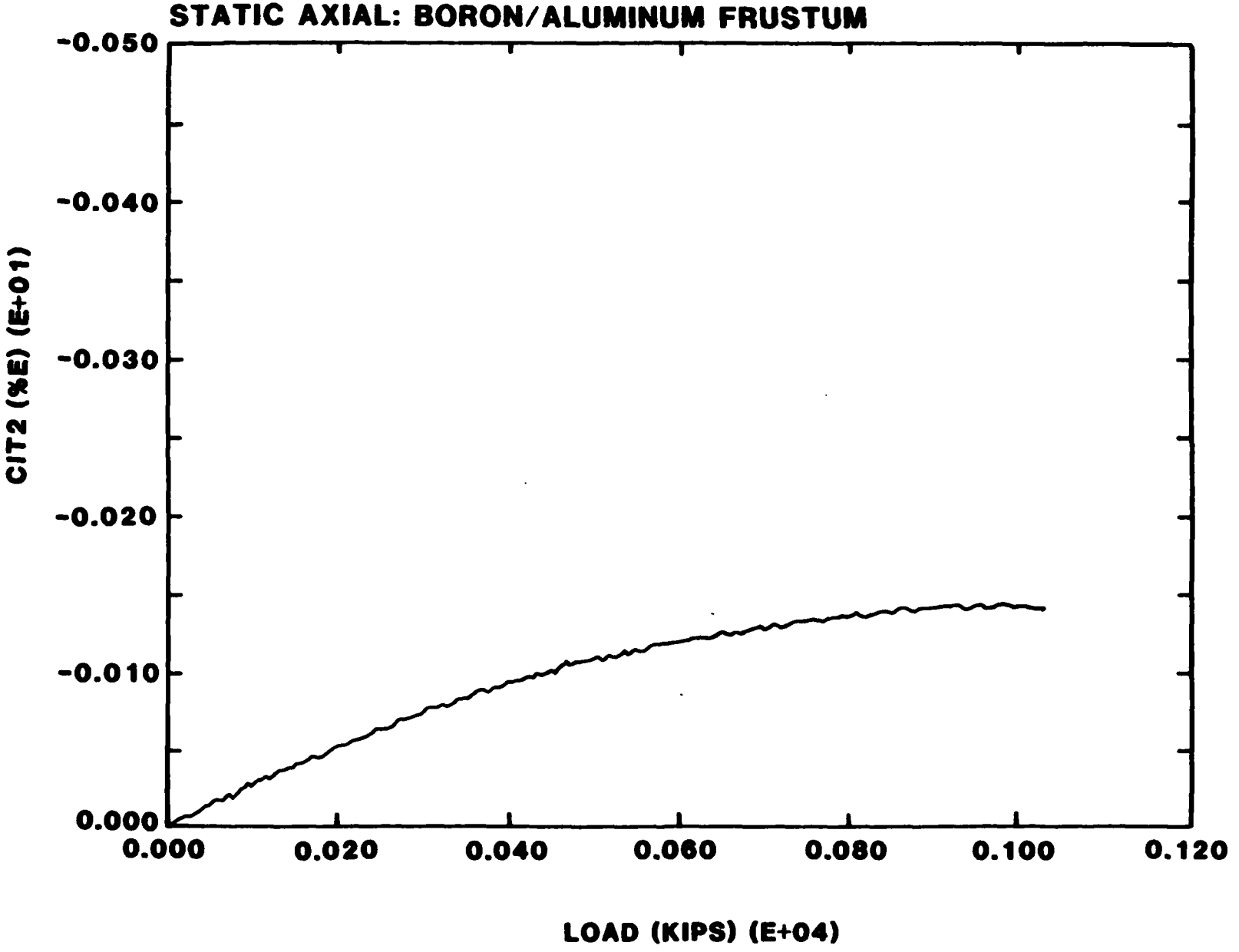
STATIC AXIAL: BORON/ALUMINUM FRUSTUM
-0.050
-0.040
-0.030
-0.020
-0.010
0.000
CIT2 (%E) (E+01)
0.000
0.020
0.040
0.060
0.080
0.100
0.120
LOAD (KIPS) (E+04)

7.5 APPENDIX E

DYNAMIC-AXIAL LOADING TEST DATA
FOR BORON/ALUMINUM FRUSTA

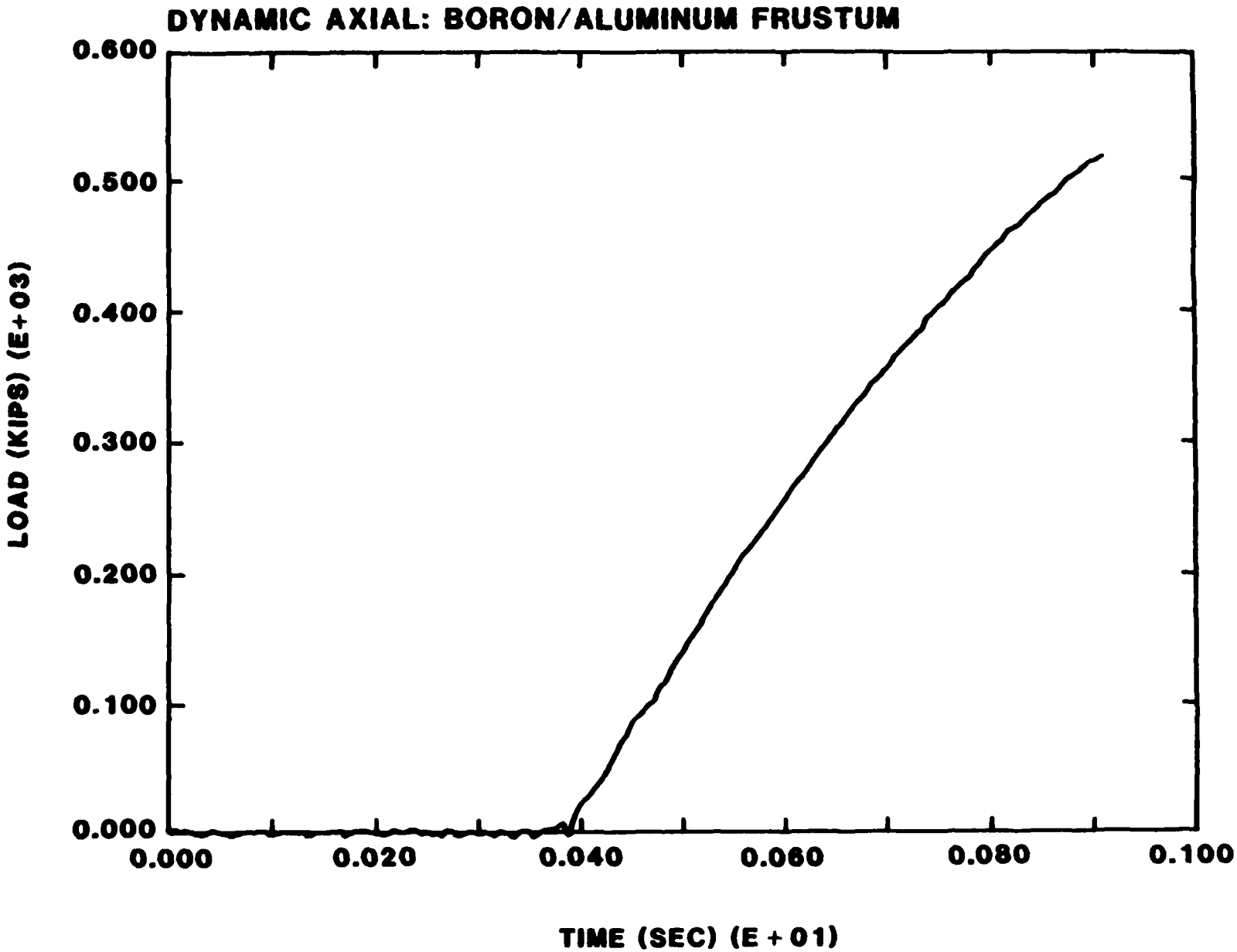
DYNAMIC AXIAL: BORON/ALUMINUM FRUSTUM
LOAD (KIPS) (E+03)
0.600
0.500
0.400
0.300
0.200
0.100
0.000
0.000
0.020
0.040
0.060
0.080
0.100
TIME (SEC) (E + 01)

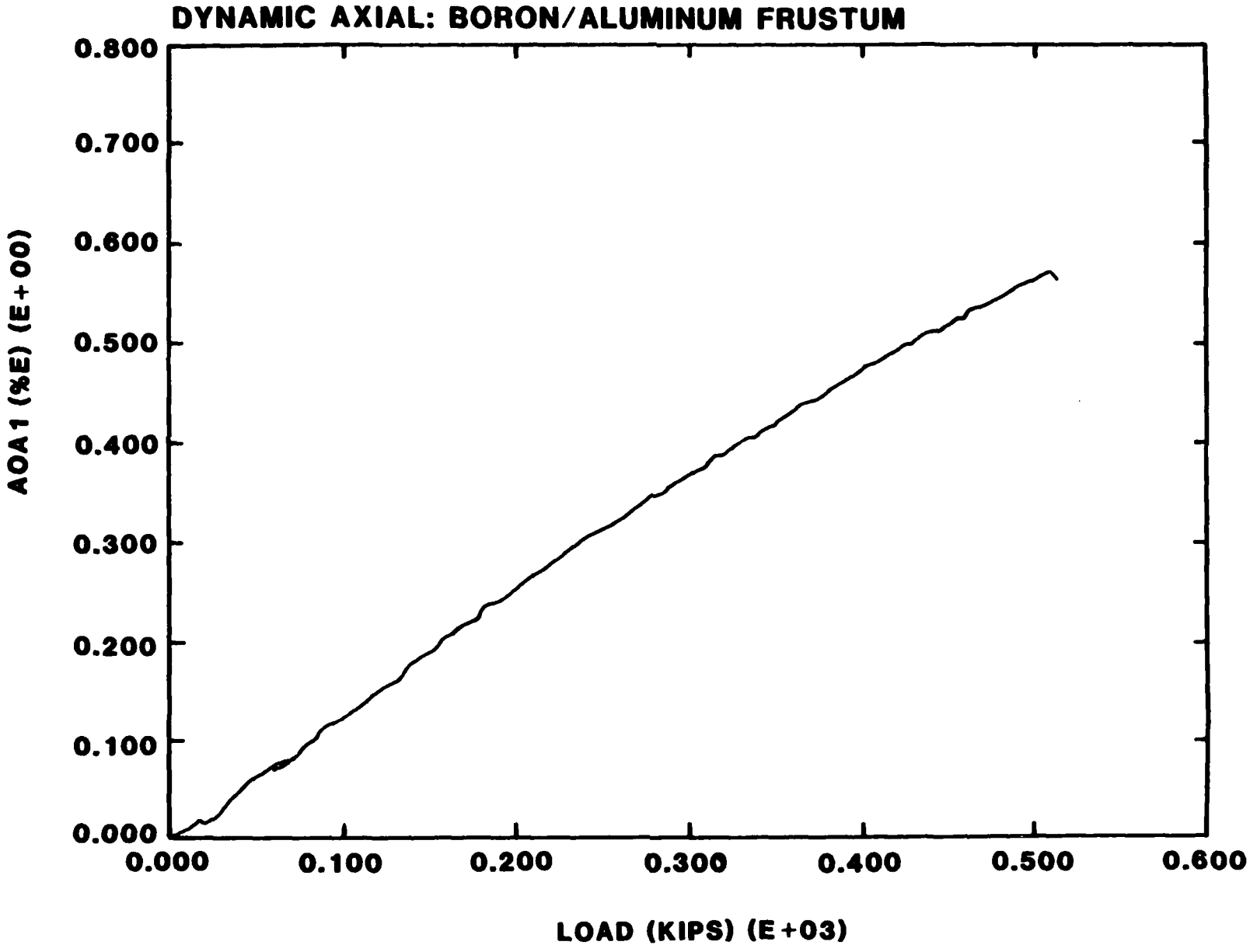
DYNAMIC AXIAL: BORON/ALUMINUM FRUSTUM
0.800
0.700
0.600
0.500
0.400
0.300
0.200
0.100
0.000
AOA1 (%E) (E+00)
0.000
0.100
0.200
0.300
0.400
0.500
0.600
LOAD (KIPS) (E+03)

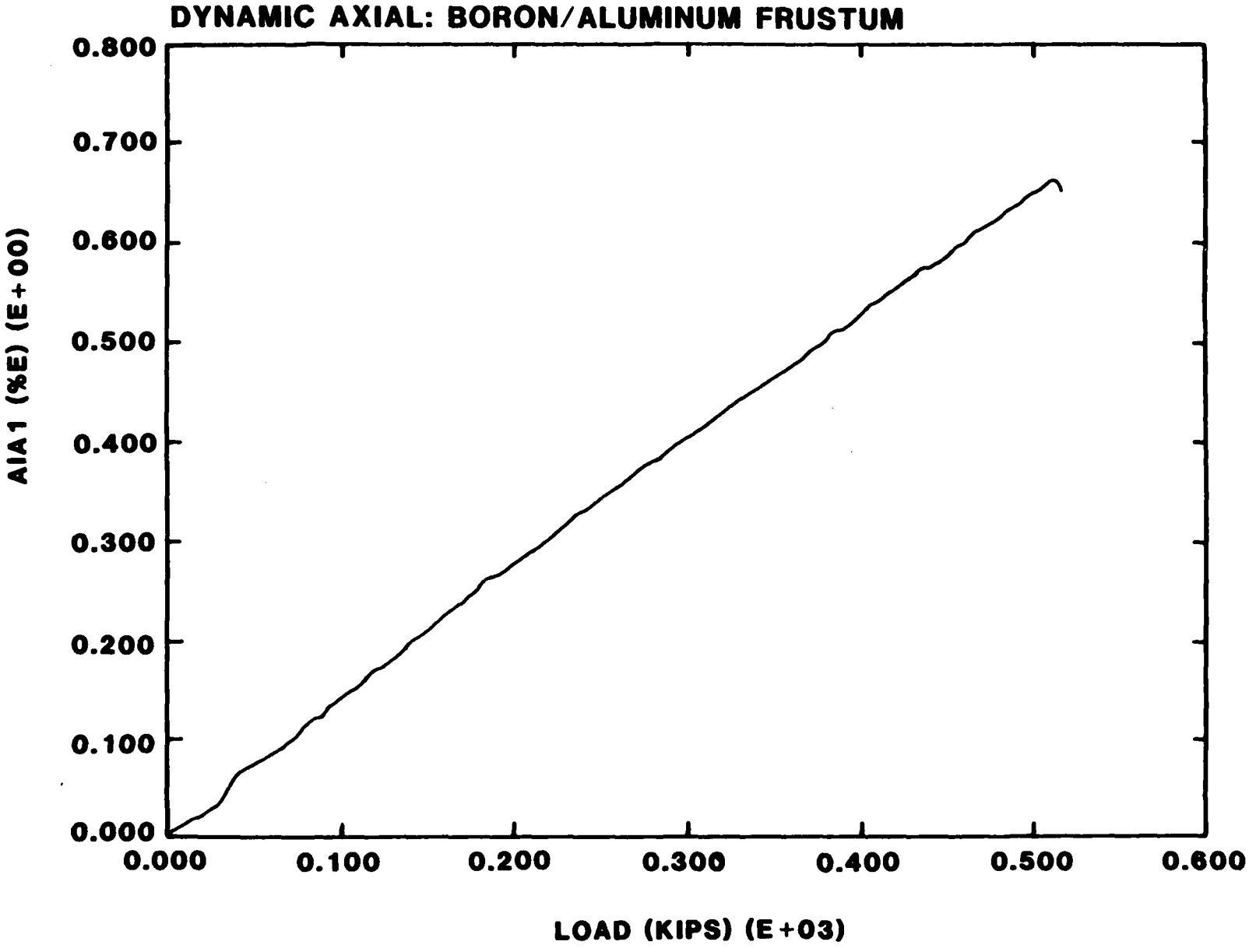
DYNAMIC AXIAL: BORON/ALUMINUM FRUSTUM
AIA1 (%E) (E+00)
0.800
0.700
0.600
0.500
0.400
0.300
0.200
0.100
0.000
0.000
0.100
0.200
0.300
0.400
0.500
0.600
LOAD (KIPS) (E+03)

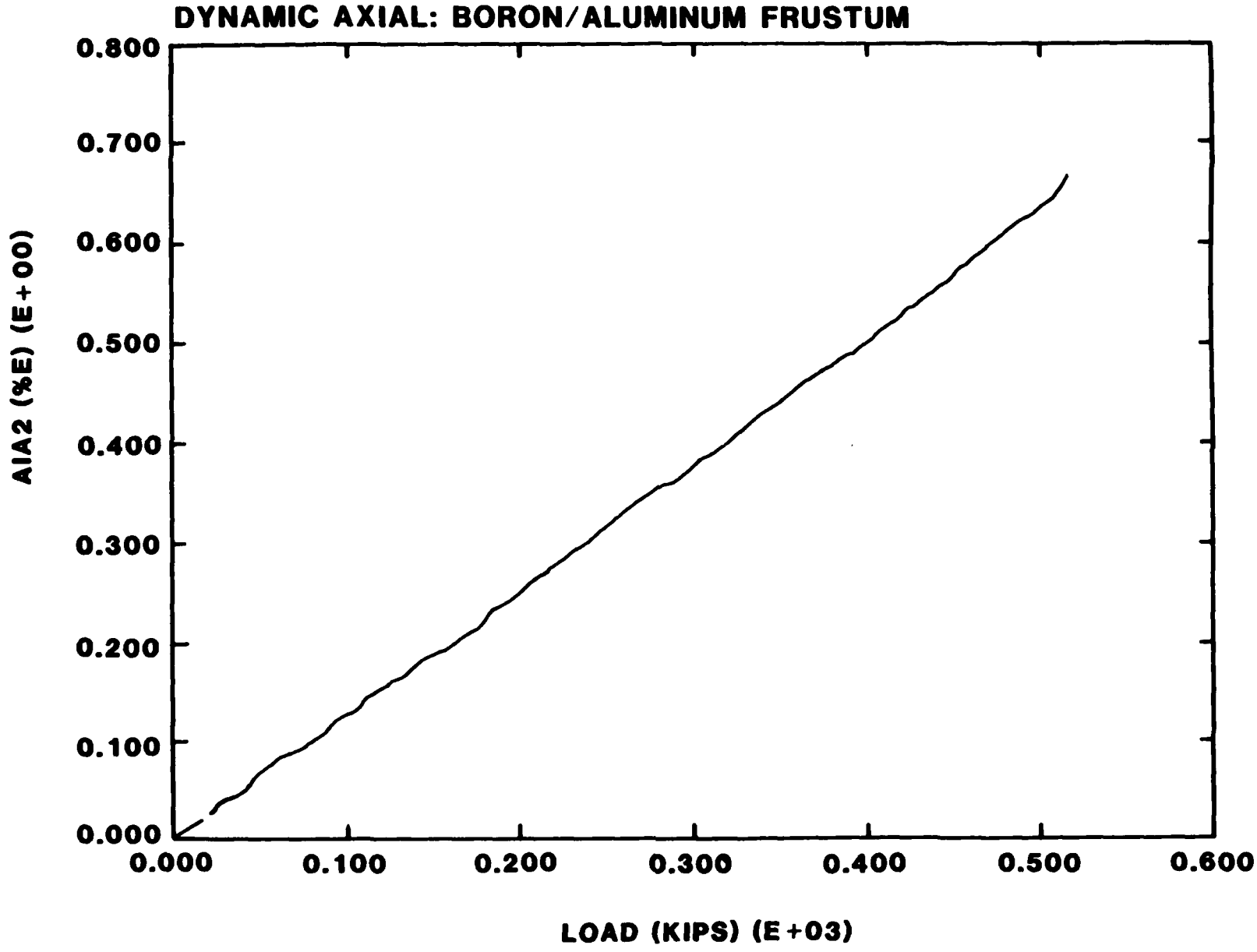
DYNAMIC AXIAL: BORON/ALUMINUM FRUSTUM
AIA2 (%E) (E+00)
0.800
0.700
0.600
0.500
0.400
0.300
0.200
0.100
0.000
0.000
0.100
0.200
0.300
0.400
0.500
0.600
LOAD (KIPS) (E+03)

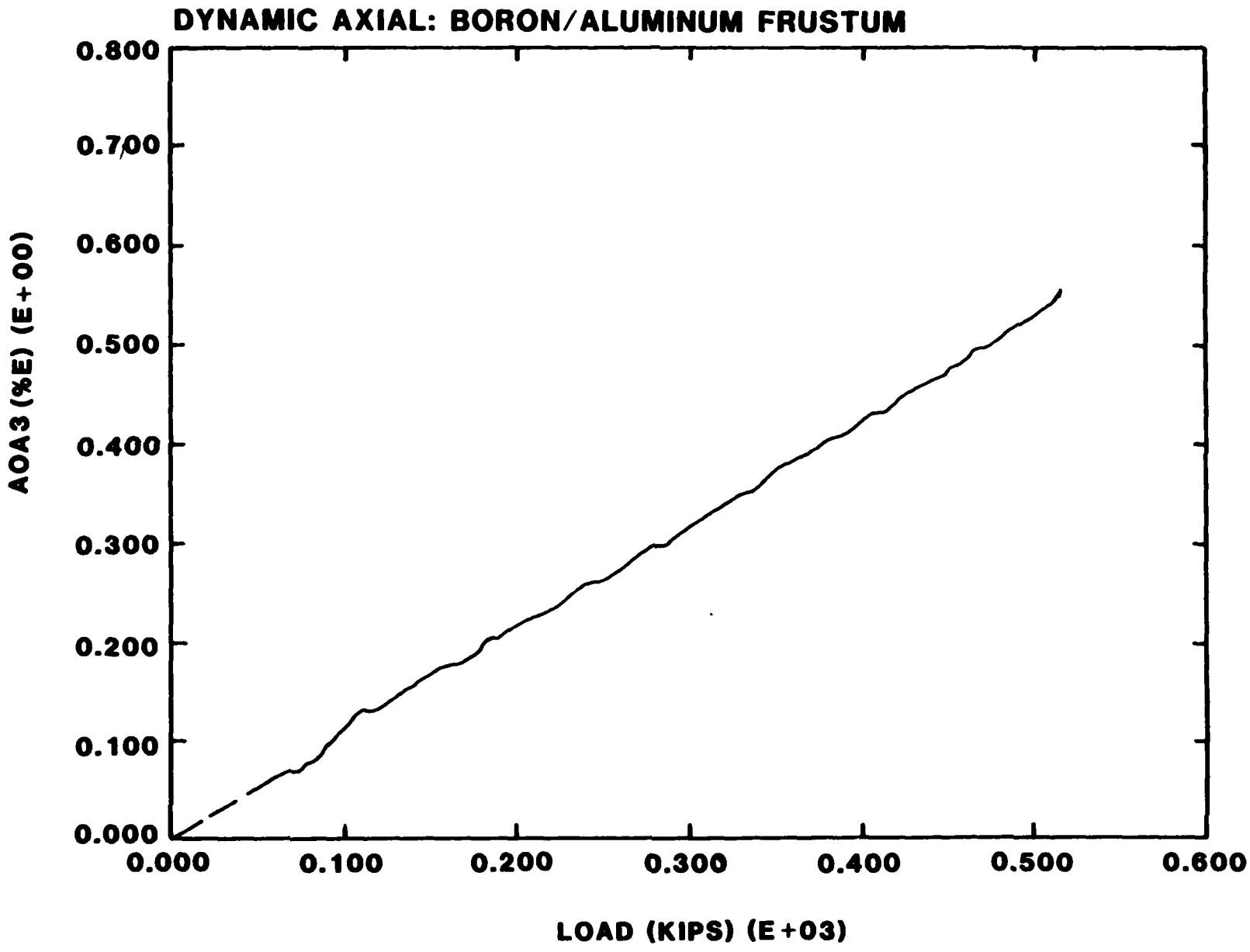
DYNAMIC AXIAL: BORON/ALUMINUM FRUSTUM
AOA3 (%E) (E+00)
0.800
0.700
0.600
0.500
0.400
0.300
0.200
0.100
0.000
0.000
0.100
0.200
0.300
0.400
0.500
0.600
LOAD (KIPS) (E+03)

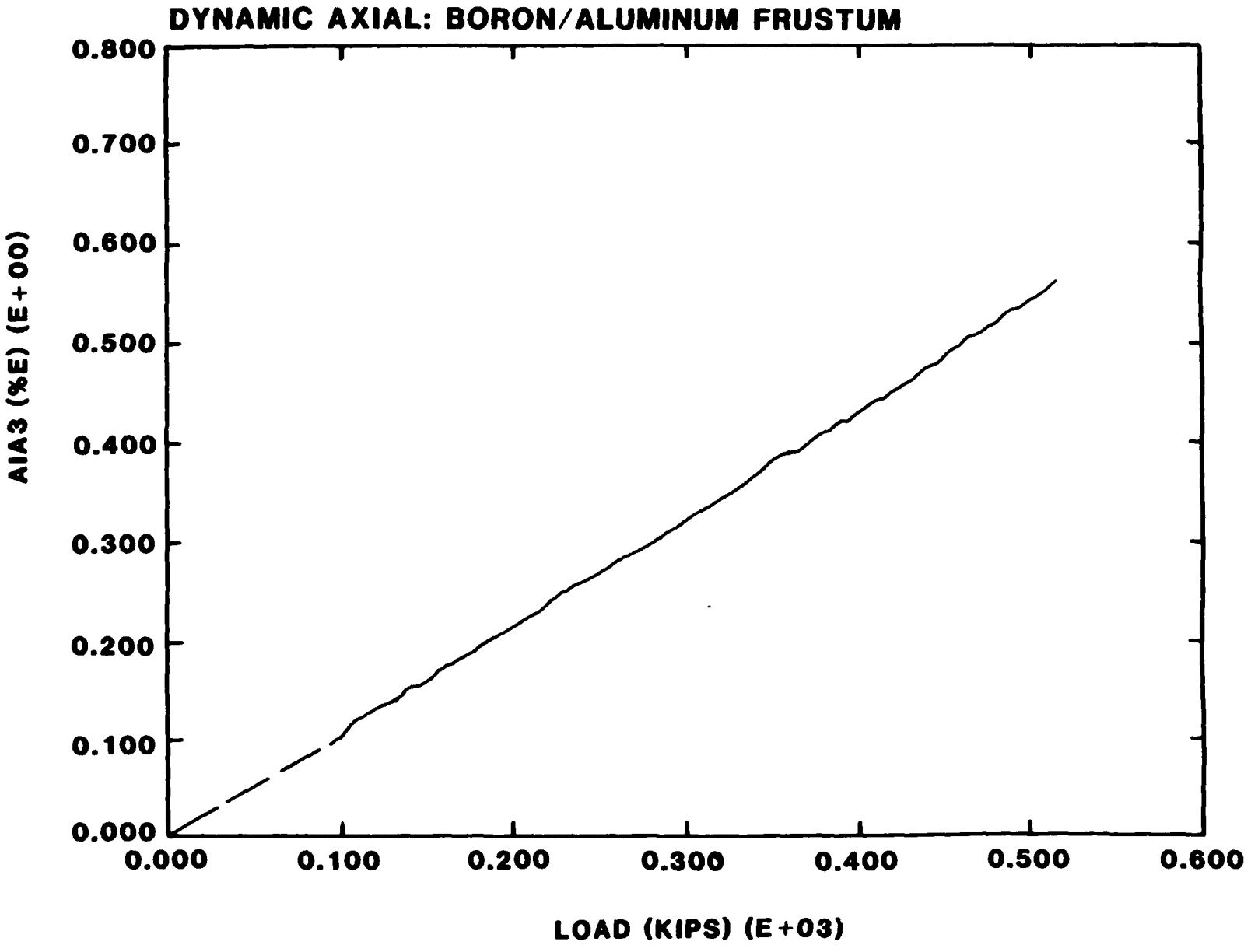
DYNAMIC AXIAL: BORON/ALUMINUM FRUSTUM
0.800
0.700
0.600
0.500
0.400
0.300
0.200
0.100
0.000
AIA3 (%E) (E+00)
0.000
0.100
0.200
0.300
0.400
0.500
0.600
LOAD (KIPS) (E+03)

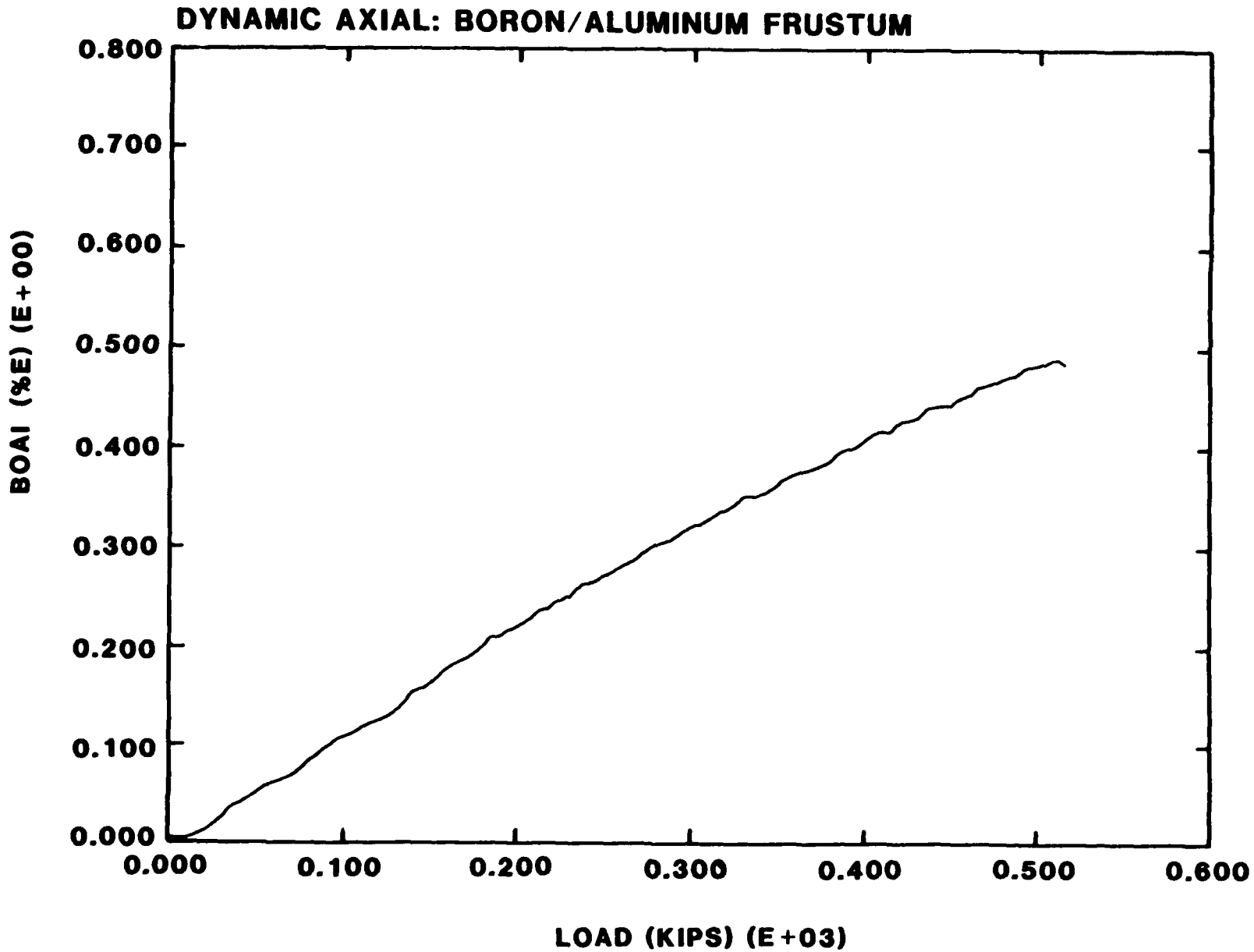
DYNAMIC AXIAL: BORON/ALUMINUM FRUSTUM
BOAI (%E) (E+00)
0.800
0.700
0.600
0.500
0.400
0.300
0.200
0.100
0.000
0.000
0.100
0.200
0.300
0.400
0.500
0.600
LOAD (KIPS) (E+03)

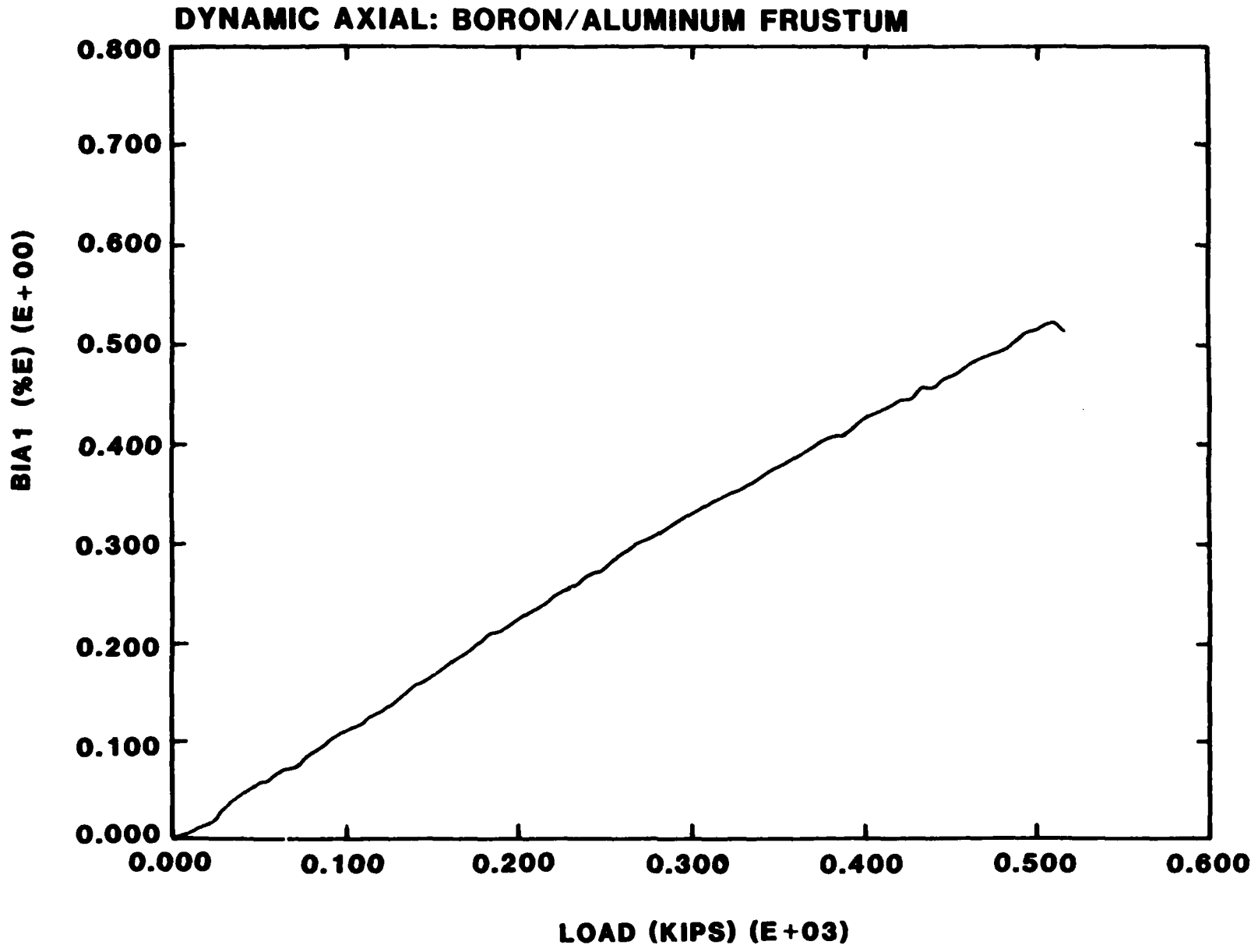
DYNAMIC AXIAL: BORON/ALUMINUM FRUSTUM
BIA1 (%E) (E+00)
0.800
0.700
0.600
0.500
0.400
0.300
0.200
0.100
0.000
0.000
0.100
0.200
0.300
0.400
0.500
0.600
LOAD (KIPS) (E+03)

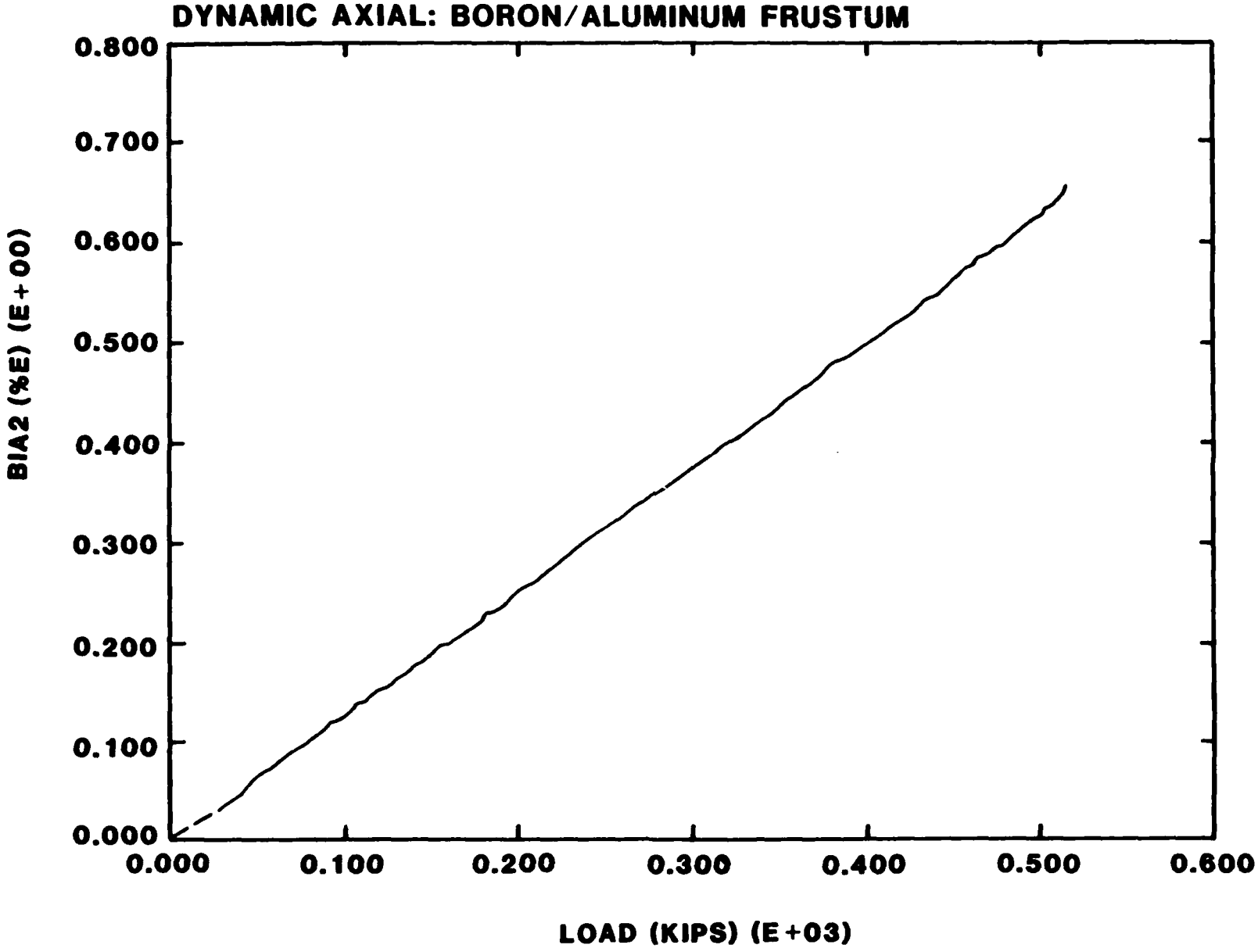
DYNAMIC AXIAL: BORON/ALUMINUM FRUSTUM
BIA2 (%E) (E+00)
0.800
0.700
0.600
0.500
0.400
0.300
0.200
0.100
0.000
0.000
0.100
0.200
0.300
0.400
0.500
0.600
LOAD (KIPS) (E+03)

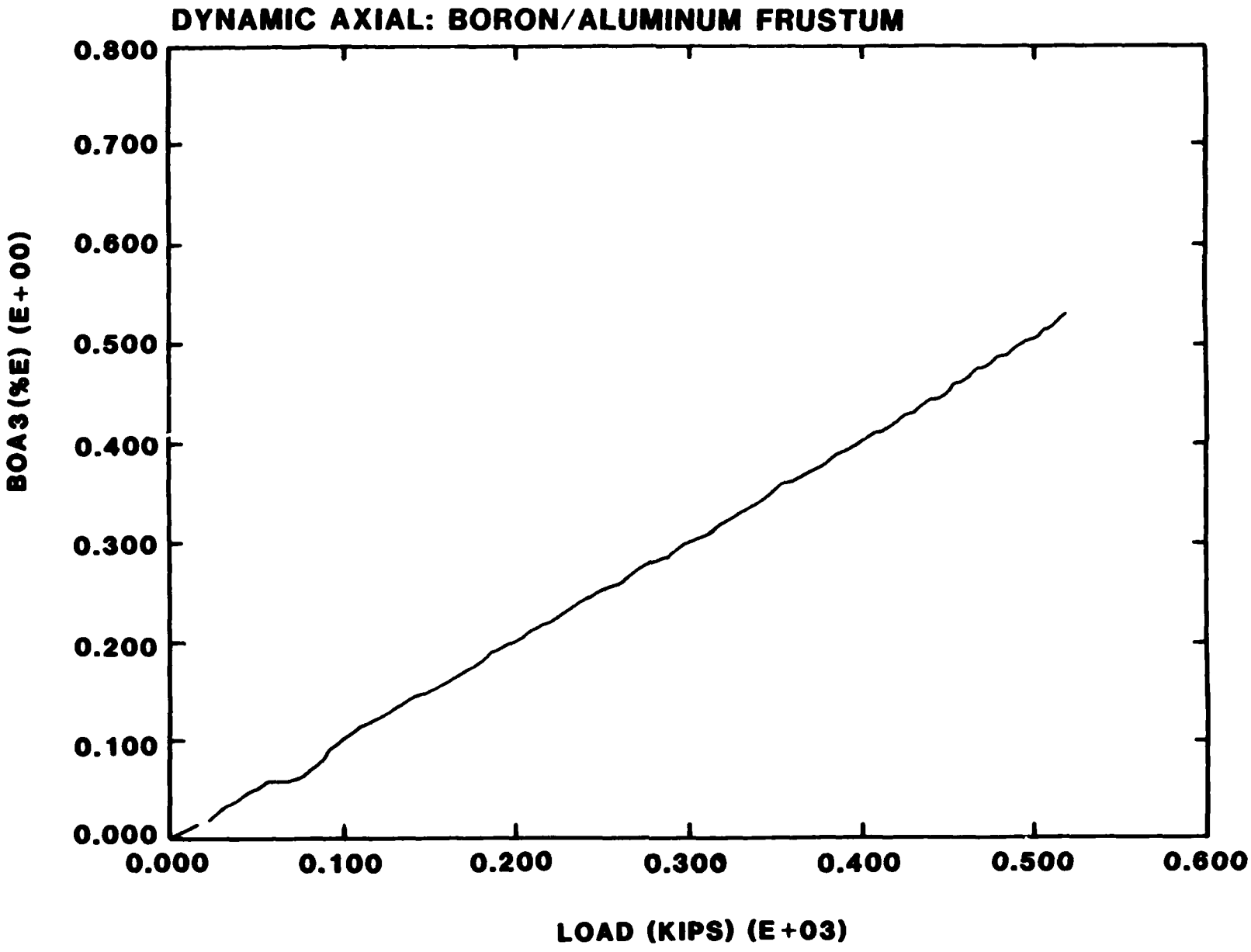
DYNAMIC AXIAL: BORON/ALUMINUM FRUSTUM
BOA3 (%E) (E+00)
0.800
0.700
0.600
0.500
0.400
0.300
0.200
0.100
0.000
0.000
0.100
0.200
0.300
0.400
0.500
0.600
LOAD (KIPS) (E+03)

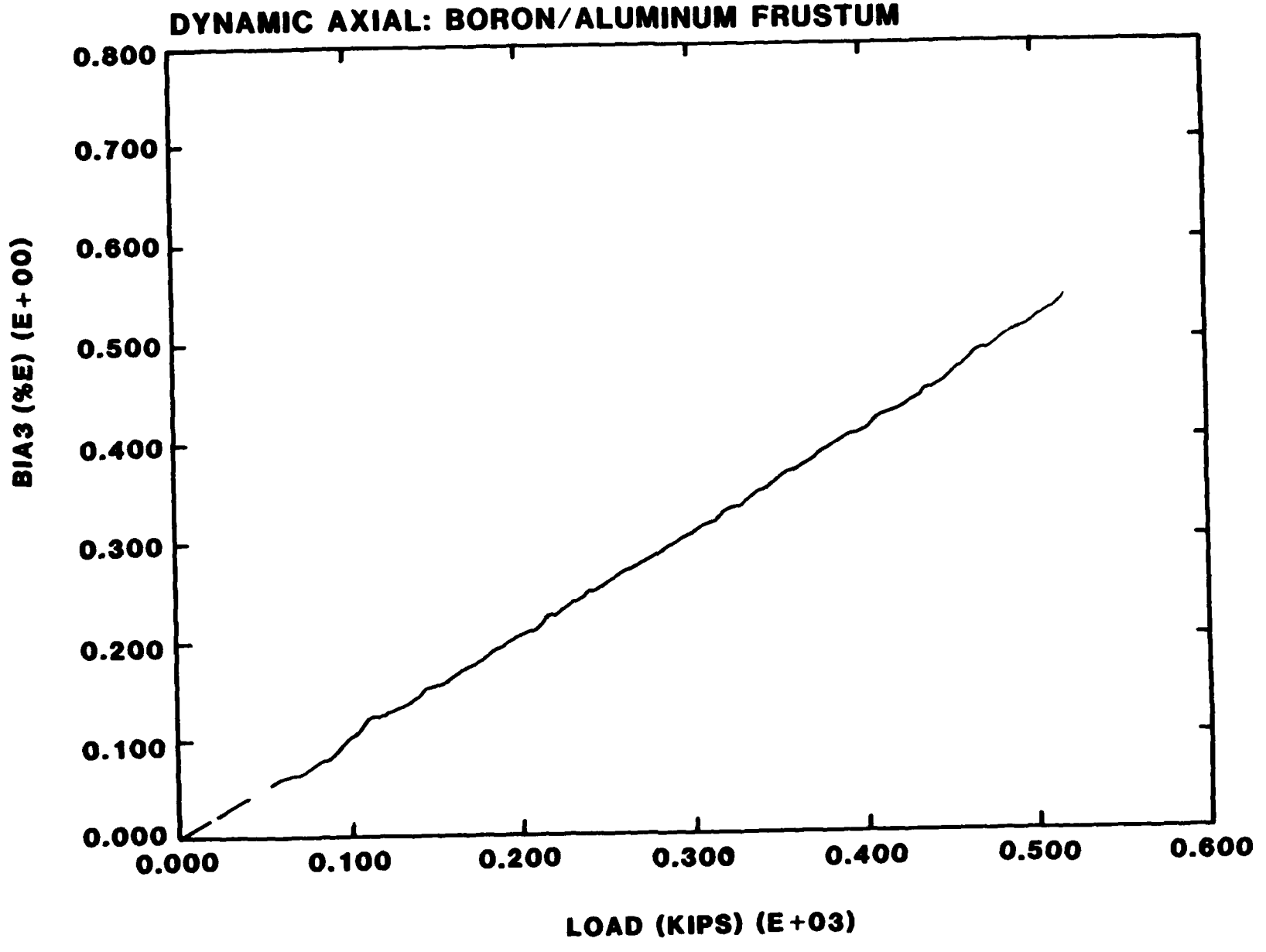
DYNAMIC AXIAL: BORON/ALUMINUM FRUSTUM
BIA3 (%E) (E+00)
0.800
0.700
0.600
0.500
0.400
0.300
0.200
0.100
0.000
0.000
0.100
0.200
0.300
0.400
0.500
0.600
LOAD (KIPS) (E+03)

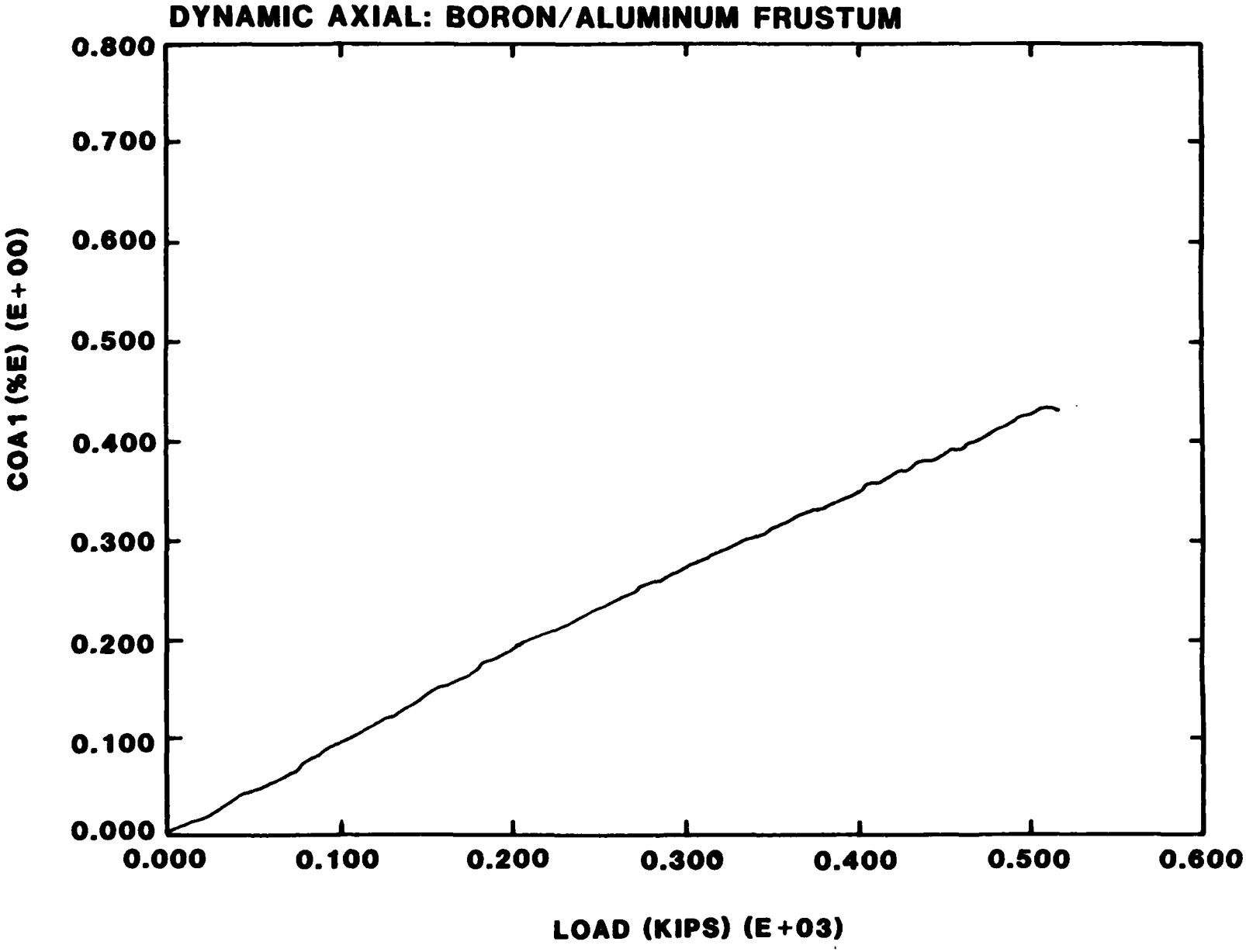
DYNAMIC AXIAL: BORON/ALUMINUM FRUSTUM
0.800
0.700
0.600
0.500
0.400
0.300
0.200
0.100
0.000
COA1 (%E) (E+00)
0.000
0.100
0.200
0.300
0.400
0.500
0.600
LOAD (KIPS) (E+03)

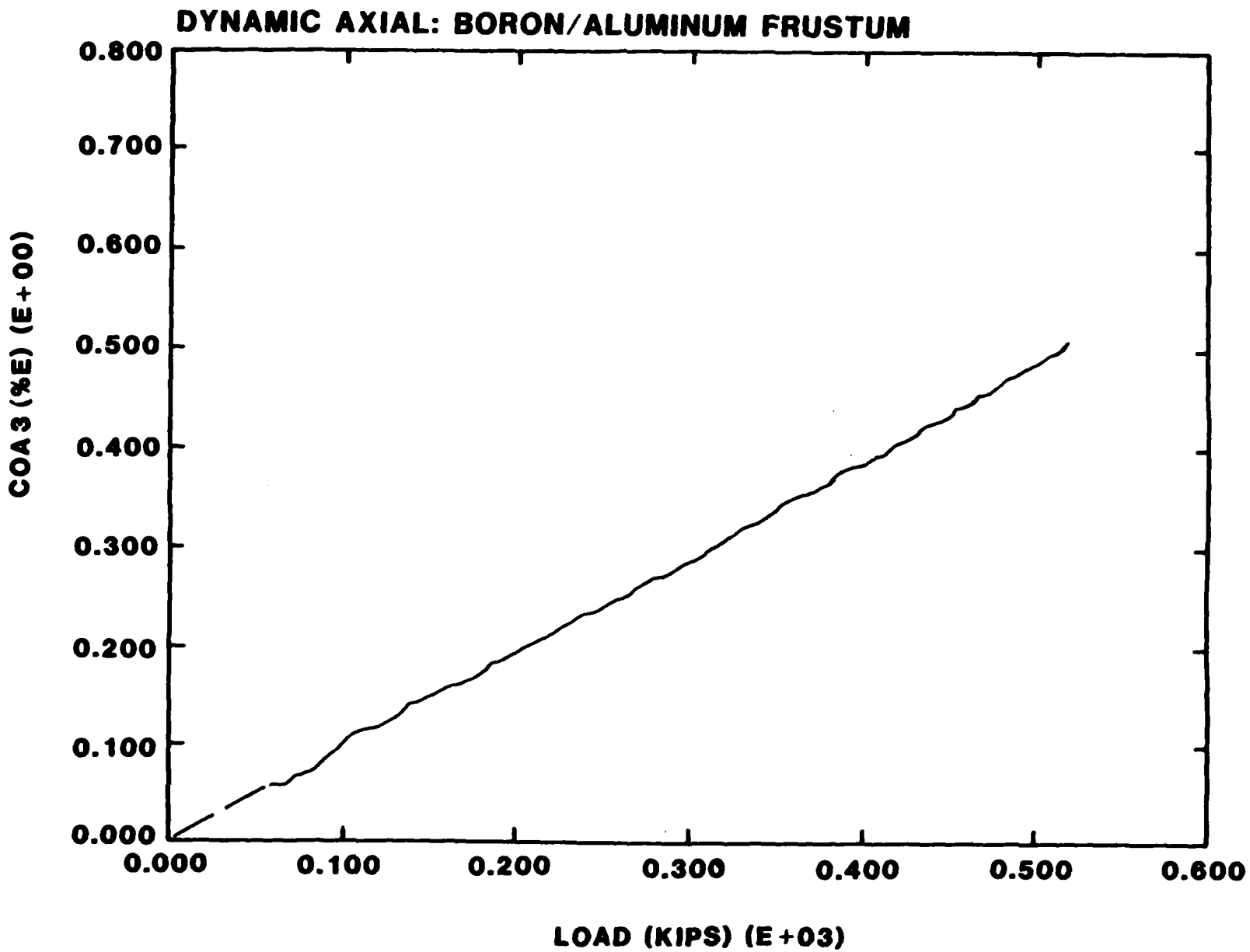
DYNAMIC AXIAL: BORON/ALUMINUM FRUSTUM
COA3 (%E) (E+00)
0.800
0.700
0.600
0.500
0.400
0.300
0.200
0.100
0.000
0.000
0.100
0.200
0.300
0.400
0.500
0.600
LOAD (KIPS) (E+03)

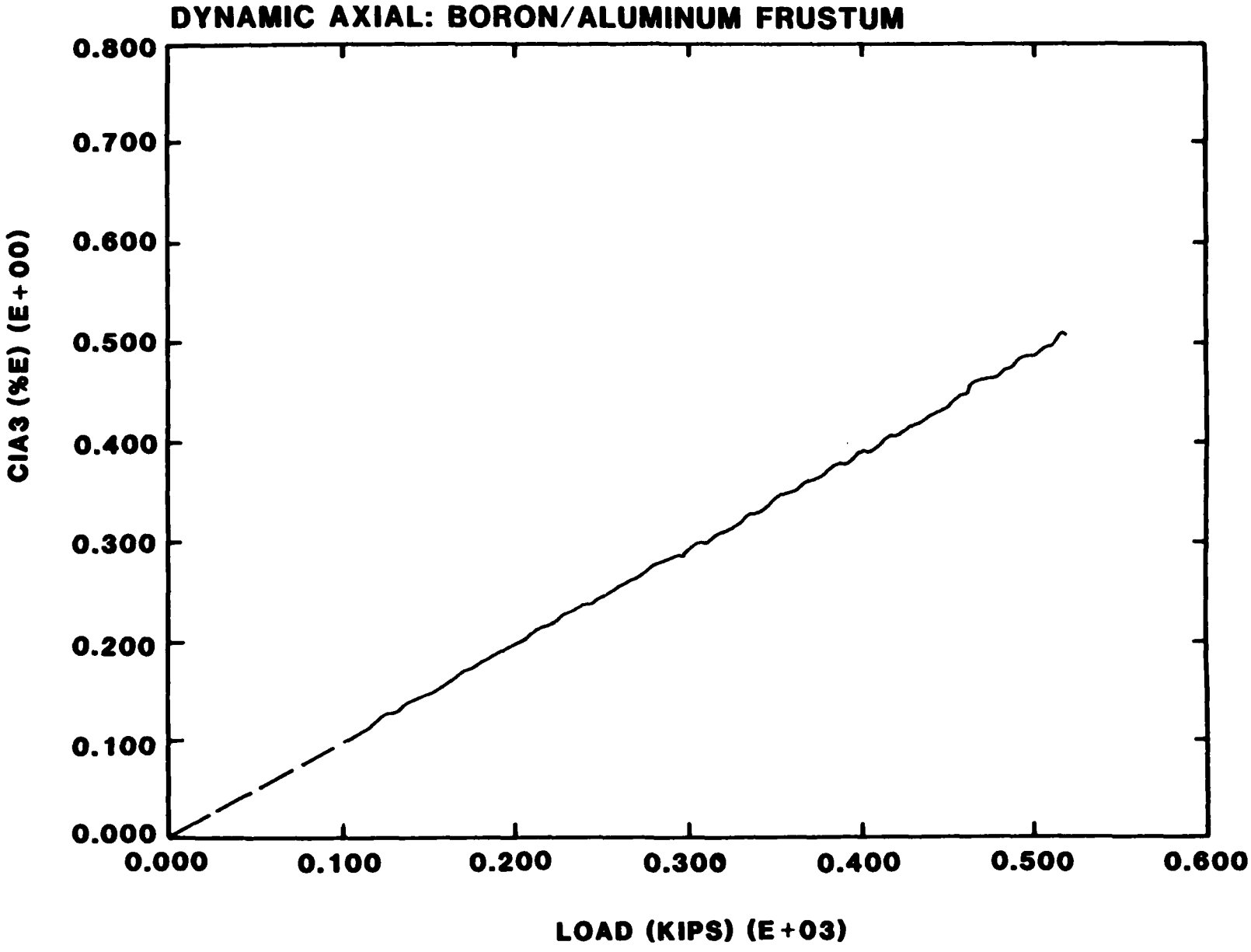
DYNAMIC AXIAL: BORON/ALUMINUM FRUSTUM
0.800
0.700
0.600
0.500
0.400
0.300
0.200
0.100
0.000
CIA3 (%E) (E+00)
0.000
0.100
0.200
0.300
0.400
0.500
0.600
LOAD (KIPS) (E+03)

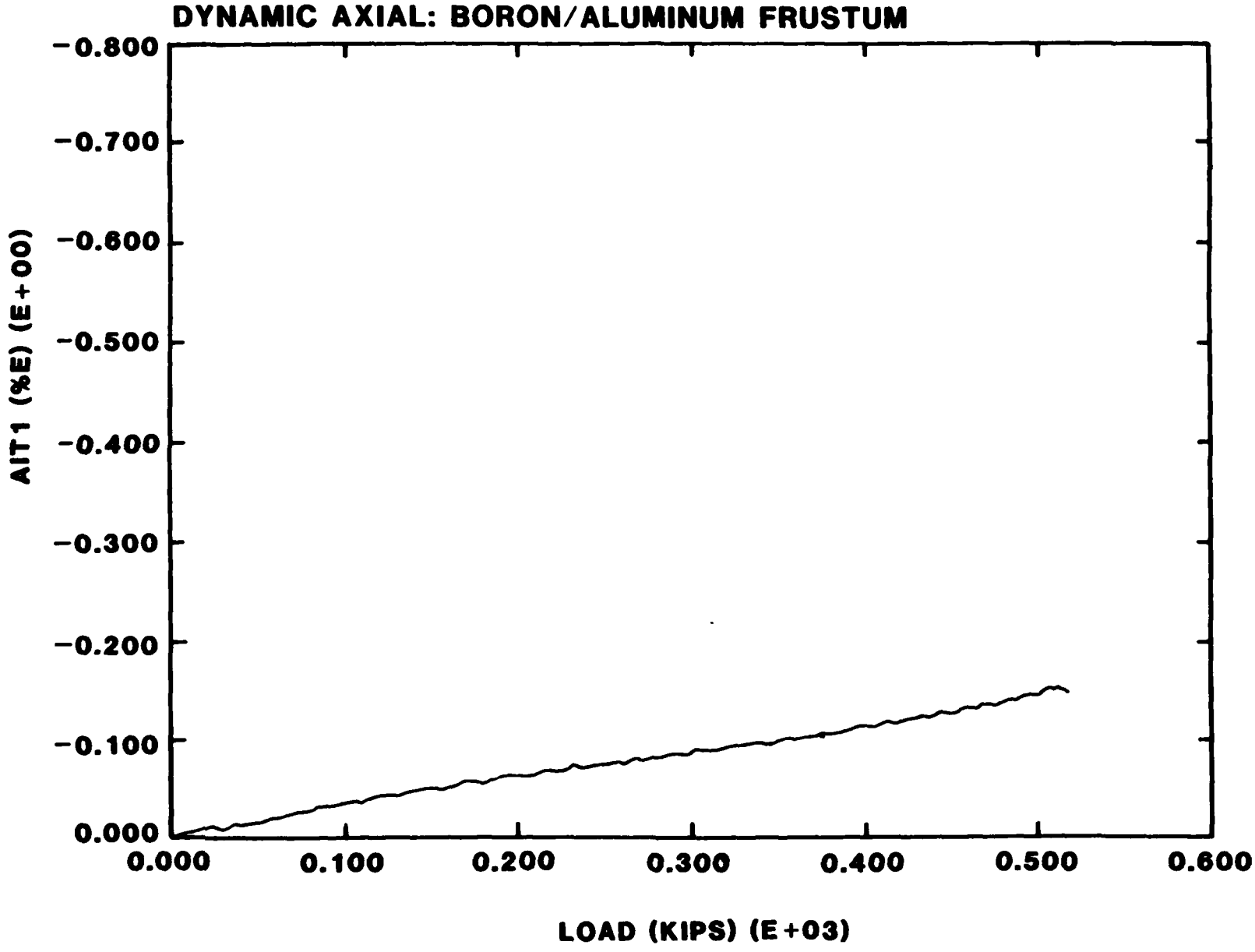
DYNAMIC AXIAL: BORON/ALUMINUM FRUSTUM
AIT1 (%E) (E+00)
-0.800
-0.700
-0.600
-0.500
-0.400
-0.300
-0.200
-0.100
0.000
0.000
0.100
0.200
0.300
0.400
0.500
0.600
LOAD (KIPS) (E+03)

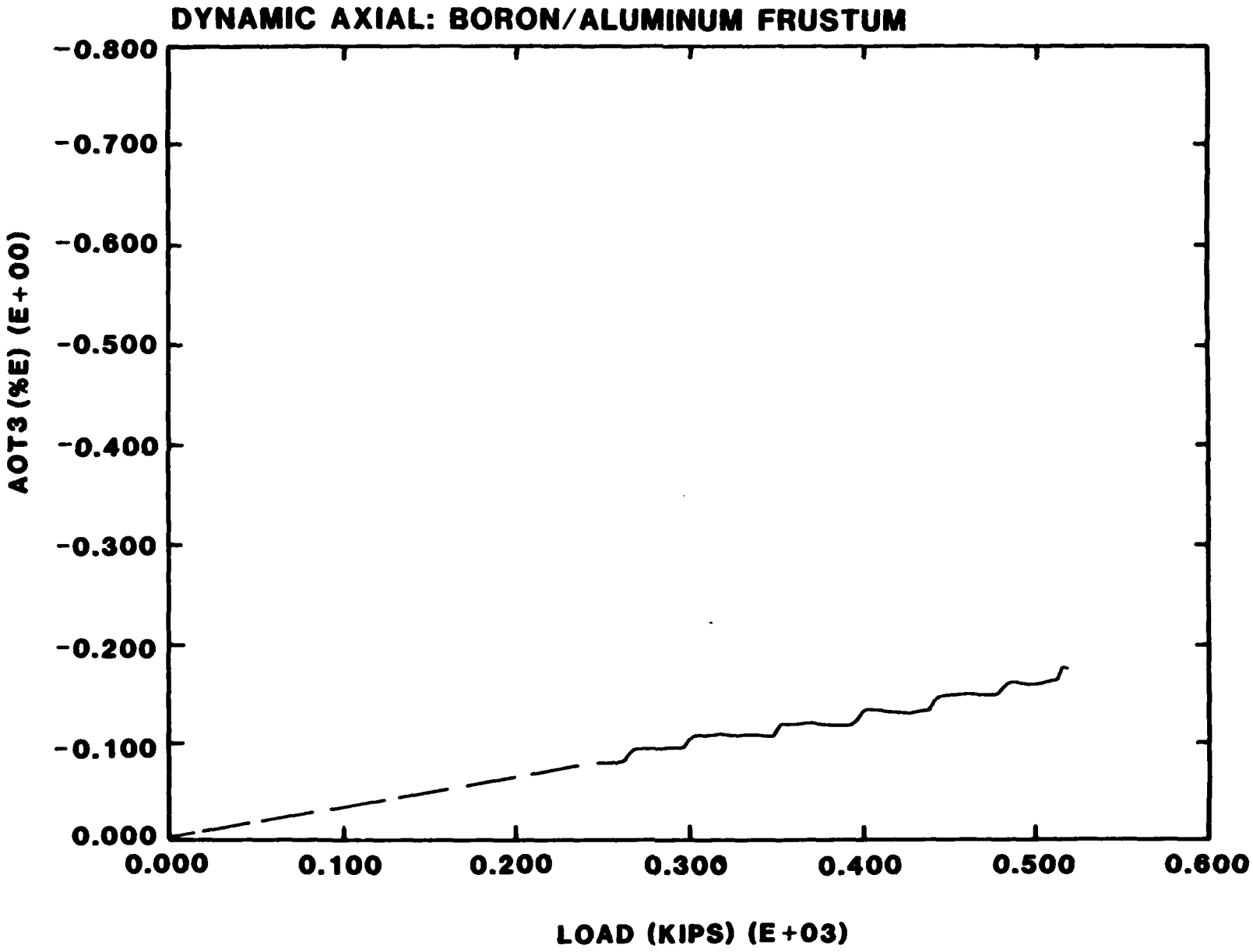
DYNAMIC AXIAL: BORON/ALUMINUM FRUSTUM
-0.800
-0.700
-0.600
-0.500
-0.400
-0.300
-0.200
-0.100
0.000
AOT3 (%E) (E+00)
0.000
0.100
0.200
0.300
0.400
0.500
0.600
LOAD (KIPS) (E+03)

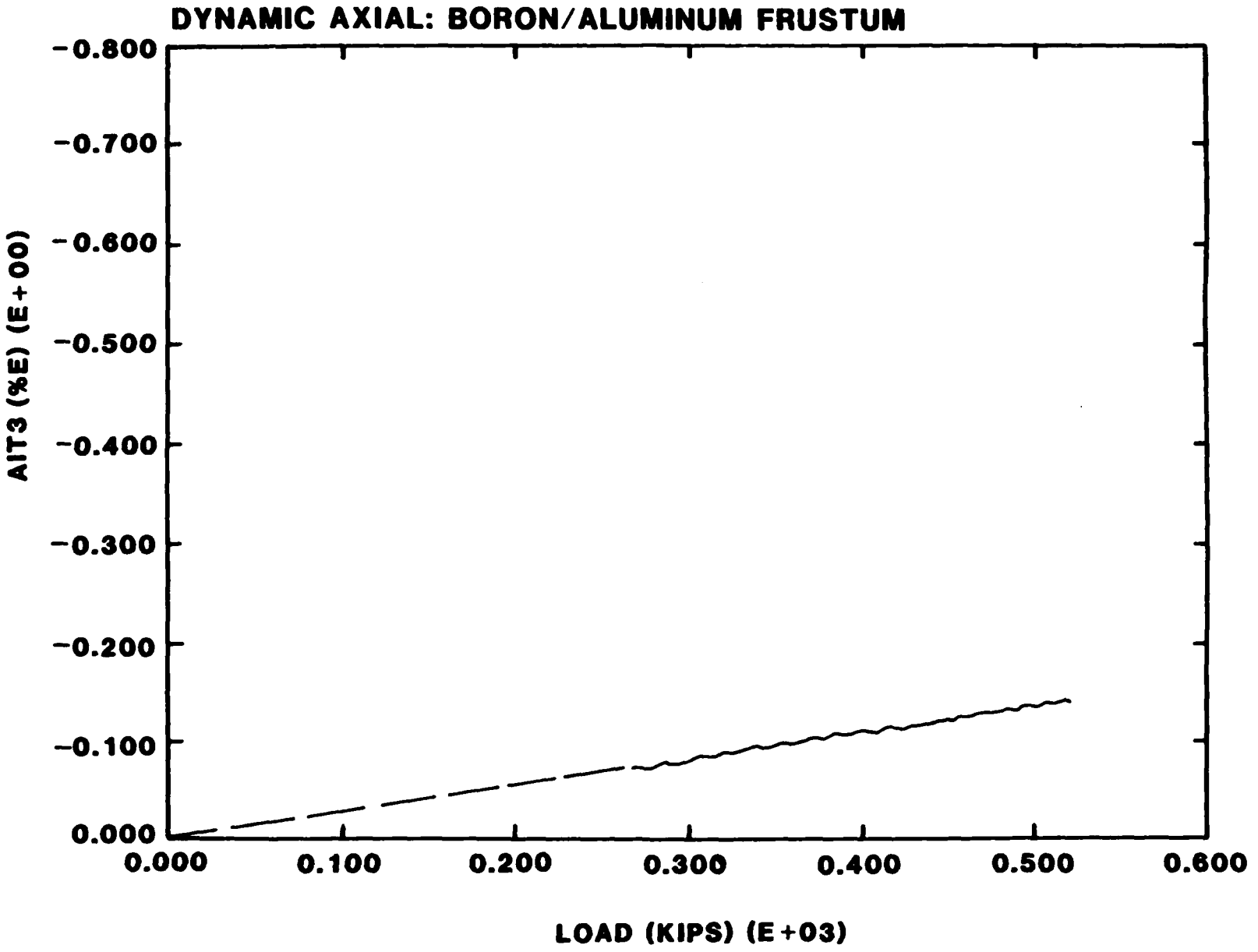
DYNAMIC AXIAL: BORON/ALUMINUM FRUSTUM
AIT3 (%E) (E+00)
-0.800
-0.700
-0.600
-0.500
-0.400
-0.300
-0.200
-0.100
0.000
0.000
0.100
0.200
0.300
0.400
0.500
0.600
LOAD (KIPS) (E+03)

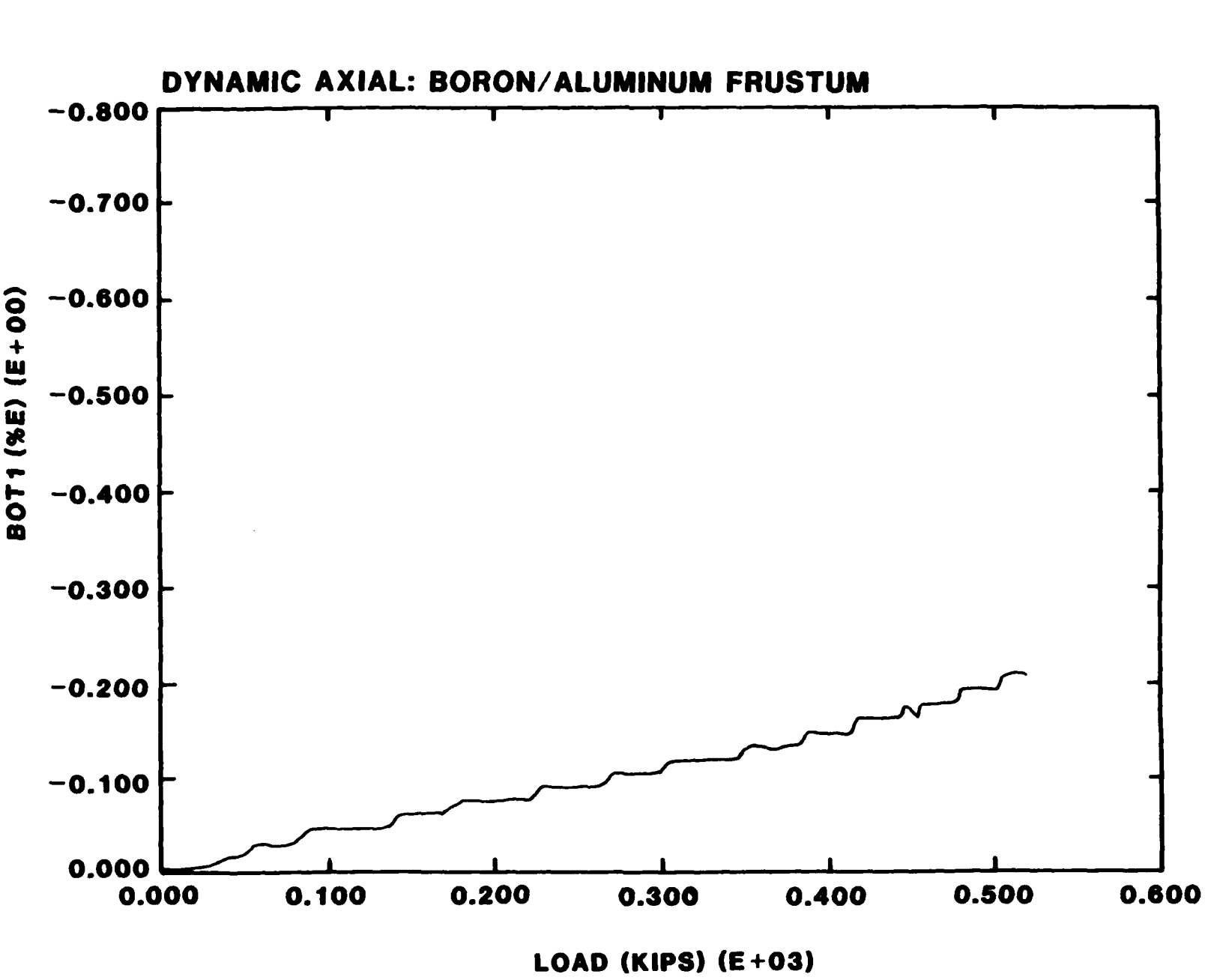
DYNAMIC AXIAL: BORON/ALUMINUM FRUSTUM
-0.800
-0.700
-0.600
-0.500
-0.400
-0.300
-0.200
-0.100
0.000
BOT1 (%E) (E+00)
0.000
0.100
0.200
0.300
0.400
0.500
0.600
LOAD (KIPS) (E+03)

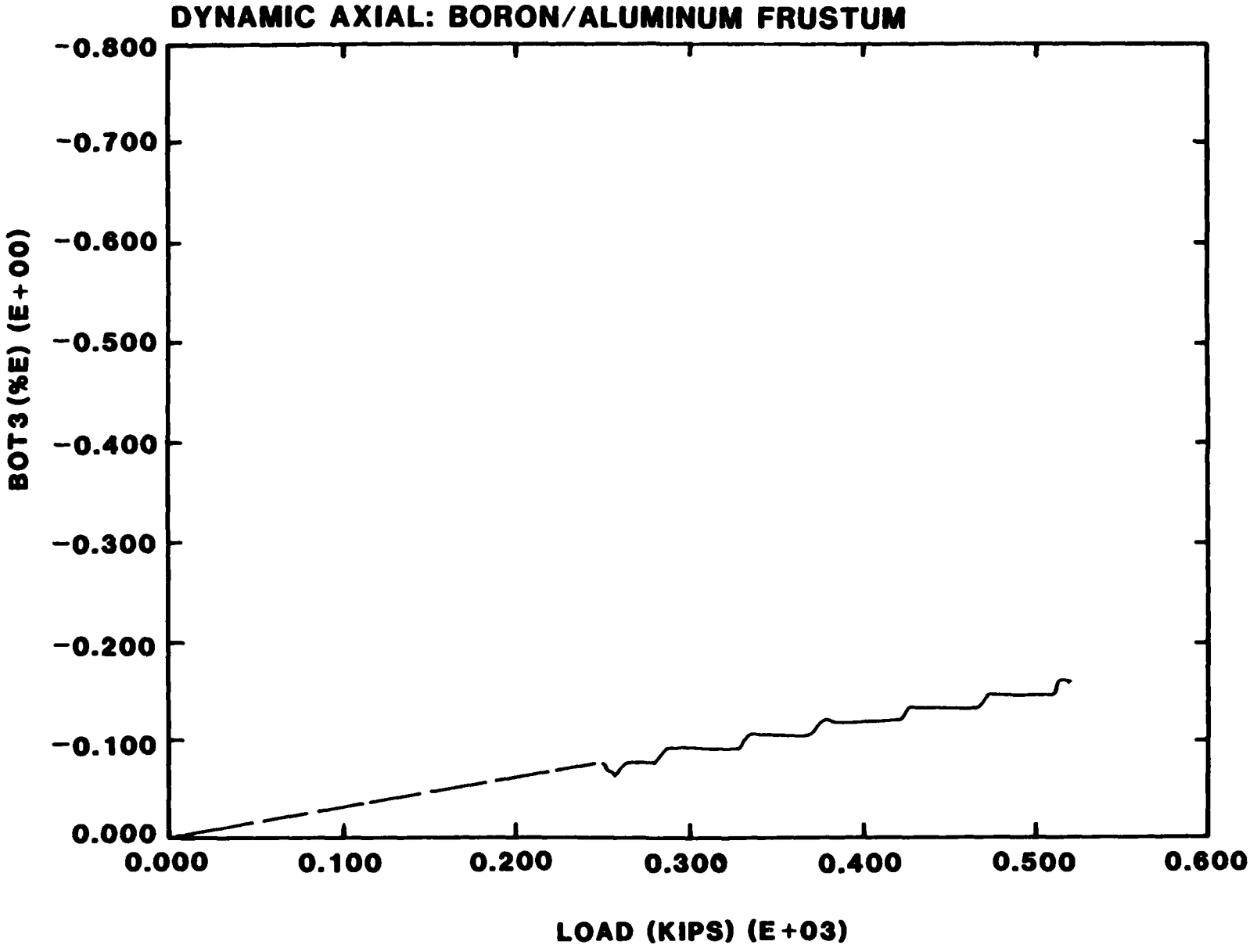
DYNAMIC AXIAL: BORON/ALUMINUM FRUSTUM
-0.800
-0.700
-0.600
-0.500
-0.400
-0.300
-0.200
-0.100
0.000
BOT3 (%E) (E+00)
0.000
0.100
0.200
0.300
0.400
0.500
0.600
LOAD (KIPS) (E+03)

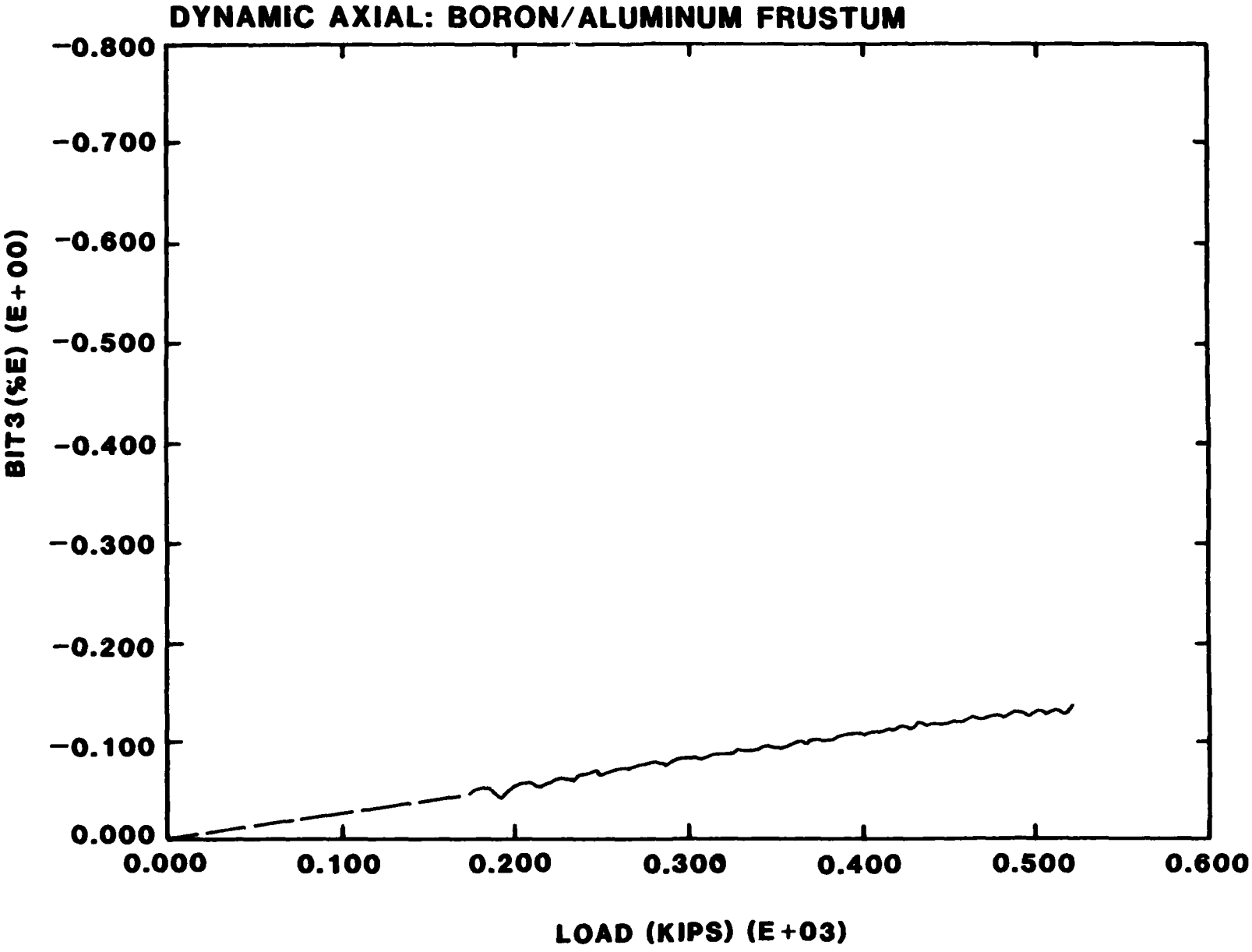
DYNAMIC AXIAL: BORON/ALUMINUM FRUSTUM
-0.800
-0.700
-0.600
-0.500
-0.400
-0.300
-0.200
-0.100
0.000
BIT3 (%E) (E+00)
0.000
0.100
0.200
0.300
0.400
0.500
0.600
LOAD (KIPS) (E+03)

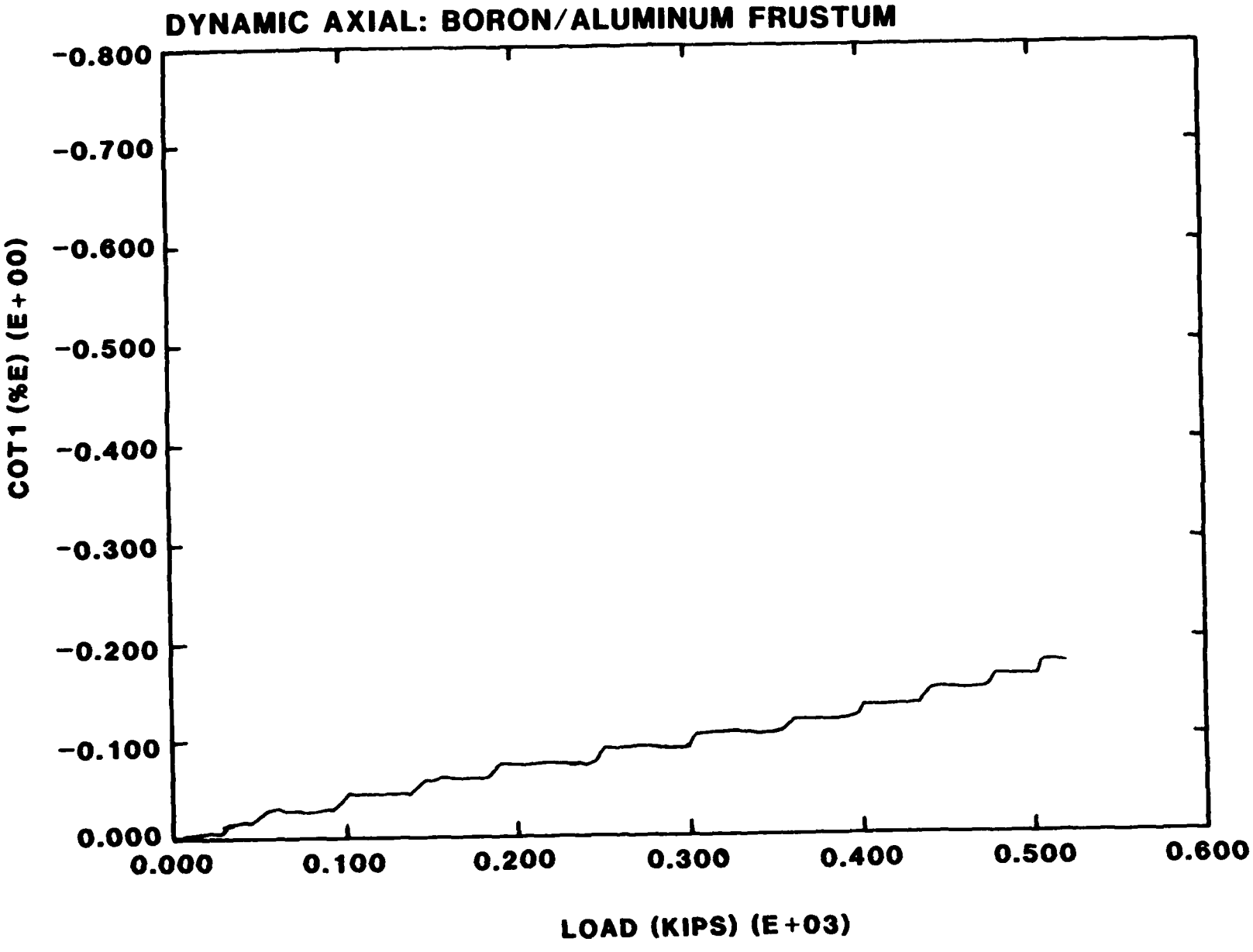
DYNAMIC AXIAL: BORON/ALUMINUM FRUSTUM
COT1 (%E) (E+00)
-0.800
-0.700
-0.600
-0.500
-0.400
-0.300
-0.200
-0.100
0.000
0.000
0.100
0.200
0.300
0.400
0.500
0.600
LOAD (KIPS) (E+03)

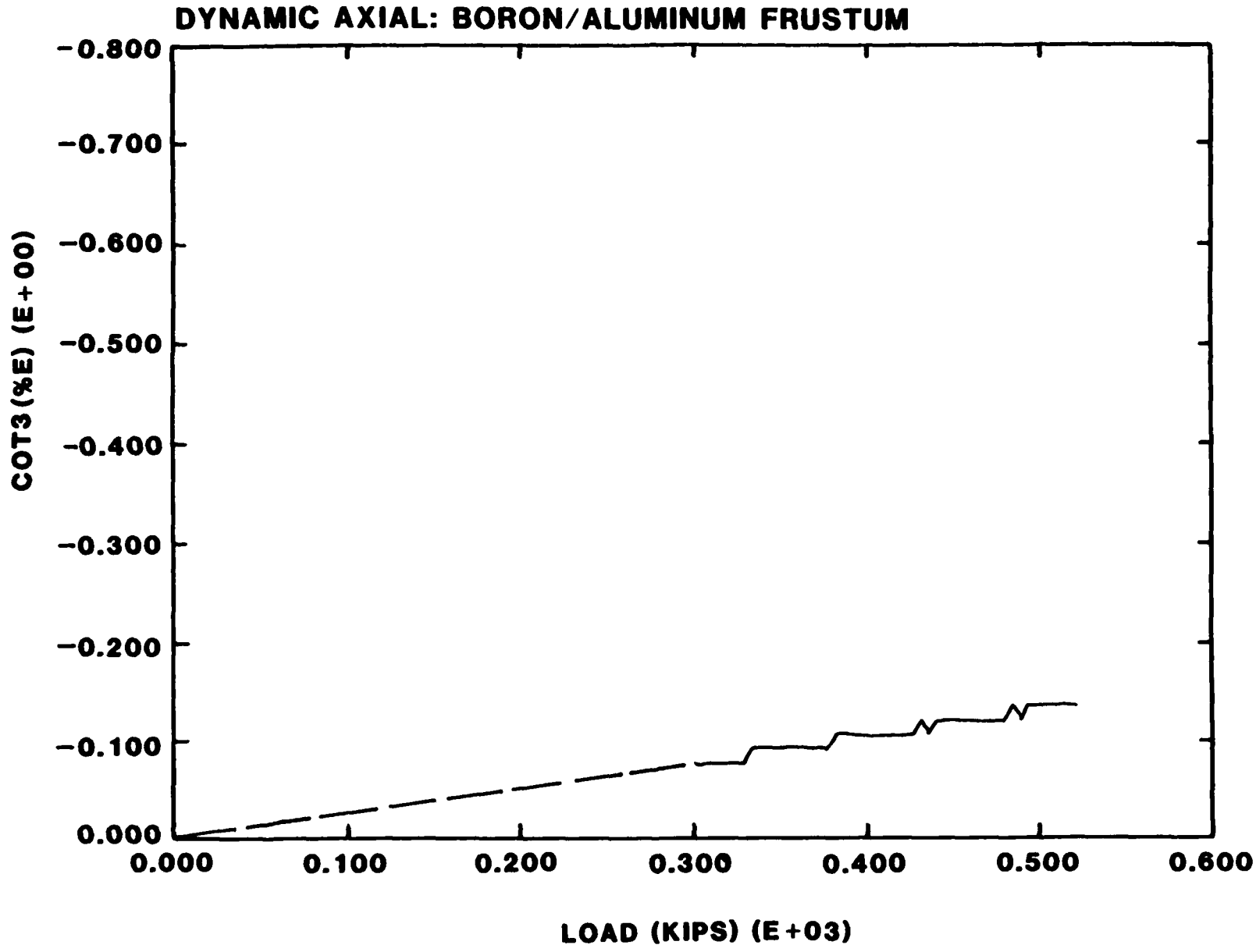
DYNAMIC AXIAL: BORON/ALUMINUM FRUSTUM
-0.800
-0.700
-0.600
-0.500
-0.400
-0.300
-0.200
-0.100
0.000
COT3 (%E) (E+00)
0.000
0.100
0.200
0.300
0.400
0.500
0.600
LOAD (KIPS) (E+03)

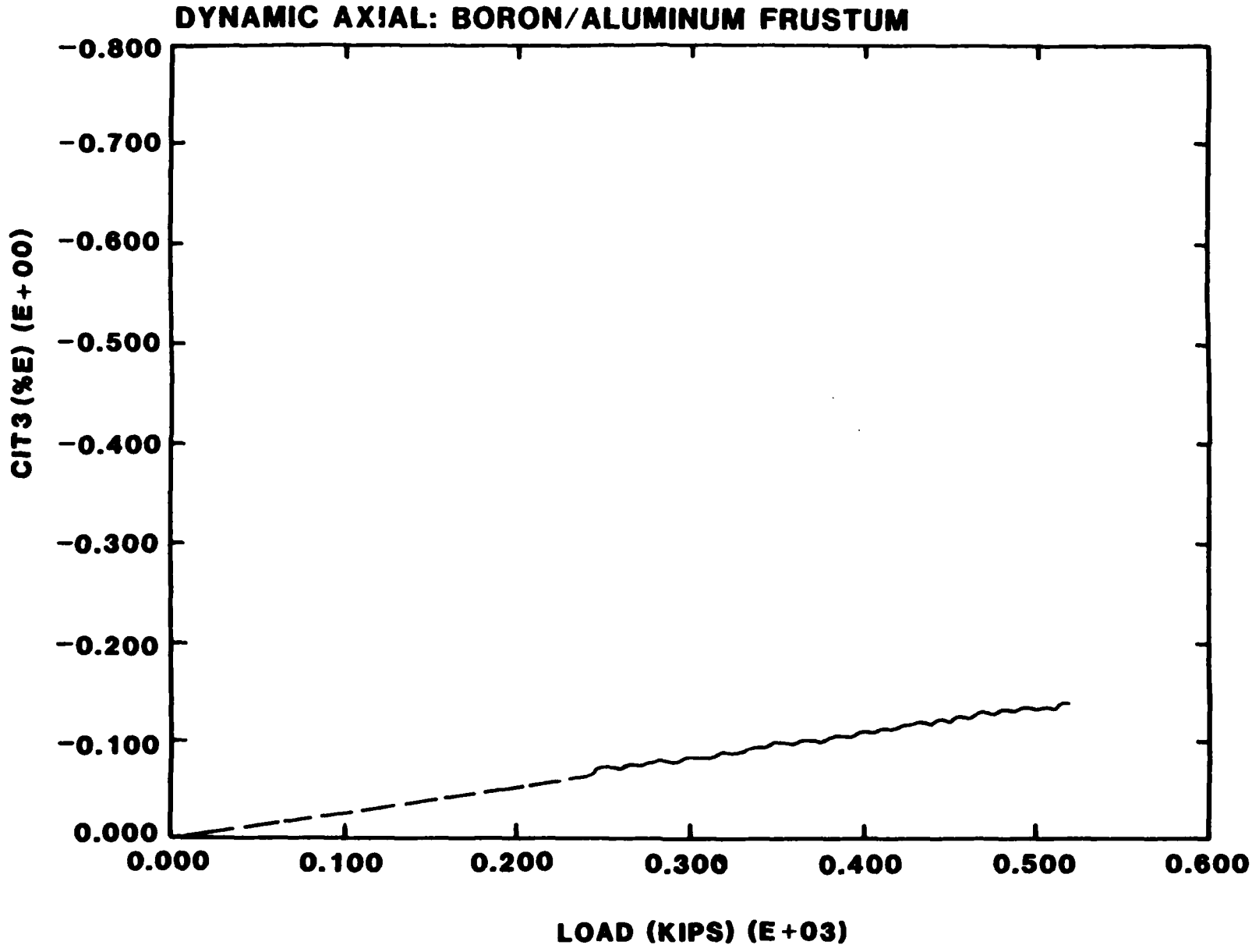
DYNAMIC AXIAL: BORON/ALUMINUM FRUSTUM
-0.800
-0.700
-0.600
-0.500
-0.400
-0.300
-0.200
-0.100
0.000
CIT3 (%E) (E+00)
0.000
0.100
0.200
0.300
0.400
0.500
0.600
LOAD (KIPS) (E+03)

7.6 APPENDIX F

STATIC-SHEAR/BEND LOADING TEST DATA
FOR BORON/ALUMINUM FRUSTA

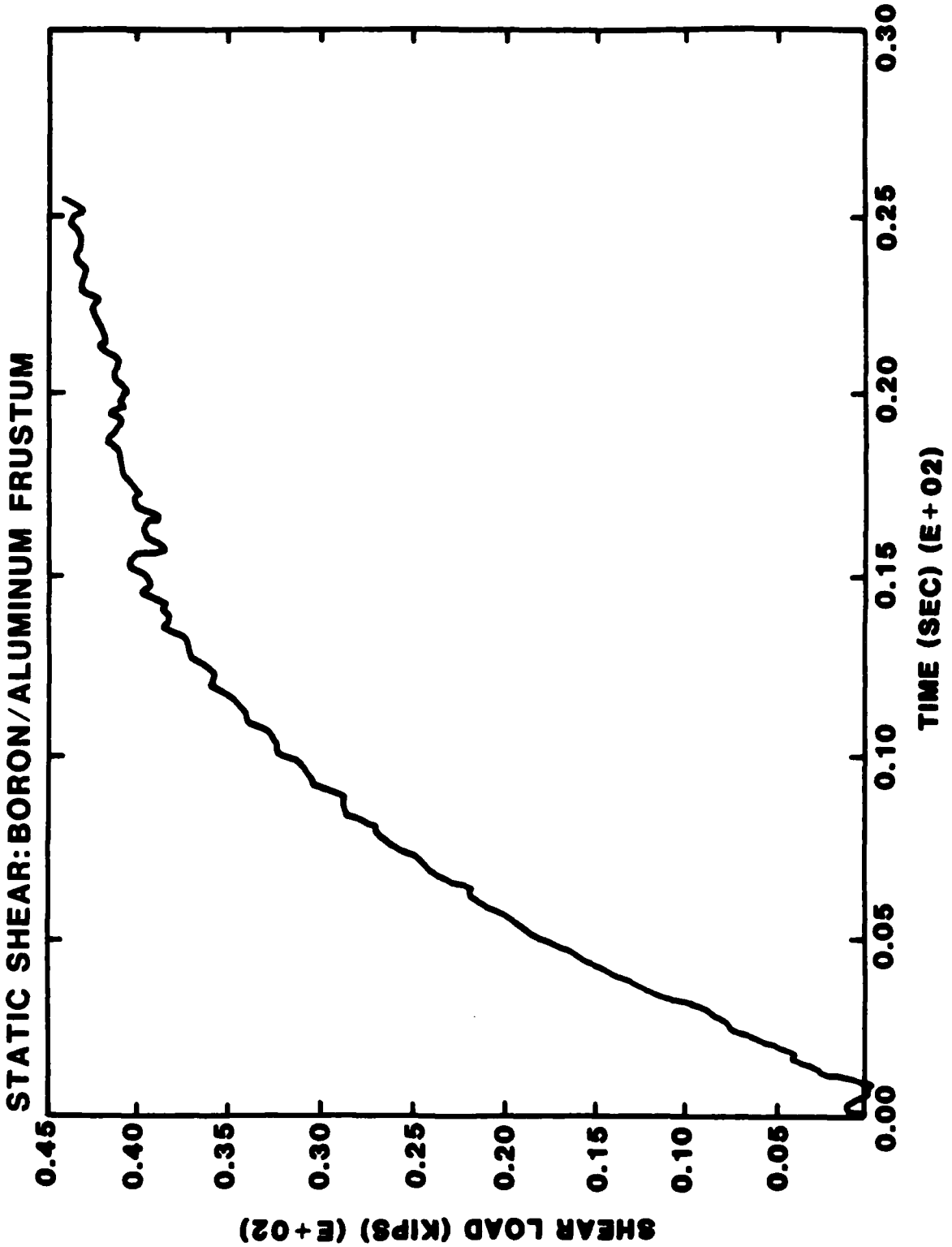
STATIC SHEAR: BORON/ALUMINUM FRUSTUM
SHEAR LOAD (KIPS) (E+02)
0.45
0.40
0.35
0.30
0.25
0.20
0.15
0.10
0.05
0.00
0.05
0.10
0.15
0.20
0.25
0.30
TIME (SEC) (E+02)

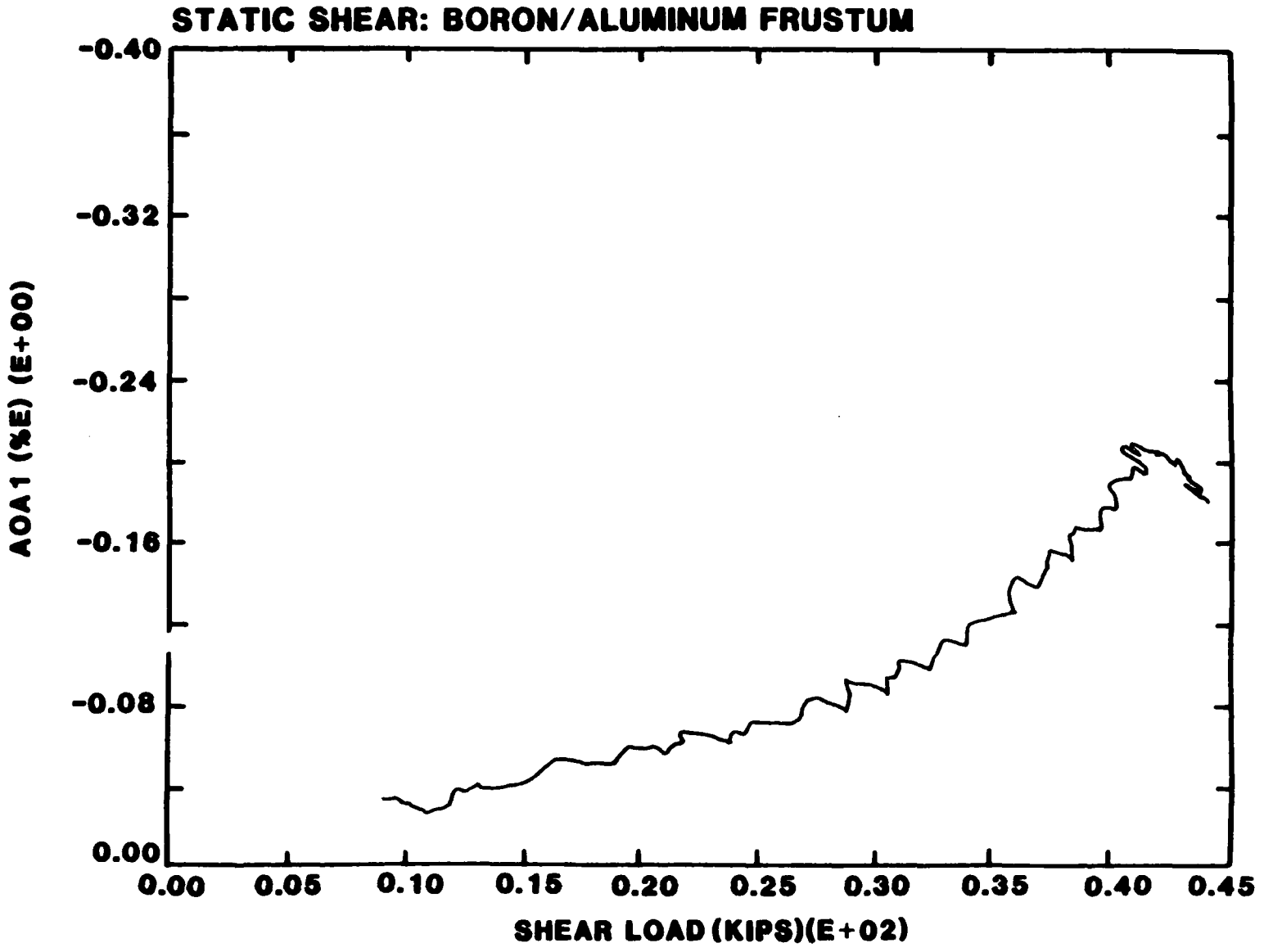
STATIC SHEAR: BORON/ALUMINUM FRUSTUM
AOA1 (%E) (E+00)
-0.40
-0.32
-0.24
-0.16
-0.08
0.00
0.00
0.05
0.10
0.15
0.20
0.25
0.30
0.35
0.40
0.45
SHEAR LOAD (KIPS)(E+02)

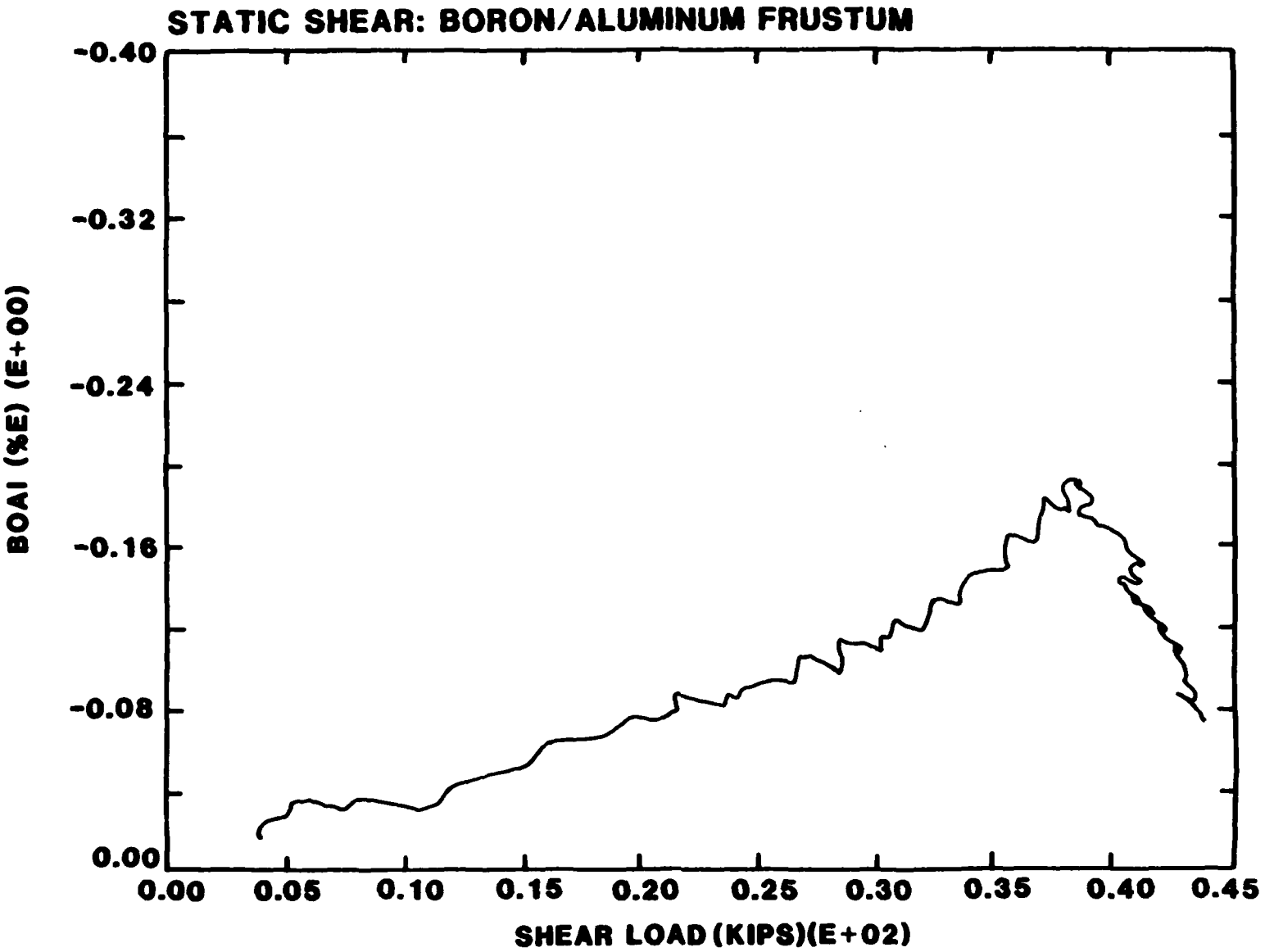
STATIC SHEAR: BORON/ALUMINUM FRUSTUM
BOAI (%E) (E+00)
-0.40
-0.32
-0.24
-0.16
-0.08
0.00
0.00
0.05
0.10
0.15
0.20
0.25
0.30
0.35
0.40
0.45
SHEAR LOAD (KIPS)(E+02)

DISTRIBUTION LIST

	No. of Copies
Office of Deputy Under Secretary of Defense for Research and Engineering (ET) ATTN: Mr. J. Persh, Staff Specialist for Materials and Structures (Room 3D1089) The Pentagon Washington, DC 20301	1
Office of Deputy Chief of Research Development and Acquisition ATTN: DAMA-CSS The Pentagon Washington, DC 20301	1
Commander U.S. Army Materiel Command ATTN: AMCLD, R. Vitali, Office of Laboratory Management 5001 Eisenhower Avenue Alexandria, VA 22333	1
Director U.S. Army Strategic Defense Command ATTN: DASD-H-L, Dr. E. Wilkinson DASD-H-L, Dr. S. Proffitt DASD-H-H, R. Buckelew DASD-H-E, J. Katechis P.O. Box 1500 Huntsville, AL 35807	1 1 1 1
Director U.S. Army Strategic Defense Command ATTN: DASD-H-Y, Col. K. Kawano DASD-H-W, D. Harmon DASD-H-W, J. Papadopoulos DASD-H-W, S. Brockway P.O. Box 1500 Huntsville, AL 35807-3801	1 1 1 1
Director Defense Nuclear Agency ATTN: SPAS, Maj. D. K. Apo SPLH, J. W. Somers SPLH, Dr. B. Steverding Washington, DC 20305-1000	1 1 1
Director Army Ballistic Research Laboratories ATTN: DRDAR-BLT, Dr. N. J. Huffington, Jr DRDAR-BLT, Dr. T. W. Wright DRDAR-BLT, Dr. G. L. Moss Aberdeen Proving Ground, MD 21005	1 1 1

	No. of Copies
Commander Air Force Materials Laboratory Air Force Systems Command ATTN: LNC, Dr. D. Schmidt Wright-Patterson Air Force Base Dayton, OH 45433	1
Commander BMO/ABRES Office ATTN: Capt. S. Opel Norton Air Force Base, CA 92409	1
Commander Air Force Materials Laboratory ATTN: AFML/MBM, Dr. S. W. Tsai Wright-Patterson Air Force Base Dayton, OH 45433	1
Commander Naval Ordinance Systems Command ATTN: ORD-03331, Mr. M. Kinna Washington, DC 20360	1
Naval Postgraduate School ATTN: Code NC4(67WT), Prof. E. M. Wu Monterey, CA 93943	1
Commander Naval Surface Weapons Center ATTN: C. Lyons C. Rowe Silver Springs, MD 20910	1 1
Defense Documentation Center Cameron Station, Bldg. 5 5010 Duke Station Alexandria, VA 22314	2
Aerospace Corporation ATTN: Dr. R. Cooper P.O. Box 92957 Los Angeles, CA 90009	1
AVCO Corporation Government Products Group ATTN: Dr. W. Reinecke P. Rolincik 201 Lowell Street Wilmington, MA 01997	1 1

	No. of Copies
ETA Corporation ATTN: D. L. Mykkinen P.O. Box 6625 Orange, CA 92667	1
Fiber Materials, Inc. ATTN: M. Subilia, Jr. L. Landers R. Burns Biddeford Industrial Park Biddeford, ME 04005	1 1 1
General Electric Company Advanced Materials Development Laboratory ATTN: K. Hall J. Brazel 3198 Chestnut Street Philadelphia, PA 19101	1 1
General Dynamics Corporation Convair Division ATTN: J. Hertz 5001 Kearny Villa Road San Diego, CA 92138	1
General Research Corporation ATTN: Dr. R. Wengler Dr. R. Parisse J. Green 5383 Hollister Avenue Santa Barbara, CA 93111	1 1 1
Hercules Aerospace Corporation ATTN: Dr. S. W. Beckwith (X2F5) P.O. Box 98 Magna, UT 84044-0098	1
Kaman Sciences Corporation ATTN: Dr. D. C. Williams P.O. Box 7463 Colorado Springs, CO 80933	1
Ktech ATTN: Dr. D. Keller 911 Pennsylvania Avenue, N.E. Albuquerque, NM 87110	1
Lawrence Livermore National Laboratory ATTN: Dr. W. W. Feng P.O. Box 808 (L-342) Livermore, CA 94550	1

	No. of Copies
Lehigh University Institute of Fracture and Solid Mechanics ATTN: Dr. George C. Sih Packard Lab, Bldg. 39 Bethlehem, PA 18015	1
Los Alamos National Laboratory ATTN: Dr. W. D. Birchler, Mail Stop G787 Henry L. Horak Los Alamos, NM 87545	1 1
Martin Marietta Aerospace ATTN: V. Hewitt Frank H. Koo P.O. Box 5837 Orlando, FL 32805	1 1
Massachusetts Institute of Technology Department of Aeronautics and Astronautics ATTN: Prof. T. H. H. Pian (Room 311, Bldg. 73) Cambridge, MA 02139	1
Pacifica Technology, Inc. ATTN: Dr. Ponsford P.O. Box 148 Del Mar, CA 92014	1
Radkowski Associates ATTN: Dr. P. Radkowski P.O. Box 5474 Riverside, CA 92507	1
Rohr Industries, Inc. ATTN: Dr. T. H. Tsiang MZ-19T P.O. Box 878 Chula Vista, CA 92012-0878	1
Sandia Laboratories ATTN: Dr. W. Alzheimer Dr. M. Forrestal Dr. E. P. Chen, Div. 1524 P.O. Box 5800 Albuquerque, NM 87115	1 1 1
Southwest Research Institute ATTN: A. Wenzel 8500 Culebra Road San Antonio, TX 78206	1
SPARTA, Inc. ATTN: J. Wonacott J. Glatz 1055 Wall Street Suite 200 P.O. Box 1354 La Jolla, CA 92038	1 1

	No. of Copies
Terra Tek, Inc. ATTN: Dr. A. H. Jones 420 Wakara Way Salt Lake City, UT 84108	1
University of Washington ATTN: K. Y. Lin FS-10, Guggenhein Bldg. Seattle, WA 98195	1
Director Army Materials Technology Laboratory ATTN: SLCMT-BM, J. F. Dignam	1
SLCMT-BM, S. C. Chou	5
SLCMT-BM, L. R. Aronin	1
SLCMT-BM, D. P. Dandekar	1
SLCMT-ISC	1
SLCMT-IML Watertown, MA 02172	2

U. S. Army Materials Technology Laboratory
Watertown, Massachusetts 02172-0001
STATIC AND DYNAMIC TESTING OF INTERCEPTOR SUBSTRUCTURES
M. L. Wilson
R. H. Todd
Terra Tek, Inc.
420 Wakara Way
Salt Lake City, Utah 84108
Technical Report MLT TR 86-5, March 1986
ills-tables, Contract DAAG46-81-C-0023
AMCMS Code: 693000.21500
Final Report - December 1980 to April 1981

AD
Unclassified
Unlimited Distribution

Key Words

Structural Testing
Frustums
Dynamic Loads
Aluminum Alloys
Boron/Aluminum Composites
Metal Matrix Composites
Fracture

Truncated, conical, half-scale, interceptor substructures were tested under axial and shear/bend loads. The substructures, designed and fabricated by General Dynamics, were manufactured with 20 ply boron/aluminum composite tape, each ply was 0.0069 to 0.0080 inch thick. Boron filaments made up 47.0 + 3.0 percent of the composite tape. Average substructure dimensions were 5.80 inches (outside) forward diameter, 7.79 inches (outside) base diameter, and 9.112 inches high (total apex angle 12.46^{0}). The wall thickness was 0.144 inches. Axial loading (both static and dynamic) as well as shear/bend loading (static only) tests were performed; one sample was tested at each test condition.

U. S. Army Materials Technology Laboratory
Watertown, Massachusetts 02172-0001
STATIC AND DYNAMIC TESTING OF INTERCEPTOR SUBSTRUCTURES
M. L. Wilson
R. H. Todd
Terra Tek, Inc.
420 Wakara Way
Salt Lake City, Utah 84108
Technical Report MLT TR 86-5, March 1986
ills-tables, Contract DAAG46-81-C-0023
AMCMS Code: 693000.21500
Final Report - December 1980 to April 1981

AD
Unclassified
Unlimited Distribution

Key Words

Structural Testing
Frustums
Dynamic Loads
Aluminum Alloys
Boron/Aluminum Composites
Metal Matrix Composites
Fracture

Truncated, conical, half-scale, interceptor substructures were tested under axial and shear/bend loads. The substructures, designed and fabricated by General Dynamics, were manufactured with 20 ply boron/aluminum composite tape, each ply was 0.0069 to 0.0080 inch thick. Boron filaments made up 47.0 + 3.0 percent of the composite tape. Average substructure dimensions were 5.80 inches (outside) forward diameter, 7.79 inches (outside) base diameter, and 9.112 inches high (total apex angle 12.46^{0}). The wall thickness was 0.144 inches. Axial loading (both static and dynamic) as well as shear/bend loading (static only) tests were performed; one sample was tested at each test condition.

U. S. Army Materials Technology Laboratory
Watertown, Massachusetts 02172-0001
STATIC AND DYNAMIC TESTING OF INTERCEPTOR SUBSTRUCTURES
M. L. Wilson
R. H. Todd
Terra Tek, Inc.
420 Wakara Way
Salt Lake City, Utah 84108
Technical Report MLT TR 86-5, March 1986
ills-tables, Contract DAAG46-81-C-0023
AMCMS Code: 693000.21500
Final Report - December 1980 to April 1981

AD
Unclassified
Unlimited Distribution

Key Words

Structural Testing
Frustums
Dynamic Loads
Aluminum Alloys
Boron/Aluminum Composites
Metal Matrix Composites
Fracture

Truncated, conical, half-scale, interceptor substructures were tested under axial and shear/bend loads. The substructures, designed and fabricated by General Dynamics, were manufactured with 20 ply boron/aluminum composite tape, each ply was 0.0069 to 0.0080 inch thick. Boron filaments made up 47.0 + 3.0 percent of the composite tape. Average substructure dimensions were 5.80 inches (outside) forward diameter, 7.79 inches (outside) base diameter, and 9.112 inches high (total apex angle 12.46^{0}). The wall thickness was 0.144 inches. Axial loading (both static and dynamic) as well as shear/bend loading (static only) tests were performed; one sample was tested at each test condition.

U. S. Army Materials Technology Laboratory
Watertown, Massachusetts 02172-0001
STATIC AND DYNAMIC TESTING OF INTERCEPTOR SUBSTRUCTURES
M. L. Wilson
R. H. Todd
Terra Tek, Inc.
420 Wakara Way
Salt Lake City, Utah 84108
Technical Report MLT TR 86-5, March 1986
ills-tables, Contract DAAG46-81-C-0023
AMCMS Code: 693000.21500
Final Report - December 1980 to April 1981

AD
Unclassified
Unlimited Distribution

Key Words

Structural Testing
Frustums
Dynamic Loads
Aluminum Alloys
Boron/Aluminum Composites
Metal Matrix Composites
Fracture

Truncated, conical, half-scale, interceptor substructures were tested under axial and shear/bend loads. The substructures, designed and fabricated by General Dynamics, were manufactured with 20 ply boron/aluminum composite tape, each ply was 0.0069 to 0.0080 inch thick. Boron filaments made up 47.0 + 3.0 percent of the composite tape. Average substructure dimensions were 5.80 inches (outside) forward diameter, 7.79 inches (outside) base diameter, and 9.112 inches high (total apex angle 12.46^{0}). The wall thickness was 0.144 inches. Axial loading (both static and dynamic) as well as shear/bend loading (static only) tests were performed; one sample was tested at each test condition.